

INVESTIGATING  
MARKET LINKAGES AND INVESTOR BEHAVIOR  
IN TIMES OF TURMOIL AND UNCERTAINTY

INVESTIGATING  
MARKET LINKAGES AND INVESTOR BEHAVIOR  
IN TIMES OF TURMOIL AND UNCERTAINTY

Philipp Prange, M.Sc.

Chair of Empirical Finance and Econometrics

A dissertation submitted to the Department of Corporate Management & Economics,  
Zeppelin University, in partial fulfillment of the requirements for the degree

Dr. rer. pol.

Dissertation of Zeppelin University

Reviewers: Prof. Dr. Franziska Peter, Prof. Dr. Robert Jung, Prof. Dr. Marcel Tyrell

Date of the disputation: February 03, 2023

Date of submission: April 14, 2022

# Contents

List of figures	iv
List of tables	vi
<b>1 Introduction</b>	<b>1</b>
1.1 Market linkages and investor behavior in times of turmoil and uncertainty . . . . .	2
1.1.1 The response of global equity markets to the outbreak of the coronavirus . . . . .	2
1.1.2 The propagation of shocks across markets . . . . .	5
1.1.3 Flights to quality and safe haven phenomena . . . . .	8
1.1.4 A new source of information on collective investor attention: Implications for prices and market dynamics . . . . .	10
1.2 Time-variation in parametric models . . . . .	15
1.2.1 Time-variation in market linkages: The case of dynamic conditional correlations . . . . .	15
1.2.2 Time-variation in parametric models: The case of the generalized autoregressive score framework . . . . .	25
1.3 Original research conducted in this dissertation . . . . .	28
<b>2 Measuring 25 years of global equity market co-movement using a time-varying spatial model</b>	<b>31</b>
2.1 Introduction . . . . .	31
2.2 Spatial modelling of stock market co-movements . . . . .	33
2.2.1 Modelling time-varying spatial dependence . . . . .	33
2.2.2 Data and descriptives . . . . .	35
2.2.3 Spatial weighting matrix . . . . .	37
2.3 Global equity market co-movement . . . . .	40
2.3.1 Time-varying co-movement across equity markets . . . . .	40
2.3.2 Contagion during recent major crises . . . . .	45

2.4	Concluding remarks . . . . .	48
2.5	Appendices . . . . .	49
2.5.1	Contagion periods depending on pre-event window lengths . . . . .	49
2.5.2	Estimated model coefficients . . . . .	50
<b>3</b>	<b>Flight to quality – Gold mining shares versus gold bullion</b>	<b>51</b>
3.1	Introduction . . . . .	51
3.2	Data . . . . .	55
3.3	Empirical analysis . . . . .	56
3.3.1	Event study methodology framework . . . . .	64
3.3.2	Profit opportunity due to recoupling . . . . .	71
3.4	Concluding remarks . . . . .	73
3.5	Appendices . . . . .	74
3.5.1	Average post-event trading volume . . . . .	74
3.5.2	Descriptive statistics . . . . .	78
<b>4</b>	<b>Does online investor attention drive the co-movement of stock, commodity, and energy markets? Insights from Google searches</b>	<b>82</b>
4.1	Introduction . . . . .	82
4.2	Data . . . . .	84
4.3	Methodology . . . . .	87
4.4	Empirical results . . . . .	88
4.5	Financial implications . . . . .	91
4.5.1	Optimal portfolio weights and hedging ratios . . . . .	91
4.5.2	Portfolio performance and hedging effectiveness . . . . .	93
4.6	Concluding remarks . . . . .	96
4.7	Appendix . . . . .	97
<b>5</b>	<b>What are you searching for? On the equivalence of proxies for online investor attention</b>	<b>98</b>
5.1	Introduction . . . . .	98
5.2	A measure of information transfer . . . . .	99
5.3	Data . . . . .	101
5.4	Empirical results . . . . .	105
5.5	Conclusion . . . . .	110

<b>6</b>	<b>News impact dynamics in the correlations of global equity returns for systemic risk measurement</b>	<b>111</b>
6.1	Introduction . . . . .	111
6.2	Time-varying correlation models with score-driven dynamics . . . . .	113
6.2.1	Dynamic conditional correlation with static news impact . . . . .	113
6.2.2	Dynamic conditional correlation with score-driven news impact . . . . .	114
6.3	Monte Carlo study . . . . .	117
6.4	Empirical study . . . . .	119
6.4.1	Data . . . . .	119
6.4.2	Empirical results . . . . .	124
6.4.3	The impact of news on global cross-market linkages . . . . .	128
6.4.4	Correlation news impact surfaces . . . . .	130
6.4.5	Model alternatives and extensions . . . . .	134
6.5	Concluding remarks . . . . .	138
6.6	Appendices . . . . .	139
6.6.1	Univariate GARCH models . . . . .	139
6.6.2	Series-specific news impact dynamics . . . . .	140
<b>7</b>	<b>Critical assessment and conclusion</b>	<b>141</b>
	<b>Bibliography</b>	<b>viii</b>

# List of Figures

1.1	Daily cumulative returns of China and G7 constituents over time . . . . .	3
1.2	Cross-sectional weighted regression of gold betas on market betas . . . . .	10
1.3	Online searches for keywords “S&P 500” and “gold price” over time . . . . .	13
1.4	Simulated true correlation processes (DCC model) . . . . .	19
1.5	Conditional correlation estimates over time . . . . .	22
1.6	News impact surfaces for correlations . . . . .	24
2.1	The relation between geographic and economic distances . . . . .	39
2.2	Time-varying spatial dependence between markets (Global) . . . . .	41
2.3	Time-varying spatial dependence (America, Europe, Asia-Pacific) . . . . .	42
2.4	Contagion after COVID-19 based on the pre-event window length . . . . .	49
2.5	Contagion after the GFC based on the pre-event window length . . . . .	49
3.1	Cross-sectional regression of gold betas on market betas . . . . .	52
3.2	Crisis period definitions (US) . . . . .	59
3.3	Average post-event trading volume (Australia) . . . . .	74
3.4	Average post-event trading volume (Canada) . . . . .	75
3.5	Average post-event trading volume (UK) . . . . .	76
3.6	Average post-event trading volume (US) . . . . .	77
4.1	Online search series over time . . . . .	85
4.2	Estimated correlations over time . . . . .	89
4.3	Optimal weights of commodities and energies over time . . . . .	92
5.1	Online searches over time for three companies . . . . .	102
6.1	Simulated true correlation processes . . . . .	118
6.2	Economic distance and stock market integration . . . . .	123
6.3	Volatility news impact curves for three assets . . . . .	126
6.4	US-German equity return correlation and global news impact . . . . .	128

## LIST OF FIGURES

---

6.5	Correlation news impact surfaces . . . . .	131
6.6	Difference between correlation news impact surfaces . . . . .	133
6.7	Time-varying global asymmetry impact . . . . .	135

# List of Tables

2.1	Descriptive statistics . . . . .	36
2.2	Average yearly co-movement . . . . .	43
2.3	Average yearly standard deviation of the co-movement parameter . . . . .	44
2.4	Contagion during selected events between 1995 and 2020 . . . . .	46
2.5	Coefficient estimates of the dynamic SAR model . . . . .	50
3.1	Market betas and gold betas per market . . . . .	57
3.2	Gold beta estimates of liquid gold mining stocks (Australia) . . . . .	60
3.3	Gold beta estimates of liquid gold mining stocks (Canada) . . . . .	61
3.4	Gold beta estimates of liquid gold mining stocks (UK) . . . . .	62
3.5	Gold beta estimates of liquid gold mining stocks (US) . . . . .	62
3.6	Gold beta estimates of combined portfolios . . . . .	63
3.7	Cumulative returns . . . . .	66
3.8	Cumulative abnormal gold returns . . . . .	69
3.9	Pooled cumulative returns and cumulative abnormal gold returns . . . . .	70
3.10	Cumulative abnormal gold returns (Long-term) . . . . .	72
3.11	Descriptive statistics (Australia) . . . . .	78
3.12	Descriptive statistics (Canada) . . . . .	79
3.13	Descriptive statistics (UK) . . . . .	81
3.14	Descriptive statistics (US) . . . . .	81
4.1	Descriptive statistics . . . . .	86
4.2	Estimated model coefficients . . . . .	90
4.3	Estimated optimal weights and hedging ratios . . . . .	94
4.4	Portfolio performance and hedging effectiveness . . . . .	95
5.1	Descriptive statistics . . . . .	104
5.2	Information transfer between Google and Wikipedia searches (2008–2017, q(5,95)) . . . . .	106



## LIST OF TABLES

---

5.3	Information transfer between Google and Wikipedia searches (2010–2017, $q(5,95)$ ) . . . . .	107
5.4	Information transfer between Google and Wikipedia searches (2008–2017, $q(10,90)$ ) . . . . .	108
5.5	Information transfer between Google and Wikipedia searches (2010–2017, $q(10,90)$ ) . . . . .	109
6.1	Performance of different correlation models . . . . .	119
6.2	Descriptive statistics . . . . .	121
6.3	Unconditional correlations between market returns . . . . .	122
6.4	GARCH model selection . . . . .	125
6.5	Parameter estimates of DCC-type models . . . . .	127
6.6	Goodness of fit comparison between models . . . . .	136
6.7	Parameter estimates of extended p-range DCC models . . . . .	137

## Acknowledgements

My academic journey has come to an end. The last three and a half years have been an outstanding experience during which I have broadened my horizons, encountered inspiring people, entered into uncharted waters, and pursued many new ideas. As a new chapter in my life is about to begin, I wish to thank the numerous people who – by the means of big and small acts of kindness and helpfulness – have knowingly or unknowingly contributed to this dissertation.

I express my deepest gratitude to Prof. Dr. Franziska Peter for being the excellent supervisor for my journey. She has been warm-hearted and caring from the beginning, has given me a great amount of freedom, has provided me with valuable insights, and has always been supportive in times of need. Further, I thank Prof. Dr. Robert Jung and Prof. Dr. Dirk Baur for their great feedback on and our discussions about numerous research projects, some of which have been conducted in joint work. My heartfelt appreciation goes to Dr. Alexander Schmidt, Dr. Karsten Schweikert, and Dr. Simon Behrendt. In them, I have found three guiding lights who have largely shaped my research interests and developments in recent years. I am sincerely grateful for our joint (co)working sessions, talks, activities, and the mental and practical guidance that they have provided me with over the course of my journey. I am also keen to remember the lunches, coffee breaks, and leisure time activities with Thomas Heil, Robert Heil, and Sascha Platschek. They have greatly contributed to the happiness and joyfulness I have experienced during my time in Friedrichshafen and I am glad to call them close friends of mine. Besides, I thank Rayan Ayari, Jasper Brühns, Sophia Gläser, Martin Haas, Markus Mößler, Dr. Konstantin Kuck, Prof. Dr. Florentina Paraschiv, Mariana Patiño, and Dorian Quelle for our joint time. I have greatly appreciated every moment. I am incredibly thankful to Lilli Krings, whose support and patience throughout the writing of this dissertation is unmatched. She was my safe haven in times of turmoil and uncertainty. Finally, I wish to thank my family – Cornelia, Peter, and Nadine Prange. I thank them so much for everything.

# Abstract

Throughout the last decades, investigations on market linkages and investor behavior in times of turmoil and uncertainty have received the attention of researchers and financial practitioners alike. This dissertation offers five distinct research papers which contribute to the existing literature on this overarching topic. First, we provide a thorough analysis of the time-varying linkages between regional and global equity markets. Second, and in line with the notion of increasing equity market integration over time, we investigate different types of flights to quality in times of stock market turmoil. Third, we provide novel empirical evidence on the usefulness of new sources of information on investor behavior towards the measurement of financial market linkages. Fourth, building on the increasing relevance of these new sources of information, we demonstrate that different measures for online investor attention do not necessarily constitute equivalent proxies for the latent variable. Last, we contribute to the strands of financial literature dealing with the estimation of dynamic linkages between financial markets and variables in the form of time-varying correlations. More specifically, we propose a score-driven extension to the well-known dynamic conditional correlation model which provides a means to quantify the time-varying influence of news on correlation dynamics. Taking the severe impact of recent and current crisis events on financial markets into consideration, the research papers comprised in this dissertation are of uttermost importance for financial market participants.

# Chapter 1

## Introduction

This dissertation is concerned with a thorough investigation on financial market linkages and investor behavior in times of turmoil and uncertainty. The first chapter serves the purpose of introducing into this general topic by reviewing some of the relevant literature for the original research conducted in this dissertation. More particularly, the literature review is concerned with (i) the response of global equity markets to the outbreak of the coronavirus, (ii) the propagation of shocks across markets, (iii) flights to quality and safe haven phenomena as patterns of collective investor behavior, and (iv) Google searches as a new source of investor attention. Besides, since many of the proceeding chapters related to the measuring of market linkages draw upon a similar framework in theory and subsequent applications, the first chapter additionally offers some preliminary methodological remarks along this dimension. While the following introduction makes no claim to completeness – neither with regards to the review of the relevant research, nor in terms of the preliminary methodological remarks – it is instead intended to provide a starting point which allows to advance both the fundamental ideas and the research avenues proposed in the later chapters of this dissertation.

The remainder of this chapter is structured as follows: Section 1.1 embeds the original research of this dissertation into the existing literature on market linkages and the behavior of financial investors in times of turmoil and uncertainty. Next, Section 1.2 provides preliminary methodological remarks on the modelling of time-variation in parametric models. These remarks are divided into two subsections, first of which introduces a specific model for the estimation of time-varying market linkages, and second of which presents a general framework for the modelling of time-variation in observation-driven models. Finally, Section 1.3 concludes the first chapter in offering a comprehensive overview on the original research conducted in this dissertation.

## 1.1 Market linkages and investor behavior in times of turmoil and uncertainty

The last decades have witnessed occurrences of financial turmoil and uncertainty with notable regularity. During such times, negatively affected markets generally exhibit an increase both in the co-movement of their returns and in their volatility levels, potentially spilling over across markets. Given the high economic and geopolitical relevance for financial practitioners and policy makers alike, investigations on the subject, nature, and channels through which shocks propagate across financial markets have sparked large strands of academic research (see, e.g., [Kling, 1985](#); [Engle \*et al.\*, 1990](#); [King and Wadhvani, 1990](#); [King \*et al.\*, 1994](#); [Karolyi, 1995](#); [Forbes and Rigobon, 2002](#); [Diebold and Yilmaz, 2012](#)).

### 1.1.1 The response of global equity markets to the outbreak of the coronavirus

To illustrate the (potential) impact of shocks on equity market linkages, consider the outbreak of the coronavirus (COVID-19) in early 2020. Shortly after the first instances of an unknown pneumonia were observed in Wuhan, China, the World Health Organization (WHO) announced that the outbreak of the virus constitutes a public health emergency of international concern. As of March 11, 2020, 118,000 cases of infections were reported in 114 countries, whilst 4,291 people have lost their lives due to the virus. That day, in response to the fast spread of COVID-19 across countries and the high level of severity, the WHO declared the outbreak of COVID-19 a global pandemic ([WHO, 2020a,b](#)). More recently, as of November 14, 2021, over 252 million confirmed cases of infections and over five million deaths have officially been reported ([WHO, 2020c](#)). From an economic perspective, the impact of the outbreak of COVID-19 on financial markets was unprecedented, causing simultaneous rises in global equity market volatility levels and rapidly declining equity market prices across the globe.

Figure 1.1 illustrates the immediate impact of the COVID-19 pandemic on international equity market indices. In more detail, the figure depicts daily cumulative returns of both China and the G7 constituent countries over the period from January 2019 to December 2020. The figure additionally highlights the time interval within that period, during which the WHO declared COVID-19 a global pandemic. As shown in the simultaneous behavior of cumulative returns in early 2020, the depicted equity markets decline sharply from their initial level in response to the outbreak of COVID-19, and partially recover thereafter.

Corresponding to the severe impact of COVID-19 on global equity markets, studies on

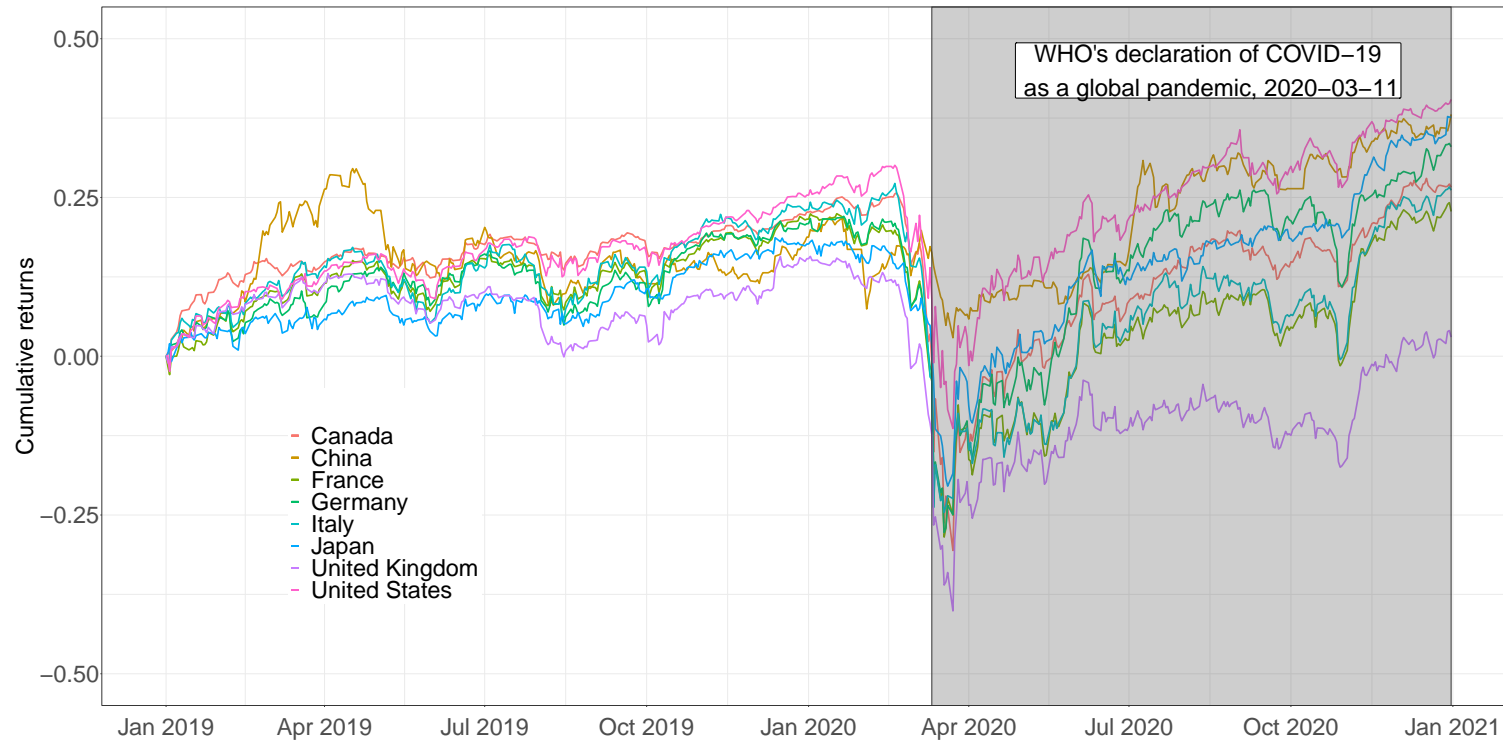


**Figure 1.1: Daily cumulative returns of China and G7 constituents over time**

This figure illustrates daily cumulative equity market returns of China and G7 constituent countries from January 2019 to December 2020. Besides, the shaded area (grey) beginning on 2020-03-11 indicates the time interval within that period during which the WHO declared COVID-19 a global pandemic.

the subject of changes in market returns, volatilities, and linkages in response to the outbreak of the virus have moved into the focus of the recent financial literature. For instance, the studies of [Baker \*et al.\* \(2020\)](#) and [Sharif \*et al.\* \(2020\)](#) investigate United States (US) equity market movements during the early phases of COVID-19. In their studies, the authors find that the US market reactions to the virus were unprecedented compared to previous periods of market turmoil. Similar investigations on equity market movements in response to the outbreak of COVID-19 have also been conducted for the international case. Along this line, the research of [Ali \*et al.\* \(2020\)](#) suggests that international equity market volatilities have increased significantly over different phases of the pandemic, and empirical evidence towards a negative response of equity market returns to the growth in confirmed cases of COVID-19 infections and corresponding death numbers is provided in [Ashraf \(2020\)](#). Besides, [Zhang \*et al.\* \(2020\)](#) and [Chakrabarti \*et al.\* \(2021\)](#) have studied country-specific as well as systemic risk in global equity markets over the course of the pandemic.

More generally, increases in equity market co-movement and the simultaneous downturn of markets in response to shocks have been witnessed in previous periods of turmoil and uncertainty, and are subject to various academic studies dealing with the issues of economic or financial integration (e.g., [Berben and Jansen, 2005](#); [Wälti, 2011](#)), asset management and portfolio diversification strategies (e.g., [Chiang \*et al.\*, 2007](#); [Driessen and Laeven, 2007](#)), systemic risk management (e.g., [Blasques \*et al.\*, 2016b](#); [Benoit \*et al.\*, 2017](#)), or financial contagion (e.g., [Forbes and Rigobon, 2002](#); [Bekaert \*et al.\*, 2014](#)). Motivated by the many different periods of market turmoil that have been studied in the literature, Chapter 2 provides a thorough investigation on the different impacts of a selection of market events on the time-varying co-movement between global, American, European, and Asian-Pacific equity markets. To study the co-movement among markets on such broad scales beyond pair-wise investigations, the empirical analysis employed in the chapter draws upon a novel methodological approach in using a dynamic version of the spatial autoregressive (SAR) model. Importantly, the co-movement within European countries is found to be generally higher compared to American and Asian-Pacific countries. Besides, whilst increasing co-movements can be witnessed prior to the global financial crisis (GFC) in 2008, the highest levels are reached over the course of the recent COVID-19 pandemic.

To facilitate a preliminary understanding of the channels through which shocks may influence the co-movement between financial markets, the following subsection introduces some of the literature concerned with the identification, measuring, and testing of different shock propagation mechanisms. Thus, the subsequent literature review sets the grounds for the proceeding chapters of this dissertation.

### 1.1.2 The propagation of shocks across markets

In view of the potentially significant impact of shocks on cross-market linkages and their importance for various common tasks in finance, theoretical financial research on the international propagation of shocks is fairly extensive. For this reason, [Forbes and Rigobon \(2001\)](#) propose to divide the related literature into two categories, i.e. (i) crisis contingent theories which suggest propagation channels and, in turn, cross-market linkages to change significantly in response to shocks, and (ii) non-crisis-contingent theories which refer to occurrences whereby propagation channels and cross-market linkages during crisis events remain identical to their initial, pre-crisis state. The fundamental difference between the two categories is whether the transmission mechanisms used to describe the propagation of shocks and, equally so, cross-market linkages, shift significantly in response to shocks. Note, however, that the transmission channels attributable to either category offer the theoretical backgrounds to explain observations of high or increased co-movement between markets over periods of turmoil. With the purpose of providing a theoretical outline for the following chapters of this dissertation, this subsection adapts the categorization proposed in [Forbes and Rigobon \(2001\)](#) to offer a brief overview on some of the different transmission channels within each category.

First, transmission channels comprised in crisis contingent theories suggest propagation mechanisms and financial market linkages to shift significantly in response to shocks. For instance, the concept of multiple equilibria in spirit of [Obstfeld \(1986\)](#) as well as both [Sachs \*et al.\* \(1996\)](#) and [Jeanne \(1997\)](#) for exchange rate crises involving self-fulfilling expectations, considers shifts in the expectations of financial investors in response to sunspot crises to explain the propagation of shocks across markets. Along this line, the study of [Masson \(1998\)](#) provides empirical evidence that both the 1994 Mexican crisis and the 1997 Asian financial crisis have negatively impacted the beliefs of investors in emerging economies unrelated to their macroeconomic fundamentals, shifting from “good” to “bad” moods. The second crisis contingent transmission channel, endogenous liquidity shocks, proposes liquidity shocks in one economy to influence the creditworthiness of other economies. Consistent with this transmission channel, the model of [Valdés \(1996\)](#) demonstrates that in instances where markets are illiquid whilst its participants are in need of liquidity, subsequent repayment issues can propagate across borders as the required liquidity is sought elsewhere. In consequence, the authors suggest this propagation mechanism to induce an increased co-movement in the creditworthiness of markets. Similar liquidity based explanations for the propagation of shocks across markets are also provoked in [Allen and Douglas \(2000\)](#), [Kyle and Xiong \(2001\)](#), [Calvo \(2004\)](#), or [Yuan \(2005\)](#). The final crisis contingent transmission channel, political contagion, describes the concept whereby political objectives inherently foster the



propagation of shocks. Akin to the concept of political contagion, [Drazen \(2000\)](#) develops a model which stresses the balance between the economic gains obtained from currency devaluation and the associated political costs arising by such policy decision making. As in the case of the European devaluations of 1992 and 1993, for instance, policy decision makers may wish to strengthen the economic and political integration between countries by refraining from competitive devaluations or, more explicitly, forming currency areas. Among others, the maintenance of a pegged exchange rate reflects a membership condition for each potential constituent of such currency area. Given that the benefits of maintaining the currency peg decrease if an “important” (potential) member of the arrangement abandons its fixed exchange rate, such occurrence increases the probability of devaluation in other countries. In turn, political contagion suggests the initial devaluation shock to propagate across international borders through a channel which becomes existent only in response to the initial shock itself.

Second, non-crisis contingent theories comprise research that suggests propagation mechanisms and market linkages in times of market turmoil to not significantly depart from their conditions in tranquil times. In other words, observations of high market co-movement are described via a continuation of linkages that already existed before the initial shock. Along this line, [Eichengreen \*et al.\* \(1996\)](#), [Glick and Rose \(1999\)](#), [Corsetti \*et al.\* \(2000\)](#), and [Kaminsky and Reinhart \(2000\)](#) consider trade linkages between countries to foster the propagation of shocks across markets. Likewise, [Gerlach and Smets \(1995\)](#) provide a model which revolves around the question how a forced depreciation in the currency of one country affects the relative competitiveness of its goods in a second country. According to their model, the negative effects on the sales of the domestic goods within the second country are stronger, the higher the trade intensity between the two countries. Besides, the role of policy coordination between countries in determining the degree of shock propagation across markets is studied in [Buiters \*et al.\* \(1998\)](#), [Loisel and Martin \(2001\)](#), and [Gai \*et al.\* \(2011\)](#), whilst [Rigobon \(1998\)](#) and [Corsetti \*et al.\* \(1999\)](#) suggest that shocks propagate across international borders as investors learn from prior crises in countries that share similar macroeconomic patterns. A final transmission channel attributable to the set of non-crises contingent theories is given by external global shocks which do not originate from one economy, but arise and affect multiple markets simultaneously instead. In this concern, the model proposed in [Dellas \(1986\)](#) points towards common (oil supply) shocks to drive the co-movement between large economies.

The quest for quantifying the transmission of shocks occurring through the channels related to either category has been pursued by a wide range of empirical approaches in the financial literature. For instance, [Calvo and Reinhart \(1996\)](#) and [Kaminsky and Reinhart](#)

(2003) study the international propagation of shocks across financial markets using principal component analysis, whereas similar endeavor is conducted in [Eichengreen \*et al.\* \(1996\)](#) by the means of binary probit models. Besides, time-varying factor models to analyze the global transmission channels in equity markets are employed in [Bekaert \*et al.\* \(2014\)](#), whilst [Acemoglu \*et al.\* \(2015\)](#) use a network approach to find the strength of the propagation of shocks across financial markets to depend on the pattern of interbank liabilities. Further, [King and Wadhvani \(1990\)](#), [Boyer \*et al.\* \(1997\)](#), [English and Loretan \(1997\)](#), [Forbes and Rigobon \(2002\)](#), [Caporale \*et al.\* \(2005\)](#), and [Chiang \*et al.\* \(2007\)](#) consider correlations, while [Baig and Goldfajn \(1999, 2000\)](#) and [De Gregorio and Valdé \(2001\)](#) use linear regressions to measure the propagation of shocks across markets. Both [Rodriguez \(2007\)](#) and [Kenourgios \*et al.\* \(2011\)](#) apply copulas whilst, more recently, [Caporin \*et al.\* \(2018\)](#) employ a Bayesian quantile regression to investigate shifts in the propagation mechanisms across European countries.

Investigating shifts in cross-market linkages in response to shocks is particularly challenging, however, due to the econometric issues arising in global financial data in the form of heteroscedasticity, simultaneous equations, and omitted variables.<sup>1</sup> Importantly, these issues lead the degree of model misspecification to change over time, rendering standard econometric techniques to test for shifts in market linkages inappropriate (e.g., [Rigobon, 2003b](#)). For instance, tests on the null hypothesis of stable market linkages might be rejected because the biases rather than the corresponding parameters change over time. Among others, methodological avenues to address these concerns are provided in [Forbes and Rigobon \(2002\)](#), [Rigobon \(2003a\)](#), and [Caporin \*et al.\* \(2018\)](#).<sup>2</sup>

Finally, the financial literature on identifying, measuring, and testing for shifts in the propagation mechanisms is closely related to several of the proceeding chapters in this dissertation. First, Chapter 2 investigates not only the co-movement between equity markets, but also shifts in the co-movement in the aftermath of a selection of events over the past two decades. Second, both Chapter 3 and 4 are concerned with the reactions of financial investors in response to shocks. Chapter 3 in particular shows that the strength of this reaction, measured by different types of flights from affected assets towards other investments, depends on the severity of the shock. Last, Chapter 6 provides a novel methodological approach to quantify the severity of shocks for the dynamic co-movement between (financial) variables. This contribution seems highly relevant, given the great interest in the topic of propagation

---

<sup>1</sup>[Forbes and Rigobon \(2002\)](#) define evidence of significant shifts in cross-market linkages after a shock to one economy (in support of crisis contingent theories) as contagion. Note, however, that different definitions of what constitutes contagion have been considered in the financial literature (For a comprehensive survey on that matter, see [Forbes, 2012](#)).

<sup>2</sup>For more throughout reviews of the theoretical literature discussing the propagation of shocks across markets, see [Goldstein \*et al.\* \(2000\)](#), [Claessens \*et al.\* \(2001\)](#), and [Forbes and Rigobon \(2001\)](#). For surveys on the related empirical literature, please refer to [Dungey \*et al.\* \(2005\)](#) and [Rigobon \(2019\)](#).

mechanisms demonstrated by the theoretical and empirical literature alike.

Building on these propagation mechanisms, the following subsection offers a foundation for Chapter 3 and 4 of this dissertation in reviewing some of the literature concerned with flights to quality and safe haven phenomena.

### 1.1.3 Flights to quality and safe haven phenomena

Taking both the various transmission channels through which shocks may propagate across markets and the simultaneous downturns of negatively affected assets into consideration, financial investors seek to find investment opportunities which explicitly reduce their losses in times of market turmoil and uncertainty (e.g., [Sherman, 1982](#); [Ang and Bekaert, 2002](#)). The related literature concerned with hedges, flights to quality or flights to safety and safe haven phenomena is particularly relevant to Chapters 3 and 4 of this dissertation. Against this backdrop, this subsection is devoted to a brief introduction on the research investigating the role of different assets and asset classes as safe havens and/ or hedges in combined portfolios.

In their study on the role of gold bullion in financial markets, [Baur and Lucey \(2010\)](#) define an asset which is uncorrelated or negatively correlated with another asset or portfolio in times of market distress and turmoil a safe haven asset. Note, that this property makes no statement about the correlation on average but only in response to the occurrence of severe negative events. Assume, for instance, an investor who adds a negatively correlated safe haven asset to the other assets in her portfolio. In tranquil times, the correlation between the safe haven asset and the other assets can thus be positive, zero, or negative. In contrast, if the prices of the other assets in the portfolio plunge in response to the occurrence of a negative shock, the negatively correlated safe haven asset would compensate the investor for her losses by exhibiting positive returns at the same time. [Baur and Lucey \(2010\)](#) further distinguish safe haven assets from hedges by the means of the temporal dimension over which these correlation properties must hold. Whilst a safe haven asset is explicitly referred to as an asset exhibiting nonpositive correlation with another asset or portfolio in extreme adverse market conditions, this characteristic must only hold on average for a hedge. In consequence, a portfolio and its hedge could be positively correlated during a crisis while being negatively correlated in tranquil times and on average.

Among others, flight to quality and safe haven phenomena have been investigated in [Kaul and Sapp \(2006\)](#), [Ranaldo and Söderlind \(2010\)](#), and [Habib and Stracca \(2012\)](#) on safe haven effects of currencies and [Gulko \(2002\)](#), [Connolly \*et al.\* \(2005\)](#), [Baur and Lucey \(2009\)](#), and [Baele \*et al.\* \(2018\)](#) on flights to quality between equity markets and bonds. Studies that analyze the financial characteristics of energy markets and the role of oil as a hedge against equity market risk are provided in [Malik and Ewing \(2009\)](#), [Arouri \*et al.\* \(2011\)](#), [Mensi \*et al.\*](#)

(2013, 2015a), and Lin *et al.* (2014). Similarly, literature on the financial characteristics of commodity markets and, more particularly, the role of gold as a hedge comprises Sherman (1982), Jaffe (1989), Capie *et al.* (2005), Faugère and Van Erlach (2005), and Lucey *et al.* (2006). Along this line, Baur and Lucey (2010) and Baur and McDermott (2010) extend the literature on the hedging property of gold towards an investigation on the commodity's safe haven characteristic. In the same vein, Ciner *et al.* (2013), Creti *et al.* (2013), Reboredo (2013), Arouri *et al.* (2015), and Chkili (2016) offer empirical evidence in support of gold's role as a safe haven asset in combined portfolios.

Chapter 3 adds to the existing literature on flights to quality or flights to safety and safe haven phenomena in distinguishing between flights to physical gold and flights to gold mining company shares. Figure 1.2 depicts this relation based on estimates obtained from a linear regression of 175 gold mining company share returns on the returns of corresponding equity market indices and the returns of gold bullion.<sup>3</sup> The figure illustrates that gold mining companies are notably distinguishable from gold bullion as no company is highly correlated with physical gold and uncorrelated with the market. Thus, whilst the related literature suggests physical gold to be uncorrelated (or negatively correlated) with the market in times of turmoil, gold mining company shares are exposed both to the market and to the price of gold. This raises the question whether gold mining company shares fall with the market or increase with the price of gold bullion during times of adverse market conditions. The thorough empirical comparison of this relative performance substantially enriches the understanding about investor behavior in response to shocks. In that regard, it is shown in Chapter 3 that the relative performance of gold mining company shares depends on the severity of the shock. When shocks to the market are less severe, e.g., the vote on the withdrawal of the United Kingdom (UK) from the European Union, investors flee from equity markets to both physical gold and gold mining shares whereby a clear preference for the latter can be witnessed. In contrast, when market shocks are more severe, e.g., the bankruptcy of Lehman Brothers, investors flee from stocks including gold mining shares to gold bullion. During such instances, the safe haven effect of gold bullion increases due to a concentration of the flight to quality.

Studies on the hedging properties of energies and commodities against the risk associated with equity market investments are also closely related to Chapter 4 of this dissertation. The main contribution of the latter, however, lies in the use of a new source of collective investor attention to enhance the estimation of the time-varying linkages between financial markets. Next, this new source of collective investor attention as well as its implications for the prices of and the dynamics between financial markets is introduced in more detail.

---

<sup>3</sup>Chapter 3 explains the data used in the figure in further detail.

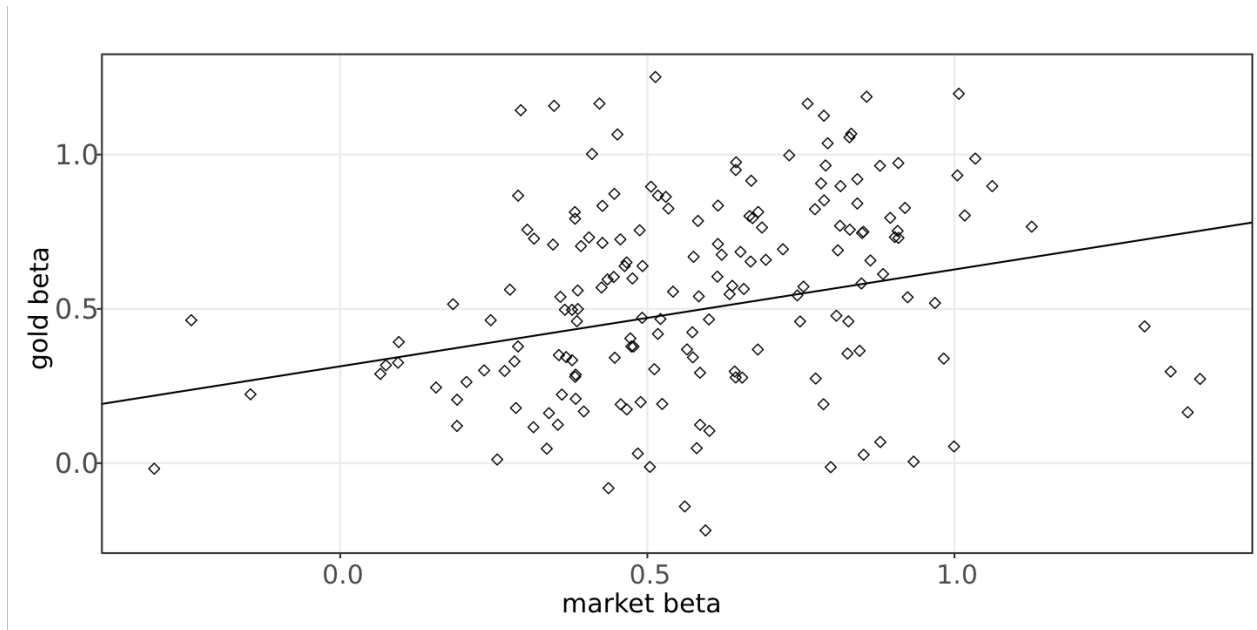


**Figure 1.2: Cross-sectional weighted regression of gold betas on market betas**

This figure plots the linear relation between gold betas and market betas. The latter are obtained from a regression of gold mining company returns on the returns of equity markets and gold bullion over the period from January 1997 to September 2018. The regression line depicted in the figure is based on a cross-sectional weighted linear regression of gold betas on market betas.

#### 1.1.4 A new source of information on collective investor attention: Implications for prices and market dynamics

According to traditional finance theory, available information is instantaneously incorporated into prices upon arrival. In spirit of the classical analysis of efficient markets coined in [Fama \(1965\)](#) as well as traditional asset pricing models proposed in both [Sharpe \(1964\)](#) and [Ross \(1976\)](#), competition among rational investors or arbitrageurs is supposed to drive prices towards fundamental values. This assumption of traditional finance theory, however, requires investors to attribute sufficient attention towards assets and to possess the specific knowledge and information that is needed to engage in arbitrage opportunities.

Traditional finance theory fails to align with real financial practice on this matter, as attention is closely related to effort and thus a scarce cognitive resource available to investors (see, e.g., [Kahnemann, 1973](#); [Pashler and Johnston, 1998](#)). More particularly, when attention is allocated towards one asset, it necessarily requires investors to substitute cognitive resources from other tasks. Given the many different investment alternatives available in financial markets, investment decision making with limited attention is inevitable for many market participants and influences both prices and market dynamics (e.g., [Miller, 1977](#); [Merton, 1987](#); [Hirshleifer and Teoh, 2003](#); [Peng and Xiong, 2006](#); [Veldkamp, 2006](#); [Veldkamp](#)

and Wolfers, 2007). Corresponding to noise trader theories inspired by Kyle (1985) and Black (1986) as well as behavioral models in line with De Long *et al.* (1990) and Shleifer and Vishny (1997), concerns of limited attention are often assigned to individual or retail investors who are likely to be at an informational disadvantage compared to institutional or other professional investors such as investment banks, hedge funds, mutual funds, or pension funds. Building on the theoretical framework on how limited attention may affect financial markets, various measures for latent investor attention have been proposed in the literature. For instance, Barber and Odean (2008) and Seasholes and Wu (2007) show that increased attention towards assets, approximated by asset appearances in newspaper articles, high trading volumes, or extreme returns, leads to attention-driven buying patterns in response. Similarly, Gervais *et al.* (2001) provide empirical evidence that assets which experience extremely high trading volumes exhibit positive excess returns thereafter. Further, Grullon *et al.* (2004) and Lou (2014) consider advertising expenditures as a measure of investor attention, and Yuan (2015) uses equity market front page appearances in newspapers to forecast market returns.

More recently, the increasing global accessibility of the internet has originated new sources of information on collective investor attention. Online search queries, referring to queries conducted on publicly available search engines such as Google or Wikipedia, have increasingly been associated with investor demand for information. As online search queries represent more unambiguous measures of latent investor attention compared to their traditional counterparts, they have raised the interest of financial practitioners and researchers alike.<sup>4</sup>

In the following, this dissertation is primarily concerned with the use of Google Trends' Search Volume Index which has recently moved into the focus of an extensive empirical literature in finance. Google Trends, a service of the company Alphabet Inc., provides data on the relative propensity of Google search queries over time. As of September 2021, Google is Alphabet Inc.'s globally leading search engine with a total market share of 86.64% (Statista, 2021). In consequence, online search queries reported by Google Trends are likely to reflect the internet searching behavior of the general population. Following Da *et al.* (2011), the related literature employs Google search queries to construct measures of the level of attention that investors attribute to assets, markets, or events and, subsequently, uses these measures to estimate their effects on and forecast the future values of various financial variables. For instance, Da *et al.* (2015) suggest to combine multiple search queries to construct an aggregate

---

<sup>4</sup>Compare, e.g., Da *et al.* (2011) who find that while traditional measures of investor attention are interesting in their own right, they are often built on unreasonable assumptions. For instance, extreme turnovers or returns can be driven by factors unrelated to investor attention and newspaper articles only generate attention when they are actually read. In contrast, actively conducting search queries is unambiguously linked to attention.



measure of investor attention and [Bleher and Dimpfl \(2019\)](#) offer an approach to construct consistent, multi-annual time series of investor attention in daily frequency from search query data. To illustrate the measure outlined in [Bleher and Dimpfl \(2019\)](#) that is used in the later chapters, [Figure 1.3](#) plots two time series of relative investor attention. In more detail, the figure shows the relative Google search volume for the keywords “S&P 500” and “gold price” over the period from January 2019 to December 2020 in daily frequency. The figure depicts that the relative search interests are particularly high during the outbreak of COVID-19 in early 2020. Besides, the search interest in “gold price” is again relatively high during August 2020 when the price of gold reaches its new all-time-high. Note, that whilst the initial search query data for any keyword is scaled between 0 and 100 relative to the observation comprising the highest search interest within a requested period, the methodology of [Bleher and Dimpfl \(2019\)](#) allows values to exceed this upper boundary.

The received measures of online investor attention from either of the proposed approaches in the literature are then employed in a wide range of empirical applications. Along this line, [Preis \*et al.\* \(2013\)](#) and [Dimpfl and Jank \(2016\)](#) demonstrate that Google searches for financial terms predict equity market returns and volatility, respectively, and [Joseph \*et al.\* \(2011\)](#) provide empirical evidence that Google searches for stock tickers can be used to predict abnormal portfolio returns and trading volume. Likewise, [Ji and Gu \(2015\)](#) and [Jain and Biswal \(2019\)](#) study the impact of Google searches on commodities and [Han \*et al.\* \(2017\)](#) and [Afkhami \*et al.\* \(2017\)](#) reveal predictability of returns and volatilities in the energy sector.

A notable part of empirical research investigating the effects of investor attention on financial markets evolves around the question how investor attention impacts individual assets. However, whilst still in its infancy, some of the recent research is also concerned with the impacts of investor attention on the co-movement between assets (e.g., [Shiyang \*et al.\*, 2019](#); [Hu \*et al.\*, 2021](#)). [Chapter 4](#) builds on this prior research in a joint framework of equity, commodity, and energy markets, and demonstrates that online investor attention, measured by Google searches, not only impacts assets at the individual level but also affects the linkages between them. More particularly, the results suggest an increase (decrease) in investor attention towards individual assets to lead to an increase (decrease) of their co-movement in response. However, this relationship is weakened or even reversed when studying times containing occurrences of severe shocks. In times of market turmoil and uncertainty, investor attention towards individual assets leads to smaller increases (or even decreases) of the co-movement between assets.

Besides, given the different sources of measures for online investor attention that have been employed in the literature, the question arises whether these constitute equivalent proxies for the latent variable. This question is closely related to the search for a preferred measure of

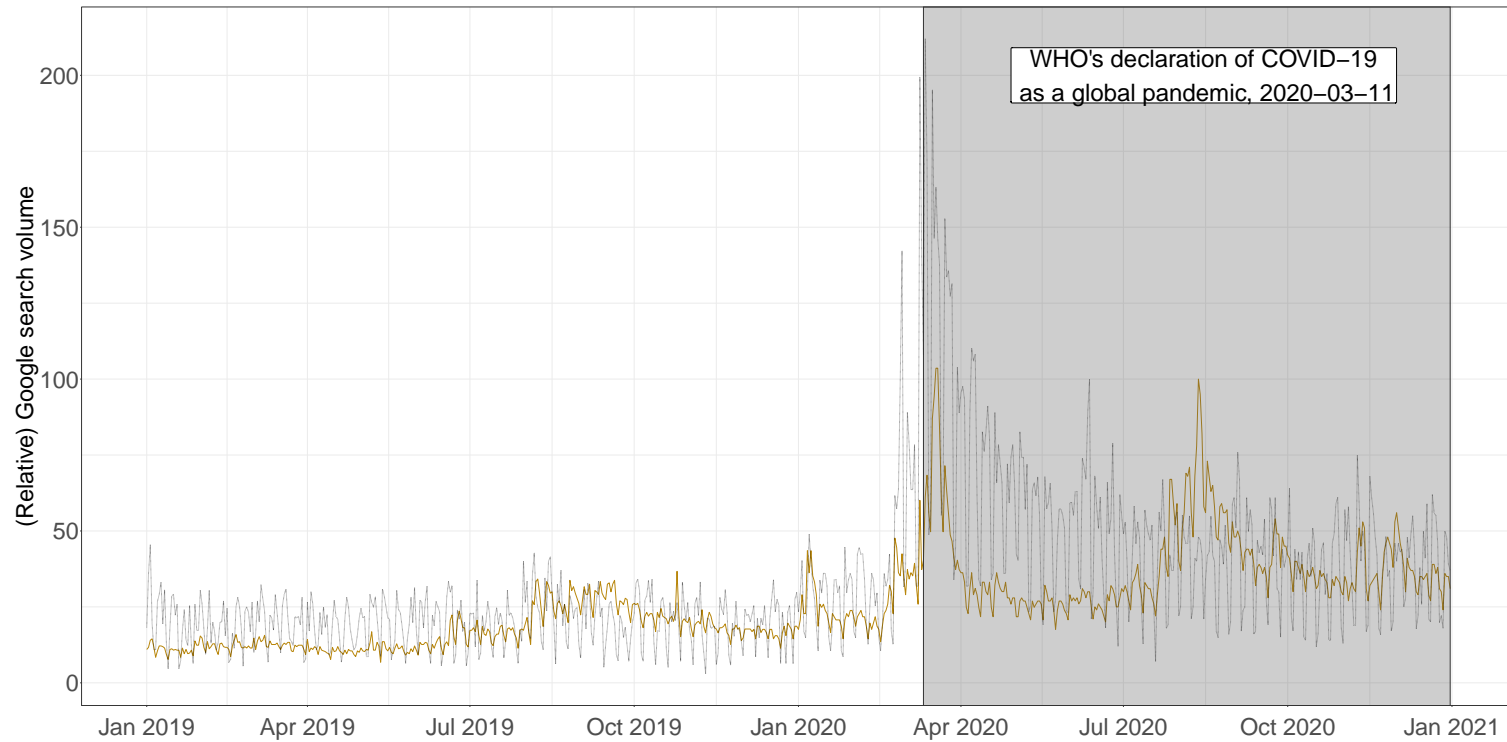


**Figure 1.3: Online searches for keywords “S&P 500” and “gold price” over time**

This figure illustrates a measure of (relative) daily Google search volume for the keywords “S&P 500” (black, dotted line) and “gold price” (gold, solid line) from January 2019 to December 2020. WHO’s declaration of COVID-19 as a global pandemic beginning on 2020-03-11 is highlighted as a shaded area (grey).



investor attention in general. Chapter 5 establishes a foundation to answering these questions in offering a throughout comparison between Google searches and Wikipedia page traffic as two prominent sources of such measures.<sup>5</sup> More particularly, the chapter draws upon Shannon transfer entropy, a measure derived from information theory, to detect and quantify both linear and nonlinear dependencies between time series (Dimpfl and Peter, 2013; Behrendt *et al.*, 2019). The empirical methodology employed in the chapter constitutes an improvement over more traditional approaches along two dimensions. First, Shannon transfer entropy provides a means to detect any statistical dependence, including nonlinear dependencies that would otherwise not be revealed by vector-autoregressive (VAR) approaches (Dimpfl and Peter, 2018; Behrendt and Schmidt, 2021). Second, the measure additionally shows the dominant direction of information transfer which constitutes an improvement over Granger (1969)'s causality test and its nonlinear extensions (e.g., Nishiyama *et al.*, 2011).

In summary, the first part of this introduction outlined some of the existing research on market linkages and investor behavior in times of turmoil and uncertainty. More particularly, the literature review introduced (i) recent equity market developments in response to COVID-19 to motivate the current relevance of the topic, (ii) theoretical and empirical research on the propagation of shocks across markets, (iii) corresponding research on flights to quality and safe haven phenomena as financial investors flee from negatively affected assets and, subsequently, (iv) research on new sources of information to measure collective investor attention towards individual assets with implications for their co-movement. Since some of the proceeding chapters related to the measuring of time-varying market linkages draw upon similar frameworks in their theory and empirical applications, the second part of this introduction provides some methodological remarks along this dimension. Thus, beyond a mere review of the related literature, the following section offers a first glance on an estimator for the time-varying correlation between (financial) variables, as well as a general framework for the modelling of time-variation in observation-driven models.

---

<sup>5</sup>For applications of Wikipedia page traffic as a measure of online investor attention in financial exercises please see, for instance, Weng *et al.* (2017), Hervé *et al.* (2019), and Behrendt *et al.* (2020).

## 1.2 Time-variation in parametric models

It is generally reasonable to assume many variables (and their relations) in finance and economics to be changing over time. Accordingly, allowing for time-variation in parametric models is important for appropriately capturing the dynamic behavior of the variables of concern in various different settings. This section is particularly interested in providing a preliminary introduction towards two of the related methodologies which are being drawn upon in the subsequent chapters of this dissertation.

First, the section introduces the estimator proposed in [Engle \(2002\)](#) for the modelling of time-varying conditional correlations. The latter measure the degree of linear dependence between two random variables or bi-variate data over time and, with reference to the previous section, are central to various common tasks in finance related to economic and financial integration, risk management and asset pricing, financial stability, or financial contagion. Second, taking a broader perspective, the section additionally introduces a general framework for the modelling of time-variation in observation-driven models.

### 1.2.1 Time-variation in market linkages: The case of dynamic conditional correlations

The methodological approaches to obtain reliable estimates of the time-varying correlations between financial variables are manifold and include, among others, rolling historical correlations (e.g., [Forbes and Rigobon, 2002](#)), exponential smoothing methods (e.g., [Zangari, 1996](#)), generalized autoregressive score (GAS) models (e.g., [Creal \*et al.\*, 2011](#); [Opschoor \*et al.\*, 2018](#)), multivariate stochastic volatility models (e.g., [Meyer and Yu, 2006](#); [Asai and McAleer, 2009](#)), and various types of multivariate generalized autoregressive conditional heteroscedasticity (MGARCH) models (e.g., [Bollerslev \*et al.\*, 1988](#); [Engle and Kroner, 1995](#); [Engle and Sheppard, 2001](#); [Engle, 2002](#); [Tse and Tsui, 2002](#); [Baur, 2006](#); [Cappiello \*et al.\*, 2006](#); [Aielli, 2013](#)).

This subsection is explicitly interested in a selection of MGARCH models to estimate the time-varying correlations between financial assets. More particularly, the subsection introduces [Engle \(2002\)](#)'s estimator for dynamic conditional correlations (DCC) as well as the subsequent extensions suggested in [Cappiello \*et al.\* \(2006\)](#). The preliminary introduction on DCC-type models is relevant to Chapter 4 and 6 of this dissertation. Whilst the former presents a novel empirical application to demonstrate the usefulness of Google search queries for the estimation of time-varying correlations, the latter takes a more general approach to advance the econometric methodology along several dimensions.

### Econometric methodology

Given an  $n$ -dimensional vector of asset returns  $r_t$  with mean zero, the conditional correlation between any two  $r_{i,t}$  and  $r_{j,t}$  with  $i = 1, \dots, n$  and  $j = 1, \dots, n$  is defined:

$$\rho_{ij,t} = \frac{E_{t-1}(r_{i,t}r_{j,t})}{\sqrt{E_{t-1}(r_{i,t}^2)}\sqrt{E_{t-1}(r_{j,t}^2)}}. \quad (1.1)$$

where the conditional correlation  $\rho_{ij,t}$  between  $r_{i,t}$  and  $r_{j,t}$  depends on all information available at time  $t$  and cannot exceed unity in absolute terms. To depict the relationship between conditional correlations and conditional covariances, denote  $r_{k,t}$ , as the conditional standard deviation  $\sigma_{k,t}$  times a Gaussian disturbance term  $\varepsilon_{k,t}$  with mean zero and unit variance:

$$\sigma_{k,t}^2 = E_{t-1}(r_{k,t}^2), \quad r_{k,t} = \sigma_{k,t}\varepsilon_{k,t}, \quad (1.2)$$

with  $k = 1, \dots, n$ . Substitution of this relation into Equation 1.1 provides a means to write the conditional correlation between any two  $r_{i,t}$  and  $r_{j,t}$  as the conditional covariance between standardized disturbances:

$$\begin{aligned} \rho_{ij,t} &= \frac{E_{t-1}(r_{i,t}r_{j,t})}{\sqrt{E_{t-1}(r_{i,t}^2)}\sqrt{E_{t-1}(r_{j,t}^2)}} \\ &= E_{t-1}(\varepsilon_{i,t}\varepsilon_{j,t}). \end{aligned} \quad (1.3)$$

Engle (2002) uses this relationship to formulate the DCC specification, which combines the flexibility of univariate GARCH models with a parsimonious parametric correlation model to obtain dynamic estimates of conditional correlations. The DCC(1,1) model can be written:

$$\begin{aligned} r_t | \mathfrak{F}_{t-1} &\sim \mathcal{N}(0, \Sigma_t), \quad \Sigma_t = D_t R_t D_t, \\ D_t^2 &= \text{diag}(\omega_i) + \text{diag}(\alpha_i) \circ r_{t-1} r_{t-1}' + \text{diag}(\beta_i) \circ D_{t-1}^2, \\ \varepsilon_t &= D_t^{-1} r_t, \\ Q_t &= (\bar{Q} - \psi_1 \bar{Q} - \psi_2 \bar{Q}) + \psi_1 \varepsilon_{t-1} \varepsilon_{t-1}' + \psi_2 Q_{t-1}, \\ R_t &= \text{diag}(Q_t)^{-1/2} Q_t \text{diag}(Q_t)^{-1/2}, \end{aligned} \quad (1.4)$$

where  $\circ$  is the Hadamard product,  $\mathfrak{F}_t$  is the information set at time  $t$ ,  $\Sigma_t$  is the covariance matrix, and  $D_t$  is a diagonal matrix comprising univariate volatility estimates of (standard) GARCH models based on unknown parameter vectors  $\omega$ ,  $\alpha$ , and  $\beta$ .<sup>6</sup> The correlation equation

<sup>6</sup>For simplicity, Equation 1.4 contains  $n$  standard GARCH(1,1) models which can be employed to estimate the respective volatility series. Note, however, that alternative volatility models can be considered.

consists of the auxiliary matrix  $Q_t$ , where  $\bar{Q}$  is the unconditional covariance matrix of  $\varepsilon_t \varepsilon_t'$ , and  $\psi_1$  and  $\psi_2$  are the unknown news impact- and smoothing parameter, respectively, to describe the evolution of correlation dynamics over time. For positive definite  $Q_t$ , a necessary and sufficient condition is  $\psi_1 + \psi_2 < 1$ . In turn,  $\text{diag}(Q_t)^{-1/2}$  is a matrix which guarantees  $R_t$  to contain estimates of the conditional correlation of form  $\rho_{ij,t} = q_{ij,t} / \sqrt{q_{ii,t} q_{jj,t}}$ , whereby  $q_{ij,t}$  refers to the  $ij$ -th element of  $Q_t$ , with ones on the main diagonal and every other element less or equal than one in absolute value.

Given the assumption of normality in Equation 1.4, Engle (2002) proposes to estimate the model parameters by the means of maximum likelihood estimation. The estimator still has a quasi-maximum likelihood interpretation if the assumption does not hold. The log-likelihood function of the estimator is represented in:

$$\mathcal{L} = -\frac{1}{2} \sum_{t=1}^T \left( n \log(2\pi) + \log |\Sigma_t| + r_t' \Sigma_t^{-1} r_t \right). \quad (1.5)$$

Coefficients of DCC-type models are commonly obtained in a two-stage maximum likelihood estimation procedure. In this concern, Engle (2002) shows that the log-likelihood function of the estimator can be written as the sum of a volatility part  $\ell_{v,t}$  and a correlation part  $\ell_{c,t}$ :

$$\mathcal{L} = \sum_{t=1}^T \ell_{v,t} + \ell_{c,t}. \quad (1.6)$$

More particularly, in Equation 1.6, the time  $t$  contribution to the volatility term is:

$$\ell_{v,t}(\theta_1) = -\frac{1}{2} \left( n \log(2\pi) + \log |D_t|^2 + r_t' D_t^{-2} r_t \right), \quad (1.7)$$

where  $\theta_1$  comprises the parameters used in the estimation of the univariate volatility series, whilst the time  $t$  contribution to the correlation part can be written:

$$\ell_{c,t}(\theta_1, \theta_2) = -\frac{1}{2} \left( \log |R| + \varepsilon_t' R^{-1} \varepsilon_t - \varepsilon_t' \varepsilon_t \right), \quad (1.8)$$

where  $\theta_2$  consists of the parameters used in the correlation equation. In the first stage of the two-stage estimation procedure, the objective is to find  $\hat{\theta}_1 = \arg \max \{ \sum_{t=1}^T \ell_{v,t}(\theta_1) \}$ . In the second stage,  $\hat{\theta}_1$  is taken as given and employed to find  $\hat{\theta}_2 = \arg \max \{ \sum_{t=1}^T \ell_{c,t}(\hat{\theta}_1, \theta_2) \}$ .

To demonstrate the performance of the DCC model in finding different correlation structures, consider a situation where the true correlation dynamics are known. In this regard, assume the data generating process to consist of two Gaussian standard GARCH models as

proposed in [Engle \(2002\)](#):

$$\begin{aligned} \begin{pmatrix} \varepsilon_{1,t} \\ \varepsilon_{2,t} \end{pmatrix} &\sim \mathcal{N} \left[ \begin{pmatrix} 0 \\ 0 \end{pmatrix}, \begin{pmatrix} 1 & \rho_t \\ \rho_t & 1 \end{pmatrix} \right], \quad r_t = D_t \varepsilon_t, \\ D_t^2 &= \begin{pmatrix} 0.01 & 0 \\ 0 & 0.5 \end{pmatrix} + \begin{pmatrix} 0.05 & 0 \\ 0 & 0.2 \end{pmatrix} \circ r_{t-1} r'_{t-1} + \begin{pmatrix} 0.94 & 0 \\ 0 & 0.5 \end{pmatrix} \circ D_{t-1}^2, \end{aligned} \quad (1.9)$$

with simulated correlations processes:

- Constant:  $\rho_t = 0.9$
- Sine:  $\rho_t = 0.5 + 0.4 \cos 2\pi t/200$
- Fast sine:  $\rho_t = 0.5 + 0.4 \cos 2\pi t/20$
- Step:  $\rho_t = 0.9 - 0.5 \cdot \mathbf{1}(t > 500)$
- Ramp:  $\rho_t = \text{mod } t/200$

In empirical applications, matters are complicated as neither periods of rapid or gradual changes in the correlation dynamics, nor periods of consistency, can usually be identified ex-ante. For this reason, the structure of the five simulated correlation processes includes periods with noticeably distinguishable behavior over their observations. For each of the proposed correlation processes, the bi-variate GARCH model in Equation 1.9 is simulated 200 times over 1000 observations. The length of the simulated observations is similar to approximately four years of daily financial data which is in line with the corresponding empirical applications presented in Chapter 4 and 6 of this dissertation.

Figure 1.4 shows the performance of the DCC estimator in finding the true correlation processes. More particularly, the figure plots the simulated true correlation processes (black lines), mean estimates obtained from the DCC model (yellow lines), and the corresponding 5% and 95% quantiles (red lines). In each instance, the DCC model is capable of replicating the true correlation process quite well. These findings are consistent with [Engle and Sheppard \(2001\)](#) and [Engle \(2002\)](#). More generally, the consistent estimation of correlation processes by the means of MGARCH models has also been studied extensively in the literature (for surveys, see [Bauwens et al., 2006](#); [Silvestrini and Veredas, 2008](#); [Engle, 2009](#); [Silvennoinen and Teräsvirta, 2009](#)).

Given the simple estimation procedure as well as the performance of the DCC model in identifying and estimating dynamic correlations between random variables, the estimator has received wide attention in the empirical financial literature over the last two decades. For instance, [Chiang et al. \(2007\)](#), [Dimitriou et al. \(2011\)](#), [Syllignakis and Kouretas \(2011\)](#),

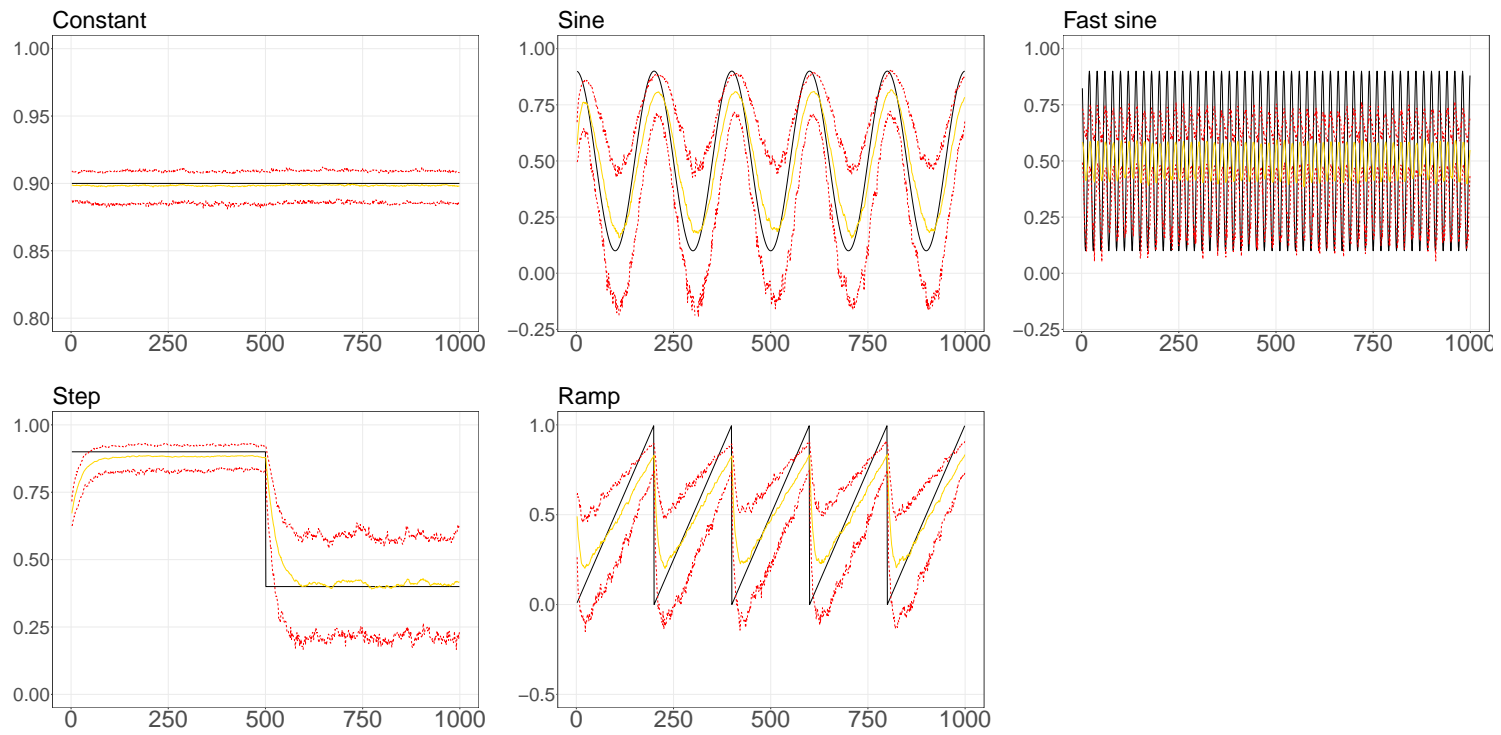


**Figure 1.4: Simulated true correlation processes (DCC model)**

This figure depicts five simulated true correlation processes (black lines), mean estimates (yellow lines), and 5% and 95% quantiles of the estimates (red lines). The figures are based on 200 simulations and 1000 observations.

and [Ahmad \*et al.\* \(2013, 2014\)](#) apply the DCC model to investigate the presence of financial contagion. More recently, similar endeavor is made in [Corbet \*et al.\* \(2020\)](#) and [Abuzayed \*et al.\* \(2021\)](#) in context of the COVID-19 pandemic. [Lahrech and Sylwester \(2011\)](#), [Sadorsky \(2014\)](#), and [Narayan \*et al.\* \(2014\)](#) use the estimator to study financial market integration, and [Asai and McAleer \(2009\)](#), [Arouri \*et al.\* \(2011, 2015\)](#), [Mensi \*et al.\* \(2015a,b\)](#), and [Chkili \(2016\)](#) consider DCC-type models to investigate portfolio risk management issues. Among others, theoretical advancements to the estimator have been suggested in [Cappiello \*et al.\* \(2006\)](#) who offer both an asymmetric and a generalized specification of the DCC model and in [Aielli \(2013\)](#) who proposes a correction for the consistent estimation of large covariance matrices. Taking the theoretical advancements provided in Chapter 6 into consideration, particular interest is devoted to the framework of [Cappiello \*et al.\* \(2006\)](#).

### Asymmetric and generalized correlation dynamics

[Cappiello \*et al.\* \(2006\)](#) extend the DCC model along two dimensions. Whilst both of the extensions can be formulated in a combined specification, the remaining chapters are solely concerned with the following extensions on an individual level.

First, the authors permit the presence of asymmetries in the modelling of conditional correlations by introducing the asymmetric DCC (ADCC) specification. Formally, the authors propose to modify the evolution of correlations suggested in Equation 1.4 as follows:

$$Q_t = \left( \bar{Q} - \psi_1 \bar{Q} - \psi_2 \bar{Q} \right) - \psi_3 \bar{N} + \psi_1 \varepsilon_{t-1} \varepsilon'_{t-1} + \psi_3 n_{t-1} n'_{t-1} + \psi_2 Q_{t-1}, \quad (1.10)$$

where  $n_t = \mathbf{1}\{\varepsilon_t < 0\} \circ \varepsilon_t$  with  $\mathbf{1}\{\cdot\}$  as the indicator function,  $\bar{N}$  is the unconditional covariance matrix of  $n_t n'_t$ , whilst  $\psi_3$  is an additional parameter to capture potential asymmetry effects in the data. A necessary and sufficient condition for positive definiteness of  $Q_t$  is  $\psi_1 + \psi_2 + \delta \psi_3 < 1$ , where  $\delta$  is the largest eigenvalue of  $\left[ \bar{Q}^{-1/2} \bar{N} \bar{Q}^{-1/2} \right]$  (see, e.g., [Ding and Engle, 2001](#); [Cappiello \*et al.\*, 2006](#)). Equation 1.10 demonstrates that the ADCC model nests the DCC specification as a special case for  $\psi_3 = 0$ .

Second, [Cappiello \*et al.\* \(2006\)](#) allow for asset-specific parameters to model the evolution of correlation dynamics over time. Whilst [Engle \(2002\)](#)'s DCC estimator assumes common news impact and smoothing parameters for all pairs of asset returns, this assumption may not be reasonable in the case of high-dimensional correlation matrices. Thus, the generalized DCC (GDCC) modification extends the DCC model by capturing potential heterogeneity across asset returns. Formally, the correlation evolution equation of the GDCC specification

can be written:

$$Q_t = (\bar{Q} - \Psi_1' \bar{Q} \Psi_1 - \Psi_2' \bar{Q} \Psi_2) + \Psi_1' \varepsilon_{t-1} \varepsilon_{t-1}' \Psi_1 + \Psi_2' Q_{t-1} \Psi_2, \quad (1.11)$$

where  $\Psi_1$  and  $\Psi_2$  are  $(n \times n)$  parameter matrices. Note, however, that the GDCC model comes at the cost of additional parameters and complexity. As such, the GDCC specification requires  $2n^2$  parameters to estimate the correlation dynamics between the returns of  $n$  assets, rendering practical applications of the extension largely limited. A more feasible approach is to assume  $\Psi_1$  and  $\Psi_2$  to be diagonal matrices instead. The GDCC specification then reduces to:

$$Q_t = \bar{Q} \circ (\iota \iota' - \psi_1 \psi_1' - \psi_2 \psi_2') + \psi_1 \psi_1' \circ \varepsilon_{t-1} \varepsilon_{t-1}' + \psi_2 \psi_2' \circ Q_{t-1}, \quad (1.12)$$

where  $\iota$  denotes a  $(n \times 1)$  vector of ones and  $\psi_1$  and  $\psi_2$  are  $(n \times 1)$  parameter vectors comprising the diagonal elements of  $\Psi_1$  and  $\Psi_2$ , respectively. The sufficient condition for  $Q_t$  to be positive definite for all  $t$  is that the intercept matrix is positive semi-definite and that  $Q_0$  is positive definite (Cappiello *et al.*, 2006).

### Correlation dynamics and news impact surfaces

Figure 1.5 displays daily conditional correlation estimates between US and German equity returns as well as the returns of gold to highlight the differences between Engle (2002)'s DCC model and Cappiello *et al.* (2006)'s asymmetric extension. The estimates for each pair of assets are received based on both the DCC model (solid lines) and the ADCC model (dotted lines) over the period from January 2019 to December 2020. The figure shows conditional correlation estimates between equity returns to generally fluctuate around 0.60 and to display large deviations over time. In contrast, the average conditional correlation between equity and gold returns is estimated to be close to zero, pointing towards gold's role as a hedge against stocks. Besides, the figure depicts a stronger reaction of estimates obtained from the ADCC model compared to the DCC model in response to the outbreak of COVID-19. This observation is hardly surprising, given that the additional parameter in the extended framework allows correlation estimates to increase stronger in response to joint negative shocks.

Alternatively, the difference between the DCC model and the ADCC model in how past shocks impact estimates of the conditional correlation can be depicted in news impact surfaces



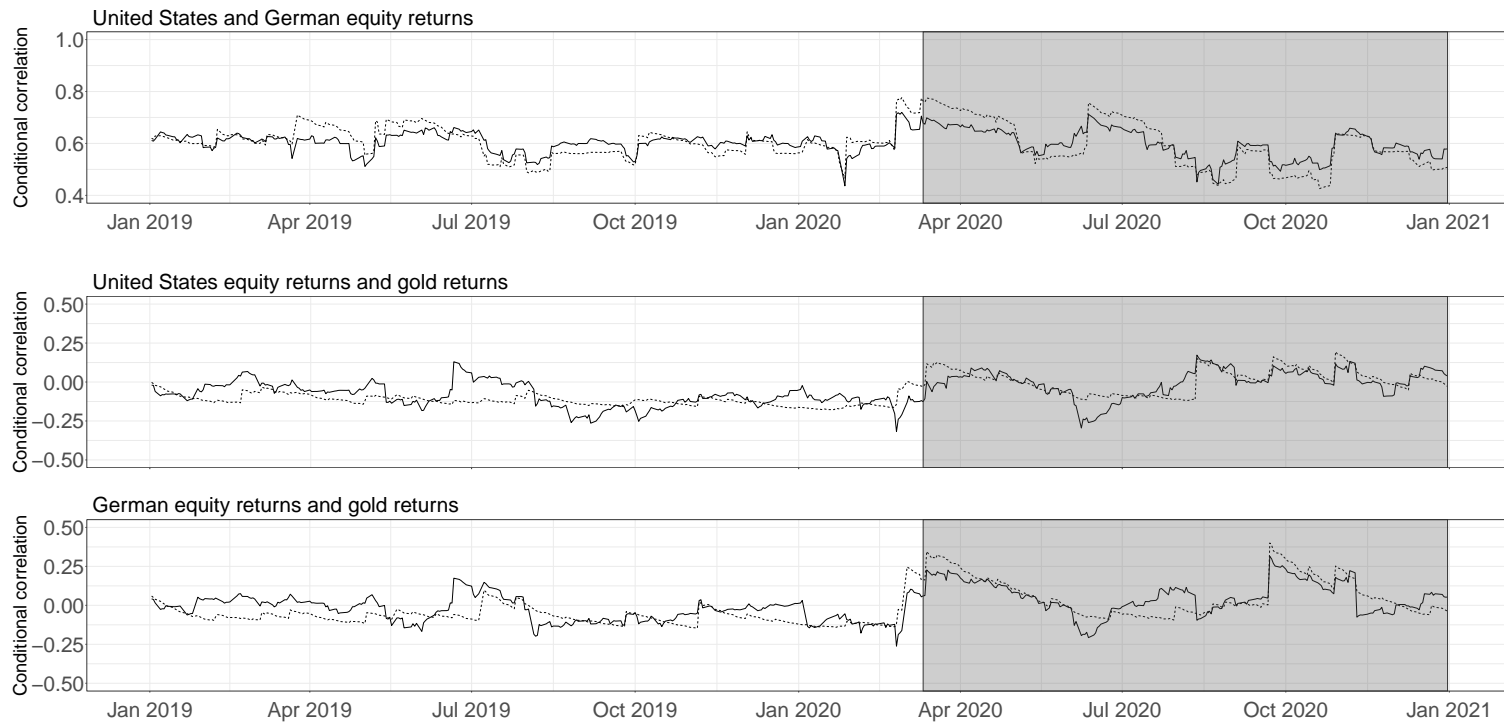


**Figure 1.5: Conditional correlation estimates over time**

This figure illustrates daily conditional correlation estimates between US and German equity returns as well as the returns of gold. The estimation period ranges from January 2019 to December 2020. Time-varying estimates between each pair of assets are obtained from the DCC model (solid lines) and the ADCC model (dotted lines), respectively. Besides, the shaded area (grey) beginning on 2020-03-11 indicates the time interval within that period during which the WHO declared COVID-19 a global pandemic.

for correlations in spirit of [Kroner and Ng \(1998\)](#). Formally:

$$\begin{aligned}
 f(\varepsilon_i, \varepsilon_j) &= \frac{c_{ij} + (\psi_1 + \psi_3)\varepsilon_i\varepsilon_j + \psi_2\bar{q}_{ij}}{\sqrt{[c_{ii} + (\psi_1 + \psi_3)\varepsilon_i^2 + \psi_2] \cdot [c_{jj} + (\psi_1 + \psi_3)\varepsilon_j^2 + \psi_2]}}, & \text{if } \varepsilon_i < 0 \text{ and } \varepsilon_j < 0, \\
 f(\varepsilon_i, \varepsilon_j) &= \frac{c_{ij} + \psi_1\varepsilon_i\varepsilon_j + \psi_2\bar{q}_{ij}}{\sqrt{[c_{ii} + \psi_1\varepsilon_i^2 + \psi_2] \cdot [c_{jj} + (\psi_1 + \psi_3)\varepsilon_j^2 + \psi_2]}}, & \text{if } \varepsilon_i \geq 0 \text{ and } \varepsilon_j < 0, \\
 f(\varepsilon_i, \varepsilon_j) &= \frac{c_{ij} + \psi_1\varepsilon_i\varepsilon_j + \psi_2\bar{q}_{ij}}{\sqrt{[c_{ii} + (\psi_1 + \psi_3)\varepsilon_i^2 + \psi_2] \cdot [c_{jj} + \psi_1\varepsilon_j^2 + \psi_2]}}, & \text{if } \varepsilon_i < 0 \text{ and } \varepsilon_j \geq 0, \\
 f(\varepsilon_i, \varepsilon_j) &= \frac{c_{ij} + \psi_1\varepsilon_i\varepsilon_j + \psi_2\bar{q}_{ij}}{\sqrt{[c_{ii} + \psi_1\varepsilon_i^2 + \psi_2] \cdot [c_{jj} + \psi_1\varepsilon_j^2 + \psi_2]}}, & \text{if } \varepsilon_i \geq 0 \text{ and } \varepsilon_j \geq 0, \quad (1.13)
 \end{aligned}$$

where  $c_{ij}$  denotes the  $ij$ -th element of the intercept matrix in the correlation equation,  $\bar{q}_{ij}$  is the corresponding element of the unconditional correlation matrix  $\bar{Q}$ , and  $\psi_3 = 0$  when considering the standard DCC model. Accordingly, [Figure 1.6](#) plots news impact surfaces for correlations between US and German equity returns based on the DCC model (left surface plot) and its asymmetric extension (right surface plot).<sup>7</sup> Whilst news impact surfaces of both models increase both towards the  $-/-$  and the  $+/+$  quadrant, the increase towards the  $-/-$  quadrant is, comparatively, much steeper in the case of the ADCC framework. The figure thus shows clear asymmetry that can be captured by the extended model, i.e., joint negative shocks have a stronger impact on correlation dynamics than joint positive shocks.

In summary, DCC-type models provide a framework to model the time-varying correlations between (financial) variables. Depending on the particular specification employed in empirical applications, different features of the data can be taken into account. Whilst the estimation procedure of DCC-type models greatly benefits from their parsimony, the static structure of either specification also imposes severe restrictions on the modelling of underlying correlation dynamics. By construction, the static model parameters cannot adapt or change in response to situations where shocks to the dynamics are severe. Given that the empirical setting of DCC-type models often revolves around times witnessing financial crises or events provoking changes of comparable scope, the assumption of a single static parameter to capture the impact of news on correlation dynamics can thus be fairly unreasonable.

[Chapter 6](#) fills this gap in the existing literature in considering an adaptive weighting of the outer product of standardized disturbances in the estimation of conditional correlations over time.

---

<sup>7</sup>Plots of news impact surfaces are limited to the case of the conditional correlations between equity returns. Even though further illustrations and discussions for the case of the conditional correlations between equity returns and the returns of gold would be interesting in their own right, this introduction solely serves the purpose to highlight the difference between the DCC and the ADCC framework.

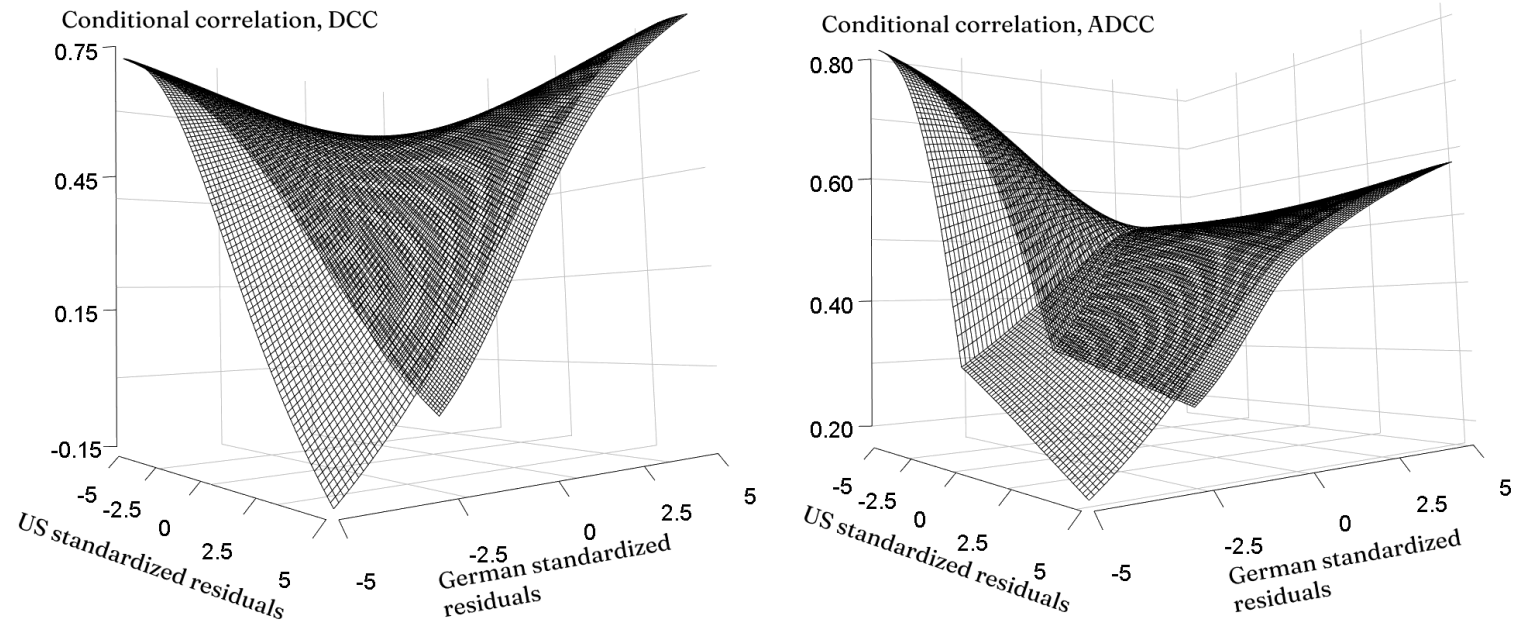


**Figure 1.6: News impact surfaces for correlations**

This figure plots news impact surfaces between US and German equity returns. The data used in this figure spans the period from January 2019 to December 2020. The left surface is based on estimates received from the DCC model. The right surface builds on the ADCC model and shows clear asymmetry in the  $-/-$  quadrant.

Beyond, it is shown that allowing for time-variation in the asymmetry parameter of [Cappiello \*et al.\* \(2006\)](#) yields important insights into the changing relevance of asymmetry effects in global equity markets. Importantly, to introduce time-variation to a selection of parameters in DCC-type models, the chapter relies on the GAS model which provides a general framework for modelling time-variation in parametric models.

Finally, given that the GAS model is essential for Chapter 6 as well as the empirical application provided in Chapter 2 of this dissertation, the following subsection establishes a preliminary understanding of the framework. More particularly, it reviews some of the existing literature on time-variation in parametric models and narrows the discussion to preparatory, methodological remarks on the GAS framework.

### 1.2.2 Time-variation in parametric models: The case of the generalized autoregressive score framework

Consider the DCC model as one tool within a large building kit of observation-driven models. The purpose of this tool in particular is to obtain reliable estimates of the time-varying correlations between random variables. More broadly, the kit comprises a wide range of similar tools, each of which provides a means to introduce time-variation to a selection of model parameters in a specific econometric setting. Alternatively, the econometrician, or craftsman in this case, can also use a second building kit containing different tools to achieve her objectives.<sup>8</sup> To comprehensively review some of the relevant literature, the existing research on dynamic parameters in time series model building can be categorized into classes of parameter-driven and observation-driven models ([Cox, 1981](#)).

#### Parameter-driven and observation-driven models

Parameter-driven models, such as the nonlinear non-Gaussian state space models formulated in both [Durbin and Koopman \(1997\)](#) and [Shepard and Pitt \(1997\)](#), stochastic volatility models provoked in [Tauchen and Pitts \(1983\)](#) and reviewed in [Shephard \(2005\)](#), and dynamic stochastic copula models in spirit of [Hafner and Manner \(2012\)](#), consider parameters to be random processes with own idiosyncratic innovations. This also reflects the appeal of parameter-driven models as, irrespective of the conditional observation density, any parameter can simply be defined as a random process with its own idiosyncratic innovations. However, the caveat of many of the parameter-driven models is that analytical expressions for the corresponding likelihood functions are not available in closed-form. In consequence, their estimation usually demands computationally intense techniques such as Markov Chain Monte Carlo or sequential Monte Carlo methods (see, e.g., [Shepard and Pitt, 1997](#);

---

<sup>8</sup>The “craftsman” is the econometrician, the two “building kits” are the two classes of parameter-driven and observation-driven models, respectively, and the “tools” refer to the specific models such as GARCH, DCC, ...

Manrique, 1998; Varin and Vidoni, 2008).<sup>9</sup>

In contrast, time-variation in observation-driven models is instead introduced by defining parameters as deterministic functions of lagged dependent variables as well as contemporaneous and lagged exogenous variables. Whilst the dynamic parameters in observation-driven models are also considered random processes, they are perfectly predictable based on the available information. Through standard prediction error decomposition, the likelihood functions of observation-driven models are known in closed-form which simplifies their evaluation procedure and has contributed to their wide popularity in theoretical and applied econometrics. Prominent examples of observation-driven models in the literature are, among others, Bollerslev (1986)'s GARCH model, Engle and Russell (1998)'s autoregressive conditional duration (ACD) model for irregularly spaced transaction data, Engle (2002)'s DCC model, Engle and Manganelli (2004)'s conditional autoregressive value at risk model, and Patton (2006)'s dynamic copula model. However, despite their wide popularity in time series model building, observation-driven models have long been short of a generalized framework. For each conditional observation density and model, new functions of the data had to be constructed to update a selection of parameters over time. Given that in some empirical frameworks the choice of such functions may not necessarily be evident, the latter has posed a common problem in the building of observation-driven models (e.g., Koopman *et al.*, 2016).

To this end, Creal *et al.* (2011, 2013) and Harvey (2013) have developed a new framework for observation-driven models which is based on the score of the predictive likelihood function. The merit of their GAS framework lies in its generality, as the model can be based on any observation density and uses the complete density structure in the updating of parameters over time.

### Econometric methodology

Following the approach outlined in Creal *et al.* (2011, 2013) and Harvey (2013), consider  $y_t$  a  $(n \times 1)$  dependent variable vector of interest,  $f_t$  a time-varying parameter vector, and  $x_t$  a vector of exogenous variables. Let  $Y^t = \{y_1, \dots, y_t\}$ ,  $F^t = \{f_0, f_1, \dots, f_t\}$ , and  $X^t = \{x_1, \dots, x_t\}$ . The available information set at time  $t$  is then given by:

$$\mathfrak{F}_t = \{Y^{t-1}, F^{t-1}, X^t\}, \quad (1.14)$$

with  $t = 1, \dots, T$ . Assume, that  $y_t$  is generated by the observation density:

$$y_t \sim p(y_t | f_t, \mathfrak{F}_t; \theta), \quad (1.15)$$

---

<sup>9</sup>For recent developments on Monte Carlo methods in the setting of nonlinear non-Gaussian state space models, see Jungbacker and Koopman (2007), Richard and Zhang (2007), and Koopman *et al.* (2015).

where  $\theta$  is a static parameter vector. The GAS(1,1) framework proposes the recursion for updating  $f_t$  over time to be given by the autoregressive updating equation:

$$f_{t+1} = \omega + A s_t + B f_t, \quad (1.16)$$

where  $\omega = \omega(\theta)$  is a parameter vector and both  $A = A(\theta)$  and  $B = B(\theta)$  are parameter matrices with appropriate dimensions, respectively. Further,  $s_t = S_t \nabla_t$ , where  $S_t = S(t, f_t, \mathfrak{F}_t; \theta)$  is a matrix function to provide a means for local scaling of the score. The latter is defined:

$$\nabla_t = \frac{\partial \log p(y_t | f_t, \mathfrak{F}_t; \theta)}{\partial f_t}. \quad (1.17)$$

In the GAS(1,1) framework formulated in Equations 1.14–1.17, the (scaled) score is used to link information received from the shape of the conditional observation density directly towards the updating of the time-varying parameter vector  $f_t$ . More particularly, the framework uses the direction of steepest ascent to enhance the fit of models based on the conditional observation density given the current location of  $f_t$ . Besides, the choice of the scaling matrix  $S_t$  provides further flexibility in how the score impacts the updating of  $f_t$  over time.<sup>10</sup>

---

<sup>10</sup>See Creal *et al.* (2013) for further insights on alternative choices for scaling matrices. For instance, if  $S_t$  is the inverted Fisher information matrix, the framework comprises Bollerslev (1986)'s GARCH model as well as the ACD model of Engle and Russell (1998). If  $S_t$  is an identity matrix, it encompasses the generalized autoregressive moving average model and the autoregressive conditional multinomial model of Benjamin *et al.* (2003) and Engle and Russel (2005), respectively.

## 1.3 Original research conducted in this dissertation

Building on the review of the relevant literature as well as the preliminary methodological remarks raised in the introduction, Chapters 2–6 are concerned with the original research conducted in this dissertation. These five chapters constitute the main part of the dissertation. Importantly, whilst each of the chapters is partially embedded into the preceding literature review, they all comprise self-contained research papers that can be considered and read independently from one another.

The overarching theme of the following chapters is an investigation on market linkages and investor behavior in times of turmoil and uncertainty. More particularly, Chapter 2 provides insights into the time-varying linkages between regional and global equity markets. Turning towards a selection of periods that are characterized by increases in the co-movement in response to shocks, the chapter further investigates the presence of global and regional contagion over the last two decades. Shifting the focus away from the linkages between equity markets, Chapter 3 is concerned with the linkages of gold mining company shares both with the equity market and with the price of gold. In more detail, the chapter uses this double exposure to deepen the understanding of investor behavior by unraveling different flights to quality based on the severity of shocks. On a similar note, Chapter 4 studies the linkages between equity, commodity, and energy markets. Along this line, Google search queries, a novel measure of online investor attention, are employed in the estimation of the time-varying correlations between asset returns. Chapter 5 adds to this research in demonstrating that alternative measures of online investor attention do not necessarily constitute equivalent proxies for the latent variable. Last, Chapter 6 offers a methodological contribution to the measuring of linkages between financial variables in the form of time-varying conditional correlations. More precisely:

- Chapter 2: **Measuring 25 years of global equity market co-movement using a time-varying spatial model**<sup>11</sup>

This study investigates linkages between global, European, American, and Asian-Pacific equity markets over various periods of turmoil and uncertainty during the last 25 years. In the empirical analysis, the investigation draws upon a dynamic version of the SAR model to reveal time-variation in the spatial dependence among global and local equity markets. The results of this study are twofold: First, the paper finds an increase in the co-movements between equity markets over time, particularly among European countries, while generally showing large fluctuations. This finding is in support of an increasing degree of equity market integration over the last two decades. Second, when considering increasing variances during events of financial turmoil and uncertainty, the results suggest that contagion on a global level, as measured by significant increases in the co-movement, has only occurred in response to the outbreak of COVID-19 in early 2020.

---

<sup>11</sup>This paper is currently under review in the *Journal of International Money and Finance*.

- Chapter 3: **Flight to quality – Gold mining shares versus gold bullion**<sup>12</sup>

This research paper employs a large sample of gold mining companies listed on four stock markets to investigate potential differences in the types of flight to quality. Motivated by the double exposure of gold mining shares to the equity market and to the price of gold, the empirical analysis finds the relative performance of gold mining shares to depend on the severity of financial shocks. After strong financial shocks, investors flee from stocks including gold mining shares towards gold bullion. In contrast, if shocks are less severe, investors only flee from stocks excluding gold mining shares. This study of gold mining companies offers important information in the context of flight to quality and safe haven effects.

- Chapter 4: **Does online investor attention drive the co-movement of stock-, commodity-, and energy markets? Insights from Google searches**<sup>13</sup>

This paper investigates whether measures for online investor attention provide valuable information for the assessment of linkages between financial markets. More particularly, the empirical analysis employs Google search queries for stocks as well as gold, silver, crude oil, and natural gas future contracts to enrich the estimation of time-varying correlations between corresponding assets. Relying on an extensive data set over six years in daily frequency, the results suggest the following: First, online investor attention towards stock, commodity, and energy markets drives the time-varying correlations between asset returns. In more detail, increases (decreases) of Google search queries for assets lead to increasing (decreasing) asset co-movements in response. This pattern reverses when market shocks are severe, implying smaller increases or even decreases of asset co-movements. Second, financial investors can improve the optimal allocation of their investments by the means of Google search queries. Taking a practical point of view, the study demonstrates that market participants can only marginally increase the hedging effectiveness of combined portfolios by considering Google searches for their investment strategies.

- Chapter 5: **What are you searching for? On the equivalence of proxies for online investor attention**<sup>14</sup>

This study investigates whether different online search queries, measured by Google searches for individual stock tickers and company-specific Wikipedia page views, constitute equivalent proxies for latent investor attention. The empirical application draws upon Shannon transfer entropy, a model-free measure to consider any kind of statistical dependence between time

---

<sup>12</sup>This paper is published originally as Baur, D., Prange, P., Schweikert, K. (2021) Flight to quality – Gold mining shares versus gold bullion, *Journal of International Financial Markets, Institutions & Money*, **71**, 101296.

<sup>13</sup>This paper is published originally as Prange, P. (2021) Does online investor attention drive the co-movement of stock-, commodity-, and energy markets? Insights from Google searches, *Energy Economics*, **99**, 105282.

<sup>14</sup>This paper is published originally as Behrendt, S., Prange, P. (2021) What are you searching for? On the equivalence of proxies for online investor attention, *Finance Research Letters*, **38**, 101401.



series, to test for and quantify the information transfer between Google searches and Wikipedia page views for 27 constituents of the Dow Jones Industrial Average (DJIA) for all trading days between January 2008 and December 2017. The methodological approach additionally allows to infer the dominant direction of information transfer which provides an improvement over more usual (non)linear Granger causality tests. The results suggest that Google searches and Wikipedia page views cannot be considered equivalent proxies for online investor attention. In particular, the study finds significant bi-directional information transfer between the different online search series across the stocks in the sample. Thus, while the employment of any of these measures may be reasonable in financial applications, both researchers and practitioners should be aware that Google searches and Wikipedia page views do not measure the same latent online investor attention for all stocks. Besides, a large part of the information transfer is found to be nonlinear, rendering linear Granger causality tests less useful for the comparison of such measures.

- **Chapter 6: News impact dynamics in the correlations of global equity returns for systemic risk measurement**<sup>15</sup>

This paper proposes a score-driven extension to the well-known DCC model. The extended model provides a means to capture the time-varying influence of news on correlation dynamics. The recursion to update the news impact parameter over time is based on the observations of past periods. The model increases the flexibility of DCC-type models whilst maintaining their appealing characteristics for applications with large cross-sections. It is demonstrated that the model performs well in a variety of different situations and shown that the incorporation of the time-varying “severity” of news enriches the assessment of correlation dynamics for a global cross-section of equity markets. In particular, this study reveals that the time-varying parameter can quantify significant increases in equity return linkages in response to plunging markets amid the outbreak of COVID-19 in early 2020 and subsequent economic recoveries.

Chapter 7 comprises a summary of the main findings of the original research conducted in this dissertation. Besides, the chapter critically reflects on Chapters 2–6 and concludes.

---

<sup>15</sup>This paper is currently submitted to the *Journal of Financial Econometrics*.

# Chapter 2

## Measuring 25 years of global equity market co-movement using a time-varying spatial model

### 2.1 Introduction

Shortly after the first cases of unknown pneumonia were detected in the city of Wuhan, China, the pandemic induced by the COVID-19 virus was declared a public health crisis of international concern. The impact on financial markets was unprecedented, causing high volatility and simultaneous downturns across equity markets around the world. Increased co-movement of equity markets during crisis periods has been witnessed in previous crisis periods and is the subject of academic studies dealing with economic and financial integration, portfolio management strategies, financial market stability or financial contagion. In this paper, we choose a data driven approach to empirically examine the co-movement in equity markets during the last 25 years. We use a dynamic spatial autoregressive model, which allows us to estimate the co-movement of equity markets on a weekly basis. Rather than modelling bi-variate correlations between pairs of countries, we seek to derive insights into the dependence of equity markets on a broader scale, such as American-, European-, and Asian-Pacific markets as well as on the global level. In doing so, we deliver a general picture on the level of equity market co-movement, as well as on its behavior during different crisis periods, such as the GFC or the COVID-19 pandemic.

Our paper touches several strands of literature. The most prominently one deals with financial contagion. [Forbes and Rigobon \(2002\)](#) define contagion as an increase in the correlation between two or more markets after a crisis event. The subject of defining, measuring and testing for contagion has stirred numerous prominent contributions, including [Bekaert \*et al.\* \(2009\)](#), [Bekaert \*et al.\* \(2014\)](#), [Bae \*et al.\* \(2003\)](#), [Longin and Solnik \(2001\)](#). For a comprehensive survey we refer to [Forbes \(2012\)](#).

Co-movement or interdependence between stock markets also plays a crucial role in risk

management and asset pricing. International diversification is based on the idea that lower levels of economic and financial integration imply low correlation between financial market returns. Recent decades, however, witnessed increased co-movement, higher equity market betas and correlations, which questions international diversification benefits (e.g., [Christoffersen \*et al.\*, 2014](#); [Baele and Soriano, 2010](#)). A recent contribution by [Raddant and Kenett \(2021\)](#) emphasizes the increased interconnectedness of global financial markets and the time-variation thereof. [Virk and Javed \(2017\)](#) analyze the integration patterns of seven leading European stock markets from 1990 to 2013 and find surging co-movement in the post-Euro period and a tendency to increase during bearish economic conditions.

The methodological approaches towards measuring co-movement and contagion are manifold, including linear correlations (e.g., [Forbes and Rigobon, 2002](#)), factor-models (e.g., [Bekaert \*et al.\*, 2009, 2014](#)), model-free or co-exceedance approaches (e.g., [Bae \*et al.\*, 2003](#); [Londono, 2019](#)), VAR models (e.g., [Boubaker \*et al.\*, 2016](#)), DCC models (e.g., [Engle, 2002](#)), and copula approaches (e.g., [Rodriguez, 2007](#); [Kenourgios \*et al.\*, 2011](#)). This paper uses a different approach. We model the global dependencies in international equity markets using spatial techniques. Spatial models are at the core of many recent studies in applied and theoretical econometric research (see, for instance, [Kelejian and Prucha, 2010](#); [Qu and Lee, 2015](#)). These approaches have an extensive history in geography literature and, since the publication of the seminal works of [Krugman \(1991, 1992\)](#), have gained attention in economics as well. Applications to financial markets include [Fernandez \(2011\)](#), who tests spatial linkages arising between financial markets in Latin-America by relying on a spatial capital asset pricing model. [Asgharian \*et al.\* \(2013\)](#) apply a static spatial model to analyze the extent to which geographic and economic relations between countries affect the co-movements among stock markets. The equity market is also studied by [Arnold \*et al.\* \(2013\)](#), who apply a spatial model within a risk management context. Recently, [Blasques \*et al.\* \(2016b\)](#) proposed an approach to model time-varying (spatial) dependence based on a GAS framework. GAS models are observation driven models, which have been introduced by [Creal \*et al.\* \(2011, 2013\)](#) and [Harvey \(2013\)](#) and are becoming increasingly popular. Their merit lies in providing a general framework for time-variation in parametric models, while offering straightforward estimation and inference, which renders them a suitable methodology for our analysis. It might also offer an interesting alternative to dynamic factor models as proposed for instance by [Jungbacker and Koopman \(2014\)](#) or [Bräuning and Koopman \(2014\)](#). However, while the aforementioned models can be used for forecasting purposes as well, our approach is solely driven by the idea of measurement, while its merit lies in its ability to express contemporaneous dependence within one time-varying parameter.

We complement the literature on equity market interdependence by analyzing global time-varying co-movement among financial markets over multiple periods of market turmoil between 1995 and 2020 using a dynamic spatial model. We examine global co-movement based on 38 stock market indices as well as subsets representative of the American-, European-, and Asian-Pacific markets. Our contributions are (i) to provide a global view by studying a large panel of stock

indices over a long period of time including various events of market turmoil and uncertainty, (ii) applying a novel model, namely a time-varying spatial dependence model recently introduced by Blasques *et al.* (2016b), which allows us to analyze the evolution of co-movements among stock markets over time, and (iii) assessing the question of whether global contagion has occurred during the major crises of the last 25 years. Implementing the time-varying spatial dependence model augmented by dynamic variances, we also account for increased volatility arising during periods of market turmoil and calculate confidence bounds for the co-movement parameters based on Blasques *et al.* (2016a).

Our results reveal a general increase in co-movement during the last 25 years which is most pronounced for European countries. Our approach shows that co-movement is also time-variant during periods of market turmoil, often exhibiting several peaks within a specific period. Allowing for temporal variances within our spatial model, we also confirm the findings by Forbes and Rigobon (2002) in that we observe a widening of confidence bounds during events or crisis periods, indicating an increase in variances. Such heteroscedasticity might bias contagion tests if not taken into account. When testing for contagion, we find evidence for global contagion during the COVID-19 pandemic while, for most of the remaining events, we conclude that it is interdependence rather than contagion that is observed.

The remainder of this paper is structured as follows. Section 2.2 presents the methodology, data and a preliminary analysis. Section 2.3 provides and discusses the results, while Section 2.4 presents the overarching conclusions.

## 2.2 Spatial modelling of stock market co-movements

### 2.2.1 Modelling time-varying spatial dependence

Spatial models offer an interesting alternative to common approaches when measuring interdependence, because they deliver a measure of co-movement that goes beyond pairwise correlations. Thereby, they are able to account for the complex dependence structure underlying global equity markets. Our analysis is based on the work of Blasques *et al.* (2016b), who introduces a dynamic spatial model based on the GAS framework offered in Creal *et al.* (2011, 2013) and Harvey (2013). We consider the SAR model in further detail to analyze spatial interactions arising across units (Cliff and Ord, 1973, 1981; Ord, 1975). Since our main interest lies within the empirical measurement of global (or regional) co-movement among equity markets rather than potential determinants, we do not include exogenous variables in our approach.

The SAR model provides a means by which to comprise the impact of the spatial lag of a cross-section on the corresponding units within that cross-section of a single scalar parameter. Denote the SAR model in period  $t = 1, \dots, T$  as:

$$y_t = \beta\iota + \rho W_t y_t + \varepsilon_t, \quad \varepsilon_t \sim p_\varepsilon(\varepsilon_t; \Sigma, \lambda), \quad (2.1)$$

where  $y_t$  is a  $(n \times 1)$  vector of cross-sectional observations,  $\beta$  is an unknown scalar parameter,  $\iota$  is a  $(n \times 1)$  vector of ones,  $\rho$  is the endogenous spatial dependence parameter,  $W_t$  is a time-varying  $(n \times n)$  spatial weights matrix, and  $\varepsilon_t$  is a  $(n \times 1)$  vector of disturbances with mean zero, covariance matrix  $\Sigma$ , and multivariate density  $p_\varepsilon(\varepsilon_t; \Sigma, \lambda)$  including  $\lambda$  to further specify the distribution of the disturbances.

The vector  $W_t y_t$  is commonly referred to as the spatial lag of the dependent variable  $y_t$ , where the weighting matrix  $W_t$  entails information on the spatial distances across units. Restricting the estimation space of the spatial dependence parameter such that  $-1/w_{t,\min}^+ < \rho < 1$ , where  $w_{t,\min}^+$  is the absolute value of the smallest eigenvalue of  $W_t$ , imposes positive definiteness on the covariance matrix (e.g., Lee, 2004; Lesage and Pace, 2009).

In Equation 2.1, the impact of the weighted dependent variable  $W_t y_t$  on  $y_t$  is captured by the static parameter  $\rho$ . The dynamic version of the SAR model based on the observation-driven GAS framework endows both the spatial dependence parameter and the covariance matrix with time-varying dynamics (Blasques *et al.*, 2016b):

$$y_t = \beta \iota + \rho_t W_t y_t + \varepsilon_t, \quad \varepsilon_t \sim p_\varepsilon(\varepsilon_t; \Sigma(f_t^\sigma), \lambda), \quad (2.2)$$

where  $\rho_t = h(f_t)$ . Thus, the time-varying spatial dependence between units is obtained as a strictly monotonic transformation of the dynamic parameter  $f_t$ . In line with Blasques *et al.* (2016b) and the conditions for positive-definite variance covariance matrices provoked in Lesage and Pace (2009), we use  $h(f_t) = \tanh(f_t)$  as a reasonable choice for the transformation to constrain  $\rho_t \in (-1, 1)$ . Further, the covariance matrix is given by  $\Sigma(f_t^\sigma) = \text{diag}(\sigma_1^2(f_{1t}^\sigma), \dots, \sigma_n^2(f_{nt}^\sigma))$  with  $\sigma_i^2(f_{it}^\sigma) = \exp(f_{it}^\sigma)$  for  $i = 1, \dots, n$ .

The GAS framework is employed to model the evolution of  $f_t$  and  $f_t^\sigma$  over time (Creal *et al.*, 2011, 2013; Harvey, 2013). More precisely, we assume that the autoregressive updating function of  $f_t$  follows a GAS(1,1)-type process:

$$f_{t+1} = \omega + A S_t \nabla_t + B f_t, \quad (2.3)$$

where  $\omega$ ,  $A$ , and  $B$  are scalar parameters,  $S_t$  is a scale matrix, and  $\nabla_t$  is the score function to link the direction of the steepest ascent of the observation density at time  $t$  to  $f_t$ . Similarly, the updating function of  $f_t^\sigma$  is assumed to follow an  $n$ -dimensional GAS(1,1)-type process:

$$f_{t+1}^\sigma = \omega^\sigma + A^\sigma S^\sigma \nabla_t^\sigma + B^\sigma f_t^\sigma, \quad (2.4)$$

where  $\omega^\sigma$  is a  $(n \times 1)$  vector containing unit-specific intercepts,  $A^\sigma$  and  $B^\sigma$  are scalar parameters,  $S^\sigma$  is a scale matrix, and  $\nabla_t^\sigma$  is the  $(n \times 1)$  score vector. Whilst intercepts are employed individually for each unit, joint  $A^\sigma$  and  $B^\sigma$  ensure parsimony of the adaptive model. In both Equations 2.3 and 2.4, we consider  $S_t$  and  $S^\sigma$  to be identity matrices. The (scaled) scores can then be denoted as the

partial derivative of the log-likelihood function at time  $t$  with regard to  $f_t$  and  $f_t^\sigma$ , respectively:

$$\nabla_t = \frac{\partial \ell_t}{\partial \rho_t} \cdot \frac{\partial \rho_t}{\partial f_t}, \quad \nabla_t^\sigma = \frac{\partial \ell_t}{\partial f_t^\sigma}, \quad (2.5)$$

where  $\partial \rho_t / \partial f_t = 1 - \tanh(f_t)^2$ . Lastly,  $\ell_t$  is given by:

$$\ell_t = \ln p_\varepsilon(\varepsilon_t; \Sigma(f_t^\sigma), \lambda) + \ln |(I - \rho_t W_t)|. \quad (2.6)$$

Considering the distribution of the disturbance vector  $\varepsilon_t$ , we assume a multivariate t-distribution with  $\lambda$  degrees of freedom, where  $\lambda$  is estimated along with the other model parameters. This distributional choice seems appropriate, since the stock return series in our application exhibits excess kurtosis (Harvey and Luati, 2014). We estimate the unknown parameter vector  $\theta = (\beta, \omega, A, B, \omega^\sigma, A^\sigma, B^\sigma; \lambda)$  using maximum likelihood estimation. While there exist robust generalized method of moments estimators for spatial autoregressive models (compare Arnold *et al.* (2013) and Wied (2013)), which also allow for inference concerning time-varying parameters, maximum likelihood has been the favorite estimation approach for score-driven models (see, for instance, Blasques *et al.* (2016b) and Gasperoni *et al.* (2022)). In a recent publication, Blasques *et al.* (2022) show strong consistency and normality of the maximum likelihood estimator for score-driven models.<sup>16</sup>

## 2.2.2 Data and descriptives

We use weekly prices of 38 stock market indices similar to Asgharian *et al.* (2013) over the sample period from January 1995 to July 2020, leaving us with 1333 observations per time series.<sup>17</sup> Price data are sourced from Refinitiv Eikon. Continuously compounded returns are calculated as the log-price changes occurring between consecutive trading weeks. Weekly rather than daily data is chosen in order to avoid or at least reduce the effect of time zone differences and differences in trading hours. Results based on daily data, however, are available upon request and lead to qualitatively similar results.

Table 2.1 offers descriptive statistics for all data used in the empirical analysis. As indicated by the high levels of kurtosis, most time series significantly depart from normality. To set up

---

<sup>16</sup>Blasques *et al.* (2016b) further offer simulation evidence that the spatial autoregressive score model is able to track the patterns of its time-varying parameters. However, their simulation study does not include time-varying variances. We conducted such a simulation study and confirm the validity of the model estimation also for this case. The results are available upon request from the authors.

<sup>17</sup>In more detail, we consider the leading market indices of 6 American countries (namely Argentina, Brazil, Canada, Chile, Mexico, and the US), 20 European countries (Austria, Belgium, Switzerland, Czech Republic, Germany, Denmark, Spain, Finland, France, UK, Greece, Hungary, Ireland, Israel, Netherlands, Norway, Poland, Portugal, Sweden, and Turkey), and 12 Asian-Pacific countries (Australia, China, Hong Kong, Indonesia, India, Japan, Korea, Malaysia, Philippines, Singapore, Thailand, and Taiwan) in our empirical analysis. In both the figures and the tables, we refer to those countries using ISO 3166-1 alpha-3 country codes to conserve space.

**Table 2.1: Descriptive statistics**

This table summarizes the data used in the empirical analysis. The data set covers the period from January 1995 to July 2020. The table offers descriptive statistics of the (log-) return series ( $r$ ) for each equity index. In more detail, we report sample mean, median, standard deviation, minimum, maximum, skewness, kurtosis, and lag-1 autocorrelation of the time series.

	Mean	Median	St. Dev.	Min.	Max.	Skewness	Kurtosis	Autocorr.
$r_{ARG}$	0.0034	0.0061	0.0513	-0.3776	0.2377	-0.6321	4.8779	0.0285
$r_{AUS}$	0.0009	0.0026	0.0206	-0.1702	0.0911	-1.1602	7.1580	0.0012
$r_{AUT}$	0.0006	0.0026	0.0316	-0.3413	0.1723	-1.8169	16.5005	0.0237
$r_{BEL}$	0.0007	0.0033	0.0279	-0.2611	0.1291	-1.4656	11.3342	-0.0287
$r_{BRA}$	0.0023	0.0049	0.0431	-0.2506	0.2176	-0.5845	3.9127	-0.0421
$r_{CAN}$	0.0010	0.0031	0.0235	-0.1754	0.1282	-1.2136	8.8497	-0.0500
$r_{CHE}$	0.0010	0.0032	0.0260	-0.2520	0.1629	-1.1792	12.1547	-0.0984
$r_{CHL}$	0.0010	0.0014	0.0218	-0.1919	0.1203	-0.9495	10.3877	0.1008
$r_{CHN}$	0.0013	0.0011	0.0366	-0.2319	0.3926	0.6048	12.4421	0.0303
$r_{CZE}$	0.0004	0.0018	0.0296	-0.3045	0.1557	-1.1541	11.2972	0.0820
$r_{DEU}$	0.0013	0.0041	0.0320	-0.2435	0.1494	-0.8364	6.0862	-0.0236
$r_{DNK}$	0.0019	0.0041	0.0268	-0.2249	0.1172	-1.2108	7.4496	-0.0395
$r_{ESP}$	0.0007	0.0035	0.0313	-0.2383	0.1359	-0.9081	6.0394	-0.0348
$r_{FIN}$	0.0012	0.0031	0.0369	-0.2316	0.1684	-0.7754	4.4343	-0.0074
$r_{FRA}$	0.0007	0.0025	0.0300	-0.2505	0.1243	-0.9484	6.8454	-0.0652
$r_{GBR}$	0.0005	0.0021	0.0240	-0.2363	0.1258	-1.2144	11.8248	-0.0691
$r_{GRC}$	-0.0003	0.0005	0.0426	-0.2254	0.2222	-0.3992	3.8148	0.0495
$r_{HKG}$	0.0009	0.0026	0.0325	-0.1992	0.1392	-0.4055	3.4113	0.0114
$r_{HUN}$	0.0024	0.0032	0.0366	-0.3302	0.1516	-1.1353	9.6635	0.0216
$r_{IDN}$	0.0018	0.0031	0.0353	-0.2330	0.1880	-0.5122	6.1690	-0.0506
$r_{IND}$	0.0017	0.0029	0.0322	-0.1738	0.1317	-0.2806	2.6549	0.0424
$r_{IRL}$	0.0009	0.0039	0.0298	-0.3174	0.1337	-1.6992	14.0005	-0.0107
$r_{ISR}$	0.0015	0.0035	0.0283	-0.1569	0.1356	-0.6185	3.2194	-0.0362
$r_{JPN}$	0.0001	0.0017	0.0306	-0.2788	0.1582	-0.8075	6.9243	-0.0412
$r_{KOR}$	0.0006	0.0026	0.0373	-0.2293	0.1744	-0.5436	5.3197	-0.0761
$r_{MEX}$	0.0020	0.0027	0.0324	-0.1793	0.1858	-0.1711	4.5063	-0.0080
$r_{MYS}$	0.0004	0.0010	0.0264	-0.1903	0.2458	0.1155	12.6506	0.0387
$r_{NLD}$	0.0008	0.0033	0.0301	-0.2875	0.1358	-1.2585	9.5525	-0.0065
$r_{NOR}$	0.0011	0.0043	0.0309	-0.2478	0.1683	-1.1126	8.4968	-0.0068
$r_{PHL}$	0.0006	0.0016	0.0322	-0.2199	0.1618	-0.6778	6.4953	0.0107
$r_{POL}$	0.0014	0.0022	0.0328	-0.2444	0.1390	-0.6623	5.4819	0.0393
$r_{PRT}$	0.0001	0.0014	0.0277	-0.2057	0.1556	-1.0416	6.9606	0.0631
$r_{SGP}$	0.0001	0.0013	0.0285	-0.2134	0.1725	-0.4817	7.3643	0.0271
$r_{SWE}$	0.0014	0.0034	0.0300	-0.2253	0.1792	-0.6091	4.9405	-0.0467
$r_{THA}$	0.0000	0.0023	0.0343	-0.2666	0.2184	-0.3988	6.3501	0.0318
$r_{TUR}$	0.0046	0.0059	0.0508	-0.3037	0.2578	-0.1278	3.9630	0.0217
$r_{TWN}$	0.0004	0.0023	0.0307	-0.1429	0.1832	-0.2851	2.9909	-0.0197
$r_{USA}$	0.0014	0.0028	0.0246	-0.2008	0.1142	-0.9145	7.4286	-0.0802

the weighting matrices, geographic distances between capital cities are sourced from the Centre d'Etudes Prospectives et d'Informations Internationales (CEPII) GeoDist database. Bilateral trade data and country-specific gross domestic products (GDP) are obtained from the Organization for Economic Co-operation and Development (OECD) and the International Trade Center (ITC) trademap databases, respectively.

### 2.2.3 Spatial weighting matrix

The weighting matrix within a standard spatial model is defined by geographic distance. While a few decades ago geographic proximity could have been regarded as a measure for economic proximity, the subsequent increase in mobility might have led to a divergence between spatial and economic distances.

A variety of papers discuss the issue of measuring economic or financial integration in relation to geographic closeness. [Portes and Rey \(2005\)](#) use a gravity model to analyze the determinants of international trade in equities and show that investment in assets is halved when the physical distance is doubled. This result is puzzling, as investors could use more distant economies to diversify their risk. More specifically, they argue that information asymmetries between investors of different countries produce borders for international financial trade. [Aviat and Coeurdacier \(2007\)](#) build on the results of [Portes and Rey \(2005\)](#) and show that there is a clear relationship between bilateral trade and bilateral asset holdings between countries. More specifically, when controlling for trade in the gravity model the impact of physical distance is drastically reduced. Therefore, trade substitutes for geographic distance, while also accounting for financial interdependence. The idea of trade as a financial distance measure is also profoundly evident within the spatial statistics literature. For instance, [Forbes and Chinn \(2004\)](#) refer to trade linkages as the predominant determinant of market integration. On a similar note, [Wälti \(2011\)](#) finds that cross-border trade fosters market integration on both the demand and the supply side. On the demand side, an increase in aggregate demand for goods in one country leads to the export growth of its trading partners and, consequently, synchronization of business cycles. On the supply side, however, the impact is ambiguous and depends on whether trade occurs within (synchronization of business cycles) or across (de-synchronization of business cycles) industries.

Based on the discussion above, we use two definitions for the weighting matrix presented in Equation 2.1 which we refer to as geographic ( $W_t^{geo}$ ) and economic weights ( $W_t^{eco}$ ), respectively. Geographic weights are based on geographic distance and remain identical for all  $t$ , while economic weights are based on a bilateral trade measure and change over time. Following [Asgharian et al. \(2013\)](#), we obtain the GDP-standardized measure of bilateral trade arising between country  $i$  and country  $j$  as:

$$E_{ij,t} = 2 - \left( \frac{ex_{ij,t}}{GDP_{j,t}} + \frac{ex_{ji,t}}{GDP_{i,t}} \right), \quad (2.7)$$

where  $ex_{ij,t}$  is the nominal export value from country  $i$  to country  $j$  measured in US-dollars, and



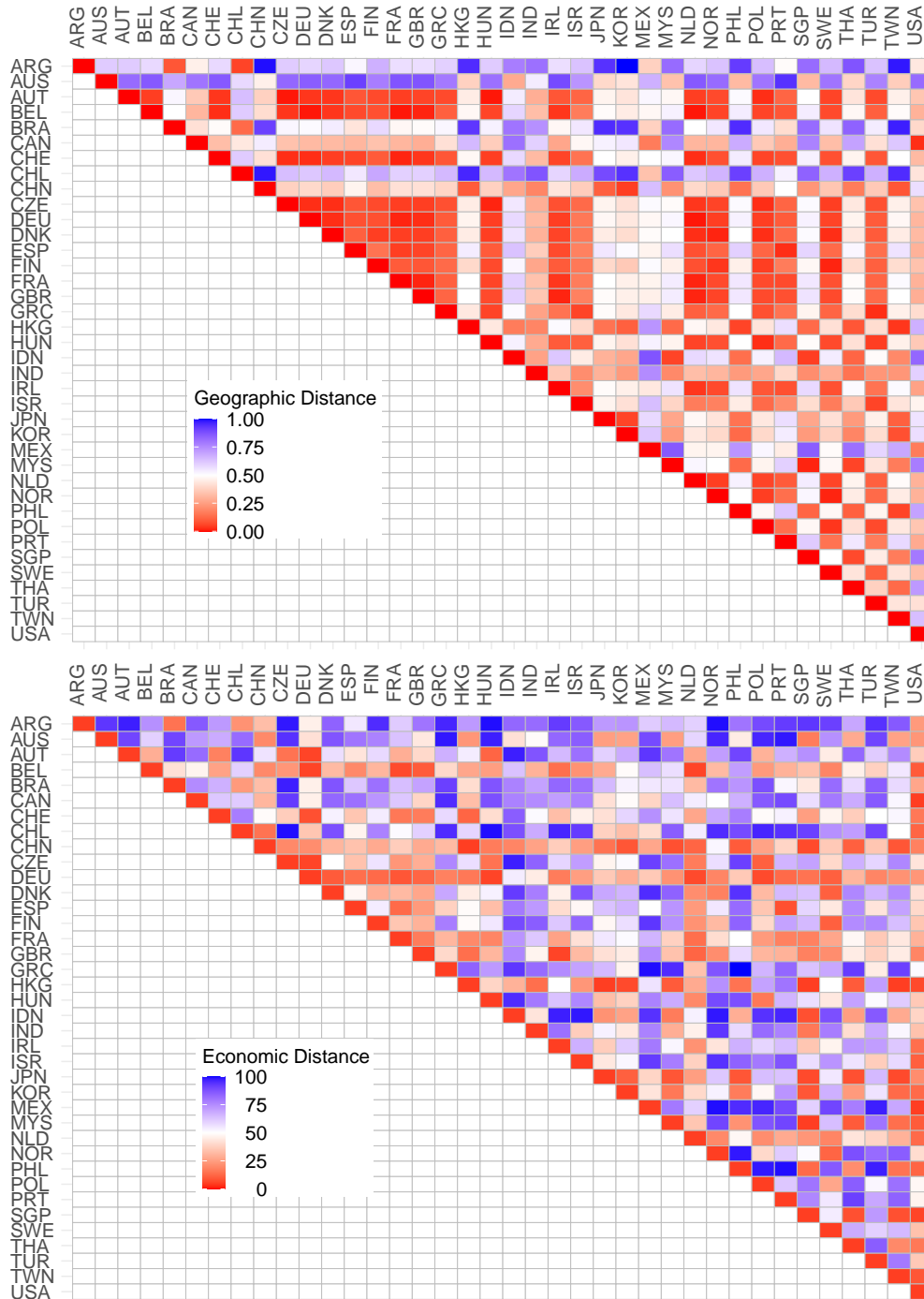
$GDP_{i,t}$  denotes the GDP of country  $i$  at time  $t$ . Besides,  $ex_{ji,t}$  denotes the nominal export value from country  $j$  to country  $i$  and  $GDP_{j,t}$  refers to the GDP of country  $j$ .

Figure 2.1 highlights that geographic and economic distance measures diverge considerably for some countries. While geographic distances cluster with respect to continents, economic distances are influenced by monetary, trade or regulatory unions. These observations highlight the importance of choosing adequate weighting matrices within spatial models.

Denote the distances between units  $i$  and  $j$  for all  $i = 1, \dots, n$  and  $j = 1, \dots, n$  at time  $t$  in a  $(n \times n)$  distance matrix  $D_t$ . The neighborhood structure for any weight matrix  $W_t$  is obtained from  $D_t$  as:

$$W_{ij,t} = \begin{cases} 1 & \text{if } D_{ij,t} \leq q_{10} \\ 0.75 & \text{if } q_{10} < D_{ij,t} \leq q_{40} \\ 0.50 & \text{if } q_{40} < D_{ij,t} \leq q_{60} \\ 0.25 & \text{if } q_{60} < D_{ij,t} \leq q_{90} \\ 0 & \text{if } q_{90} < D_{ij,t}, \end{cases} \quad (2.8)$$

where  $q_{10}$ ,  $q_{40}$ ,  $q_{60}$ , and  $q_{90}$  refer to the 10%, 40%, 60%, and 90% quantile of the empirical distribution of  $D_t$ , respectively. Note, that the  $i$ -th row in  $W_t$  comprises all spatial weights impacting unit  $i$ . Thus, we set the main diagonal to zero and, in line with prior literature, row-standardize  $W_t$  such that for each  $i$ ,  $\sum_j W_{ij,t} = 1$  (e.g., [Ord, 1975](#); [Anselin, 1982](#)). This results in an asymmetric spatial weight matrix  $W_t$ . Finally, the asymmetric spatial lag may be interpreted as a (geographically or economically) weighted average of all neighbors.



**Figure 2.1: The relation between geographic and economic distances**

This figure depicts the relation between geographic and economic distances for the entire cross-section of market indices. Geographic distances (upper panel) are scaled by the maximum geographic distance in our sample to be restricted within 0 and 1. Economic distances between countries (lower panel) are displayed by their affiliation to the empirical distribution of mean economic distances over the full sample period and range from 0 to 100.

## 2.3 Global equity market co-movement

### 2.3.1 Time-varying co-movement across equity markets

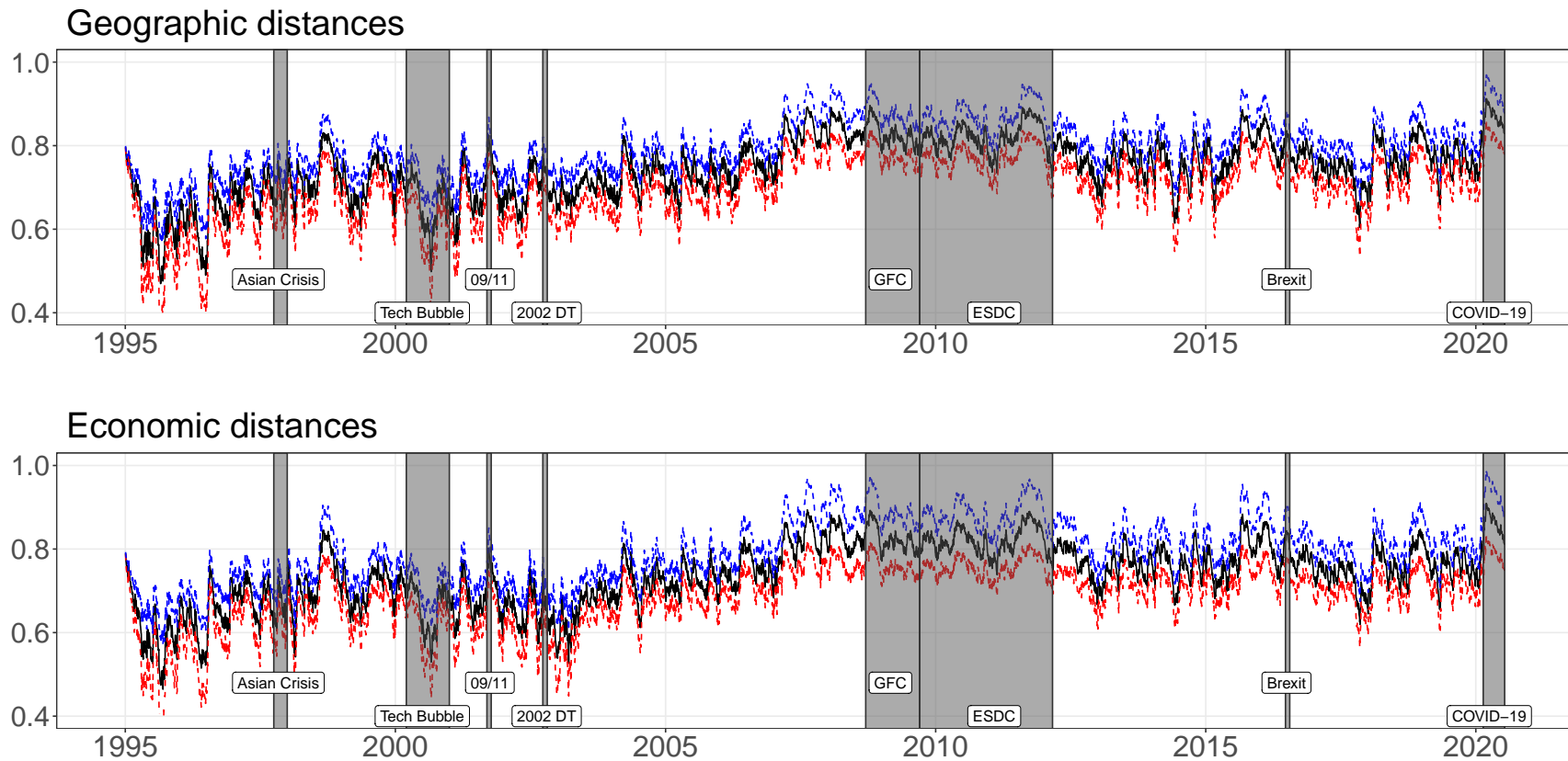
We estimate the SAR model using the full set of sample countries (global) as well as subsets referring to the American, European, and Asian-Pacific regions. Figure 2.2 illustrates the global dynamic spatial dependence parameter based on the geographic (upper panel) and economic distance measure (lower panel).<sup>18</sup> Irrespective of the weighting scheme, we observe an increase in co-movement until the late 1990s. Thereafter, the graph reveals constant or even decreasing co-movement in the early 2000s which then transitions into another upward trend until around 2010. The weighting scheme does not seem to have a decisive impact on the dynamics of the spatial dependence parameter. However, as is evident from the widening confidence bounds occurring during crisis periods, volatility increases during such crises. As noted by [Forbes and Rigobon \(2002\)](#), this observed heteroscedasticity might bias contagion tests and it is therefore crucial to account for this pattern.

Figure 2.3 displays the time-varying co-movement parameters for American, European, and Asian-Pacific countries. We observed a higher degree of spatial dependence for European countries as compared to American and Asian-Pacific countries. This result is hardly surprising, when considering the geographic, economic, and political proximity of European countries as compared to the two other groups. American countries tend to exhibit the lowest spatial dependence parameters, which jumped upwards during the first wave of the COVID-19 pandemic in 2020. Equity markets across the American and Asian-Pacific countries also seem to drive the trending patterns which we observe for the global co-movement in Figure 2.2.

Table 2.2 shows yearly averages of the estimated spatial parameters. The corresponding standard deviations can be found in Table 2.3. These statistics confirm the indications from Figures 2.2 and 2.3 as they reveal the highest yearly average spatial dependence parameter for the European countries, followed by the Asian-Pacific, and then the American countries. We further observe a slightly higher variation in the spatial dependence parameter on an annualized basis for Asian-Pacific countries as compared to the European and American countries. During the GFC, we observe an increase in co-movement, albeit only slightly, which might be due to the already very high level of co-movement. Another rise in the global dependence occurs during 2016, which coincides with the Chinese stock market turbulences and the Brexit vote in the UK. The highest co-movement is, however, observed in the early months of 2020 when the COVID-19 pandemic spread.

---

<sup>18</sup>Summary statistics for these estimation results can be found in Table 2.5 in Appendix 2.5.2.



**Figure 2.2: Time-varying spatial dependence between markets (Global)**

This figure depicts mean estimates of the weekly spatial dependence for all market indices over the sample period from January 1995 to July 2020. We provide time-varying estimates based on Student-t distributed disturbances and time-varying volatilities. The red and blue line depict the 2.5% and 97.5% quantile of the distribution, respectively.

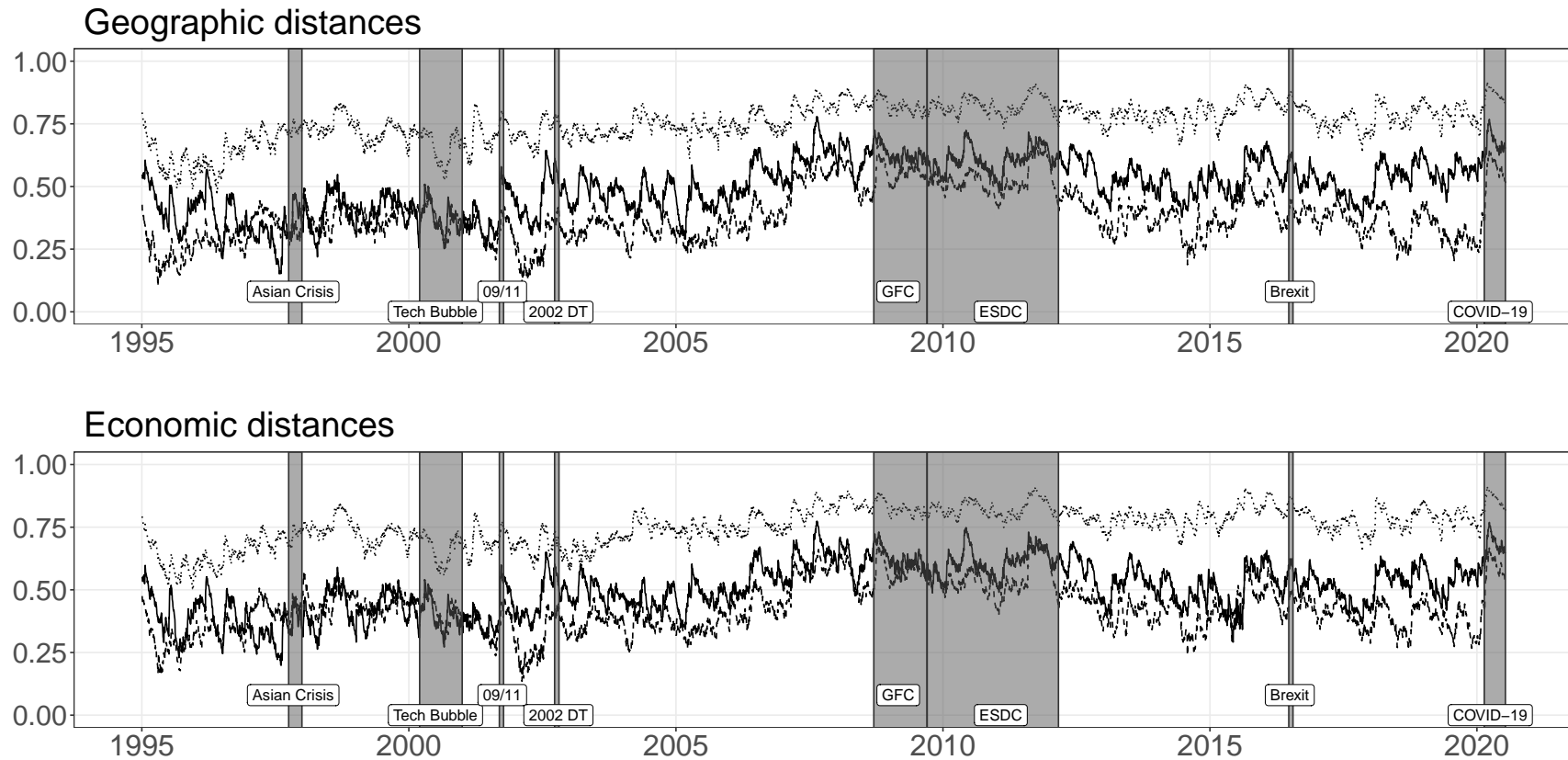


**Figure 2.3: Time-varying spatial dependence (America, Europe, Asia-Pacific)**

This figure depicts mean estimates of the weekly spatial dependence for three market sets over the sample period from January 1995 to July 2020. The sets comprise American countries (dashed lines), European countries (dotted lines), and Asian-Pacific countries (solid lines). For each set of constituents, we provide time-varying estimates based on Student-t distributed disturbances and time-varying volatilities.

**Table 2.2: Average yearly co-movement**

This table provides the arithmetic mean of the time-varying spatial dependence parameter based on both the geographic and economic distance measure. In each case, we report values for the global and the regional samples from January 1995 to July 2020.

	(a) Geographic distance				(b) Economic distance			
	Global	American	European	Asian-Pacific	Global	American	European	Asian-Pacific
1995	0.7327	0.3288	0.7164	0.5589	0.7343	0.3929	0.7364	0.5319
1996	0.6742	0.3641	0.6382	0.4800	0.6884	0.4163	0.6701	0.4686
1997	0.7622	0.4540	0.7824	0.3580	0.7707	0.5128	0.7778	0.3752
1998	0.7698	0.5112	0.7799	0.4557	0.7649	0.5590	0.7828	0.5002
1999	0.7709	0.4719	0.7511	0.4622	0.7732	0.5243	0.7643	0.4805
2000	0.7340	0.4860	0.7138	0.4618	0.7385	0.5257	0.7117	0.4994
2001	0.7540	0.4508	0.7591	0.4501	0.7603	0.4825	0.7463	0.4890
2002	0.7854	0.3920	0.7805	0.5184	0.7640	0.4295	0.7619	0.5443
2003	0.7627	0.4132	0.7626	0.5231	0.7364	0.4568	0.7400	0.5469
2004	0.7605	0.4209	0.7638	0.5395	0.7564	0.4593	0.7661	0.5338
2005	0.7582	0.4270	0.7394	0.5328	0.7674	0.4670	0.7533	0.5379
2006	0.7845	0.4627	0.7744	0.5788	0.7968	0.5082	0.7806	0.6040
2007	0.8358	0.5504	0.8331	0.6209	0.8370	0.5737	0.8353	0.6437
2008	0.8601	0.5766	0.8516	0.6981	0.8619	0.6004	0.8525	0.7062
2009	0.8668	0.6171	0.8413	0.7090	0.8706	0.6325	0.8502	0.7056
2010	0.8434	0.5739	0.8300	0.6661	0.8494	0.5852	0.8349	0.6571
2011	0.8412	0.5596	0.8235	0.6755	0.8461	0.5748	0.8224	0.6843
2012	0.8255	0.5153	0.8162	0.6727	0.8329	0.5329	0.8194	0.6606
2013	0.7834	0.4195	0.7886	0.6003	0.7968	0.4516	0.7931	0.5956
2014	0.7874	0.3934	0.8045	0.5559	0.8094	0.4381	0.8073	0.5458
2015	0.8097	0.4772	0.8239	0.5906	0.8127	0.5217	0.8248	0.5278
2016	0.8290	0.4914	0.8370	0.6607	0.8325	0.5290	0.8367	0.6338
2017	0.7644	0.4039	0.7680	0.5681	0.7699	0.4287	0.7695	0.5524
2018	0.8091	0.4379	0.8098	0.6047	0.8003	0.4777	0.8041	0.6067
2019	0.8166	0.4007	0.8104	0.6269	0.8114	0.4629	0.8082	0.5972
2020	0.8563	0.5343	0.8535	0.6863	0.8580	0.5877	0.8501	0.6943

**Table 2.3: Average yearly standard deviation of the co-movement parameter**

This table provides the yearly standard deviation of the time-varying spatial dependence parameter based on both the geographic and economic distance measure. In each case, we report values for the global and the regional samples from January 1995 to July 2020.

	(a) Geographic distance				(b) Economic distance			
	Global	American	European	Asian Pacific	Global	American	European	Asian Pacific
1995	0.0413	0.0683	0.0316	0.0356	0.0440	0.0620	0.0332	0.0543
1996	0.0412	0.0297	0.0468	0.0327	0.0303	0.0379	0.0241	0.0329
1997	0.0183	0.0398	0.0262	0.0330	0.0157	0.0286	0.0244	0.0511
1998	0.0290	0.0684	0.0329	0.0582	0.0434	0.0605	0.0288	0.0620
1999	0.0282	0.0384	0.0323	0.0208	0.0262	0.0324	0.0225	0.0315
2000	0.0194	0.0333	0.0233	0.0362	0.0156	0.0309	0.0188	0.0397
2001	0.0482	0.0368	0.0562	0.0364	0.0421	0.0380	0.0501	0.0443
2002	0.0203	0.0349	0.0213	0.0349	0.0168	0.0414	0.0169	0.0421
2003	0.0112	0.0460	0.0218	0.0210	0.0184	0.0401	0.0181	0.0245
2004	0.0217	0.0343	0.0200	0.0220	0.0222	0.0380	0.0166	0.0359
2005	0.0156	0.0203	0.0218	0.0199	0.0194	0.0218	0.0172	0.0282
2006	0.0259	0.0223	0.0299	0.0365	0.0221	0.0268	0.0306	0.0387
2007	0.0334	0.0501	0.0298	0.0710	0.0338	0.0487	0.0264	0.0778
2008	0.0204	0.0713	0.0238	0.0222	0.0223	0.0839	0.0232	0.0315
2009	0.0186	0.0282	0.0276	0.0198	0.0179	0.0295	0.0225	0.0354
2010	0.0209	0.0367	0.0246	0.0181	0.0222	0.0465	0.0222	0.0294
2011	0.0389	0.0685	0.0494	0.0363	0.0385	0.0854	0.0482	0.0424
2012	0.0248	0.0559	0.0229	0.0247	0.0229	0.0554	0.0230	0.0389
2013	0.0167	0.0500	0.0159	0.0200	0.0186	0.0449	0.0149	0.0345
2014	0.0294	0.0352	0.0259	0.0257	0.0201	0.0423	0.0216	0.0302
2015	0.0276	0.0581	0.0187	0.0465	0.0238	0.0583	0.0134	0.0742
2016	0.0242	0.0544	0.0178	0.0233	0.0242	0.0508	0.0166	0.0272
2017	0.0254	0.0319	0.0260	0.0425	0.0266	0.0396	0.0266	0.0530
2018	0.0350	0.0794	0.0344	0.0386	0.0350	0.0781	0.0343	0.0440
2019	0.0193	0.0706	0.0189	0.0147	0.0180	0.0593	0.0181	0.0264
2020	0.0526	0.1437	0.0563	0.0645	0.0503	0.1333	0.0513	0.0863

### 2.3.2 Contagion during recent major crises

We now turn to specific crisis periods and analyze the potential occurrence of contagion. Based on the definition of contagion by [Forbes and Rigobon \(2002\)](#), we examine whether there is evidence of contagion on a global scale or at a regional level. To this end, we estimate confidence bounds based on the Delta-method in-sample confidence bands for time-varying parameters as introduced by [Blasques \*et al.\* \(2016a\)](#). Since our model also allows for temporal variances, these bounds also account for potentially increased volatility arising during crisis periods. However, this approach, as well as further approaches offered in [Blasques \*et al.\* \(2016a\)](#) and theories offered in [Blasques \*et al.\* \(2022\)](#) are based on the assumption of a correctly specified model. Thereby our standard errors and confidence bounds do not account for filtering uncertainty. A potential solution might lie in an adequate bootstrap method as proposed by [Zamojski \(2017\)](#) or [Beutner \*et al.\* \(2020\)](#), but developing such a procedure is beyond the scope of the paper.

More particularly, we examine potential contagion (as defined as increased co-movement) during the first weeks of the Asian crisis, the bursting of the tech bubble in March 2000, the September 11, 2001, terrorist attacks (9/11), the 2002 downturn (2002 DT), the GFC, the European sovereign debt crisis (ESDC), Brexit, and the outbreak of COVID-19.

Adapting the definition of [Forbes and Rigobon \(2002\)](#), we define contagion as a significant increase in co-movement arising during a crisis period or in the direct aftermath of a crisis event. Consequently, we assess whether the global and regional time-varying spatial dependence parameters increase significantly during the considered crisis periods. A significant increase is defined as non-overlapping of at least two consecutive weeks of the crisis/post-event lower ( $c_{t_c}^{LOW}$ ) confidence bounds and the arithmetic mean of the pre-event upper ( $c_{t_p}^{UP}$ ) confidence bounds:

$$\frac{1}{N} \sum_{p=n}^{n+N} c_{t_p}^{UP} < c_{t_c}^{LOW} \quad t_c \in \{t_m, t_{m+1}, \dots, t_{m+M}\}$$

$$\text{with } t_{n+N} < t_m. \tag{2.9}$$

To determine the crisis periods ( $t_c$ ), we rely on the previous literature, while the pre-crisis period is defined as one month preceding the start of the crisis. We consider the 0.025 and 0.975 quantiles for lower and upper bounds, respectively. The results are given in [Table 2.4](#).

With respect to the Asian crisis, [Figures 2.2 and 2.3](#) reveal an increase in co-movement among global and regional equity markets. However, we cannot detect a significant increase corresponding to non-overlapping pre-crisis upper and crisis lower confidence bounds as indicated in [Table 2.4](#). Since our approach accounts for dynamic volatility, the co-movement parameters visible from [Figure 2.3](#) are quite volatile, rendering a detection of contagion, as defined in [Equation 2.9](#), rather difficult. This is particularly noticeable when dealing with a longer crisis period, as for the Asian crisis. Consequently, our results do not support those of [Baig and Goldfajn \(1999\)](#), [Caporale \*et al.\* \(2005\)](#),



**Table 2.4: Contagion during selected events between 1995 and 2020**

This table provides an overview on the presence of contagion during selected event periods between January 1995 and July 2020. We also tabulate the mean of the upper confidence bound for each pre-event period as well as the minimum of the lower confidence bound during contagion periods. Finally, the table highlights the presence of regional or global contagion for each of the events considered.

	Event period	mean( $c_{t_p}^{UP}$ )	Contagion period	min( $c_{t_e}^{LOW}$ )
<b>Global</b>				
Asian crisis	1997-10-01/1997-12-31	0.8206	No contagion	
Tech bubble	2000-03-15/2000-12-31	0.8176	No contagion	
9/11	2001-09-11/2001-10-10	0.8113	No contagion	
2002 DT	2002-09-24/2002-10-24	0.8378	No contagion	
GFC	2008-09-15/2009-09-14	0.8839	No contagion	
ESDC	2009-09-15/2012-03-01	0.9095	No contagion	
Brexit	2016-06-23/2016-07-22	0.8853	No contagion	
COVID-19	2020-02-20/2020-07-31	0.8470	2020-03-20/2020-05-01	0.8501
<b>America</b>				
Asian crisis	1997-10-01/1997-12-31	0.5748	No contagion	
Tech bubble	2000-03-15/2000-12-31	0.6131	No contagion	
9/11	2001-09-11/2001-10-10	0.4920	No contagion	
2002 DT	2002-09-24/2002-10-24	0.5136	No contagion	
GFC	2008-09-15/2009-09-14	0.5841	2008-10-17/2008-12-19	0.5936
ESDC	2009-09-15/2012-03-01	0.7411	No contagion	
Brexit	2016-06-23/2016-07-22	0.5740	No contagion	
COVID-19	2020-02-20/2020-07-31	0.5099	2020-03-27/2020-07-14	0.5387
<b>Europe</b>				
Asian crisis	1997-10-01/1997-12-31	0.8868	No contagion	
Tech bubble	2000-03-15/2000-12-31	0.8061	No contagion	
9/11	2001-09-11/2001-10-10	0.8490	No contagion	
2002 DT	2002-09-24/2002-10-24	0.8687	No contagion	
GFC	2008-09-15/2009-09-14	0.9107	No contagion	
ESDC	2009-09-15/2012-03-01	0.9500	No contagion	
Brexit	2016-06-23/2016-07-22	0.9213	No contagion	
COVID-19	2020-02-20/2020-07-31	0.8464	No contagion	
<b>Asia-Pacific</b>				
Asian crisis	1997-10-01/1997-12-31	0.8294	No contagion	
Tech bubble	2000-03-15/2000-12-31	0.7657	No contagion	
9/11	2001-09-11/2001-10-10	0.6864	No contagion	
2002 DT	2002-09-24/2002-10-24	0.8751	No contagion	
GFC	2008-09-15/2009-09-14	1.2724	No contagion	
ESDC	2009-09-15/2012-03-01	1.5725	No contagion	
Brexit	2016-06-23/2016-07-22	0.9963	No contagion	
COVID-19	2020-02-20/2020-07-31	0.9906	No contagion	

and [Chiang \*et al.\* \(2007\)](#), who find evidence of regional market contagion over the Asian crisis period. Moreover, global equity market co-movement increased sharply from a monthly average of 0.7157 in July 1998 to 0.7801 in August of the same year and as far as 0.7980 in September, reverting to pre-crisis levels in November 1998.

Turning to the bursting of the tech bubble in March 2000 (e.g., [Griffin \*et al.\*, 2011](#); [Ljungqvist and Wilhelm Jr., 2003](#)), we do not detect any evidence of financial contagion, nor do we detect global contagion during the GFC, perhaps surprisingly, but rather there is evidence of significant increases in co-movement for the American sample over two months following the collapse of Lehman Brothers in September 2008, which is commonly considered to be the starting date for the GFC (e.g., [Mollah \*et al.\*, 2016](#)). These findings are in line with those of [Bekaert \*et al.\* \(2014\)](#), who studied contagion among equity markets during the GFC and found that there was only weak evidence of global contagion.

The ongoing high degree of co-movement arising after the end of the financial crisis of 2009 may be linked to the start of the European sovereign debt crisis. [Pragidis \*et al.\* \(2015\)](#) analyzed contagion effects from 10-year government bond yields arising from the Greek debt crisis to other European countries, denoting a timeline of European debt crisis events running from 2009 to 2013. Moreover, [Beirne and Fratzscher \(2013\)](#) noted an increase in sovereign risk from 2008 to 2011 which ultimately resulted in the European sovereign debt crisis of 2010. Accordingly, fundamental contagion was observed during that epoch. Finally, [Broto and Perez-Quiros \(2015\)](#) defined the beginning of the sovereign debt crisis as being October 2010, extending at least until March 2012 when Greece was finally held accountable for its debt. Moreover, they found significant evidence for contagion throughout the sovereign debt crisis. Another rise in global and regional co-movement was observed from late 2015 to 2016, which might be attributed to the uncertainty surrounding the UK's potential departure from the European Union, culminating in the referendum of June 2016 and the decision in favor of Brexit.

With respect to the pandemic-induced crisis period, commencing in February 2020, we find evidence for global contagion. Overall, the economic downturn induced by the COVID-19 pandemic constitutes the only event for which we find a significant increase in co-movement over several weeks arising among international equity markets, despite the generally high level of co-movement brought about by increasing market integration over the past two decades. Overall, our findings support those of [Forbes and Rigobon \(2002\)](#). When accounting for heteroscedasticity in terms of the increasing variance arising during crisis periods, we often observe *no contagion, only interdependence*. These results are robust to alternative definitions of the pre-event windows (see Figures 2.4 and 2.5 in Appendix 2.5.1).

## 2.4 Concluding remarks

We empirically examine the co-movement arising across equity markets around the world. On the basis of a time-varying spatial model, we estimate global co-movement as well as co-movement among the sub-samples of American, European, and Asian-Pacific countries from January 1995 to July 2020. Our approach not only captures the time-variation within such co-movements, but also accounts for increasing variances during events or crisis periods. Using confidence intervals, we are able to test for contagion, as measured by a significant increase in co-movement during an event. First, our results indicate that contagion on a global level has occurred only once in the past 25 years, specifically during the first wave of the COVID-19 pandemic which took place in the first quarter of 2020. Second, our results highlight that equity market co-movement increased over the last two decades, particularly among European countries, while generally exhibiting a high level of fluctuation. In contrast, standard approaches, such as correlation analysis, overlook the time-variant behavior of co-movement. For this reason, our results provide a more generalized view of co-movement beyond pairwise correlation and highlight the high degree of global equity market integration. Finally, in support of the findings of [Forbes and Rigobon \(2002\)](#), market dynamics which are often considered to represent contagion are perhaps better described as instances of interdependence when accounting for concurring increases in variances.

## 2.5 Appendices

### 2.5.1 Contagion periods depending on pre-event window lengths

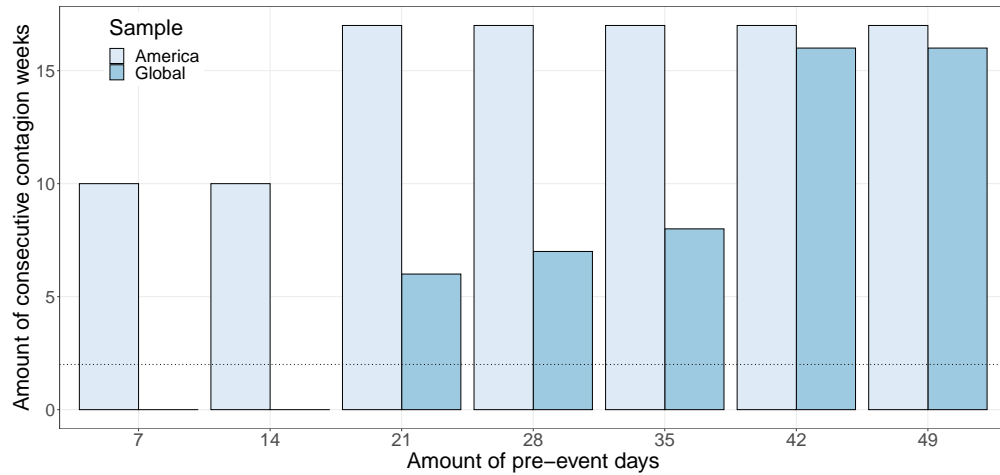


**Figure 2.4: Contagion after COVID-19 based on the pre-event window length**

This figure depicts the relation between (i) the number of consecutive weeks of contagion and (ii) the number of days contained in the pre-event window. Additionally, the figure contains a horizontal, dashed line. The latter shows the minimum required number of consecutive weeks of contagion used in the manuscript. The results are fairly robust to changes in either dimension. We do not find evidence of contagion within the European or Asian sample.

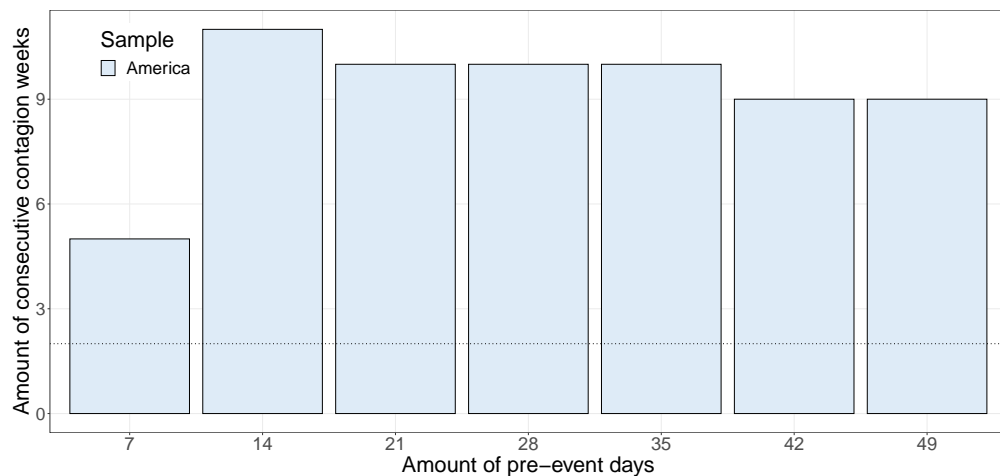


**Figure 2.5: Contagion after the GFC based on the pre-event window length**

This figure depicts the relation between (i) the number of consecutive weeks of contagion and (ii) the number of days contained in the pre-event window. Additionally, the figure contains a horizontal, dashed line. The latter shows the minimum required number of consecutive weeks of contagion used in the manuscript. The results are fairly robust to changes in either dimension. We do not find evidence of contagion within the global, European, or Asian sample.

## 2.5.2 Estimated model coefficients

**Table 2.5: Coefficient estimates of the dynamic SAR model**

This table details results for the dynamic SAR models based on the sample period from January 1995 to July 2020. For each combination of constituents, we report coefficients based on geographic and economic spatial weight matrices and Student-t distributed error terms. Besides, we provide the maximized log-likelihood value ( $\mathcal{L}$ ), the Akaike information criterion (AIC), and the Bayesian information criterion (BIC). \*\*\*, \*\*, and \* denote statistical significance at the 1%, 5%, and 10% levels, respectively.

	Global		America		Europe		Asia-Pacific	
	$W_t^{geo}$	$W_t^{eco}$	$W_t^{geo}$	$W_t^{eco}$	$W_t^{geo}$	$W_t^{eco}$	$W_t^{geo}$	$W_t^{eco}$
$\beta$	0.0003***	0.0004***	0.0011***	0.0010***	0.0004***	0.0005***	0.0007***	0.0008***
$\omega$	0.0186***	0.0188***	0.0138**	0.0217**	0.0230**	0.0191**	0.0028	0.0077
$A$	0.0090***	0.0093***	0.0095***	0.0124***	0.0108***	0.0098***	0.0066***	0.0092**
$B$	0.9828***	0.9830***	0.9737***	0.9621***	0.9790***	0.9827***	0.9961***	0.9888***
$\omega_{ARG}^\sigma$	-0.0719***	-0.0725***	-0.1530***	-0.1451***				
$\omega_{AUS}^\sigma$	-0.0906***	-0.0932***					-0.0673***	-0.0690***
$\omega_{AUT}^\sigma$	-0.0863***	-0.0872***			-0.0844***	-0.0848***		
$\omega_{BEL}^\sigma$	-0.0922***	-0.0926***			-0.0914***	-0.0914***		
$\omega_{BRA}^\sigma$	-0.0773***	-0.0780***	-0.1625***	-0.1549***				
$\omega_{CAN}^\sigma$	-0.0954***	-0.0967***	-0.2000***	-0.1901***				
$\omega_{CHE}^\sigma$	-0.0923***	-0.0928***			-0.0907***	-0.0913***		
$\omega_{CHL}^\sigma$	-0.0880***	-0.0894***	-0.1908***	-0.1816***				
$\omega_{CHN}^\sigma$	-0.0767***	-0.0774***					-0.0591***	-0.0601***
$\omega_{CZE}^\sigma$	-0.0873***	-0.0880***			-0.0851***	-0.0850***		
$\omega_{DEU}^\sigma$	-0.0896***	-0.0897***			-0.0886***	-0.0884***		
$\omega_{DNK}^\sigma$	-0.0863***	-0.0872***			-0.0847***	-0.0850***		
$\omega_{ESP}^\sigma$	-0.0877***	-0.0883***			-0.0867***	-0.0866***		
$\omega_{FIN}^\sigma$	-0.0848***	-0.0860***			-0.0843***	-0.0848***		
$\omega_{FRA}^\sigma$	-0.0922***	-0.0921***			-0.0917***	-0.0916***		
$\omega_{GBR}^\sigma$	-0.0955***	-0.0959***			-0.0937***	-0.0936***		
$\omega_{GRC}^\sigma$	-0.0760***	-0.0767***			-0.0746***	-0.0744***		
$\omega_{HKG}^\sigma$	-0.0833***	-0.0841***					-0.0626***	-0.0634***
$\omega_{HUN}^\sigma$	-0.0799***	-0.0806***			-0.0776***	-0.0777***		
$\omega_{IDN}^\sigma$	-0.0810***	-0.0818***					-0.0618***	-0.0622***
$\omega_{IND}^\sigma$	-0.0809***	-0.0818***					-0.0610***	-0.0617***
$\omega_{IRL}^\sigma$	-0.0877***	-0.0885***			-0.0863***	-0.0866***		
$\omega_{ISR}^\sigma$	-0.0830***	-0.0839***			-0.0778***	-0.0801***		
$\omega_{JPN}^\sigma$	-0.0830***	-0.0840***					-0.0619***	-0.0627***
$\omega_{KOR}^\sigma$	-0.0837***	-0.0846***					-0.0638***	-0.0641***
$\omega_{MEX}^\sigma$	-0.0846***	-0.0854***	-0.1797***	-0.1712***				
$\omega_{MYS}^\sigma$	-0.0885***	-0.0894***					-0.0690***	-0.0693***
$\omega_{NLD}^\sigma$	-0.0938***	-0.0936***			-0.0925***	-0.0927***		
$\omega_{NOR}^\sigma$	-0.0864***	-0.0875***			-0.0842***	-0.0844***		
$\omega_{PHL}^\sigma$	-0.0806***	-0.0814***					-0.0615***	-0.0618***
$\omega_{POL}^\sigma$	-0.0852***	-0.0859***			-0.0823***	-0.0825***		
$\omega_{PRT}^\sigma$	-0.0877***	-0.0887***			-0.0860***	-0.0860***		
$\omega_{SGP}^\sigma$	-0.0892***	-0.0897***					-0.0673***	-0.0682***
$\omega_{SWE}^\sigma$	-0.0887***	-0.0901***			-0.0876***	-0.0886***		
$\omega_{THA}^\sigma$	-0.0819***	-0.0827***					-0.0618***	-0.0624***
$\omega_{TUR}^\sigma$	-0.0705***	-0.0711***			-0.0695***	-0.0692***		
$\omega_{TWN}^\sigma$	-0.0842***	-0.0850***					-0.0648***	-0.0654***
$\omega_{USA}^\sigma$	-0.0943***	-0.0944***	-0.1963***	-0.1847***				
$A^\sigma$	0.0996***	0.0999***	0.1769***	0.1713***	0.1083***	0.1088***	0.1318***	0.1303***
$B^\sigma$	0.9894***	0.9893***	0.9772***	0.9784***	0.9897***	0.9896***	0.9919***	0.9918***
$\lambda$	10.0466***	9.8244***	8.6307***	8.8158***	10.0908***	10.0843***	9.5612***	9.5805***
$\mathcal{L}$	126572	126285	19173	19233	68540	68627	38285	38293
AIC	-253054	-252480	-38319	-38440	-137027	-137199	-76533	-76547
BIC	-252820	-252247	-38252	-38373	-136886	-137059	-76434	-76449

# Chapter 3

## Flight to quality – Gold mining shares versus gold bullion

### 3.1 Introduction

*Imagine a port for boats. Whenever there is a storm forecast, boats will seek the shelter of the port and only leave the port when the storm dissipates. Some types of boats are always in the proximity of the port and only need to seek shelter if the storm is severe. When boats seek shelter, the port becomes crowded and the price of shelter increases.*

The above is an analogy for the role of gold and gold mining companies in the financial system.<sup>19</sup> When there is a severe shock or financial turmoil, investors sell shares and buy gold as a safe haven. Gold mining shares are correlated with gold and only sold if the shock is severe.

This paper is motivated by a key difference of gold and gold mining shares. Gold is uncorrelated with the stock market whereas gold mining shares are correlated with gold and the stock market. We seek to use this difference to learn more about the flight to quality phenomenon and gold's safe haven property.

Figure 3.1 presents evidence that gold mining company shares are related to the price of gold and to the stock market. The gold and market betas are positively related and the majority of firms exhibit betas between zero and one. No gold mining company perfectly resembles gold as no company is uncorrelated with the market and highly correlated with gold. Most gold mining companies that exhibit gold betas close to one also exhibit market betas well above zero. The full sample including relatively illiquid gold mining companies exhibits smaller market betas and gold betas compared to the liquid sub-sample because non-trading days and implied zero returns reduce market and gold betas towards zero.

---

<sup>19</sup>Stocks are the “boats”, gold is the “port”, gold mining company stocks are the “boats in the proximity of the port”, financial turmoil is the “storm” and flight to quality is the “boats seeking shelter”.

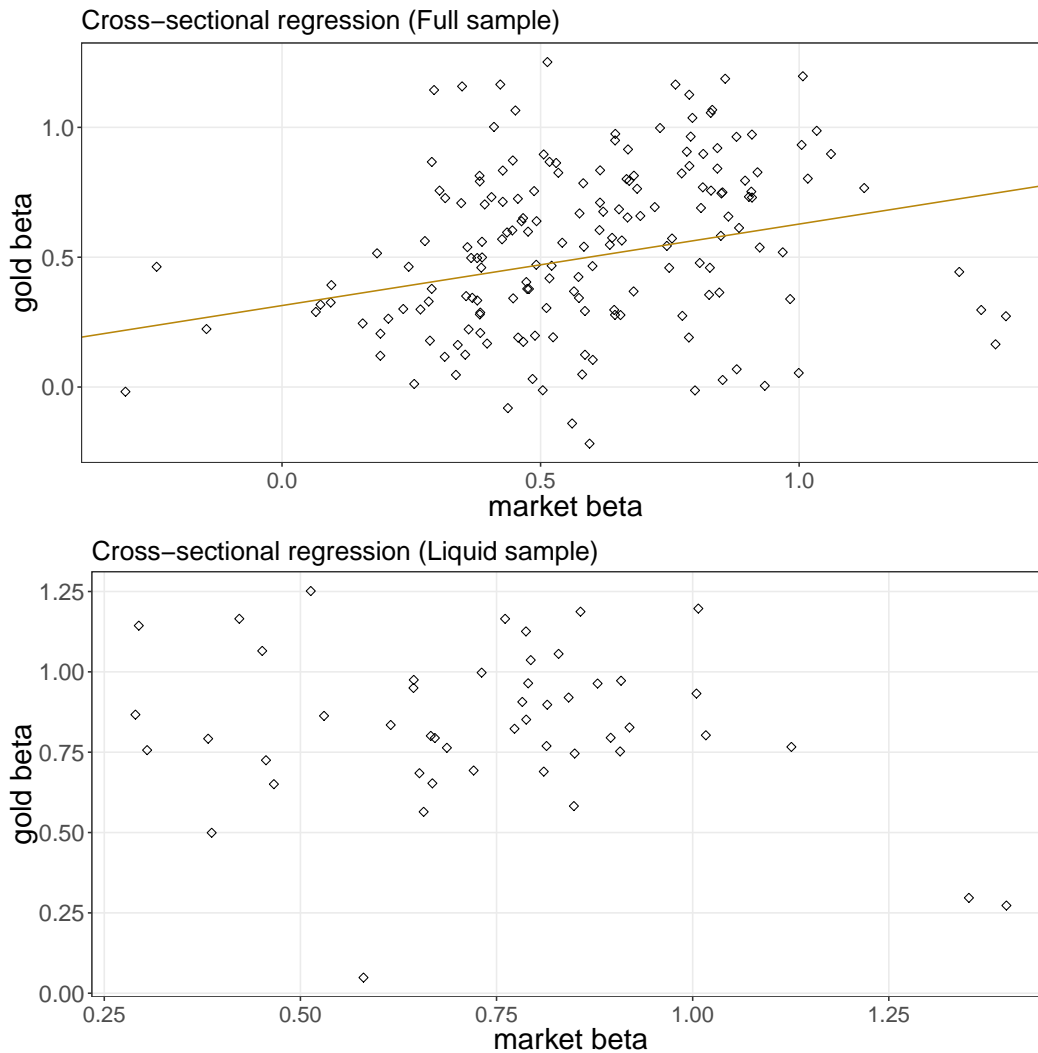


**Figure 3.1: Cross-sectional regression of gold betas on market betas**

Full sample (upper panel) and liquid sub-sample (lower panel). The regression line is depicted in the upper panel. Since the slope coefficient is insignificant for the liquid sub-sample, we exclude the regression line from the lower panel.

The double exposure of gold mining companies to gold price risk and market risk leads to some important questions. What happens in a crisis when gold assumes its safe haven characteristic? Do the prices of gold mining shares increase with the price of gold or fall with the market in a crisis period? We exploit the cross-section of gold mining companies to answer these questions and to enhance our understanding of the role of gold and gold mining companies in normal times and during financial turmoil.

We find that the performance of gold mining companies relative to gold depends on the severity of the financial shock or crisis. If the shock is extreme and consistent with a black swan event, e.g., the bankruptcy of Lehman Brothers, there is a flight to gold (“quality”) from all stocks including the stocks of gold mining companies. In contrast, if the shock is less extreme, e.g., after the Brexit

vote, there is a flight to both gold and gold mining shares inconsistent with a “classical” flight to quality.<sup>20</sup> One explanation for the difference between gold mining shares and gold bullion is that investors prefer physical and thus tangible gold in periods of extreme turmoil but are less concerned about the tangibility in less extreme periods.

The Brexit results even reveal an extreme (and unusual) case of flight to gold with gold mining shares significantly exceeding the positive returns of gold. We argue that this effect suggests that investors use the safe haven characteristic of gold not to reduce the risk but rather to increase the risk of their portfolios by investing in gold-related assets employing a (risky) “safe haven trade”.<sup>21</sup>

The analysis also shows that many gold mining shares are rather illiquid which implies that they cannot be traded in a crisis period at low cost (if at all) and that there is a flight to liquid gold mining shares or the more liquid gold bullion. Finally, we also uncover a link between the strength of the flight to gold bullion and the flight from gold mining companies, i.e., the stronger the flight from gold mining companies is, the stronger is the flight to gold bullion and vice versa. Whilst it is not surprising that the price effect is stronger if investors focus on one asset (gold) than on many assets (gold and gold mining shares), this finding is still novel and important to fully understand the flight to quality and safe haven phenomena.

The related literature covers studies on flight to quality or flight to safety and safe haven phenomena that do not analyze gold or gold mining companies, e.g., [Kaul and Sapp \(2006\)](#) and [Ranaldo and Söderlind \(2010\)](#) on safe haven effects of currencies and [Gulko \(2002\)](#), [Connolly \*et al.\* \(2005\)](#), [Baur and Lucey \(2009\)](#) and [Baele \*et al.\* \(2018\)](#) on flight to quality between stocks and bonds. [Beber \*et al.\* \(2009\)](#) investigate investors’ demand for quality and liquidity in different market conditions and find that liquidity is more important than quality.

Studies that analyze the financial characteristics of gold and its role as a hedge include [Sherman \(1982\)](#), [Jaffe \(1989\)](#), [Capie \*et al.\* \(2005\)](#), [Faugère and Van Erlach \(2005\)](#), and [Lucey \*et al.\* \(2006\)](#). An extension of the hedge characteristic of gold to periods of financial turmoil was introduced by [Baur and Lucey \(2010\)](#) for stocks and bonds and extended to a more comprehensive sample of markets in [Baur and McDermott \(2010\)](#). [Chan \*et al.\* \(2011\)](#) and [Ciner \*et al.\* \(2013\)](#) further expanded the analysis and included commodities (oil) and real estate and find that Treasury bonds and gold act as safe havens. [Creti \*et al.\* \(2013\)](#) examine links between 25 commodities and the stock market and find empirical evidence in support of the safe haven role of gold. [Reboredo \(2013\)](#) uses copulas to model the relationship between gold and the US-Dollar and finds strong support for the role of gold as a hedge and a safe haven (see also [Beckmann \*et al.\* \(2013\)](#) and [Bredin \*et al.\* \(2015\)](#)).

The value of gold mining companies and their exposure to the price of gold is analyzed in [Tufano \(1996\)](#), [Baur \(2014\)](#), [Lucey and O’Connor \(2017\)](#), and [Manas \*et al.\* \(2019\)](#). [Rockerbie](#)

---

<sup>20</sup>The Brexit vote can be defined as unlikely but expected albeit with a low probability whereas the September 11, 2001, terrorist attacks and the Lehman Brothers collapse can be defined as extremely unlikely or even unexpected and thus more consistent with a black swan event.

<sup>21</sup>This conclusion is based on the assumption that gold stocks are more risky than gold bullion. An alternative view would be that an investment in a portfolio of gold bullion and gold stocks is more diversified and thus less risky than an undiversified investment into gold bullion.



(1999), Selvanathan and Selvanathan (1999), and Moel and Tufano (2002) study the real option of gold mining companies to open and close mines. Adam *et al.* (2017) address the question why companies engage in selective hedging and find that smaller gold mining companies speculate more than larger ones. Other studies on the relationship between gold bullion and gold mining shares include Borenstein and Farrell (2008), Batten *et al.* (2017), and Reboredo and Ugolini (2017). Areal *et al.* (2013) find that US gold stocks act neither as a hedge nor as a safe haven for the US stock market. Using a wavelet methodology, Dar *et al.* (2019) find that gold mining stocks and gold are positively correlated.

We investigate the dynamic relationship of gold mining companies and gold bullion in times of financial turmoil. In the following, we define financial turmoil either as periods in which financial assets exhibit significant price declines or as periods of increased uncertainty in financial markets. Specifically, we analyze whether the share prices of gold mining companies increase with the price of gold or decouple from the price of gold when stock markets exhibit extreme negative returns and high volatility. We use this information to infer the severity of extreme events based on the different responses of gold prices and prices of gold mining shares after such events.

To the best of our knowledge there is no study that distinguishes between a flight to (physical) gold and a flight to gold mining companies and no study that uses this distinction to assess the severity of crises and the strength of flight to quality. Moreover, there is no study that uses a large and global sample of small cap, mid cap, and large cap gold mining companies to measure flight to quality or, more precisely, flight to gold.

We contribute to the literature with an identification of different types of flight to quality. This distinction provides a deeper understanding of investor behavior in response to different types of financial shocks. A detailed analysis of three selected events allows us to derive hypotheses about the relationship between the type of financial shock and the corresponding investor behavior. The roles of the liquidity of gold mining shares and the size of gold mining companies are also examined. Finally, we also contribute to the literature with an analysis of potential profit opportunities originating from a decoupling of gold mining companies from the price of gold during a crisis and an eventual recoupling after a crisis.

The paper is structured as follows: Section 3.2 introduces the data and presents descriptive statistics of the global sample of gold mining companies, gold, and stock markets. Section 3.3 presents the empirical analysis with the econometric modelling framework, the estimation results and a detailed discussion and interpretation of the results. Finally, Section 3.4 summarizes the main findings and provides concluding remarks.

## 3.2 Data

Our initial sample consists of 648 mining companies whose primary resource exploration, production or processing activities are attributed to the gold market according to Refinitiv Eikon.<sup>22</sup> While companies of our initial sample are being traded on nineteen distinct markets, the vast majority of mining stocks is listed on either the Australian, Canadian, UK or US market. Thus, we constrain our sample to these markets, leaving us with 609 gold mining companies to cover approximately 85% of the total market capitalization of the global gold mining sector.

Daily prices from January 1997 until September 2018 are obtained from Refinitiv Eikon, resulting in more than 5,000 observations per firm. Whilst the large number of gold mining companies allows a broader and potentially deeper analysis of the flight to gold phenomenon, it is important to note that many gold mining companies are relatively small and their shares illiquid, i.e., there are many days, often more than 50%, when there is no price change.

The concept of liquidity is generally considered as elusive and implies difficulties in both its definition and approximation (e.g., [Stoll, 2000](#); [Lesmond, 2005](#); [Chang et al., 2010](#)). Commonly employed estimators of market liquidity in the literature may be categorized into three distinct classes. The first class comprises estimators based on bid-ask quotes (e.g., [Chordia et al., 2000, 2001, 2004](#)). Despite the natural relation between quote information and liquidity, quote data accessibility is comparatively difficult to obtain and thus rare. This concern is especially relevant if the cross-section and/ or the time period becomes large, as it is the case in our sample of gold mining stocks. The second class of estimators is constructed from trade volume data as in Amihud’s ratio between absolute returns and trading volume (e.g., [Rouwenhorst, 1999](#); [Amihud, 2002](#); [Bekaert et al., 2007](#)). Since volume-based measures are not defined for zero volume days they are not suitable for this study. Finally, the third class of liquidity estimators is constructed from price data exclusively (e.g., [Roll, 1984](#); [Lesmond et al., 1999](#)). In view of the challenges in defining and measuring liquidity for a large sample of gold mining firms over multiple crisis periods, we adhere to [Lesmond et al. \(1999\)](#)’s suggestion to measure liquidity of such stocks based on the proportion of days with zero returns.<sup>23</sup> According to their study, informed investors avoid trading when transaction costs surpass the expected profits from trading, resulting in a zero return observation on that day. Employing this framework, we base our analysis on stocks which have at least 50% non-zero return observations over their complete sample period, leaving us with 175 out of 609 companies in our full sample. To shed light on the role of liquidity for the safe haven property, we additionally identify a more liquid sub-sample consisting of stocks that possess at least 80% non-zero return observations (49 out of 175 companies).<sup>24</sup>

---

<sup>22</sup>In more detail, Refinitiv Eikon allows to classify equities by industry sectors. We use this categorization to identify all 648 globally listed firms in the gold mining sector.

<sup>23</sup>Formally,  $ILL_i = \sum_{t=1}^{T_i} \mathbb{1}\{r_{i,t} = 0\} / T_i$ , where  $T_i$  is the total number of return observations of stock  $i$ , and the indicator function  $\mathbb{1}\{\cdot\}$  takes value of 1 for zero returns  $r$  of stock  $i$  at time  $t$ .

<sup>24</sup>[Lesmond et al. \(1999\)](#) provide evidence that the 80% threshold is in line with an approximate 5% difference between the observed and effective proportion of zero returns. Thus, we balance the need to obtain

Classifying gold mining companies based on different company characteristics is a difficult endeavor. For instance, grade, mining methods, and mine-types are highly complex characteristics and may even vary across different mines of a single firm (Ulrich *et al.*, 2019). Given the complex nature of alternative characteristics, we consider firm size as the best practical choice to further categorize the gold mining stocks in our sample. More specifically, we employ market capitalization (cap) as a measure of firm size. We divide the gold stocks of our full sample into three equally-sized groups composed of small cap, medium cap and large cap companies. Given the findings in Ulrich *et al.* (2019), we assume a positive relation between the size of gold assets (firms) and profitability, because larger mines usually have lower costs.

The sample also consists of the daily price of gold in US-Dollars per Troy ounce from the London Bullion Market and four stock market indices (Australian Stock Exchange (ASX) 200 for Australia, Toronto Stock Exchange (TSX) Composite for Canada, Financial Times Stock Exchange (FTSE) All Share for the UK, and Standard and Poor’s (S&P) 500 for the US) corresponding to the four markets on which the gold mining companies are listed.

Tables 3.11–3.14 in Appendix 3.5.2 present descriptive statistics of the returns on gold mining shares, gold returns and market returns. They reveal that gold mining companies exhibit both lower returns and higher risk than gold. For example, Table 3.14 shows that only one out of eleven gold mining companies listed in the US exhibits a higher average return and all gold mining shares are more risky than gold. Additional analyses of the Archipelago Exchange (NYSE ARCA) Gold Bugs and the Gold Miners price indices confirm this result.<sup>25</sup>

### 3.3 Empirical analysis

There are many studies that have shown that gold is uncorrelated with the market in normal times and in crisis times. In other words, gold has a market beta of zero and, per definition, a gold beta of one. In contrast, there are less studies on gold mining companies, their market betas and gold betas (see Baur (2014) and references therein). Figure 3.1 displays the distribution of market betas and gold betas for all gold mining companies in scatter plots pooled over the four markets considered (Australia, Canada, the UK, and the US). A summary of the estimates is presented in Table 3.1 for the full sample of gold mining companies and a sub-sample of companies with liquid gold mining shares. It shows that the market betas and gold betas generally deviate substantially from zero and one, i.e., from the gold benchmark. This implies that most gold mining companies are very different from gold on average. The coefficient estimates are generally larger for the liquid sub-sample, making it more gold-like in terms of the gold beta but also less gold-like in terms of the market beta.

---

a sufficiently large sample with an accurate identification of liquid stocks.

<sup>25</sup>For the 2010–2019 sample period, the daily returns of the NYSE ARCA Gold Bugs and Gold Miners indices are -0.037% and -0.028%, and the standard deviations of the returns are 2.4 and 2.1, respectively. The mean gold bullion return and standard deviation for the same period are 0.008% and 0.99, respectively.

**Table 3.1: Market betas and gold betas per market**

This table reports average market beta ( $\hat{\beta}_M$ ) and gold beta ( $\hat{\beta}_G$ ) across all gold mining companies. In addition,  $sd(\cdot)$  denotes the estimated (cross-sectional) standard deviation.

	$\hat{\beta}_M$	$sd(\hat{\beta}_M)$	$\hat{\beta}_G$	$sd(\hat{\beta}_G)$
<b>Panel A: Full sample</b>				
Australia	0.66	0.26	0.35	0.26
Canada	0.60	0.27	0.64	0.26
UK	0.32	0.35	0.66	0.47
US	0.32	0.35	0.66	0.47
<b>Panel B: Liquid sub-sample</b>				
Australia	0.83	0.30	0.63	0.21
Canada	0.76	0.20	0.86	0.16
UK	0.76	0.22	0.98	0.16
US	0.50	0.21	0.90	0.41

Estimating average market and gold betas do not automatically imply that the relationships among gold mining shares, the stock market and gold bullion are constant during crisis periods. Since the correlation of gold with the market varies in normal periods and in crisis periods, it is possible that gold mining betas vary through time and gold mining shares become more or less gold-like in crisis periods. We test this hypothesis with the following models:

$$r_{i,t} = a + \beta_1 r_{Gold,t} + \beta_2 r_{Gold,t} \mathbb{1}\{r_{S,t} < q_5\} + \varepsilon_{i,t}, \quad (3.1)$$

$$r_{i,t} = b + \gamma_1 r_{Gold,t} + \gamma_2 r_{Gold,t} D_1 + \gamma_3 r_{Gold,t} D_2 + \gamma_4 r_{Gold,t} D_3 + \varepsilon_{i,t}, \quad (3.2)$$

$$r_{i,t} = a + \delta_1 r_{Gold,t} + \delta_2 r_{Gold,t} \mathbb{1}\{\sigma_{S,t} > q_{95}\} + \varepsilon_{i,t}, \quad (3.3)$$

where  $r_{i,t}$  denotes the return of gold mining company  $i$  at time  $t$ ,  $r_{Gold,t}$  denotes the gold bullion return,  $r_{S,t}$  denotes the return of the domestic stock market index and  $\sigma_{S,t}$  denotes the estimated volatility of the domestic stock market index at time  $t$ . Using the first model, we investigate if gold betas increase in response to extreme negative daily shocks in the stock market (below the 5% quantile over a rolling window of two years denoted  $q_5$ ). The model closely follows the safe haven literature (Baur and Lucey, 2010). The second model focuses on three financial turmoil periods, the September 11, 2001, terrorist attacks, the bankruptcy of Lehman Brothers in September 2008, and the Brexit vote in June 2016. Those three events have very different characteristics. The September 11, 2001, terrorist attacks and the bankruptcy of Lehman Brothers were both largely unexpected events with extremely low probabilities and near-zero probabilities for the September 11 event consistent with a black swan event. In contrast, the Brexit vote was a shock to investors but not as unexpected and unlikely as the former two events. We use 20 trading days as duration of the events for an initial analysis but also study shorter and longer event windows. The third model considers periods in which the volatility of the domestic stock market exceeds its 95% quantile, denoted  $q_{95}$ . The chosen 95% quantile threshold yields 284 extreme periods and corresponds roughly to our pre-

selected crisis events. In general, the specification of thresholds, i.e., choosing the corresponding quantile in Equation 3.1 and Equation 3.3, determines how extreme the selected days (events) are. Figure 3.2 illustrates for the US sample how different specifications of our thresholds lead to the identification of different shock or crisis periods across the three models.

The graph illustrates that the shocks are too scattered in Equation 3.1 to identify clear and unique safe haven events and that Equation 3.2 and Equation 3.3 provide a more reliable identification of extreme financial shocks, most likely because of volatility clustering. We therefore use the 95% quantile for Equation 3.3 to balance the need for extreme periods and a sufficiently large sample size. Choosing higher threshold values, e.g., the 99% quantile (second panel of Figure 3.2), only selects periods during the global financial crisis (including the bankruptcy of Lehman Brothers) which makes our analysis too narrow and reduces the available number of observations to estimate the effect of extreme days. Instead, choosing quantiles between 75% and 90% provides very similar results for the Australian, the UK, and the US sample compared with the 95% benchmark.<sup>26</sup> We interpret this finding with the fact that volatility clusters and that high volatility periods are persistent. For the Canadian sample, the reaction is stronger if higher quantiles are chosen.

The estimation results presented in Tables 3.2–3.5 for the models provided in Equations 3.1–3.3 show that there is no homogeneous reaction of the gold betas to extreme negative shocks. The majority of estimates are positive for all countries except for the UK where the same number of statistically significant positive and negative  $\beta_2$  coefficients is reported for the model given in Equation 3.1. The crisis-specific reaction is more homogeneous with the first and second crises displaying mostly negative beta estimates ( $\gamma_2$  and  $\gamma_3$ ). The third event (Brexit) within Equation 3.2 exhibits positive crisis-betas for almost all firms across all countries. Finally, the third model based on extreme volatility yields negative beta estimates on average (summary panel in each table) for all countries except for the US.

These results indicate varying exposures of gold mining shares to the price of gold with a clear decoupling from the price of gold in response to large shocks, in specific crisis periods and in periods of high volatility. In the majority of cases there is a flight from gold mining companies to gold (bullion) represented by negative beta estimates. Only in response to the Brexit vote there is a flight to gold mining companies represented by positive beta estimates.

On a similar note, Table 3.6 provides gold beta estimates of equally weighted portfolios consisting of liquid gold mining stocks divided into different groups by their market capitalization.<sup>27</sup> The results demonstrate a similar reaction of gold shares in response to large shocks, specific crisis periods and periods of financial turmoil.

<sup>26</sup>The results for the models using different thresholds are not reported to conserve space but can be obtained from the authors upon request.

<sup>27</sup>Alternatively, we could estimate gold betas of a portfolio in which stocks are weighted based on their market capitalization. Since our sample contains some very large gold mining companies and many small ones, we prefer to assign them equal weights within their sub-categorization to ensure that each gold mining company has the same importance. Otherwise, our results could be primarily driven by the largest gold mining companies.

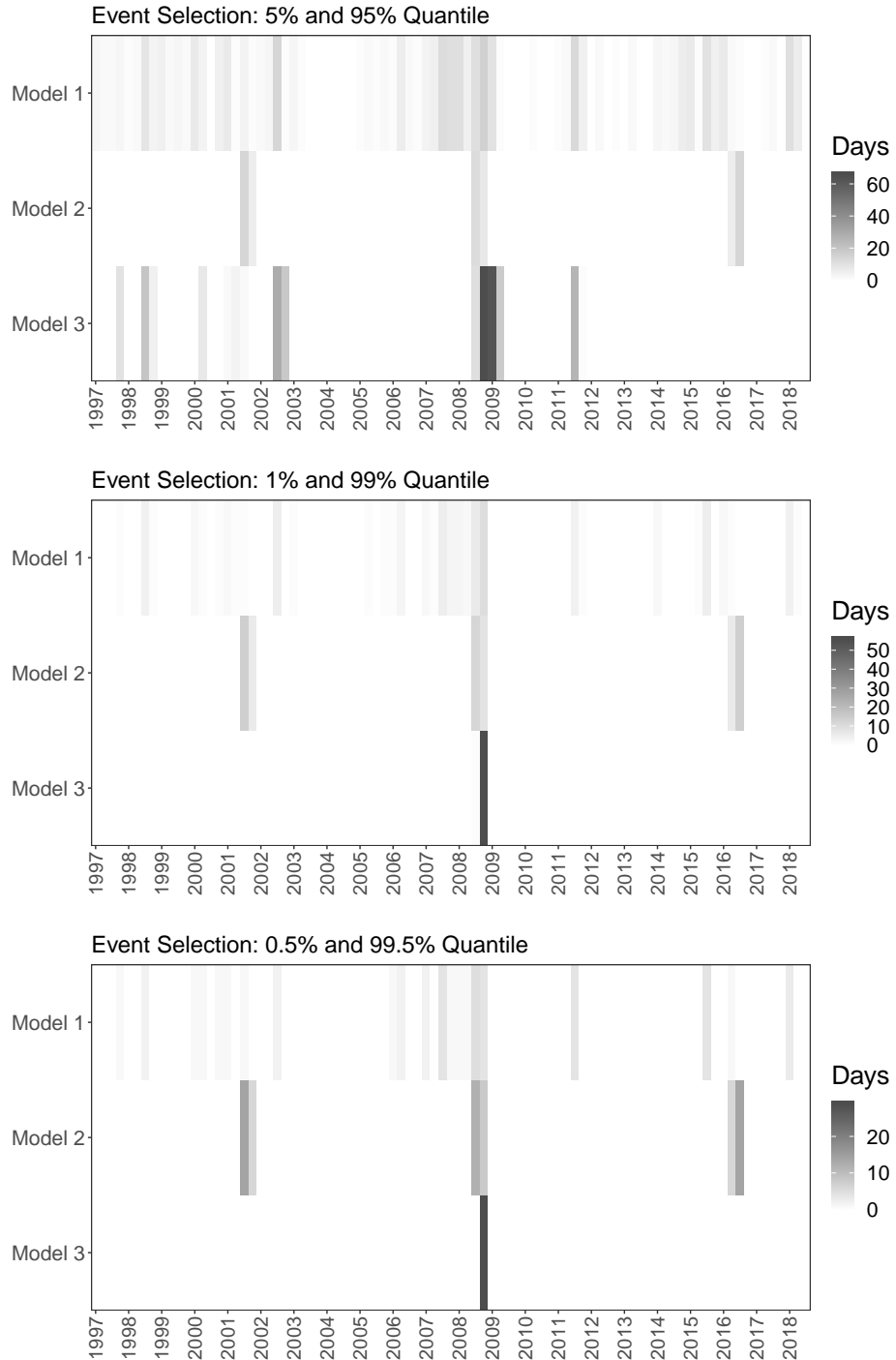


**Figure 3.2: Crisis period definitions (US)**

This figure depicts crisis period definitions based on different extreme stock market return and volatility thresholds for the US. The coloring indicates the number of event days that occur within each quarter between 1997 and 2018. Darker (brighter) coloring reflects a higher (lower) number of event days per quarter.

**Table 3.2: Gold beta estimates of liquid gold mining stocks (Australia)**

This table reports gold beta estimates of liquid Australia-listed gold mining companies. In more detail,  $\hat{\beta}_1$  and  $\hat{\beta}_2$  are the estimated model coefficients of Equation 3.1,  $\hat{\gamma}_1$ ,  $\hat{\gamma}_2$ ,  $\hat{\gamma}_3$  and  $\hat{\gamma}_4$  are the estimated model coefficients of Equation 3.2, and  $\hat{\delta}_1$  and  $\hat{\delta}_2$  are based on Equation 3.3. \*\*\*, \*\*, \* denote statistical significance at the 1%, 5%, and 10% level.

Company	Model 1 Return threshold		Model 2 Crisis events				Model 3 Volatility threshold	
	$\hat{\beta}_1$	$\hat{\beta}_2$	$\hat{\gamma}_1$	$\hat{\gamma}_2$	$\hat{\gamma}_3$	$\hat{\gamma}_4$	$\hat{\delta}_1$	$\hat{\delta}_2$
NEWCREST MINING	0.66***	0.38***	0.71***	-0.34	-0.50***	1.15**	0.74***	-0.27***
OZ MINERALS	0.35***	0.29*	0.40***	-3.06***	-0.10	-0.23	0.39***	-0.07
INDEPENDENCE GROUP	0.35***	0.18	0.38***		-0.28	0.50	0.40***	-0.15
OCEANAGOLD CDI	0.80***	0.42*	0.88***		-0.97***	1.03	0.98***	-0.49***
RESOLUTE MINING	0.96***	-0.09	0.97***	-0.49	-0.63**	1.89***	1.06***	-0.59***
PERSEUS MINING	0.76***	-0.08	0.80***		-1.29***	1.78**	0.88***	-0.55***
SILVER LAKE RESOURCES	0.93***	-0.46*	0.92***		-0.65**	1.27	1.08***	-0.64***
DORAY MINERALS	0.71***	-0.08	0.69***			0.85	0.67***	0.28
MEDUSA MINING	0.59***	0.18	0.63***		-0.48*	0.91	0.65***	-0.17
KINGSGATE CONSOLIDATED	0.63***	0.08	0.67***	-1.22*	-0.67**	-0.66	0.65***	-0.09
<i>Summary of estimated coefficients</i>								
Number of obs.	10.00	10.00	10.00	4.00	9.00	10.00	10.00	10.00
Mean	0.67	0.08	0.70	-1.28	-0.62	0.85	0.75	-0.27
Median	0.68	0.13	0.70	-0.85	-0.63	0.97	0.71	-0.22
Minimum	0.35	-0.46	0.38	-3.06	-1.29	-0.66	0.39	-0.64
Maximum	0.96	0.42	0.97	-0.34	-0.10	1.89	1.08	0.28
25% Quantile	0.60	-0.08	0.64	-1.68	-0.67	0.59	0.65	-0.54
75% Quantile	0.79	0.26	0.86	-0.45	-0.48	1.24	0.95	-0.10

**Table 3.3: Gold beta estimates of liquid gold mining stocks (Canada)**

This table reports gold beta estimates of liquid Canada-listed gold mining companies. In more detail,  $\hat{\beta}_1$  and  $\hat{\beta}_2$  are the estimated model coefficients of Equation 3.1,  $\hat{\gamma}_1$ ,  $\hat{\gamma}_2$ ,  $\hat{\gamma}_3$  and  $\hat{\gamma}_4$  are the estimated model coefficients of Equation 3.2, and  $\hat{\delta}_1$  and  $\hat{\delta}_2$  are based on Equation 3.3. \*\*\*, \*\*, \* denote statistical significance at the 1%, 5%, and 10% level.

Company	Model 1 Return threshold		Model 2 Crisis events				Model 3 Volatility threshold	
	$\hat{\beta}_1$	$\hat{\beta}_2$	$\hat{\gamma}_1$	$\hat{\gamma}_2$	$\hat{\gamma}_3$	$\hat{\gamma}_4$	$\hat{\delta}_1$	$\hat{\delta}_2$
BARRICK GOLD TSX	0.77***	0.40***	0.85***	-0.87*	-0.82***	1.19***	0.81***	0.09
GOLDCORP	0.86***	0.26***	0.92***	-1.27**	-0.80***	0.55	0.87***	0.12
AGNICO EAGLE MINES	0.88***	0.30***	0.95***	-0.36	-0.78***	0.58	0.93***	-0.02
KINROSS GOLD	1.02***	0.18	1.07***	-0.25	-0.77***	0.96	1.05***	-0.07
B2GOLD	0.90***	0.07	0.96***		-1.13***	1.94***	1.05***	-0.58***
OCEANAGOLD	1.00***	0.75***	1.13***		-0.76***	0.57	1.17***	-0.36**
IAMGOLD	1.02***	0.10	1.07***	-1.01	-1.07***	1.07*	1.03***	0.02
ALAMOS GOLD	0.86***	0.25*	0.93***		-0.91***	1.23*	0.99***	-0.54***
DETOUR GOLD	1.25***	0.55***	1.39***		-1.30***	0.56	1.29***	0.15
CENTERRA GOLD	0.85***	0.49***	0.99***		-1.51***	-0.05	0.92***	0.02
OSISKO GOLD ROYALTIES	0.75***	0.05	0.75***			0.16	0.76***	
SEMAFO	0.97***	0.27	1.05***	-2.86***	-1.03***	1.34	1.06***	-0.30*
ELDORADO GOLD	1.07***	0.26*	1.13***	1.55**	-0.83***	0.83	1.11***	0.00
NEW GOLD	0.79***	0.33*	0.86***	-1.07	-0.69**	1.25	0.78***	0.35**
CHINA GOLD INT RES	0.81***	0.10	0.84***	-0.85	-0.27	0.85	0.79***	0.21
ALACER GOLD	0.84***	0.34**	0.95***		-1.34***	0.19	0.90***	-0.05
DUNDEE PRCS MTLs	0.76***	0.06	0.80***	-0.12	-0.93***	-0.34	0.81***	-0.26***
TERANGA GOLD	0.78***	0.79***	0.87***			0.82	0.89***	0.07
TMAC RESOURCES	0.80***	-0.55	0.76***			-0.36	0.74***	
GOLDEN STAR RESOURCES	1.19***	0.54***	1.29***	0.08	-0.88**	0.29	1.25***	0.10
CORVUS GOLD	0.90***	0.90***	1.02***			-0.16	1.03***	-1.68
GOLD RESERVE A	0.71***	-0.16	0.75***	-2.29**	-1.09***	-2.27**	0.62***	0.47***
OREZONE GOLD	1.12***	0.18	1.15***			-0.68	1.13***	0.12
CHESAPEAKE GOLD	0.57***	-0.17	0.56***		-0.81***	2.34***	0.58***	-0.21
ALIO GOLD	0.94***	0.36*	1.06***		-1.32***	1.78**	1.16***	-0.72***
TANZANIAN RTY EXP A	0.72***	0.30	0.79***	-1.93*	-0.60	0.47	0.78***	-0.12
<i>Summary of estimated coefficients</i>								
Number of obs.	26.00	26.00	26.00	13.00	21.00	26.00	26.00	24.00
Mean	0.89	0.27	0.96	-0.86	-0.94	0.58	0.94	-0.13
Median	0.86	0.27	0.95	-0.87	-0.88	0.58	0.92	-0.01
Minimum	0.57	-0.55	0.56	-2.86	-1.51	-2.27	0.58	-1.68
Maximum	1.25	0.90	1.39	1.55	-0.27	2.34	1.29	0.47
25% Quantile	0.78	0.10	0.84	-1.27	-1.09	0.17	0.79	-0.27
75% Quantile	0.99	0.39	1.06	-0.25	-0.78	1.16	1.06	0.10



**Table 3.4: Gold beta estimates of liquid gold mining stocks (UK)**

This table reports gold beta estimates of liquid UK-listed gold mining companies. In more detail,  $\hat{\beta}_1$  and  $\hat{\beta}_2$  are the estimated model coefficients of Equation 3.1,  $\hat{\gamma}_1$ ,  $\hat{\gamma}_2$ ,  $\hat{\gamma}_3$  and  $\hat{\gamma}_4$  are the estimated model coefficients of Equation 3.2, and  $\hat{\delta}_1$  and  $\hat{\delta}_2$  are based on Equation 3.3. \*\*\*, \*\*, \* denote statistical significance at the 1%, 5%, and 10% level.

Company	Model 1 Return threshold		Model 2 Crisis events				Model 3 Volatility threshold	
	$\hat{\beta}_1$	$\hat{\beta}_2$	$\hat{\gamma}_1$	$\hat{\gamma}_2$	$\hat{\gamma}_3$	$\hat{\gamma}_4$	$\hat{\delta}_1$	$\hat{\delta}_2$
RANDGOLD RESOURCES	1.04***	0.28***	1.09***	-1.22**	-0.56***	1.88***	1.07***	0.00
POLYMETAL INT	0.93***	-0.01	0.92***			0.57	0.93***	-0.39
HOCHSCHILD MINING	1.02***	-0.45***	1.01***		-0.76***	1.22**	1.08***	-0.44***
HIGHLAND GOLD MINING	0.73***	0.54***	0.79***		-0.06	0.68	0.84***	-0.21
ACACIA MINING	1.27***	-0.01	1.23***			2.33***	1.29***	-0.27
PETROPAVLOVSK	1.02***	-0.28*	1.05***		-1.32***	-0.98	1.01***	-0.15
<i>Summary of estimated coefficients</i>								
Number of obs.	6.00	6.00	6.00	1.00	4.00	6.00	6.00	6.00
Mean	1.00	0.01	1.01	-1.22	-0.67	0.95	1.04	-0.24
Median	1.02	-0.01	1.03	-1.22	-0.66	0.95	1.04	-0.24
Minimum	0.73	-0.45	0.79	-1.22	-1.32	-0.98	0.84	-0.44
Maximum	1.27	0.54	1.23	-1.22	-0.06	2.33	1.29	-0.00
25% Quantile	0.95	-0.21	0.94	-1.22	-0.90	0.59	0.95	-0.36
75% Quantile	1.04	0.21	1.08	-1.22	-0.43	1.72	1.08	-0.17

**Table 3.5: Gold beta estimates of liquid gold mining stocks (US)**

This table reports gold beta estimates of liquid US-listed gold mining companies. In more detail,  $\hat{\beta}_1$  and  $\hat{\beta}_2$  are the estimated model coefficients of Equation 3.1,  $\hat{\gamma}_1$ ,  $\hat{\gamma}_2$ ,  $\hat{\gamma}_3$  and  $\hat{\gamma}_4$  are the estimated model coefficients of Equation 3.2, and  $\hat{\delta}_1$  and  $\hat{\delta}_2$  are based on Equation 3.3. \*\*\*, \*\*, \* denote statistical significance at the 1%, 5%, and 10% level.

Company	Model 1 Return threshold		Model 2 Crisis events				Model 3 Volatility threshold	
	$\hat{\beta}_1$	$\hat{\beta}_2$	$\hat{\gamma}_1$	$\hat{\gamma}_2$	$\hat{\gamma}_3$	$\hat{\gamma}_4$	$\hat{\delta}_1$	$\hat{\delta}_2$
NEWMONT MINING	0.75***	0.25**	0.80***	-0.32	-0.65***	0.53	0.80***	-0.13
ROYAL GOLD	0.83***	0.22*	0.87***	0.39	-0.40*	0.33	0.87***	-0.07
HECLA MINING	1.11***	0.24	1.14***	0.73	-0.23	0.19	1.10***	0.22
COEUR MINING	1.07***	0.19	1.08***	0.32	0.25	0.78	1.03***	0.36**
MCEWEN MINING	1.17***	-0.17	1.17***	-1.02	-0.76*	1.49	1.16***	-0.05
VISTA GOLD ASE	1.14***	-0.03	1.14***	1.30	-0.68	2.80**	1.07***	0.38
US GOLD	0.06	-0.26	0.05	-1.76*	-0.62*	1.33	0.11	-0.46***
<i>Summary of estimated coefficients</i>								
Number of obs.	7.00	7.00	7.00	7.00	7.00	7.00	7.00	7.00
Mean	0.87	0.06	0.89	-0.05	-0.44	1.06	0.88	0.04
Median	1.07	0.19	1.08	0.32	-0.62	0.78	1.03	-0.05
Minimum	0.06	-0.26	0.05	-1.76	-0.76	0.19	0.11	-0.46
Maximum	1.17	0.25	1.17	1.30	0.25	2.80	1.16	0.38
25% Quantile	0.79	-0.10	0.83	-0.67	-0.67	0.43	0.83	-0.10
75% Quantile	1.12	0.23	1.14	0.56	-0.31	1.41	1.08	0.29

**Table 3.6: Gold beta estimates of combined portfolios**

This table provides gold beta estimates of combined portfolios comprising liquid gold mining stocks. In more detail,  $\hat{\beta}_1$  and  $\hat{\beta}_2$  are the estimated model coefficients of Equation 3.1,  $\hat{\gamma}_1$ ,  $\hat{\gamma}_2$ ,  $\hat{\gamma}_3$  and  $\hat{\gamma}_4$  are the estimated model coefficients of Equation 3.2, and  $\hat{\delta}_1$  and  $\hat{\delta}_2$  are based on Equation 3.3. \*\*\*, \*\*, \* denote statistical significance at the 1%, 5%, and 10% level.

	Model 1 Return threshold		Model 2 Crisis events				Model 3 Volatility threshold	
	$\hat{\beta}_1$	$\hat{\beta}_2$	$\hat{\gamma}_1$	$\hat{\gamma}_2$	$\hat{\gamma}_3$	$\hat{\gamma}_4$	$\hat{\delta}_1$	$\hat{\delta}_2$
<b>Australia</b>								
<i>Sub-categorization by market capitalization</i>								
Large cap	0.66***	0.24**	0.70***	-1.06**	-0.44***	0.99**	0.74***	-0.30***
Mid cap	0.63***	0.08	0.67***	-1.22*	-0.67**	-0.66	0.65***	-0.09
<i>Combined portfolio of liquid gold mining shares</i>								
All stocks	0.65***	0.21**	0.69***	-1.09***	-0.48***	0.66	0.72***	-0.26***
<b>Canada</b>								
<i>Sub-categorization by market capitalization</i>								
Large cap	0.83***	0.23***	0.90***	-0.73*	-0.77***	0.63	0.87***	-0.06
Mid cap	0.72***	0.30	0.79***	-1.93*	-0.60	0.47	0.78***	-0.12
<i>Combined portfolio of liquid gold mining shares</i>								
All stocks	0.82***	0.24***	0.89***	-0.81*	-0.76***	0.62	0.87***	-0.07
<b>UK</b>								
<i>Sub-categorization by market capitalization</i>								
Large cap	1.04***	0.28***	1.09***	-1.22**	-0.56***	1.88***	1.07***	-0.01
<i>Combined portfolio of liquid gold mining shares</i>								
All stocks	1.04***	0.28***	1.09***	-1.22**	-0.56***	1.88***	1.07***	-0.01
<b>US</b>								
<i>Sub-categorization by market capitalization</i>								
Large cap	0.90***	0.23**	0.94***	0.16	-0.34*	0.47	0.92***	0.05
Mid cap	1.16***	-0.12	1.16***	-0.25	-0.74**	1.92**	1.13***	0.09
Small cap	0.06	-0.26	0.05	-1.76*	-0.62*	1.33	0.11	-0.46***
<i>Combined portfolio of liquid gold mining shares</i>								
All stocks	0.86***	0.09	0.88***	-0.08	-0.47***	1.00**	0.87***	0.02

The results for the full sample including companies with relatively illiquid shares yield similar results in general. However, due to the lower liquidity, the gold beta estimates are generally smaller in absolute terms compared to the more liquid sub-sample. This finding is intuitive, given that the number of non-trading zero return observations for gold mining companies not included in the liquid sub-sample is higher, which leads to lower absolute betas.

### 3.3.1 Event study methodology framework

Since the beta estimates may be noisy due to the relatively short crises periods, we also consider an alternative framework based on an event study methodology. We calculate (i) cumulative returns (CR) conditional on a crisis period but unconditional on any factor such as gold or market returns, and (ii) cumulative abnormal gold returns (CAGR) conditional on a crisis period and on gold returns for each gold mining company. While the CR estimates do not require any model, the CAGR estimates are based on a simple market model with gold returns being the market. The two models also differ in another and more important aspect: The CR analysis investigates if gold mining companies hold their pre-crisis value in a crisis and thus act as a safe haven whereas the CAGR analysis evaluates whether investors show a preference for gold mining companies over gold during a crisis.

#### Cumulative returns

We calculate the cumulative returns (CR) for each gold mining company  $i$  over the crisis window  $[\tau_1, \tau_2]$ ,

$$CR_i = \sum_{t=\tau_1}^{\tau_2} r_{i,t}, \quad (3.4)$$

and interpret the sign of the CRs over different event windows. More specifically, we use the cumulative returns (CR) to identify if gold and gold mining companies act as a weak or strong safe haven as follows:

- CR = 0: weak safe haven
- CR > 0: strong safe haven
- CR < 0: no safe haven

If the cumulative return is not different from zero, the gold mining company exhibits the dynamics of a weak safe haven. If the cumulative return is greater than zero, the company exhibits the dynamics of a strong safe haven and if the cumulative return is smaller than zero the company does not display features of a safe haven. We analyze cumulative returns for all gold mining companies divided into groups by their respective market capitalization and exploit the full cross-section of companies to obtain average estimates of the safe haven effect.

Table 3.7 shows the evolution of the unconditional cumulative returns of gold, small cap, mid cap, and large cap gold miners and the respective market over the three crisis periods. The last row of the table presents the cross-sectional average over all gold mining companies in each country and a cross-sectional test that the average is zero.

The strongest negative reaction is observed after the bankruptcy of Lehman Brothers whilst the strongest positive reaction is observed after the Brexit vote. Although the results for 9/11 are less clear-cut, they indicate that some gold mining companies acted as a safe haven during that period. It seems that gold mining stocks negatively decoupled from the price of gold during the bankruptcy of Lehman Brothers and positively decoupled from the price of gold after the Brexit vote.

The fact that there is no clear pattern across the size of companies, across countries, and across crisis events is related to the heterogeneity of gold firms, firm-specific differences, and country-specific differences such as different costs per ounce, different environmental regulations, and different hedging practices. These differences may result in different performances during periods of financial turmoil across firms and countries.

Our CR estimates also reveal a negative relationship between the magnitude of the gold safe haven effect and the reaction of gold mining companies, i.e., the larger and stronger the gold price reaction is, the stronger is the decoupling and vice versa. In other words, if investors flee from stocks and even from gold mining companies, the effect on gold is stronger compared with a situation when investors flee from stocks but not from gold mining companies. If the flight is concentrated on one asset, the price impact is stronger than if the flight is distributed over a larger set of assets, in our case gold and gold mining shares. During the Lehman Brothers crisis, it seems that the flight to gold was focused on gold and did not include gold mining companies, resulting in the strongest positive gold price reaction and the strongest negative gold mining share price reaction in comparison with the 9/11 crisis and the Brexit vote.

### Cumulative abnormal gold returns

In a second step, we use a “classical” event study framework following [MacKinlay \(1997\)](#) and analyze abnormal gold returns in a crisis period.

It is important to note that this framework is not employed to find abnormal portfolio returns relative to the market but instead to analyze the performance of gold mining shares relative to gold bullion in a crisis period. Consequently, the approach exclusively provides a means to assess deviations between the returns of gold mining shares and gold bullion. We henceforth refer to the cumulative abnormal returns of gold mining shares over gold bullion simply as CAGR.

We estimate the following gold market model based on a 2-year pre-crisis period estimation window for each gold mining firm  $i$ :

$$r_{i,t} = a + b r_{Gold,t} + \varepsilon_{i,t}. \quad (3.5)$$

**Table 3.7: Cumulative returns**

This table provides percentage cumulative returns over 5, 10, 15, and 20 trading days for three defined crisis events. The respective panels show (i) cumulative returns sub-categorized by market capitalization, (ii) a proportional division into positive and negative cumulative returns, and (iii) the average cumulative returns of all liquid mining companies. \*\*\*, \*\*, \* denote statistical significance at the 1%, 5%, and 10% level.

Event	9/11				Lehman Brothers				Brexit			
Holding period	5	10	15	20	5	10	15	20	5	10	15	20
<b>Australia</b>												
<i>Sub-categorization by market capitalization</i>												
Gold	7.71	5.97	6.80	7.23	14.69	18.42	9.86	18.25	4.38	7.71	5.98	3.96
Index	-9.28	-10.32	-4.53	-3.22	-2.05	0.02	-4.34	-21.36	-2.47	-1.40	2.21	4.05
Large cap	-1.63	-8.10	-3.33	2.75	8.53	18.31	1.50	-22.39	7.27	21.61	25.94	19.39
Mid cap	-9.55	-0.38	-0.38	11.39	19.97	14.74	6.03	-17.52	4.85	17.71	17.90	12.45
<i>Proportional return-sign allocation of CR</i>												
Positive CR	0.50	0.25	0.25	0.50	0.78	1.00	0.56	0.22	0.78	1.00	1.00	1.00
Negative CR	0.50	0.75	0.75	0.50	0.22	0.00	0.44	0.78	0.22	0.00	0.00	0.00
<i>CR average of gold mining shares</i>												
All stocks	-3.61	-6.17	-2.59	4.91	11.07	17.52	2.51	-21.30	6.74	20.74	24.16	17.85
<b>Canada</b>												
<i>Sub-categorization by market capitalization</i>												
Gold	7.71	5.97	6.80	7.23	14.69	18.42	9.86	18.25	4.38	7.71	5.98	3.96
Index	-6.13	-9.76	-7.72	-6.33	1.12	-5.17	-16.72	-34.26	0.23	1.61	3.44	3.71
Large cap	6.53	4.01	13.52	7.38	4.38	6.74	-9.21	-27.54	5.44	14.76	13.93	7.22
Mid cap	0.00	-8.70	-18.23	-21.62	-2.70	-2.13	-11.13	-15.66	17.38	40.83	34.91	30.04
<i>Proportional return-sign allocation of CR</i>												
Positive CR	0.80	0.64	0.82	0.75	0.57	0.70	0.24	0.14	0.92	0.92	0.88	0.76
Negative CR	0.20	0.36	0.18	0.25	0.43	0.30	0.76	0.86	0.08	0.08	0.12	0.24
<i>CR average of gold mining shares</i>												
All stocks	7.18	3.22	11.87	4.96	3.36	5.75	-9.49	-25.84	7.39	18.72	17.11	10.87
<b>UK</b>												
<i>Sub-categorization by market capitalization</i>												
Gold	7.71	5.97	6.80	7.23	14.69	18.42	9.86	18.25	4.38	7.71	5.98	3.96
Index	-3.41	-9.83	-6.32	-1.72	-1.76	-6.56	-8.91	-31.45	0.13	1.12	4.84	5.85
Large cap	-0.52	-0.43	3.51	-6.20	10.66	10.00	-10.54	-27.19	14.83	30.46	31.23	26.40
<i>Proportional return-sign allocation of CR</i>												
Positive CR	0.00	0.00	1.00	0.00	0.75	0.75	0.50	0.25	0.83	1.00	1.00	0.83
Negative CR	1.00	1.00	0.00	1.00	0.25	0.25	0.50	0.75	0.17	0.00	0.00	0.17
<i>CR average of gold mining shares</i>												
All stocks	-0.52	-0.43	3.51	-6.20	10.66	10.00	-10.54	-27.19	14.83	30.46	31.23	26.40
<b>US</b>												
<i>Sub-categorization by market capitalization</i>												
Gold	7.71	5.97	6.80	7.23	14.69	18.42	9.86	18.25	4.38	7.71	5.98	3.96
Index	-5.05	-8.51	-5.07	-2.79	0.27	-3.14	-12.99	-33.07	-0.71	0.68	3.16	4.11
Large cap	11.61	10.99	22.67	20.42	13.05	11.17	-12.48	-14.92	7.14	19.69	24.06	18.22
Mid cap	15.86	13.68	9.04	20.06	21.90	24.90	-1.61	-28.70	26.39	30.67	30.27	9.68
Small cap	-7.59	-0.94	-6.09	-9.97	-14.41	-12.97	-20.42	-53.51	-10.38	-20.22	-40.55	-27.37
<i>Proportional return-sign allocation of CR</i>												
Positive CR	0.86	0.86	0.71	0.86	0.71	0.86	0.29	0.14	0.86	0.86	0.86	0.86
Negative CR	0.14	0.14	0.29	0.14	0.29	0.14	0.71	0.86	0.14	0.14	0.14	0.14
<i>CR average of gold mining shares</i>												
All stocks	10.08	10.06	14.67	15.98	11.65	11.64	-10.51	-24.37	10.14	17.13	16.60	9.27
<b>Global</b>												
<i>CR average of gold mining shares</i>												
	5.31***	3.36***	9.43***	7.70***	7.18**	9.61	-7.13	-24.72	8.60***	20.48**	20.28***	13.95***

We define gold bullion as our market to precisely measure the individual gold mining company's performance relative to gold bullion in crisis periods. We predict the returns in the event window,  $\hat{r}_{i,t}$ , using the coefficient estimates of Equation 3.5 and calculate the abnormal gold returns  $\widehat{AGR}_{i,t}$  as:

$$\widehat{AGR}_{i,t} = r_{i,t} - \hat{r}_{i,t}, \quad t = \tau_1, \tau_1 + 1, \dots, \tau_2, \quad (3.6)$$

for the event window  $[\tau_1, \tau_2]$ . The cumulative abnormal gold returns are the sum of all abnormal gold returns over the event window:

$$\widehat{CAGR}_{i,t} = \sum_{t=\tau_1}^{\tau_2} \widehat{AGR}_{i,t}. \quad (3.7)$$

To evaluate whether the CAGRs are significantly different from zero, we compute the test statistic:

$$\frac{1}{\sqrt{\tau_2 - \tau_1}} (\widehat{CAGR}_{i,t} / \hat{\sigma}_i), \quad (3.8)$$

where  $\hat{\sigma}_i^2$  is the sample variance estimated from the residuals of Equation 3.5 over the full sample. The factor  $1/\sqrt{\tau_2 - \tau_1}$  adjusts for the event window length over which the cumulative abnormal gold returns are computed. Rejecting the null hypothesis means that gold mining company  $i$  performs significantly different from gold bullion in a crisis period. The signs of our estimated CAGRs do not only provide us with information about what type of assets investors buy and sell but also their preference for gold mining shares versus gold bullion. We propose the following interpretation of zero, positive and negative CAGRs:

- CAGR = 0: weak flight to gold (bullion)
- CAGR > 0: no “classical” flight to gold (bullion) but to gold mining shares (safe haven trade)
- CAGR < 0: strong flight to gold (bullion)

While CRs identify the existence of the safe haven property of gold mining companies, CAGRs determine the strength of a flight to gold. Should the CAGRs be zero, prices for gold mining shares follow similar trajectories as gold bullion and we interpret this as evidence for investors not having a preference for gold (bullion) over gold mining shares in crisis periods. This, in turn, means that if the flight to gold includes gold mining shares there is a weak flight to gold (bullion) and if the flight to gold excludes gold mining shares (negative CAGRs, i.e., a flight from gold mining shares) there is a strong flight to gold (bullion). Positive CAGRs display a preference for gold mining shares and thus a non-classical flight to quality as the “quality” is not a low risk asset but a high risk asset. In this scenario, investors trade on the safe haven property assuming that gold mining shares are strongly linked to gold.

CAGRs computed in this way do not only enable us to identify a potential preference for gold mining shares relative to gold but also a longer-term decoupling of gold mining shares from gold. We investigate such decoupling phenomena by analyzing the evolution of CAGRs over time after the

crisis event. This analysis is motivated by the idea that a crisis-induced decoupling of the price of gold mining shares from the price of gold implies a temporary mispricing and an expected recoupling with the price of gold to its pre-crisis relationship.

Table 3.8 shows the results of the CAGR analysis for liquid stocks and offers various interesting results. Firstly, we find an average preference for gold bullion in the 9/11 crisis (reported in the panel labelled “Global”), a very strong preference for gold bullion in the Lehman Brothers crisis, and a clear preference for gold mining shares after Brexit contrasting the preference for gold observed in the 9/11 and 2008 crises. However, there are variations from this general observation when we turn to the individual markets. For instance, Canadian gold miners outperform gold in the first 5 days after 9/11 and US large cap miners outperform gold over 10, 15, and 20 days after the event. Secondly, the results show that small cap miners do not perform well over all three events compared with larger mining companies and clearly underperform larger miners following the Brexit vote. Since the Brexit reaction can be considered a risky safe haven trade one explanation is that investors preferred less risky large cap or medium cap gold miners over riskier small cap miners.

To better understand the role of company size on both the safe haven property and the strength of the flight to gold phenomenon, we pool all liquid stocks and re-estimate the CRs and CAGRs. The gold shares are categorized into large cap shares (larger than 1 billion US-Dollars), mid cap shares (between 100 million and 1 billion US-Dollars), and small cap shares (less than 100 million US-Dollars).<sup>28</sup> Table 3.9 comprises the results of the CR and CAGR estimates for the global cross-section of firms.<sup>29</sup> The table indicates a weaker reaction, i.e., smaller absolute returns, for large cap shares than for mid cap shares. In addition, we find that small cap shares underperform mid cap shares in all event periods. The results indicate that larger gold firms are less risky than smaller gold firms.

Finally, we analyze the trading volume of large cap, mid cap, and small cap miners for all markets and all three crisis-periods with the aim to better understand the role of liquidity for flights to gold.<sup>30</sup> We hypothesize that investors prefer the more liquid gold bullion over the less liquid gold mining shares and within the group of gold mining shares, we expect that investors prefer the more liquid large cap firms over the less liquid mid cap and small cap firms.

Figures 3.3–3.6 in Appendix 3.5.1 present the trading volume for the three crisis periods and confirm the hypotheses that large cap miners are more liquid than mid cap miners which in turn

---

<sup>28</sup>To investigate the role of company size towards CRs and CAGRs in the pooled sample, we rely on different rules to categorize companies into groups than in the initial market-specific analysis. In turn, however, these rules allow us to obtain a more even balancing of companies per group. We also explore 30 million and 300 million US-Dollars as different thresholds of market capitalization to categorize the global cross-section of gold mining shares into groups. The results are qualitatively similar and available upon request.

<sup>29</sup>While pooling gold mining companies across different markets ignores that prices are formed over different trading periods, the number of liquid gold mining shares is too small to conduct the same analysis for each market with a sufficient number of observations.

<sup>30</sup>The link between crisis periods and liquidity has been established empirically in Longstaff (2004), Chordia *et al.* (2005), Goyenko and Ukhov (2009), and Florackis *et al.* (2014).

**Table 3.8: Cumulative abnormal gold returns**

This table provides percentage cumulative abnormal gold returns over 5, 10, 15, and 20 trading days for three defined crisis events. The respective panels show (i) cumulative abnormal gold returns sub-categorized by market capitalization, (ii) a proportional division into positive and negative cumulative abnormal gold returns, and (iii) the average cumulative abnormal gold returns of all liquid mining companies. \*\*\*, \*\*, \* denote statistical significance at the 1%, 5%, and 10% level.

Event	9/11				Lehman Brothers				Brexit			
Holding period	5	10	15	20	5	10	15	20	5	10	15	20
<b>Australia</b>												
<i>Sub-categorization by market capitalization</i>												
Large cap	-5.60	-10.23	-8.95	-5.96	-0.98	9.75	-2.49	-37.24	2.79	13.67	19.49	14.70
Mid cap	-14.68	-4.05	-10.95	-2.13	16.34	10.07	3.23	-22.47	0.29	6.76	8.85	7.40
<i>Proportional return-sign allocation of CAGR</i>												
Positive CAGR	0.25	0.00	0.25	0.25	0.57	1.00	0.43	0.14	0.70	0.90	0.90	0.90
Negative CAGR	0.75	1.00	0.75	0.75	0.43	0.00	0.57	0.86	0.30	0.10	0.10	0.10
<i>CAGR average of gold mining shares</i>												
All stocks	-7.87	-8.69	-9.45	-5.00	3.97	9.84	-0.86	-33.02	2.04	11.60	16.30	12.51
<b>Canada</b>												
<i>Sub-categorization by market capitalization</i>												
Large cap	1.17	-2.75	2.70	-0.78	-4.88	-4.28	-13.85	-36.01	0.11	4.91	6.38	1.83
Mid cap	1.20	-11.10	-20.92	-24.39	-11.15	-12.73	-16.85	-26.20	12.35	32.12	29.08	27.45
<i>Proportional return-sign allocation of CAGR</i>												
Positive CAGR	0.67	0.58	0.42	0.50	0.33	0.28	0.11	0.00	0.48	0.88	0.80	0.40
Negative CAGR	0.33	0.42	0.58	0.50	0.67	0.72	0.89	1.00	0.52	0.12	0.20	0.60
<i>CAGR average of gold mining shares</i>												
All stocks	1.17	-3.44	0.73	-2.75	-5.93	-5.69	-14.35	-34.38	2.07	9.27	10.01	5.93
<b>UK</b>												
<i>Sub-categorization by market capitalization</i>												
Large cap	-3.84	-4.70	-6.05	-23.08	-8.76	-8.72	-22.90	-40.68	9.57	21.19	23.86	21.27
<i>Proportional return-sign allocation of CAGR</i>												
Positive CAGR	0.00	0.00	0.00	0.00	0.33	0.33	0.00	0.00	0.83	0.83	0.83	0.83
Negative CAGR	1.00	1.00	1.00	1.00	0.67	0.67	1.00	1.00	0.17	0.17	0.17	0.17
<i>CAGR average of gold mining shares</i>												
All stocks	-3.84	-4.70	-6.05	-23.08	-8.76	-8.72	-22.90	-40.68	9.57	21.19	23.86	21.27
<b>US</b>												
<i>Sub-categorization by market capitalization</i>												
Large cap	-4.64	10.76	12.71	14.87	3.16	-0.98	-18.34	-26.28	0.32	7.66	14.54	11.64
Mid cap	-7.36	-3.04	4.21	8.40	9.67	10.46	-7.05	-40.61	19.15	17.89	20.07	2.51
Small cap	-1.00	-4.41	-3.84	-12.02	-14.47	-12.52	-18.87	-51.69	-9.77	-18.84	-37.64	-22.90
<i>Proportional return-sign allocation of CAGR</i>												
Positive CAGR	0.00	0.57	0.71	0.71	0.57	0.57	0.14	0.14	0.57	0.86	0.86	0.86
Negative CAGR	1.00	0.43	0.29	0.29	0.43	0.43	0.86	0.86	0.43	0.14	0.14	0.14
<i>CAGR average of gold mining shares</i>												
All stocks	-4.89	4.65	7.92	9.18	2.50	0.64	-15.19	-34.01	4.26	6.80	8.66	4.10
<b>Global</b>												
<i>CAGR average of gold mining shares</i>												
	-2.31	-2.01	0.85	-0.49	2.51	-1.58	-12.55***	-34.57***	3.32***	10.88***	12.85***	8.95***



**Table 3.9: Pooled cumulative returns and cumulative abnormal gold returns**

This table offers percentage cumulative returns and percentage cumulative abnormal gold returns over 5, 10, 15, and 20 trading days for three defined crisis events. We report the results for a global cross-section of gold mining shares, categorized into different groups based on their market capitalization. More specifically, we distinguish between large cap miners (market capitalization above 1 billion US-Dollars), mid cap miners (market capitalization between 100 million and 1 billion US-Dollars), and small cap miners (market capitalization below 100 million US-Dollars).

Event	9/11				Lehman Brothers				Brexit			
	Holding period	5	10	15	20	5	10	15	20	5	10	15
<b>Cumulative returns</b>												
<i>Sub-categorization by market capitalization</i>												
Gold	7.71	5.97	6.80	7.23	14.69	18.42	9.86	18.25	4.38	7.71	5.98	3.96
Large cap	3.00	0.04	6.49	1.97	7.58	13.25	-4.68	-20.98	6.67	17.89	18.63	11.50
Mid cap	8.03	5.77	13.56	14.81	7.60	6.24	-9.85	-24.70	10.09	24.46	24.46	18.79
Small cap	8.07	11.34	11.15	13.57	4.80	8.26	-6.78	-36.02	10.09	15.88	12.18	5.50
<i>Proportional return-sign allocation of CR</i>												
Positive CR	0.70	0.58	0.67	0.71	0.66	0.78	0.34	0.17	0.88	0.94	0.92	0.81
Negative CR	0.30	0.42	0.33	0.29	0.34	0.22	0.66	0.83	0.12	0.06	0.08	0.19
<i>CR average of gold mining shares</i>												
All stocks	5.54	3.36	9.43	7.70	7.18	9.61	-7.13	-24.72	8.60	20.33	20.12	13.66
<b>Cumulative abnormal gold returns</b>												
<i>Sub-categorization by market capitalization</i>												
Large cap	-5.29	-1.83	-2.07	-5.76	-3.57	0.94	-10.75	-31.39	1.90	9.10	11.84	7.06
Mid cap	2.41	-2.93	2.37	4.84	-0.36	-5.02	-15.65	-36.72	4.34	14.34	16.67	13.70
Small cap	-2.00	-0.33	9.42	8.11	-4.45	-1.21	-10.60	-39.82	4.64	6.34	5.01	1.06
<i>Proportional return-sign allocation of CAGR</i>												
Positive CAGR	0.38	0.46	0.46	0.50	0.43	0.49	0.17	0.06	0.58	0.88	0.83	0.62
Negative CAGR	0.62	0.54	0.54	0.50	0.57	0.51	0.83	0.94	0.42	0.12	0.17	0.38
<i>CAGR average of gold mining shares</i>												
All stocks	-2.31	-2.01	0.85	-0.49	-2.51	-1.58	-12.55	-34.57	3.32	10.88	12.85	8.95

are more liquid than small cap miners (in line with, e.g., [Brunnermeier, 2009](#); [Anand et al., 2013](#); [Florackis et al., 2014](#)). The crisis-specific performance of the miners is aligned with the trading volume, i.e., large cap miners often perform best within the group of gold mining shares whereas small cap miners often perform worst within this group.

The results suggest that investors do not sell bullion in a crisis but rather the less liquid gold mining shares with trading volumes concentrated at large cap gold mining shares.<sup>31</sup>

<sup>31</sup>Estimates by the World Gold Council and CME Group data on gold futures indicate that gold bullion is more liquid than gold mining shares and even more liquid than a hypothetical portfolio of very large gold miners. Daily trading volume of 145 billion US-Dollars for gold bullion ([World Gold Council, 2021](#)) is larger than the average daily trading volume of 20 million US-Dollars for Barrick Gold, one of the largest gold mining companies ([Bloomberg, 2021](#)). Even if the sample of gold mining companies consisted of 1,000 large cap gold miners with a daily trading volume of 20 million US-Dollars each, the aggregate trading volume (20

### 3.3.2 Profit opportunity due to recoupling

This section analyzes if any mispricing of gold mining shares due to a decoupling of the share price from the price of gold leads to a correction and realignment of the share price and the gold price to pre-crisis levels over the subsequent year. Table 3.10 displays long-term CAGR estimates and shows whether there is a reversal over 50, 100, 150 or 200 days with respect to the start of the crisis period.<sup>32</sup>

The negative mispricing and decoupling from gold (prices of gold mining shares fell by more than implied by the pre-crisis gold relationship) in the 9/11 and Lehman Brothers crises and the positive mispricing and decoupling (prices of gold mining shares increased by more than implied by the pre-crisis gold relationship) after the Brexit vote are fully corrected over longer horizons. Specifically, based on the average effect across all stocks (last line labelled “Global” in the table) the negative decoupling for the 9/11 crisis is fully corrected after 100 days but only after 200 days for the Lehman Brothers event; the positive decoupling after the Brexit vote is fully corrected after 50 days. These results vary across countries, e.g., the correction after the 9/11 event takes longer for the UK-listed miners (150 days) and less time for the Australia-listed miners (50 days).

These corrections and re-alignments to the pre-crisis gold price relationship imply very large returns for some post-crisis periods and some gold mining companies. For example, the percentage return of an investment in large cap gold miners in response to a decoupling yield returns of almost 60% for Canadian and US-listed shares and up to 80% for Australian shares after the 9/11 crisis. The returns are generally smaller but qualitatively similar for a larger sample including less liquid gold mining companies.

---

billion US-Dollars) would still be significantly below that of gold bullion (145 billion US-Dollars).

<sup>32</sup>The decoupling and recoupling is also observed for an alternative market model with both gold and stock index returns included.

**Table 3.10: Cumulative abnormal gold returns (Long-term)**

This table provides percentage cumulative abnormal gold returns over 50, 100, 150, and 200 trading days for three defined crisis events. The respective panels show (i) cumulative abnormal gold returns sub-categorized by market capitalization, (ii) a proportional division into positive and negative cumulative abnormal gold returns, and (iii) the average cumulative abnormal gold returns of all liquid mining companies. \*\*\*, \*\*, \* denote statistical significance at the 1%, 5%, and 10% level.

Event	9/11				Lehman Brothers				Brexit			
Holding period	50	100	150	200	50	100	150	200	50	100	150	200
<b>Australia</b>												
<i>Sub-categorization by market capitalization</i>												
Large cap	14.15	44.93	59.70	79.25	-69.70	-38.40	-20.96	-4.06	3.83	19.18	15.55	-3.60
Mid Cap	32.76	50.79	70.58	101.33	-70.95	-5.09	28.93	52.87	-5.23	-21.55	-33.68	-46.57
<i>Proportional return-sign allocation of CAGR</i>												
Positive CAGR	0.75	1.00	1.00	1.00	0.14	0.29	0.57	0.57	0.60	0.70	0.40	0.40
Negative CAGR	0.25	0.00	0.00	0.00	0.86	0.71	0.43	0.43	0.40	0.30	0.60	0.60
<i>CAGR average of gold mining shares</i>												
All stocks	18.80	46.39	62.42	84.77	-70.06	-28.88	-6.70	12.20	1.11	6.96	0.78	-16.49
<b>Canada</b>												
<i>Sub-categorization by market capitalization</i>												
Large cap	-4.20	16.94	36.94	57.64	-40.32	3.50	3.80	19.31	-7.43	-8.81	-5.66	-12.63
Mid cap	-27.82	-5.56	35.95	77.40	-32.42	-23.24	-15.22	-23.79	12.56	21.01	22.28	8.68
<i>Proportional return-sign allocation of CAGR</i>												
Positive CAGR	0.33	0.75	0.92	0.92	0.17	0.61	0.61	0.61	0.36	0.32	0.36	0.36
Negative CAGR	0.67	0.25	0.08	0.08	0.83	0.39	0.39	0.39	0.64	0.68	0.64	0.64
<i>CAGR average of gold mining shares</i>												
All stocks	-6.17	15.07	36.86	59.29	-39.00	-0.96	0.63	12.13	-4.23	-4.04	-1.19	-9.22
<b>UK</b>												
<i>Sub-categorization by market capitalization</i>												
Large cap	-2.42	-5.89	2.51	3.79	-45.63	-10.94	-13.37	2.00	14.20	28.95	25.36	23.51
<i>Proportional return-sign allocation of CAGR</i>												
Positive CAGR	0.00	0.00	1.00	1.00	0.33	0.33	0.33	0.33	0.83	1.00	1.00	0.67
Negative CAGR	1.00	1.00	0.00	0.00	0.67	0.67	0.67	0.67	0.17	0.00	0.00	0.33
<i>CAGR average of gold mining shares</i>												
All stocks	-2.42	-5.89	2.51	3.79	-45.63	-10.94	-13.37	2.00	14.20	28.95	25.36	23.51
<b>US</b>												
<i>Sub-categorization by market capitalization</i>												
Large cap	1.38	17.27	64.13	95.14	-61.88	-30.93	-24.64	-16.30	9.73	14.64	13.97	-6.16
Mid cap	-6.82	-13.39	5.95	46.51	-39.04	42.33	55.20	58.68	-25.53	-17.32	-10.53	-23.41
Small cap	2.66	23.58	4.77	-54.56	-54.84	-40.85	-35.34	-4.02	-29.84	-50.54	7.99	-2.60
<i>Proportional return-sign allocation of CAGR</i>												
Positive CAGR	0.57	0.57	0.86	0.71	0.14	0.43	0.57	0.43	0.43	0.43	0.71	0.14
Negative CAGR	0.43	0.43	0.14	0.29	0.86	0.57	0.43	0.57	0.57	0.57	0.29	0.86
<i>CAGR average of gold mining shares</i>												
All stocks	-0.78	9.41	39.03	59.86	-54.35	-11.42	-3.36	6.88	-6.00	-3.80	6.12	-10.58
<b>Global</b>												
<i>CAGR average of gold mining shares</i>												
	-0.28	17.76**	40.32***	61.39***	-48.85***	-9.49	-2.83	10.22	-1.07	2.41	3.60	-6.84

### 3.4 Concluding remarks

This paper uses a large sample of gold mining companies traded on four stock markets to identify different types of flight to gold. After extreme financial shocks, we observe that investors flee from stocks including gold mining shares to gold bullion. However, if the financial shock is less extreme, investors only flee from stocks excluding gold mining shares. This highlights that the study of gold mining companies provides important additional information in the context of flight to quality and safe haven effects. The analysis of three crisis periods reveals that the bankruptcy of Lehman Brothers in 2008 and the subsequent global financial crisis was the most severe in this sense with a strong flight from gold mining shares to gold. The September 11, 2001, terrorist attacks do not display an equally strong flight to gold and no clear flight from gold mining shares. The Brexit vote in 2016 reveals a very different pattern, a flight to gold mining shares that we interpret as a safe haven trade, i.e., investors speculate on a safe haven effect increasing the price of gold and gold mining companies. The Brexit results suggest that investors learned from the safe haven performance of gold in the past and used the gold share – gold bullion relationship to profit from the safe haven effect.

We also exploit the crisis-specific cross-sectional effects across gold mining companies and find a negative relationship between the strength of the safe haven effect of gold and the strength of the flight from gold mining shares. The broader a flight to quality is, i.e., from stocks to gold and gold mining shares, the lower is the concentration and thus price pressure on gold. In contrast, the narrower a flight to quality is, i.e., from stocks including gold mining shares to gold, the stronger is the concentration and effect on the gold price.

Our study shows that gold mining companies play a critical role in crisis periods and that this information can be used to enhance our understanding about investor behavior during times of financial turmoil. The relationship between gold mining shares and the price of gold also implies that a flight to gold from stocks including gold mining shares leads to a temporary decoupling and thus long-term profit opportunities based on an expected recoupling of gold mining shares with the price of gold.

This paper contributes to the literature on gold as a safe haven and flight to quality and touches upon liquidity and tangibility. However, more research on the role of liquidity is needed and more research on the role of physical assets and their tangibility in comparison with the non-tangible gold shares is required. Do investors seek out liquid and safe assets in a crisis or are they content with a relatively or temporarily illiquid asset that holds its value during a crisis? This may depend on whether investors want to sell the asset in a crisis or whether they want to use it merely as collateral.

Since even large cap and thus relatively liquid gold mining shares are sold in times of severe financial turmoil, the findings suggest that investors assign special value to physical gold and thus physical assets. This provides interesting research avenues with regard to the financialization and the digitalization of assets.

### 3.5 Appendices

#### 3.5.1 Average post-event trading volume

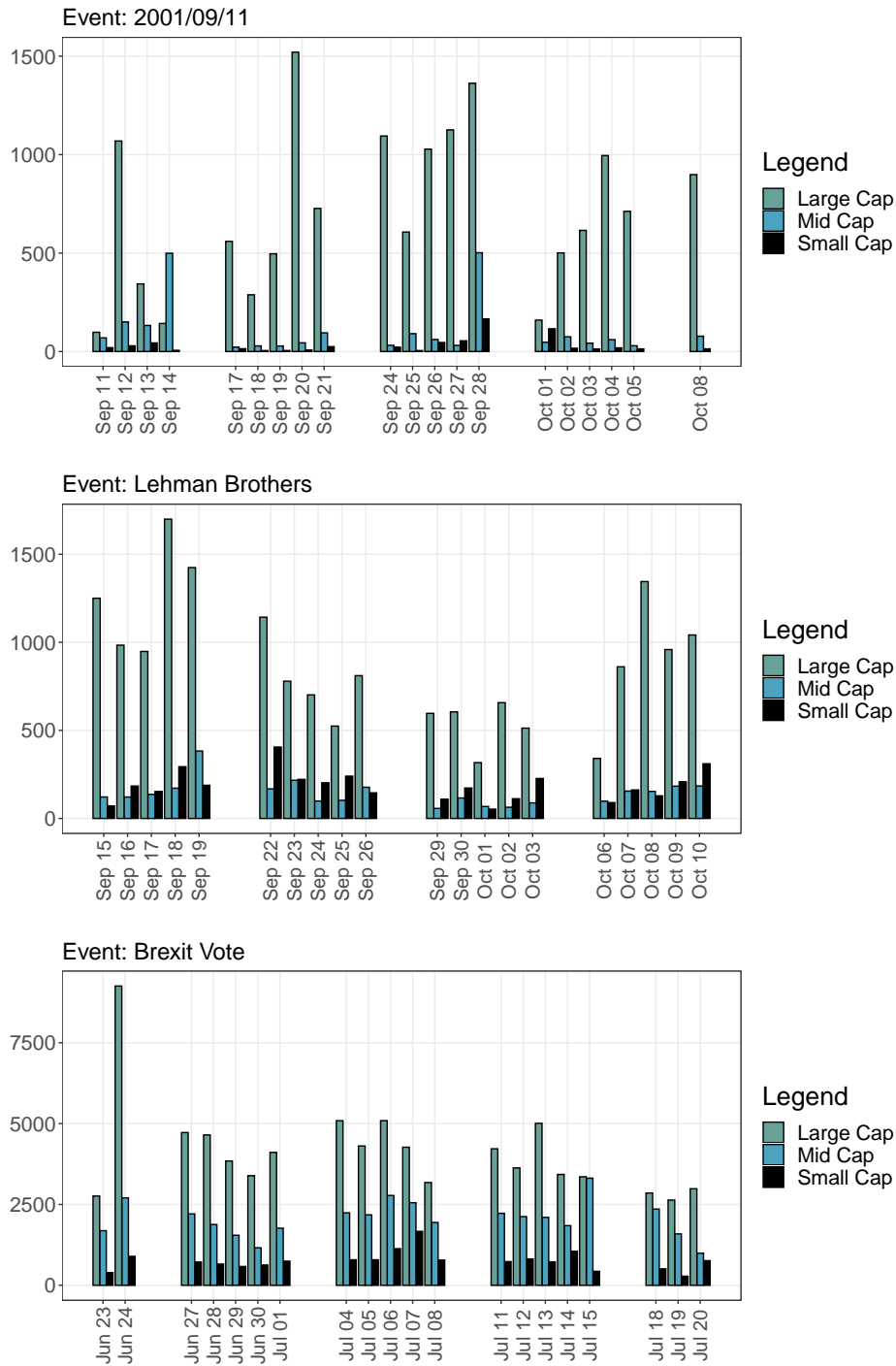


**Figure 3.3: Average post-event trading volume (Australia)**  
 Average trading volume of Australia-listed gold mining shares in post-event periods.

CHAPTER 3. FLIGHT TO QUALITY – GOLD MINING SHARES VERSUS GOLD BULLION

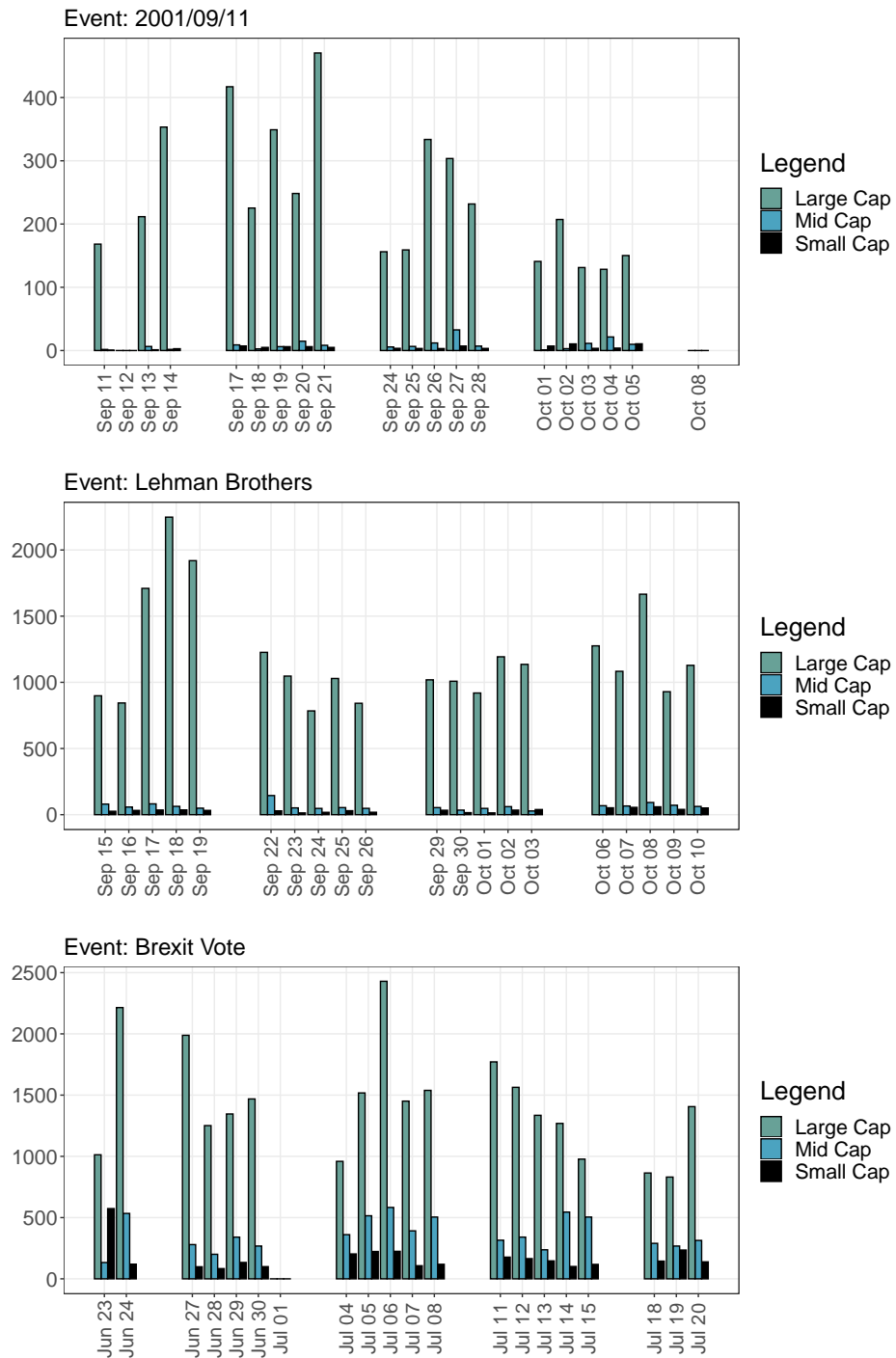


**Figure 3.4: Average post-event trading volume (Canada)**  
Average trading volume of Canada-listed gold mining shares in post-event periods.

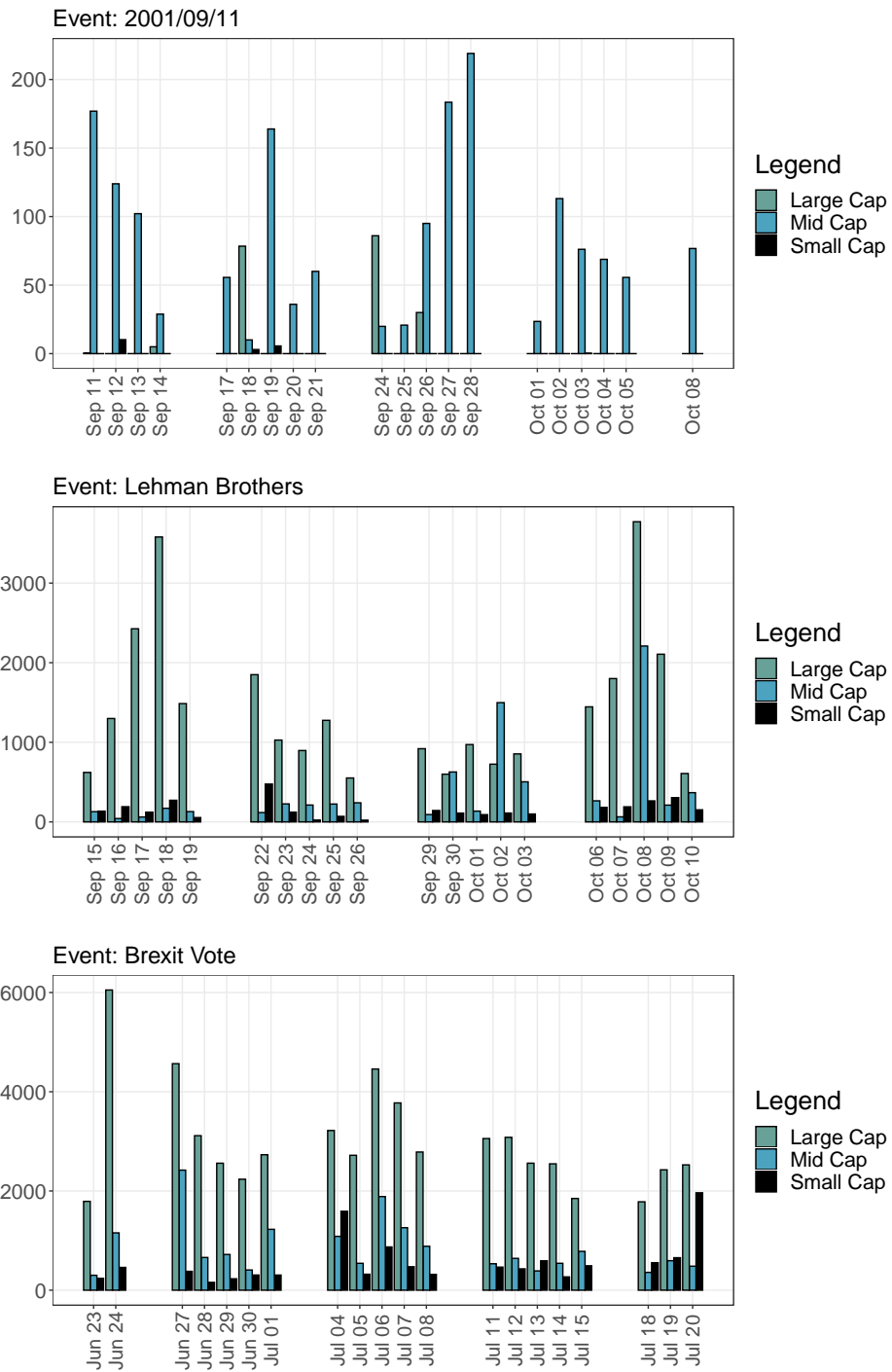


**Figure 3.5: Average post-event trading volume (UK)**  
 Average trading volume of UK-listed gold mining shares in post-event periods.

CHAPTER 3. FLIGHT TO QUALITY – GOLD MINING SHARES VERSUS GOLD BULLION

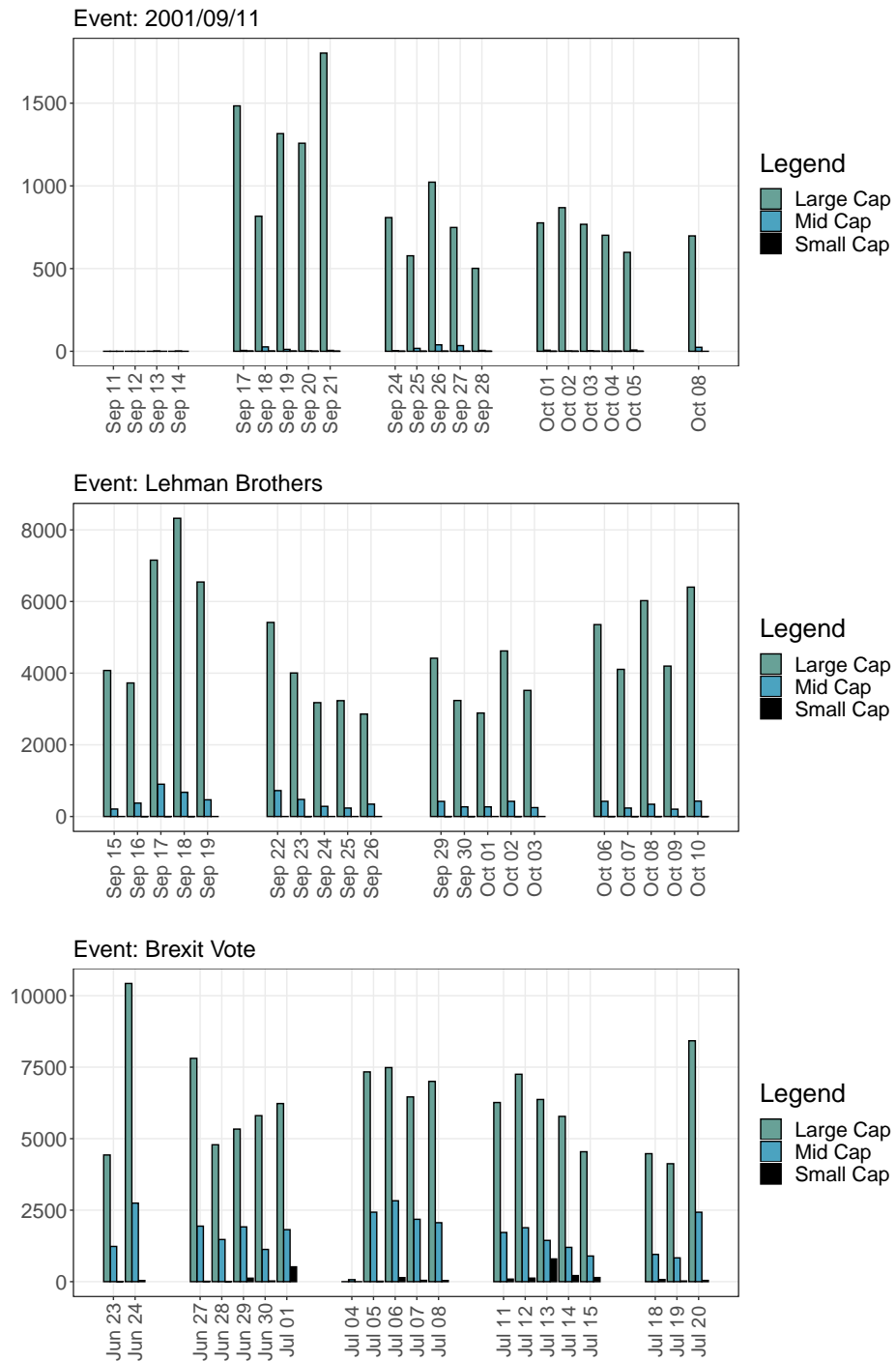


**Figure 3.6: Average post-event trading volume (US)**  
Average trading volume of US-listed gold mining shares in post-event periods.



### 3.5.2 Descriptive statistics

**Table 3.11: Descriptive statistics (Australia)**

Market capitalization in million US-Dollars. All remaining figures are computed for percentage returns. Daily data between January 1997 and September 2018 is used. Superscript  $L$  indicates stocks of the liquid sub-sample.

Company	Market cap	Mean	St. Dev.	Min.	Max.	Skewness	Kurtosis
<b>Large cap</b>							
NEWCREST MINING <sup>L</sup>	10834.27	0.03	2.63	-18.47	16.91	-0.03	7.00
NORTHERN STAR	3934.92	0.10	5.14	-48.77	50.83	0.19	16.87
EVOLUTION MINING	3283.99	0.02	4.71	-46.10	43.99	0.63	14.60
OZ MINERALS <sup>L</sup>	2061.87	0.02	3.70	-26.58	38.82	0.59	13.61
INDEPENDENCE GROUP <sup>L</sup>	1921.60	0.07	3.31	-17.95	42.38	0.63	11.63
OCEANAGOLD CDI <sup>L</sup>	1785.87	0.00	4.06	-36.08	23.10	-0.15	9.11
REGIS RESOURCES	1418.80	-0.03	5.22	-75.38	109.86	0.08	75.60
ST. BARBARA	1384.58	-0.00	4.61	-32.22	41.70	0.35	8.31
SANDFIRE RESOURCES	807.22	0.08	4.93	-51.15	52.84	0.65	20.12
RESOLUTE MINING <sup>L</sup>	576.50	-0.04	4.00	-34.51	33.03	0.30	8.11
GOLD ROAD RESOURCES	394.33	0.04	5.46	-62.80	62.80	0.56	22.47
DACIAN GOLD	365.24	0.09	4.07	-29.55	19.68	-0.30	9.49
PERSEUS MINING <sup>L</sup>	258.78	0.02	4.41	-42.93	39.21	0.09	10.45
SILVER LAKE RESOURCES <sup>L</sup>	189.59	0.01	4.47	-26.57	23.64	0.21	6.10
RAMELIUS RESOURCES	183.87	0.03	4.87	-28.35	93.83	2.46	43.50
WEST AFRICAN RESOURCES	145.21	0.01	5.20	-25.95	34.83	0.54	7.97
<b>Mid cap</b>							
GASCOYNE RESOURCES	117.47	0.02	5.02	-24.78	49.90	0.96	13.59
DORAY MINERALS <sup>L</sup>	108.46	0.02	4.36	-30.42	100.33	5.55	128.80
ALKANE RESOURCES	88.03	-0.01	4.37	-24.51	32.77	0.55	6.68
BEADELL RESOURCES	63.08	-0.07	5.50	-60.49	49.90	0.21	20.18
DGR GLOBAL	53.33	-0.01	5.81	-40.55	45.17	0.40	11.17
MEDUSA MINING <sup>L</sup>	52.71	0.01	3.84	-18.23	29.38	0.22	7.05
ORION MINERALS	47.53	-0.15	6.75	-69.31	83.28	0.10	18.77
BLACKHAM RESOURCES	42.19	-0.04	6.64	-81.57	57.90	0.22	18.57
DE GREY MINING	40.75	-0.07	10.49	-69.31	109.86	0.43	30.16
BASSARI RESOURCES	35.54	-0.08	7.29	-87.42	67.08	0.03	16.97
ARAFURA RESOURCES	35.07	-0.01	5.08	-45.36	47.46	0.32	9.53
TROY RESOURCES	34.97	-0.03	3.98	-42.61	29.51	-0.11	11.19
SUMATRA COPPER & GOLD	33.77	-0.13	6.34	-34.48	40.55	0.35	8.79
KINGSGATE CONSOLIDATED <sup>L</sup>	33.62	-0.02	3.97	-38.14	44.63	0.58	15.75
AXIOM MINING	30.27	-0.12	7.00	-69.31	69.31	-0.21	17.53
KINGSROSE MINING	30.16	-0.06	4.33	-33.65	35.67	0.20	12.42
<b>Small cap</b>							
TANAMI GOLD	29.81	-0.08	5.36	-59.78	56.80	0.33	17.71
TRITON MINERALS	28.35	-0.07	6.22	-35.97	87.56	2.80	35.20
CHALICE GOLD MINES	26.09	-0.00	3.90	-22.26	29.54	0.48	9.08
FOCUS MINERALS	25.83	-0.08	5.12	-36.29	37.16	0.27	8.85
ORINOCO GOLD	19.68	-0.09	5.82	-37.45	55.34	0.59	15.07
SIHAYO GOLD	18.82	-0.08	7.05	-59.47	69.31	0.49	12.60
BARRA RESOURCES	15.39	-0.04	6.70	-51.08	79.11	0.50	13.76
CITIGOLD	10.91	-0.06	5.46	-48.95	79.49	1.24	20.92
AZUMAH RESOURCES	10.77	-0.07	5.37	-34.63	44.80	0.42	8.54
INTREPID MINES	10.29	-0.07	5.62	-79.85	87.55	-1.04	62.52
DRAGON MINING	9.66	-0.03	5.47	-38.87	55.96	0.35	11.09
AUSTAR GOLD	6.93	-0.12	8.51	-40.68	98.08	1.23	14.16
KALNORTH GOLD MINES	4.54	-0.08	5.87	-45.20	51.08	0.08	19.57
GREAT WSTN EXPLORATION	4.00	-0.11	7.58	-74.78	53.90	0.41	14.50
CRATER GOLD MINING	3.65	-0.16	10.70	-69.31	69.31	0.18	23.26
BERKUT MINERALS	3.17	-0.20	6.01	-30.11	40.55	0.13	9.27
METMINCO	2.65	-0.26	7.65	-45.20	51.01	0.23	9.20
Average	624.98	-0.04	5.51	-44.56	54.42	0.52	19.13
Gold		0.02	1.06	-9.60	7.01	-0.19	9.50
Index		0.02	0.96	-8.70	5.72	-0.48	9.11

## CHAPTER 3. FLIGHT TO QUALITY – GOLD MINING SHARES VERSUS GOLD BULLION

**Table 3.12: Descriptive statistics (Canada)**

Market capitalization in million US-Dollars. All remaining figures are computed for percentage returns. Daily data between January 1997 and September 2018 is used. Superscript *L* indicates stocks of the liquid sub-sample.

Company	Market cap	Mean	St. Dev.	Min.	Max.	Skewness	Kurtosis
<b>Large cap</b>							
BARRICK GOLD TSX <sup>L</sup>	12359.42	-0.02	2.58	-17.91	28.11	0.17	9.67
GOLDCORP <sup>L</sup>	9379.60	0.02	2.80	-22.12	22.56	0.16	8.53
AGNICO EAGLE MINES <sup>L</sup>	8160.14	0.02	3.08	-28.41	21.62	-0.02	9.07
KIRKLAND LAKE GOLD	3812.75	-0.04	6.28	-40.38	76.48	0.80	14.24
KINROSS GOLD <sup>L</sup>	3766.04	-0.04	3.51	-23.94	24.79	0.28	7.75
B2GOLD <sup>L</sup>	2214.54	0.01	3.85	-16.71	25.49	0.33	6.03
OCEANAGOLD <sup>L</sup>	1855.40	0.00	4.26	-25.13	39.30	0.10	10.23
IAMGOLD <sup>L</sup>	1827.06	-0.00	3.58	-21.68	24.50	0.17	6.35
ALAMOS GOLD <sup>L</sup>	1803.46	0.04	3.63	-25.97	30.16	0.07	7.77
ENDEAVOUR MINING	1727.37	-0.01	4.11	-25.34	25.93	0.03	8.86
DETOUR GOLD <sup>L</sup>	1557.07	0.04	3.98	-35.97	25.18	-0.32	10.75
CENTERRA GOLD <sup>L</sup>	1239.98	0.00	4.02	-40.10	50.34	-0.21	22.03
OSISKO GOLD ROYALTIES <sup>L</sup>	1185.18	-0.03	2.12	-12.93	12.70	-0.23	7.65
SEMAFO <sup>L</sup>	794.74	-0.01	5.13	-44.18	33.65	0.06	9.37
ELDORADO GOLD <sup>L</sup>	754.33	-0.04	4.25	-32.63	47.69	0.36	11.00
FORTUNA SILVER MINES	713.67	0.07	4.09	-30.54	79.11	1.63	37.87
TOREX GOLD RESOURCES	712.91	0.00	7.92	-47.00	76.55	0.57	11.93
NEW GOLD <sup>L</sup>	643.70	0.02	5.22	-55.96	60.61	0.16	21.97
CHINA GOLD INT RES <sup>L</sup>	597.06	0.07	5.21	-34.69	91.63	1.89	29.84
ALACER GOLD <sup>L</sup>	490.22	0.02	4.18	-21.02	56.10	0.93	15.84
CONTINENTAL GOLD	484.71	-0.04	8.96	-73.40	139.95	1.47	35.08
GOLD STANDARD VENTURES	441.48	-0.06	6.21	-82.67	69.31	0.25	30.28
DUNDEE PRCS MTL <sup>L</sup>	405.37	-0.00	3.03	-24.54	20.54	0.06	8.90
OSISKO MINING	388.83	-0.17	6.39	-51.12	38.30	-0.84	17.25
WESDOME GOLD MINES	368.93	-0.01	4.45	-26.93	40.10	0.48	8.38
TERANGA GOLD <sup>L</sup>	342.37	-0.06	3.64	-17.44	27.63	0.16	6.44
TMAC RESOURCES <sup>L</sup>	311.10	-0.03	3.11	-18.07	17.02	0.03	8.79
ATLANTIC GOLD	296.01	-0.00	5.24	-48.10	38.30	0.15	10.06
GOLDEN STAR RESOURCES <sup>L</sup>	285.32	-0.05	5.39	-42.69	42.59	0.36	9.04
CORVUS GOLD <sup>L</sup>	264.41	0.09	5.07	-26.63	43.40	0.64	7.84
ROXGOLD	253.58	-0.06	9.99	-98.08	99.33	0.31	20.34
GOLD RESERVE A <sup>L</sup>	253.34	-0.02	4.95	-48.40	52.41	0.51	15.08
<b>Mid cap</b>							
SABINA GOLD & SILVER	247.61	0.03	6.95	-77.32	102.96	0.88	52.20
ARGONAUT GOLD	245.82	-0.06	5.37	-95.55	135.81	3.64	196.77
VICTORIA GOLD	197.97	-0.02	7.82	-55.96	85.57	0.85	18.33
GREAT PANTHER SILVER	156.67	-0.05	6.40	-51.08	109.86	1.19	32.58
MIDAS GOLD	154.07	-0.07	3.96	-14.75	20.48	0.42	5.01
BARKERVILLE GOLD MINES	135.88	-0.09	7.66	-76.10	65.06	0.11	10.38
LYDIAN INT	119.52	-0.00	6.58	-91.63	156.06	5.56	149.13
OREZONE GOLD <sup>L</sup>	103.65	0.01	5.18	-50.00	41.69	0.19	11.46
GOLDMINING	88.73	-0.01	4.02	-33.65	34.74	0.35	11.43
BONTERRA RESOURCES	86.75	-0.08	10.16	-69.31	69.31	0.14	25.39
BELO SUN MINING	85.47	0.00	8.48	-55.96	91.63	0.59	14.78
INTL TWR HILL MNS	80.81	-0.02	5.20	-78.41	105.46	0.77	52.07
RUPERT RES	80.20	-0.01	8.71	-76.21	91.63	0.43	12.39
CALEDONIA MINING CORP	71.50	-0.05	7.08	-36.30	69.53	0.69	10.86
ALMADEN MINERALS	68.12	-0.01	5.36	-55.96	39.02	0.14	12.93
AURA MINERALS	63.65	-0.08	6.06	-70.77	51.99	-0.05	17.47
CHESAPEAKE GOLD <sup>L</sup>	62.66	0.00	3.57	-31.73	27.81	0.36	10.24
ALIO GOLD <sup>L</sup>	59.54	-0.05	4.90	-31.47	35.67	0.35	9.43
BARSELE MINERALS	56.65	0.16	6.50	-51.08	31.02	-0.21	12.56
LIBERTY GOLD	54.38	-0.11	4.09	-15.86	24.12	0.56	5.81
ROBEX RESOURCES	51.47	-0.05	8.20	-61.90	69.31	0.37	9.18
DYNACOR GOLD MINES	49.67	0.03	5.59	-41.36	49.64	0.69	13.90
METANOR RESOURCES	48.03	-0.08	5.28	-34.65	36.77	0.27	7.45
AVINO SILVER & GD.MINES	47.84	-0.01	7.25	-49.06	81.83	0.52	13.54
TANZANIAN RTY EXP A <sup>L</sup>	46.10	-0.01	5.94	-41.06	62.25	0.45	11.98

## 3.5. APPENDICES

GOGOLD RESOURCES	43.24	0.01	3.82	-31.02	41.87	0.60	17.55
GOLDEN QUEEN MNG	39.41	-0.05	7.88	-51.08	96.14	0.49	14.95
TERRAX MINERALS	36.01	0.00	7.82	-69.31	91.63	0.82	24.92
KERR MINES	34.57	-0.11	8.74	-69.31	69.31	0.27	11.19
MAWSON RES	34.45	-0.03	6.97	-47.00	71.91	0.79	11.85
COLUMBUS GOLD	33.72	-0.04	6.44	-65.39	62.42	0.75	17.06
<b>Small cap</b>							
TREASURY METALS	33.27	-0.06	6.95	-47.96	69.31	0.36	16.47
FORTUNE MINERALS	31.38	-0.08	6.41	-51.08	69.31	0.31	17.54
RED EAGLE MINING	30.89	-0.13	6.10	-38.30	51.08	0.18	10.21
EURO SUN MINING	30.69	-0.04	10.66	-69.31	109.86	0.31	21.33
ATICO MINING	30.43	-0.02	4.90	-29.95	36.42	0.51	8.38
AMARILLO GOLD	24.75	-0.04	8.60	-98.08	69.31	0.13	14.70
ESKAY MINING	23.41	-0.03	10.30	-58.78	69.31	0.34	8.27
IDM MINING	22.55	-0.17	6.84	-40.55	91.63	1.14	21.41
AXMIN	20.16	-0.05	10.74	-69.31	69.31	0.22	23.74
SIRIOS RES	18.42	-0.05	9.69	-89.20	102.40	0.69	15.51
PUDO	17.23	0.06	10.53	-87.55	87.55	0.17	19.82
ATLATSA RESOURCES	17.13	-0.08	7.29	-69.31	69.31	0.37	17.55
MARLIN GOLD MINING A	16.57	-0.10	6.90	-43.24	60.22	0.56	11.78
ORVANA MINERALS	15.83	-0.07	6.07	-49.25	60.61	0.29	14.55
LUPAKA GOLD	15.07	-0.09	7.29	-35.67	38.30	0.30	5.77
OROSUR MINING	13.62	-0.03	6.25	-81.09	84.73	0.19	29.79
CORAL GOLD RESOURCES	13.37	-0.06	7.63	-42.29	71.02	0.60	9.54
STRIKEPOINT GOLD	12.30	-0.04	9.89	-69.31	91.63	0.36	11.63
MUNDORO CAPITAL	9.37	-0.07	6.03	-57.54	61.90	0.27	15.91
FREEGOLD VENTURES	8.74	-0.10	8.12	-47.00	58.78	0.28	7.83
COLORADO RESOURCES	8.17	-0.09	7.41	-48.73	121.64	2.17	42.14
MINERAL MOUNTAIN RES	7.89	-0.11	8.02	-45.68	40.55	-0.01	6.08
CANARC RESOURCE	5.91	-0.07	8.24	-69.31	51.08	0.13	9.08
INT GOLD AND METALS	5.48	-0.10	10.56	-69.31	84.87	0.17	13.38
EAGLE GRAPHITE	4.39	-0.14	10.20	-91.63	79.85	-0.02	14.74
MINCO GOLD	3.92	-0.06	6.82	-62.42	81.09	0.48	13.90
PELANGIO EXPLORATION	3.07	-0.08	8.40	-36.77	61.90	0.37	7.70
DYNASTY GOLD	2.47	-0.12	12.54	-69.31	138.63	0.26	15.27
ATLANTA GOLD	2.36	-0.14	8.96	-69.31	69.31	0.03	18.79
MIRANDA GD	1.54	-0.09	7.58	-76.21	47.00	-0.11	12.06
COLOMBIA CREST GOLD	0.52	-0.14	10.68	-69.31	109.86	0.29	18.39
INFINITO GOLD	0.48	-0.11	8.97	-69.31	69.31	-0.20	20.01
Average	661.32	-0.04	6.46	-50.45	62.96	0.47	18.55
Gold		0.02	1.06	-9.60	7.01	-0.19	9.50
Index		0.02	1.06	-9.79	9.37	-0.70	12.85

## CHAPTER 3. FLIGHT TO QUALITY – GOLD MINING SHARES VERSUS GOLD BULLION

**Table 3.13: Descriptive statistics (UK)**

Market capitalization in million US-Dollars. All remaining figures are computed for percentage returns. Daily data between January 1997 and September 2018 is used. Superscript  $L$  indicates stocks of the liquid sub-sample.

Company	Market cap	Mean	St. Dev.	Min.	Max.	Skewness	Kurtosis
<b>Large cap</b>							
RANDGOLD RESOURCES <sup>L</sup>	6012.35	0.04	2.79	-56.56	30.51	-1.42	43.68
POLYMETAL INT <sup>L</sup>	3735.32	-0.02	2.36	-20.30	11.30	-0.50	8.93
CENTAMIN	1478.85	0.06	3.26	-64.32	22.36	-2.10	49.44
HOCHSCHILD MINING <sup>L</sup>	1073.48	-0.02	3.54	-26.20	22.43	0.13	8.39
HIGHLAND GOLD MINING <sup>L</sup>	606.71	-0.01	3.84	-84.60	47.91	-2.20	69.97
ACACIA MINING <sup>L</sup>	578.50	-0.08	3.28	-35.23	15.86	-1.21	15.05
PETROPAVLOVSK <sup>L</sup>	277.09	-0.05	3.68	-35.19	53.74	0.37	22.87
<b>Mid cap</b>							
GRIFFIN MINING	214.56	0.02	3.90	-35.14	78.28	2.70	58.73
AVESORO RESOURCES DI	204.88	-0.21	4.07	-62.86	28.77	-2.13	44.75
HUMMINGBIRD RESOURCES	126.40	-0.09	2.81	-23.27	22.12	0.91	14.73
CHAARAT GOLD HDG DI	118.33	-0.03	3.97	-92.46	42.65	-3.39	115.86
ANGLO ASIAN MINING	88.93	-0.01	5.31	-41.55	53.29	0.55	13.68
SHANTA GOLD	51.34	-0.05	4.27	-74.19	77.65	0.78	81.80
<b>Small cap</b>							
CONDOR GOLD	31.88	-0.05	5.92	-57.05	69.31	1.46	25.76
ALTYN	29.62	-0.04	4.03	-33.94	39.05	0.61	14.98
CHINA NONFERROUS GD	22.64	-0.02	3.62	-22.31	38.87	1.46	18.93
PATAGONIA GOLD	21.81	-0.04	4.25	-46.61	34.18	0.62	14.04
XTRACT RESOURCES	4.73	-0.17	6.71	-57.54	92.68	1.32	29.21
ECR MINERALS	3.27	-0.27	5.90	-80.18	69.31	0.33	28.84
AVOCET MINING	3.10	-0.09	4.19	-72.27	38.81	-0.52	36.26
Average	734.19	-0.06	4.09	-51.09	44.45	-0.11	35.79
Gold		0.02	1.06	-9.60	7.01	-0.19	9.50
Index		0.01	1.09	-8.71	8.81	-0.22	9.15

**Table 3.14: Descriptive statistics (US)**

Market capitalization in million US-Dollars. All remaining figures are computed for percentage returns. Daily data between January 1997 and September 2018 is used. Superscript  $L$  indicates stocks of the liquid sub-sample.

Company	Market cap	Mean	St. Dev.	Min.	Max.	Skewness	Kurtosis
<b>Large cap</b>							
NEWMONT MINING <sup>L</sup>	16812.73	-0.01	2.69	-18.26	22.45	0.34	8.24
ROYAL GOLD <sup>L</sup>	5149.14	0.03	3.27	-39.52	26.46	-0.05	11.16
HECLA MINING <sup>L</sup>	1450.12	-0.01	4.40	-35.12	31.67	0.07	8.76
COEUR MINING <sup>L</sup>	1069.99	-0.06	4.53	-40.55	33.78	-0.11	10.25
<b>Mid cap</b>							
MCEWEN MINING <sup>L</sup>	654.30	0.01	6.00	-58.82	73.08	0.66	15.23
VISTA GOLD ASE <sup>L</sup>	48.79	-0.06	7.64	-84.73	102.96	0.44	20.65
PERSHING GOLD	35.65	-0.06	5.19	-79.85	65.94	0.40	59.34
<b>Small cap</b>							
US GOLD <sup>L</sup>	18.33	-0.09	4.85	-41.29	46.43	0.55	13.18
BULLFROG GOLD	8.11	-0.11	10.70	-91.63	82.10	0.11	10.93
LONE STAR GOLD	0.72	-0.02	17.37	-73.09	476.12	10.13	278.06
BONANZA GOLDFIELDS	0.65	-0.26	16.23	-69.31	138.63	0.77	13.20
Average	2295.32	-0.06	7.53	-57.47	99.97	1.21	40.82
Gold		0.02	1.06	-9.60	7.01	-0.19	9.50
Index		0.02	1.18	-9.47	10.96	-0.25	11.45

# Chapter 4

## Does online investor attention drive the co-movement of stock, commodity, and energy markets? Insights from Google searches

### 4.1 Introduction

The dependence between stock, commodity, and energy markets is of great interest for both policy makers and financial practitioners. In particular, market participants need to know how shocks transmit to level and risk across different markets over time (Kling, 1985; Engle *et al.*, 1990; King and Wadhvani, 1990; Karolyi, 1995). This is due to two reasons. Firstly, taking a macroeconomic point of view, the dynamic co-movement between the energy sector and macroeconomic variables are of key interest for policy makers. For instance, an increase in the price of oil may induce inflation, and consequently impact interest and foreign exchange rates, business cycles, and economic development. In turn, oil price movements may spill over towards the stock market as investors need to adjust their positions to new economic conditions. Amongst others, the dependence between oil and stock markets has been investigated upon in Sadorsky (1999), Park and Ratti (2008), Kilian and Park (2009), and Jiang and Yoon (2020). More recently, Zolfaghari *et al.* (2020) study spillover effects within energy markets and between energy markets and macroeconomic variables, highlighting the importance of the energy-macro nexus to policy makers. Secondly, taking a more practical point of view, the financialization of energy- and commodity markets has offered new opportunities for financial investors (e.g., Hillier *et al.*, 2006; Baur and Lucey, 2010; Daskalaki and Skiadopoulos, 2011). For instance, Mensi *et al.* (2013), Mensi *et al.* (2015a), Arouri *et al.* (2015), and Chkili (2016) provide empirical evidence that adding commodities to purely stock-diversified portfolios may increase both risk-adjusted returns and hedging effectiveness of the portfolios. In the same

vein, [Malik and Ewing \(2009\)](#), [Aroui \*et al.\* \(2011\)](#), and [Lin \*et al.\* \(2014\)](#) propose hedging stocks with energies.

Another strand of economic literature uses investor attention to explain the co-movement of asset prices (e.g., [Peng and Xiong, 2006](#); [Veldkamp, 2006](#); [Veldkamp and Wolfers, 2007](#)). Whilst the theoretical literature suggests that high attention towards individual assets decreases the amount of attention given to common shocks, thus implying lower return correlations, the empirical evidence to investigate this relation is still in its infancy (e.g., [Shiyang \*et al.\*, 2019](#); [Hu \*et al.\*, 2021](#)). In contrast, measures to approximate investor attention have received considerable attention in the literature throughout recent years. More recently, online search queries have increasingly been associated with investor demand for information and, henceforth, been used as a novel measure of the latent variable. A profound example of such online investor attention measure is provided by Google Trends' Search Volume Index, which has been employed in a variety of applications in recent years ([Da \*et al.\*, 2011](#)). For instance, [Ji and Gu \(2015\)](#) investigate the influence of investor attention on energy and commodity market returns, and [Han \*et al.\* \(2017\)](#) reveal predictability of crude oil price movements by means of Google searches. Likewise, [Jain and Biswal \(2019\)](#) show that an increase in Indian investor attention towards the gold price induces an increase of the latter in response. Finally, [Afkhami \*et al.\* \(2017\)](#) explore different Google keywords to optimally forecast volatility in the energy sector, and [Aromi and Clements \(2019\)](#) analyze the influence of investor attention on volatility, correlation, and directional spillovers between the crude oil and stock market.

To the best of our knowledge, however, there is yet no study to investigate the role of investor attention towards market dependence in a joint framework of stock, commodity, and energy markets. Besides, and perhaps more importantly, there is yet no study to consider investor attention in the modelling of the linkages between assets. This is the contribution of our paper. To this end, we use the model proposed in [Vargas \(2008\)](#) which allows to include exogenous variables in the correlation equation of [Engle \(2002\)](#)'s DCC model. In our case, the exogenous variables are given by information received from Google search requests, which we allow to drive the correlation between asset returns. Our results, which are based on a sample of daily observations over almost six years, suggest that online investor attention is a statistically significant determinant of the time-varying correlation. Moreover, we provide a brief financial exercise to demonstrate the implications of our findings to market participants. In particular, we consider an investor who uses online investor attention in the allocation of her portfolio and investigate the effect towards portfolio performance. By and large, the benefits are marginal, rendering online investor attention less useful in context of such asset allocation strategies.

The remainder of this paper is structured as follows: Section [4.2](#) describes our data set and Section [4.3](#) outlines the empirical methodology used to estimate the time-varying conditional correlations. Next, Section [4.4](#) presents the results, which are then employed in the financial application outlined in Section [4.5](#). Lastly, Section [4.6](#) concludes.

## 4.2 Data

In this paper, we use daily prices and Google search requests for the iShare Dow Jones US ETF as well as gold, silver, crude oil, and natural gas future contracts over the sample period from January 2015 to September 2020, leaving us with 1,488 observations per time series. Data are received from Refinitiv Datastream and Google Trends, respectively.<sup>33</sup> To obtain data from Google Trends in daily frequency, we follow the instructions provided in [Bleher and Dimpfl \(2019\)](#). Figure 4.1 depicts the initial time series of asset prices (solid lines) and Google search volume (dashed lines) over time. In each case, we find a tendency for increasing Google search requests in times of asset price movements. For instance, over the period of plunging stock markets following the beginning of the COVID-19 pandemic, Google searches for all assets rise in comparison to their prior level.

In more detail, Google Trends provides information on the relative propensity of search queries over time ([Bleher and Dimpfl, 2019](#)). In our case, the keywords of interest are “dow”, “gold price”, “silver price”, “oil price”, and “gas price”.<sup>34</sup> Within any requested period beginning in January 2004, all values are scaled between 0 and 100, relative to the observation which possesses the highest search interest. Note, however, that this information is offered in weekly frequency for requests which exceed 270 continuous days, and offered in monthly frequency for requests which exceed 1,890 continuous days.

Thus, the six year period of interest in our sample gives reason to implement the algorithm of [Bleher and Dimpfl \(2019\)](#) to construct consistent, multi-annual time series of daily observations. Sourcing data based on this algorithm allows values to exceed the initial upper boundary of 100. For the empirical analysis, we compute daily logarithmic returns of asset prices and Google search requests. In line with the literature examining the linkage between Google searches and volatility, we henceforth consider unexpected Google searches and refer to the final time series of processed Google search requests simply as Google searches.<sup>35</sup>

Table 4.1 offers descriptive statistics for all data employed in the empirical analysis. In addition to the first sample which covers the period from January 2015 to September 2020, we consider a restricted sample to account for potential regime shifts due to the COVID-19 pandemic. Consequently, the restricted sample covers the period from January 2015 to December 2019. For each of these samples, we assess stationarity of all variables using augmented Dickey-Fuller (ADF) and Kwiatkowski–Phillips–Schmidt–Shin (KPSS) tests. Whereas the former tests for the null-hypothesis of a unit root process in the data, the latter tests for the null-hypothesis of stationarity. The corresponding test statistics suggest that all time series are stationary over their respective sample periods and are available upon request.

<sup>33</sup>Please find more information on Google Trends on [www.google.com/trends](http://www.google.com/trends).

<sup>34</sup>To ensure that our keywords are linked to financial requests, we make use of Google Trends’ setting to exclude non-finance related queries from the data. Google, however, does not disclose the algorithm that is used to filter the corresponding search data.

<sup>35</sup>The final (unexpected) Google search series for any given search request (SR) are obtained simply as the residual series from the regression  $\Delta(\log SR_t) = a + b\Delta(\log SR_{t-1}) + \varepsilon_t$  with  $t = 1, \dots, T$ .

CHAPTER 4. DOES ONLINE INVESTOR ATTENTION DRIVE THE CO-MOVEMENT OF STOCK, COMMODITY, AND ENERGY MARKETS?

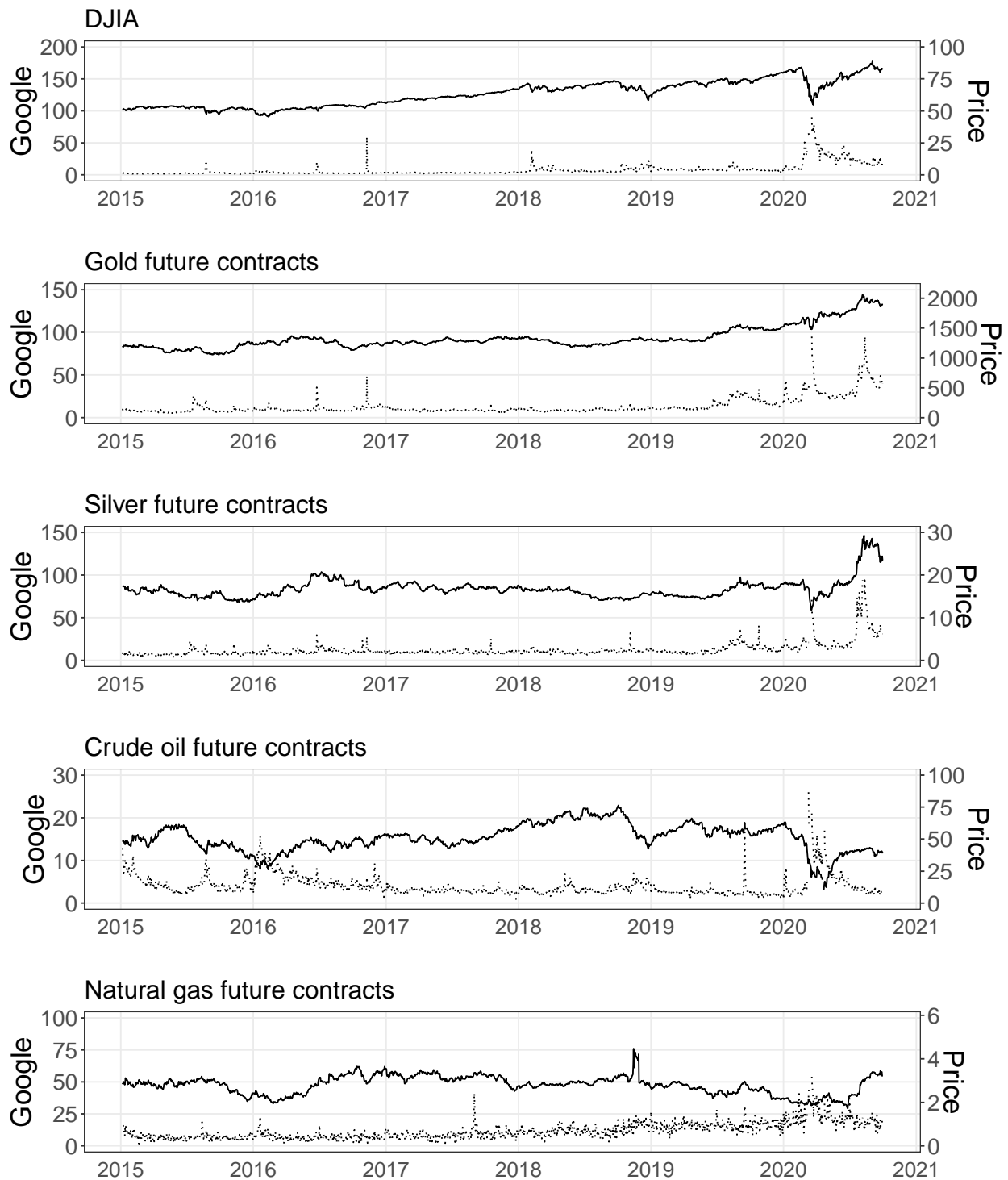


**Figure 4.1: Online search series over time**

This figure illustrates daily relative Google search volume (dashed lines) and prices in US Dollars (solid lines) of the DJIA (“dow”), and gold (“gold price”), silver (“silver price”), crude oil (“crude oil price”), and natural gas (“gas price”) future contracts from January 2015 to September 2020.



**Table 4.1: Descriptive statistics**

This table summarizes the data used in the empirical analysis. The data set covers 1,488 trading days from January 2015 to September 2020. We report descriptive statistics of returns and Google searches ( $G_t$ ) for DJIA (*dow*) spot prices and gold (*gold*), silver (*silver*), crude oil (*oil*), and natural gas (*gas*) future contracts. Panel A and B refer to sample period January 2015 to September 2020, and January 2015 to December 2019, respectively. More precisely, we report the sample mean, median, standard deviation, minimum, maximum, skewness, kurtosis, and lag-1 autocorrelation for each time series.

	Mean	Median	St. Dev.	Min.	Max.	Skewness	Kurtosis	Autocorr.
<b>Panel A: 2015-01-01/2020-09-30</b>								
$r_{dow}$	0.0006	0.0004	0.0105	-0.0614	0.0953	0.6254	11.8981	-0.0649
$r_{gold}$	0.0004	0.0000	0.0087	-0.0475	0.0580	0.2632	5.6416	-0.0225
$r_{silver}$	0.0004	0.0000	0.0161	-0.1160	0.0724	-0.3829	7.0034	-0.0117
$r_{oil}$	0.0005	0.0003	0.0292	-0.2818	0.2239	0.6960	16.1321	-0.0344
$r_{gas}$	0.0001	0.0000	0.0247	-0.3770	0.2679	-1.4208	52.3083	-0.0706
$G_{dow}$	0.0000	-0.0022	0.2677	-1.5428	2.8112	0.7745	14.3209	-0.0682
$G_{gold}$	0.0000	-0.0061	0.1382	-0.6421	1.6066	2.2682	23.0137	-0.0368
$G_{silver}$	0.0000	-0.0052	0.2045	-0.8086	1.3001	0.2443	2.4380	-0.0753
$G_{oil}$	0.0001	-0.0050	0.2097	-0.9163	1.8353	1.0886	9.3007	-0.0478
$G_{gas}$	0.0002	0.0116	0.3632	-1.3439	1.1582	-0.3314	0.6542	-0.1274
<b>Panel B: 2015-01-01/2019-12-31</b>								
$r_{dow}$	0.0003	0.0002	0.0083	-0.0404	0.0491	-0.5136	3.8106	0.0097
$r_{gold}$	0.0002	0.0000	0.0078	-0.0339	0.0459	0.2591	3.1904	-0.0397
$r_{silver}$	0.0000	0.0000	0.0134	-0.0758	0.0521	-0.2530	3.5391	-0.0333
$r_{oil}$	0.0002	0.0004	0.0234	-0.0907	0.1369	0.1852	2.8216	-0.0748
$r_{gas}$	-0.0002	0.0000	0.0238	-0.3770	0.1863	-2.9352	56.3153	-0.0869
$G_{dow}$	0.0000	-0.0014	0.2745	-1.5427	2.8120	0.8017	14.6487	-0.0703
$G_{gold}$	0.0000	-0.0058	0.1400	-0.6291	1.6111	2.4258	25.0052	-0.0509
$G_{silver}$	0.0001	-0.0032	0.2077	-0.7874	1.3026	0.2017	2.4788	-0.0885
$G_{oil}$	0.0001	-0.0072	0.1977	-0.8513	1.8388	0.7239	7.2384	-0.0556
$G_{gas}$	0.0002	0.0084	0.3734	-1.3420	1.1636	-0.3386	0.5607	-0.1280

### 4.3 Methodology

Firstly, following Engle (2002), the DCC methodology is employed to estimate time-varying conditional correlations between asset returns  $r_t \in \mathbb{R}^n$  with  $t = 1, \dots, T$ . More precisely, consider:

$$r_t | \mathfrak{F}_{t-1} \sim \mathcal{N}(0, \Sigma_t), \quad (4.1)$$

where  $\mathfrak{F}_{t-1}$  denotes the information set at time  $t-1$  and  $\Sigma_t$  is the time-varying ( $n \times n$ ) conditional covariance matrix. Decompose the conditional covariance matrix as  $\Sigma_t = D_t R_t D_t$ , where  $D_t$  is a matrix comprising univariate volatility estimates on the diagonal. We consider a range of univariate volatility models to obtain the corresponding estimates.<sup>36</sup> The choice concerning the appropriate univariate volatility model is based on the Bayesian information criterion (BIC). Further, the time-varying correlation dynamics are modelled by writing the conditional correlation matrix  $R_t$  as  $R_t = \text{diag}(Q_t)^{-\frac{1}{2}} Q_t \text{diag}(Q_t)^{-\frac{1}{2}}$ , and defining a dynamic equation for the auxiliary matrix  $Q_t$ . We assume that the conditional correlation evolves linearly according to a GARCH(1,1)-type structure. Thus, the DCC(1,1) process can be written as:

$$Q_t = (1 - \psi_1 - \psi_2) \bar{Q} + \psi_1 \varepsilon_{t-1} \varepsilon'_{t-1} + \psi_2 Q_{t-1}, \quad (4.2)$$

where  $\bar{Q}$  is given by the unconditional covariance matrix of standardized disturbances  $\varepsilon_t$ , implying that the time-varying conditional correlation between  $r_i$  and  $r_j$  with  $i = 1, \dots, n$  and  $j = 1, \dots, n$  is given as the  $ij$ -th element of  $R_t$  in form  $\rho_{ij,t} = q_{ij,t} / \sqrt{q_{ii,t} q_{jj,t}}$ .

Secondly, we follow Vargas (2008) to investigate the effect of the change in investor attention on the time-varying conditional correlation by introducing the DCCX(1,1) specification:

$$Q_t = (1 - \psi_1 - \psi_2) \bar{Q} - K \circ \bar{G} + \psi_1 \varepsilon_{t-1} \varepsilon'_{t-1} + \psi_2 Q_{t-1} + K \circ G_{t-1}, \quad (4.3)$$

where  $\circ$  is the Hadamard product,  $K$  and  $G_t$  are diagonal matrices with parameters  $\xi_1, \dots, \xi_n$  and Google searches  $G_1, \dots, G_n$  on the diagonal, respectively, and  $\bar{G} = T^{-1} \sum_{t=1}^T G_t$ . Whilst the approach in Equation 4.3 is still restrictive, i.e., investor attention towards assets  $i$  and  $j$  only affects elements  $q_{ii}$  and  $q_{jj}$  on the diagonal of  $Q_t$ , their conditional correlation may still be influenced indirectly through the relation  $\rho_{ij,t} = q_{ij,t} / \sqrt{q_{ii,t} q_{jj,t}}$ . As such, the DCCX model provides a means to reveal and interpret potential effects of investor attention on the conditional correlation between asset returns. For instance, positive (negative) coefficients imply that an increase in investor attention towards individual assets leads to a decrease (increase) of their conditional correlation in response. Finally, positive definiteness of  $\Sigma_t$  is ensured by restricting the parameter space such that the minimum eigenvalue of  $Q_t$  remains positive for all  $t$ .

---

<sup>36</sup>Please see Appendix 4.7 for an overview on the different GARCH class models considered in this study.

## 4.4 Empirical results

To investigate whether Google searches provide valuable information for latent correlations between stock, commodity, and energy market returns, we rely on the flexibility of univariate volatility models intertwined with two parsimonious parametric correlation models. To be more precise, we conduct a joint estimation of the conditional mean and variance equations to obtain time-varying univariate volatility estimates for each time series. Besides, we consider both the standard DCC model and the DCCX specification augmented with Google searches as an external regressor. Whilst the former allows to receive dynamic estimates of the conditional correlation between the return series, the latter provides means to reveal the existence of linear relations between Google searches and the time-varying return correlations. We consider the estimation periods from January 2015 to September 2020, and from January 2015 to December 2019 for the analysis.

Figure 4.2 depicts the estimated correlation series between stock, commodity, and energy market returns over time. The correlation estimates between the DJIA, gold, silver, crude oil, and natural gas future contracts are based on the standard DCC model (solid lines) and the extended DCCX model (dashed lines). Even though the suggested estimates differ only slightly across models, some divergences are clearly noticeable. In particular, this holds true for the time-varying correlations between the DJIA and crude oil and between crude oil and natural gas. In context of the dynamic correlation series based on commodity future contracts, the resulting estimates can barely be distinguished. In general, we find the conditional correlations between the DJIA and precious metals to fluctuate around zero, which provides additional empirical evidence in support of their hedging property against stock market risk. Further, we observe a decrease in the correlations in response to the outbreak of the COVID-19 pandemic, indicating the safe haven property of both gold and silver. In contrast, whilst the correlation between the stock market and natural gas future contracts also fluctuates around zero, the dependence between the DJIA and crude oil future contracts deviates substantially from zero and is much more volatile overall.

Moreover, Table 4.2 reports the estimated coefficients of the volatility and correlation models. Several interesting findings can be obtained from this table: Firstly, we find that Google searches are a statistically significant determinant of the time-varying correlation between asset returns. More particularly, when considering the restricted estimation period, the signs of the estimated coefficients are all negative, indicating that an increase (decrease) in investor attention towards individual assets leads to an increase (decrease) of their co-movement in response. Secondly, our results point towards a reversal of this relationship over crisis events which also contain a higher propensity of investor attention. When including the COVID-19 pandemic, we find that the coefficients are less negative (and even positive in case of investor attention towards crude oil and natural gas future contracts).

We interpret this finding as follows: In the presence of severe common shocks towards assets, investor attention towards individual assets leads to a smaller increase (or even a decrease) of their co-movement compared with tranquil times. This finding is in line with the theory outlined in Peng and Xiong (2006), Veldkamp (2006), and Veldkamp and Wolfers (2007) and helps to deepen our

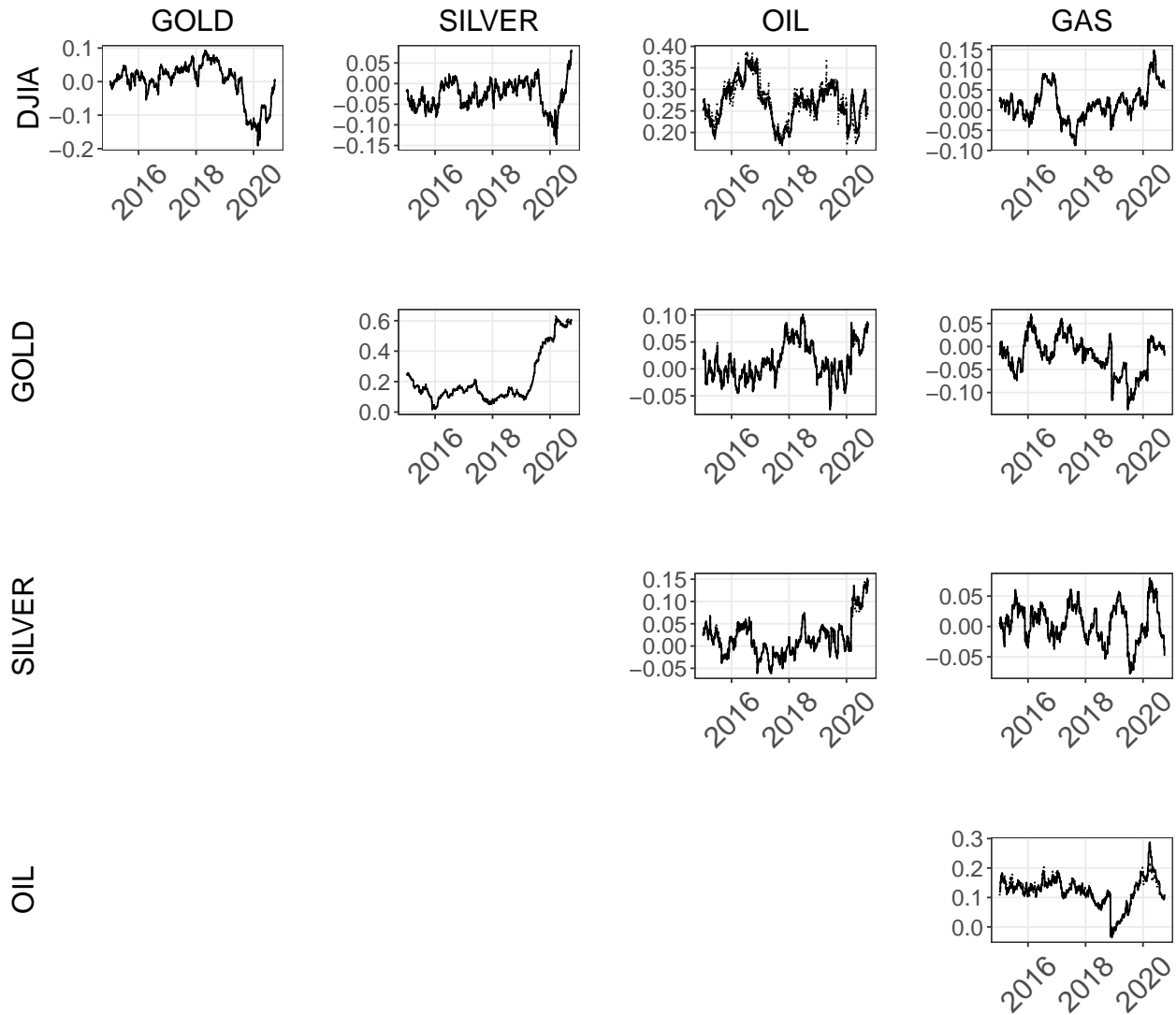


**Figure 4.2: Estimated correlations over time**

This figure plots daily conditional correlation estimates based on the DCC (solid lines) and the DCCX model (dashed lines) over the full estimation period. More precisely, the figure shows estimated correlations between returns of the DJIA, gold, silver, crude oil, and natural gas future contracts between January 2015 and September 2020.

**Table 4.2: Estimated model coefficients**

This table provides estimated coefficients for a) the univariate GARCH models and b) the multivariate DCC(X) models. Panel A and B distinguish the estimation period from January 2015 to September 2020, and the estimation period from January 2015 to December 2019. Of particular interest are  $\xi_{\text{dow}}$ ,  $\xi_{\text{gold}}$ ,  $\xi_{\text{silver}}$ ,  $\xi_{\text{oil}}$ , and  $\xi_{\text{gas}}$ , which show the influence of Google searches on the estimated correlation between the return series. \*\*\*, \*\*, and \* denote statistical significance at the 1%, 5%, and 10% level, respectively.

	a) Univariate components					b) Multivariate components	
	DJIA	Gold	Silver	Oil	Gas	DCC	DCCX
<b>Panel A: 2015-01-01/2020-09-30</b>							
$\omega$	-0.3811***	0.0000***	-0.1989***	0.0000***	0.0000		
$\alpha$	-0.1377***	0.0221***	0.0346***	0.0635***	0.0347***		
$\beta$	0.9643***	0.9623***	0.9807***	0.8767***	0.8537***		
$\gamma$	0.1870***	-0.0151***	0.0699***		-0.0400***		
$\psi_1$						0.0054***	0.0053***
$\psi_2$						0.9912***	0.9911***
$\xi_{\text{dow}}$							-0.0219***
$\xi_{\text{gold}}$							-0.0407***
$\xi_{\text{silver}}$							-0.1636***
$\xi_{\text{oil}}$							0.4048***
$\xi_{\text{gas}}$							0.1804***
<b>Panel B: 2015-01-01/2019-12-31</b>							
$\omega$	-0.5927***	0.0000	-0.0491***	0.0000***	0.0000***		
$\alpha$	-0.1931***	0.0106***	0.0150***	0.0443***	0.0529***		
$\beta$	0.9435***	0.9859***	0.9950***	0.9201***	0.8620***		
$\gamma$	0.1211***	-0.0087***	0.0048***		-0.0608***		
$\psi_1$						0.0052***	0.0038***
$\psi_2$						0.9877***	0.9916***
$\xi_{\text{dow}}$							-0.1385***
$\xi_{\text{gold}}$							-0.9317***
$\xi_{\text{silver}}$							-0.8777***
$\xi_{\text{oil}}$							-0.0105***
$\xi_{\text{gas}}$							-0.1967***

understanding of the role that investor attention assumes in determining the dynamic co-movement between asset returns. Further, our results may have important considerations for policy makers and financial investors. In the following, we therefore want to use our results in a brief financial exercise to investigate whether market participants can use the information entailed in Google searches to enhance the optimal allocation of their investments.

## 4.5 Financial implications

### 4.5.1 Optimal portfolio weights and hedging ratios

In context of optimal portfolio allocation, sound risk management decision-making depends on the precise construction of the dynamic covariance matrix between returns. Thus, investors are well advised to incorporate all relevant information available into its estimation. Considering the information of online investor attention as potentially valuable, we demonstrate the implications of changes to the dynamic covariance matrix for an investor in a brief financial exercise: Firstly, we construct optimal portfolio weights and hedging ratios in the two-asset framework based on the DCC(X) models. Secondly, we analyze the hedging effectiveness of the resulting portfolios.

Suppose an investor attempts to protect herself from stock price movement exposure by investing in commodity or energy future contracts. We consider the framework of [Kroner and Ng \(1998\)](#), assuming the investor seeks to minimize portfolio risk without lowering expected returns and define the optimal weight of the second asset in a 1 US-Dollar portfolio at time  $t$  as:

$$w_{c,t} = \frac{\sigma_{d,t}^2 - \sigma_{cd,t}^2}{\sigma_{c,t}^2 - 2\sigma_{cd,t}^2 + \sigma_{d,t}^2},$$

$$w_{c,t} = \begin{cases} 0, & \text{if } w_{c,t} < 0 \\ w_{c,t}, & \text{if } 0 \leq w_{c,t} \leq 1 \\ 1, & \text{if } w_{c,t} > 1, \end{cases} \quad (4.4)$$

where  $\sigma_{d,t}^2$  and  $\sigma_{c,t}^2$  indicate the time-varying conditional variance of the DJIA and the future contract returns, respectively, and  $\sigma_{cd,t}^2$  is the dynamic conditional covariance between DJIA and future contract returns. Note, that the framework provided in Equation 4.4 imposes a constraint on the mean-variance portfolio optimization approach, as short selling is not allowed. Subsequently, suppose the objective of the investor is to minimize the risk of her stock market investment based on the available information set. In a two-asset framework, [Kroner and Sultan \(1993\)](#) suggest a long position of 1 US-Dollar in the stock market to be hedged by a short position of  $\beta_{c,t}$  US-Dollar in the second market:

$$\beta_{c,t} = \frac{\sigma_{cd,t}^2}{\sigma_{c,t}^2}. \quad (4.5)$$

Figure 4.3 illustrates the optimal portfolio weights based on the DCC model (solid lines) and DCCX model (dashed lines) over time. Clearly, the suggested optimal weights of each future contract in the two-asset portfolios are highly volatile over time, yet demonstrate only marginal dissimilarities across models. Note, however, that optimal weights are a function of both individual asset variances and their covariance. Thus, deviations in the employed covariance estimates may only have partial influence on the calculated ratios.

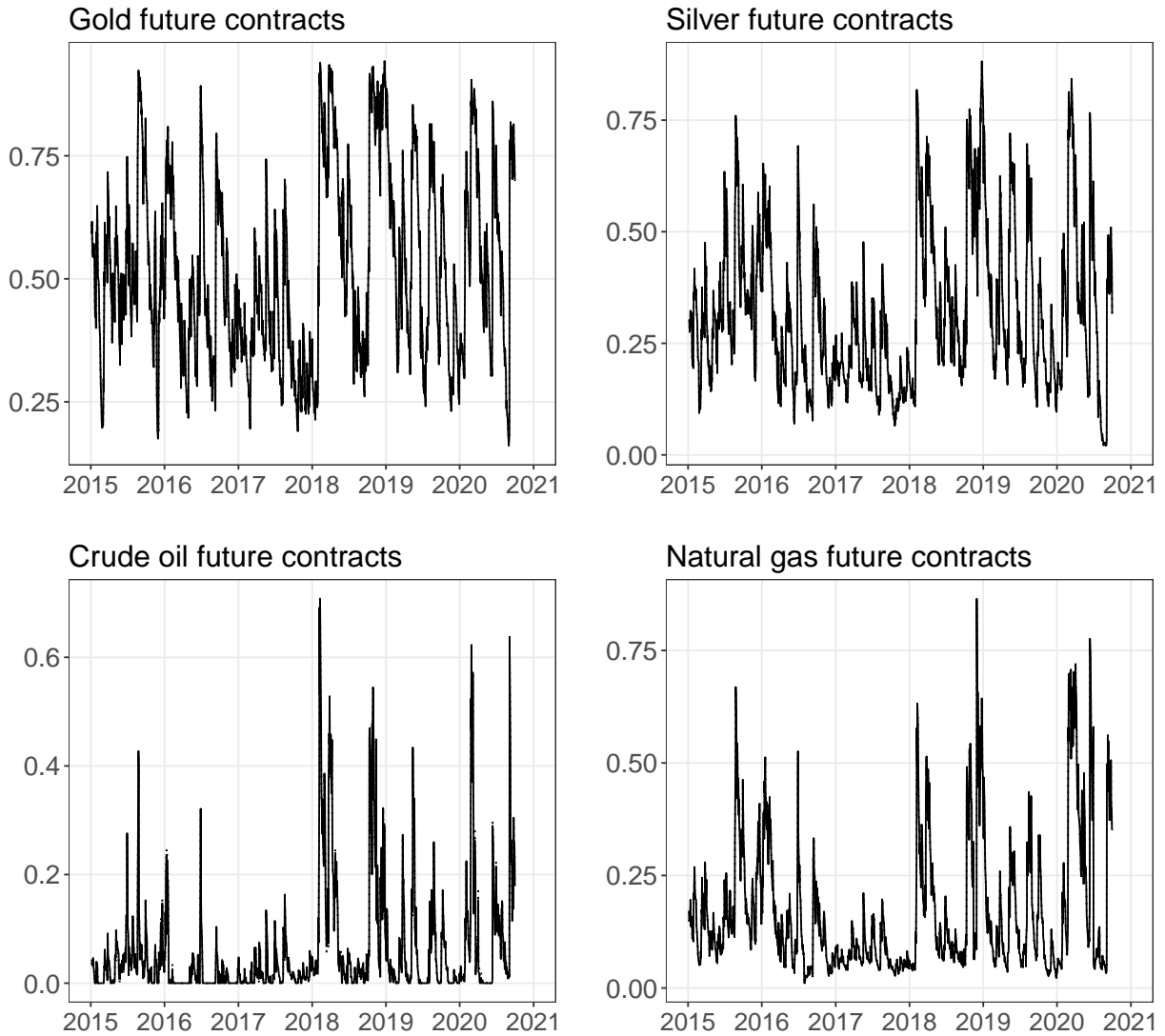


**Figure 4.3: Optimal weights of commodities and energies over time**

This figure plots estimates of daily optimal commodity and energy weights for four hedged portfolios over the period from January 2015 to September 2020. Weights to minimize the risk of DJIA investments by the means of investments in gold (top left panel), silver (top right panel), crude oil (bottom left panel), and natural gas (bottom right panel) future contracts are estimated through the DCC (solid line) and DCCX (dashed line) model.

Moreover, Table 4.3 presents summary statistics of optimal portfolio weights and hedging ratios. To this end, we denote hedged portfolios based on the DCC model and DCCX model as  $PF_{c,DCC}$  and  $PF_{c,DCCX}$ , respectively. As can be seen, estimates of optimal weights vary substantially across estimation period but not across models. For instance, the average optimal weights of gold, silver, crude oil, and natural gas future contracts in the two-asset portfolios decrease from approximately 52%, 32%, 6%, and 17% to 50%, 31%, 5%, and 14%, respectively, when restricting the estimation to the pre-COVID-19 period. This finding is not surprising, as it suggests that the stock market risk during the COVID-19 pandemic is considerably higher. Turning to the average optimal hedging ratios, the table depicts low absolute values for all future contracts. For instance, a long position of 1 US-Dollar on the stock market should on average be hedged by an approximately 0.1 cent long position on the gold market over the full estimation period. Restricting the estimation to the pre-COVID-19 period, the investor should take a 1 cent short position on the gold market. Again, this indicates that the investor requires more gold in her portfolio to minimize the risk of her stock market investment during times of financial turmoil.

In summary, our findings on the optimal ratios of commodity and energy future contracts to hedge DJIA investments, accompanied by low and/ or negative hedging ratios, coincide with the notion that both precious metals and natural gas future contracts may enrich purely stock-diversified portfolios. This finding is less pronounced for the case of crude oil future contracts. Moreover, the consideration of Google searches as a determinant of the time-varying correlation between asset returns only leads to marginal changes in asset allocation decisions.

## 4.5.2 Portfolio performance and hedging effectiveness

Next, we examine the actual performance of the hedged portfolios. We follow [Ku \*et al.\* \(2007\)](#), who propose hedging effectiveness as the gain (or loss) in the variance of the hedged portfolio compared to the variance of the unhedged portfolio  $PF_d$ :

$$HE_{c,m} = \frac{\sigma_{PF_d}^2 - \sigma_{PF_{c,m}}^2}{\sigma_{PF_d}^2}, \quad (4.6)$$

where  $\sigma_{PF_d}^2$  refers to the variance of the benchmark portfolio, and  $\sigma_{PF_{c,m}}^2$  is the variance of the hedged portfolio with  $m \in \{DCC, DCCX\}$ . Risk reduction increases as  $HE_{c,m}$  approaches unity.

Table 4.4 provides descriptive statistics and hedging effectiveness of the portfolios, whereby superior model performance is highlighted in boldface. Our results indicate that taking the information from Google searches into consideration may improve the hedging effectiveness in the majority of hedged portfolios. However, we find the improvements to be marginal in magnitude, as incorporating Google searches does not improve the hedging effectiveness by more than 1%. Thus, whilst our results show that investor attention is a significant determinant of the linkages between assets, they also shed light on the limitations of Google searches in financial application, rendering the measure less useful in the designing of optimal portfolios and their corresponding risk reduction.



**Table 4.3: Estimated optimal weights and hedging ratios**

This table summarizes estimated a) optimal commodity future contract weights and b) hedging ratios for all hedged portfolios considered in this study. In more detail, we report the corresponding mean, median, standard deviation, minimum, and maximum. Panel A and B refer to the estimation period from January 2015 to September 2020, and January 2015 to December 2019, respectively.

	a) Optimal weights					b) Hedging ratios				
	Mean	Median	St. Dev.	Min.	Max.	Mean	Median	St. Dev.	Min.	Max.
<b>Panel A: 2015-01-01/2020-09-30</b>										
PF <sub>gold,DCC</sub>	0.5153	0.4841	0.1878	0.1608	0.9422	-0.0009	0.0124	0.0811	-0.6302	0.2459
PF <sub>gold,DCCX</sub>	0.5153	0.4842	0.1877	0.1606	0.9421	-0.0013	0.0118	0.0798	-0.6266	0.2412
PF <sub>silver,DCC</sub>	0.3212	0.2878	0.1732	0.0204	0.8819	-0.0195	-0.0139	0.0302	-0.2580	0.0802
PF <sub>silver,DCCX</sub>	0.3211	0.2876	0.1733	0.0204	0.8818	-0.0194	-0.0137	0.0303	-0.2710	0.0795
PF <sub>oil,DCC</sub>	0.0602	0.0205	0.1032	0.0000	0.7081	0.0988	0.0881	0.0497	0.0207	0.3400
PF <sub>oil,DCCX</sub>	0.0597	0.0191	0.1035	0.0000	0.7072	0.0993	0.0899	0.0492	0.0180	0.3349
PF <sub>gas,DCC</sub>	0.1673	0.1119	0.1464	0.0107	0.8649	0.0096	0.0055	0.0259	-0.0496	0.1731
PF <sub>gas,DCCX</sub>	0.1672	0.1119	0.1464	0.0108	0.8652	0.0096	0.0056	0.0251	-0.0474	0.1642
<b>Panel B: 2015-01-01/2019-12-31</b>										
PF <sub>gold,DCC</sub>	0.4967	0.4600	0.1806	0.1601	0.9445	0.0124	0.0135	0.0452	-0.2022	0.2049
PF <sub>gold,DCCX</sub>	0.4966	0.4600	0.1810	0.1572	0.9472	0.0146	0.0136	0.0401	-0.1810	0.1818
PF <sub>silver,DCC</sub>	0.3096	0.2617	0.1635	0.0696	0.8542	-0.0286	-0.0245	0.0241	-0.1706	0.0190
PF <sub>silver,DCCX</sub>	0.3094	0.2613	0.1635	0.0710	0.8533	-0.0290	-0.0232	0.0237	-0.2312	0.0066
PF <sub>oil,DCC</sub>	0.0473	0.0115	0.0929	0.0000	0.7375	0.0961	0.0829	0.0481	0.0321	0.3911
PF <sub>oil,DCCX</sub>	0.0470	0.0109	0.0929	0.0000	0.7419	0.0966	0.0832	0.0489	0.0331	0.4122
PF <sub>gas,DCC</sub>	0.1394	0.1001	0.1149	0.0080	0.8730	-0.0012	-0.0008	0.0130	-0.0733	0.0540
PF <sub>gas,DCCX</sub>	0.1396	0.1010	0.1149	0.0100	0.8734	-0.0015	-0.0011	0.0111	-0.0651	0.0443

**Table 4.4: Portfolio performances**

This table summarizes the performance of all hedged portfolios considered in this study. In more detail, we report mean, median, standard deviation, minimum, maximum, skewness, kurtosis and hedging effectiveness of returns from DJIA investments hedged with gold ( $PF_{gold,m}$ ), silver ( $PF_{silver,m}$ ), crude oil ( $PF_{oil,m}$ ) and natural gas ( $PF_{gas,m}$ ) future contracts. In the table,  $m$  refers to the DCC or DCCX specification used to compute the share of assets in each portfolio. Panel A and B refer to the estimation period from January 2015 to September 2020, and January 2015 to December 2019, respectively. Superior portfolio performance is highlighted in bold face.

	Mean	Median	St. Dev.	Min.	Max.	Skewness	Kurtosis	HE (%)
<b>Panel A: 2015-01-01/2020-09-30</b>								
$PF_{dow}$	0.0006	0.0004	0.0105	-0.0614	0.0953	0.6254	11.8981	
$PF_{gold,DCC}$	0.0004	0.0004	0.0065	-0.0436	0.0657	0.5595	12.3387	<b>61.5031</b>
$PF_{gold,DCCX}$	0.0004	0.0004	0.0065	-0.0436	0.0657	0.5592	12.3396	61.5024
$PF_{silver,DCC}$	0.0005	0.0006	0.0085	-0.0699	0.0795	-0.1409	14.1630	34.2954
$PF_{silver,DCCX}$	0.0005	0.0006	0.0085	-0.0699	0.0796	-0.1399	14.1554	<b>34.3070</b>
$PF_{oil,DCC}$	0.0004	0.0003	0.0107	-0.0685	0.0910	0.2363	10.5661	-4.4133
$PF_{oil,DCCX}$	0.0004	0.0003	0.0107	-0.0684	0.0895	0.2184	10.4232	<b>-4.2346</b>
$PF_{gas,DCC}$	0.0004	0.0004	0.0099	-0.0491	0.1612	2.8979	50.5654	11.9145
$PF_{gas,DCCX}$	0.0004	0.0004	0.0099	-0.0490	0.1611	2.8966	50.5206	<b>11.9367</b>
<b>Panel B: 2015-01-01/2019-12-31</b>								
$PF_{dow}$	0.0003	0.0002	0.0083	-0.0404	0.0491	-0.5136	3.8106	
$PF_{gold,DCC}$	0.0002	0.0003	0.0053	-0.0259	0.0268	-0.1299	2.3511	<b>60.1276</b>
$PF_{gold,DCCX}$	0.0002	0.0003	0.0053	-0.0259	0.0268	-0.1290	2.3515	60.1228
$PF_{silver,DCC}$	0.0003	0.0005	0.0064	-0.0332	0.0404	-0.0878	3.0740	41.2693
$PF_{silver,DCCX}$	0.0003	0.0005	0.0064	-0.0332	0.0404	-0.0871	3.0733	<b>41.2722</b>
$PF_{oil,DCC}$	0.0002	0.0002	0.0084	-0.0458	0.0576	-0.4072	5.0130	-2.1081
$PF_{oil,DCCX}$	0.0002	0.0002	0.0084	-0.0458	0.0575	-0.4108	4.9772	<b>-1.9863</b>
$PF_{gas,DCC}$	0.0002	0.0003	0.0074	-0.0347	0.0334	-0.3970	3.1898	19.7802
$PF_{gas,DCCX}$	0.0002	0.0003	0.0074	-0.0346	0.0334	-0.3970	3.1858	<b>19.8158</b>

## 4.6 Concluding remarks

Linkages between financial markets are highly relevant for both policy makers conducting research related to the energy-macro nexus, and financial practitioners interested in increasing the benefits from their investments. Consequently, finding drivers of such linkages is important for financial researchers and practitioners alike. Whilst investor attention has already been considered theoretically as one of these drivers, the empirical evidence to assess this relation is still in its infancy. We add to filling this gap in the literature and investigate the impact of online investor attention on the linkages between stock, commodity, and energy markets. More particularly, we draw upon an extension of the DCC model to find online investor attention, measured by Google searches for individual assets, to be a statistically significant driver of the time-varying correlation between their returns. Our results suggest that when common shocks towards assets are severe, investor attention towards individual assets leads to smaller increases (or even decreases) of their co-movement compared with tranquil times. This finding provides novel empirical evidence with regards to the information that may be entailed by measures for online investor attention, and motivates additional investigations in further research. Moreover, we demonstrate the implications of our findings to market participants in a portfolio construction exercise. Even though the effects from incorporating the information provided by Google searches into the portfolio design are small in magnitude, marginal benefits are revealed for the majority of the considered portfolios and estimation periods.

## 4.7 Appendix

We consider the BIC to choose the univariate GARCH specification from the following three GARCH-type models:

- Standard GARCH (Bollerslev, 1986)

$$\sigma_t^2 = \omega + \alpha r_{t-1}^2 + \beta \sigma_{t-1}^2$$

- Exponential GARCH (Nelson, 1991)

$$\log \sigma_t^2 = \omega + \alpha \frac{r_{t-1}}{\sigma_{t-1}} + \gamma \left( \frac{|r_{t-1}|}{\sigma_{t-1}} - E \left[ \frac{|r_{t-1}|}{\sigma_{t-1}} \right] \right) + \beta \log \sigma_{t-1}^2$$

- GJR-GARCH (Glosten *et al.*, 1993)

$$\sigma_t^2 = \omega + \alpha r_{t-1}^2 + \gamma \mathbb{1}\{r_{t-1}^2\} + \beta \sigma_{t-1}^2$$

The employed GARCH-type models are capable to account for the characteristic properties observable in univariate financial time series to different extents. The exponential GARCH and GJR-GARCH model, for instance, can capture volatility persistence in addition to potential leverage and asymmetry effects.

# Chapter 5

## What are you searching for? On the equivalence of proxies for online investor attention

### 5.1 Introduction

Investor attention is a potentially valuable input factor for many financial forecasting exercises. However, it is also a latent variable, and several different proxies for investor attention have been employed in the past. In recent years, online searches have increasingly been associated with the informational demand of investors and, consequently, have been used as a measure of online investor attention. In line both with noise trader theories in the spirit of [Kyle \(1985\)](#) and [Black \(1986\)](#) as well as with behavioral models inspired by [De Long \*et al.\* \(1990\)](#) and [Shleifer and Vishny \(1997\)](#), such online information gathering is often attributed to retail investors. The latter are generally perceived to be at an informational disadvantage compared to institutional investors.

Online investor attention measured by online search queries, primarily Google and Wikipedia searches, has been at the center of an extensive empirical literature in finance. For instance, [Da \*et al.\* \(2011\)](#) show that the Google Search Volume Index constitutes a more convincing measure of investor attention than other indirect proxies, such as extreme returns and abnormal trading volume (e.g., [Barber and Odean, 2008](#)). Similarly, [Preis \*et al.\* \(2013\)](#) and [Moat \*et al.\* \(2013\)](#) provide empirical evidence that Google and Wikipedia searches for financial terms, respectively, predict stock market movements. Besides, [Dimpfl and Jank \(2016\)](#) find that Google searches can be used to augment forecasts of realized volatility on the index level, and [Audrino \*et al.\* \(2020\)](#) discover a similar result for individual-level stocks. Beyond, [Joseph \*et al.\* \(2011\)](#) find that stock ticker searches on Google predict abnormal portfolio returns and trading volume. They highlight the significance of ticker searches since these are directly linked to stock performance, while broader company-related search terms may also lead to search results that are not primarily related to a company's performance on

the stock market. On a similar note, [Behrendt \*et al.\* \(2020\)](#) find that company-specific Wikipedia page views help to predict collective investor behavior.

Even though different sources of online search queries are considered in the literature, the question remains whether these constitute equivalent proxies for online investor attention. This is associated with the ongoing search for a preferred proxy. We make use of an extensive data set consisting of Google stock ticker searches and company-specific Wikipedia searches for the constituents of the DJIA covering ten years from 2008 until 2017 to investigate this question. Our empirical analysis draws upon Shannon transfer entropy, a model-free measure derived from information theory that can be used to test for and quantify the transfer of information between time series ([Dimpfl and Peter, 2013](#); [Behrendt \*et al.\*, 2019](#)). The measure detects any statistical dependence, including nonlinear relations that are not revealed by VAR approaches (e.g., [Dimpfl and Peter, 2018](#); [Behrendt and Schmidt, 2021](#)). Moreover, it is possible to determine the *dominant direction* of the information transfer, which constitutes an improvement over the Granger causality test ([Granger, 1969](#)) and its nonlinear extensions (e.g., [Nishiyama \*et al.\*, 2011](#)).

While we discover a significant bi-directional information transfer for most companies' online search series, we cannot confirm that Google searches and Wikipedia searches are equivalent proxies of investor attention based on information-theoretical arguments. There emerges no clear pattern of *dominant directions* of the information transfer across companies. Using any of these measures may be reasonable in financial applications, but one should be aware that they do not measure the same online investor attention for all stocks, which may influence empirical findings. Moreover, some of the information transfer is nonlinear, rendering linear correlations or linear Granger causality tests less useful for comparisons of such online investor attention measures.

The remainder of this paper is structured as follows: Section [5.2](#) briefly outlines the concept of Shannon transfer entropy, and Section [5.3](#) describes our data set. Next, Section [5.4](#) presents the results, and Section [5.5](#) concludes.

## 5.2 A measure of information transfer

Denote by  $I$  a discrete random variable which can take on  $n$  distinct values, where  $i$  indicates one possible realization of  $I$ , and by  $p(i)$  the probability mass function (pmf) of  $I$ . Shannon entropy ([Shannon, 1948](#)) states that the average number of bits required to optimally encode independent draws from the distribution of  $I$  can be calculated as:

$$H_I = \mathbb{E}(\eta(i)) = - \sum_i p(i) \cdot \log_2(p(i)), \quad (5.1)$$

where  $\eta(i) = -\log_2(p(i))$  denotes a measure of information content. By construction,  $\eta(i)$  is large (small) for small (large)  $p(i)$ , i.e., rare outcomes convey more information than frequent outcomes. Consequently, Shannon entropy measures the expected informational content over all realizations  $i$ .

A bi-variate measure of the expected information content, called mutual information, is based on the Kullback-Leibler divergence (Kullback and Leibler, 1951). Introducing a second discrete random variable  $J$ , we let  $p(i)$  and  $p(j)$  denote the marginal pmf's of  $I$  and  $J$ , respectively. Moreover,  $p(i, j)$  is the joint pmf of both random variables. Mutual information is then given by:

$$M_{IJ} = \sum_i \sum_j p(i, j) \cdot \log_2 \left( \frac{p(i, j)}{p(i)p(j)} \right). \quad (5.2)$$

Mutual information measures the decrease in uncertainty for the case that  $I$  and  $J$  are not statistically independent. However, an asymmetric measure would be desirable for the quantification of the information transfer between two time series.

On this note, Schreiber (2000) introduces time series dynamics into the above formulation by considering transition probabilities. Now, let  $I$  and  $J$  denote stationary Markov processes of order  $l$  and  $h$ , respectively. Measuring the deviation from the generalized Markov property  $p(i_{t+1}|i_t^{(l)}, j_t^{(h)}) = p(i_{t+1}|i_t^{(l)})$ , where  $i_t^{(l)} = (i_t, \dots, i_{t-l+1})'$  and  $j_t^{(h)} = (j_t, \dots, j_{t-h+1})'$ , Schreiber (2000) quantifies the information transfer from discrete process  $J$  to  $I$  by means of the Shannon transfer entropy:

$$T_{J \rightarrow I} = \sum_i \sum_j p(i_{t+1}, i_t^{(l)}, j_t^{(h)}) \cdot \log_2 \left( \frac{p(i_{t+1}|i_t^{(l)}, j_t^{(h)})}{p(i_{t+1}|i_t^{(l)})} \right). \quad (5.3)$$

We can determine the *dominant direction* of the information transfer by taking the difference of  $T_{J \rightarrow I}$  and  $T_{I \rightarrow J}$ , where  $T_{I \rightarrow J}$  denotes the information flow from  $I$  to  $J$ .

Basing Shannon transfer entropy on discrete random variables allows us to bootstrap the underlying Markov processes along the lines of Horowitz (2003) and to provide basic statistical inference. In order to obtain such discretized time series, we follow Dimpfl and Peter (2013) and Behrendt *et al.* (2019) by partitioning our time series into three bins and using an encoded time series for estimation. A partitioning into three bins is reasonable in our application since we are interested in general tail events (low or high volumes of daily online searches). Besides, a partitioning into more bins would require more data. In the following, we specify two quantiles,  $q_1$  and  $q_2$ , of the empirical distribution of the observed online search series  $\{x_t\}_{t=1}^T$ . An encoded time series  $\{S_t\}_{t=1}^T$  is obtained as:

$$S_t = \begin{cases} 1 & \text{for } x_t \leq q_1 \\ 2 & \text{for } q_1 < x_t < q_2 \\ 3 & \text{for } x_t \geq q_2 \end{cases} \quad \forall t. \quad (5.4)$$

Thus, the chosen encoding replaces each observed value in  $\{x_t\}_{t=1}^T$  by one of the three integers  $\{1, 2, 3\}$ , according to Equation 5.4. These quantiles can be varied as a robustness test.

Lastly, following Marschinski and Kantz (2002), we calculate an effective transfer entropy to

mitigate a potential bias due to finite sample effects:

$$ET_{J \rightarrow I} = T_{J \rightarrow I} - T_{J_{\text{shuffled}} \rightarrow I}, \quad (5.5)$$

where  $T_{J_{\text{shuffled}} \rightarrow I}$  denotes the Shannon transfer entropy with a shuffled time series for  $J$ . A shuffled time series is obtained by sampling from the original series and aligning the sampled observations to a new series. Thus, any statistical dependence between  $J_{\text{shuffled}}$  and  $I$  is destroyed. While  $T_{J_{\text{shuffled}} \rightarrow I}$  converges to zero for increasing  $T$  in the case of no bias, a non-zero value is an indication for the existence of a finite sample bias.

## 5.3 Data

Our data set comprises daily Google stock ticker searches and company-specific Wikipedia searches for 27 constituents of the DJIA for all trading days over ten years from January 2008 until December 2017. Raw data are sourced from Google Trends and the Wikimedia data dump following the approaches outlined in [Bleher and Dimpfl \(2019\)](#) and [Behrendt \*et al.\* \(2020\)](#), respectively.<sup>37</sup> This leaves us with 2,505 observations per company and online source. Before elaborating further on the data, [Figure 5.1](#) illustrates raw relative Google search volume and absolute Wikipedia page views for the three companies with the highest average market capitalization over the full sample period, i.e., Microsoft (MSFT), JPMorgan Chase & Co. (JPM), and Johnson & Johnson (JNJ). As can be seen, the online search time series display pronounced co-movements for some time periods.

To be more precise, Google Trends' Search Volume Index comprises a measure of the relative propensity of any given keyword (here: stock tickers) over time. Its values are scaled between 0 and 100, where 100 reflects the maximum search interest within the requested period. Since we use the algorithm of [Bleher and Dimpfl \(2019\)](#) to source values at daily frequency, it is possible to obtain values greater than 100 as depicted in [Figure 5.1](#). We compute first differences of this measure to avoid persistence introduced by a potential unit root and to comply with preceding literature (e.g., [Dzielinski, 2012](#); [Chronopoulos \*et al.\*, 2018](#)). We refer to these series simply as Google searches. The Wikipedia page views time series constitute daily counts of the number of times a company's Wikipedia page is visited, accounting for all languages the respective page is translated into.<sup>38</sup> In order to obtain time series that better conform to the Google search series and that can be tested for stationarity with the usual statistical tests, we take the first difference of each Wikipedia page views time series and scale with the respective sample mean, obtaining a measure of relative change

---

<sup>37</sup>Three stock tickers are excluded from the analysis due to imprecise symbols, i.e., AT&T Inc. ( $T$ ), Visa Inc. ( $V$ ), and Dow Chemical ( $DOW$ ). For information about Google Trends, see [www.google.com/trends](http://www.google.com/trends). For Wikimedia, see <https://dumps.wikimedia.org/>. Further information about the data handling procedures can be found in [Bleher and Dimpfl \(2019\)](#) and [Behrendt \*et al.\* \(2020\)](#).

<sup>38</sup>The raw Wikipedia data consists of roughly 10 TB. Bash-scripts and the GNU parallel library ([Tange, 2011](#)) are used to filter for each respective company page.



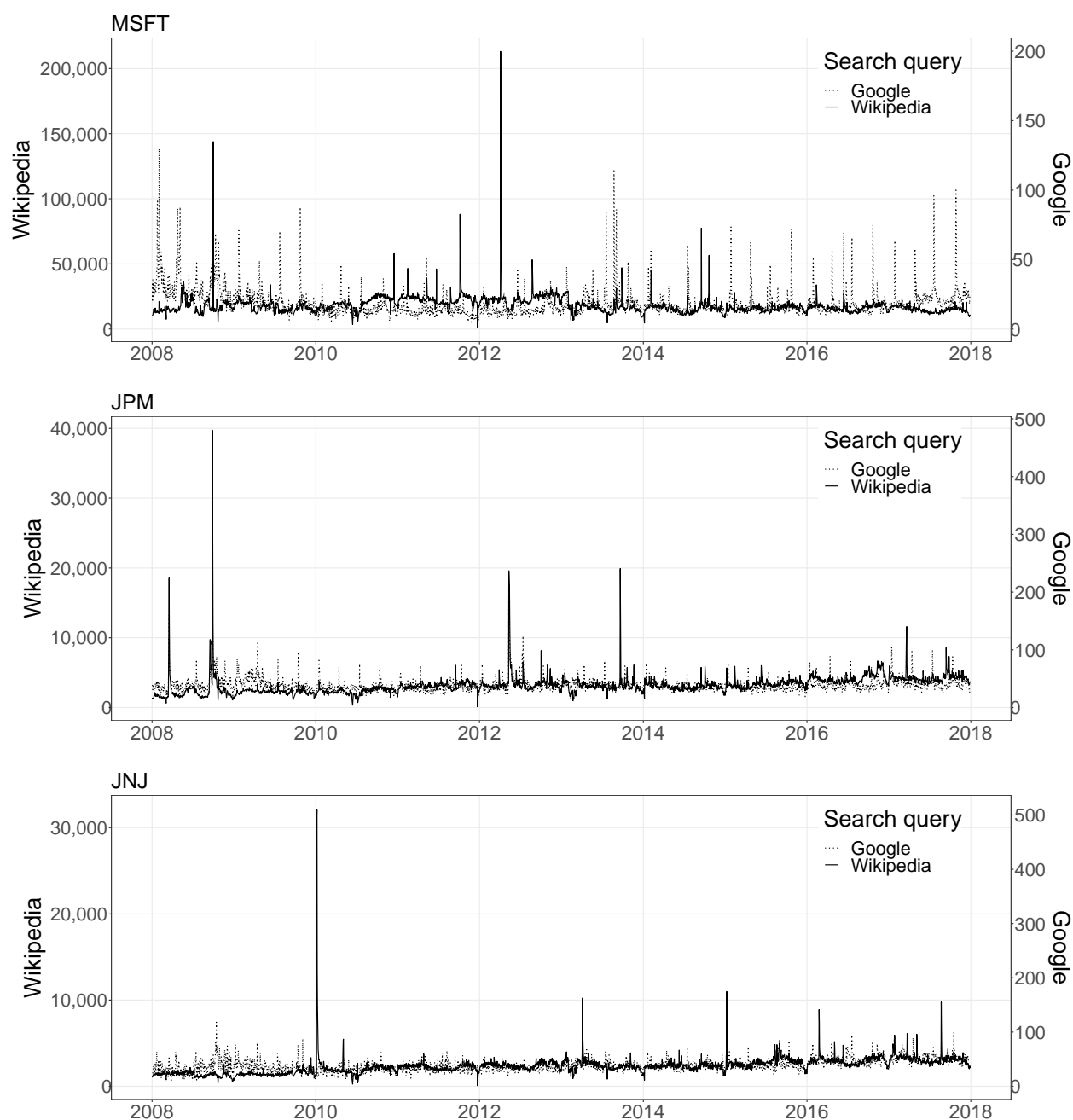


**Figure 5.1: Online searches over time for three companies**

This figure plots raw daily relative Google stock ticker search volume (dashed line) and absolute company-specific Wikipedia page views (solid line) for the companies Microsoft (MSFT), JPMorgan Chase & Co. (JPM), and Johnson & Johnson (JNJ) from January 2008 to December 2017. The y-axis on the left-hand side refers to Wikipedia page views, measured in counts, while the y-axis on the right-hand side specifies a relative measure of Google search volume (see [Bleher and Dimpfl, 2019](#)).

of Wikipedia page views from one trading day to the next.<sup>39</sup> Again, we refer to these series simply as Wikipedia searches.<sup>40</sup> Based on ADF tests, we can reject the null-hypothesis of a unit root process for each of the Google and Wikipedia search time series in our sample.

Table 5.1 provides descriptive statistics for Google and Wikipedia search time series for all 27 companies. It is obvious that many time series exhibit an excess kurtosis, which is important for the application we have in mind since we are especially interested in extreme tail events, i.e., extremely low or high Google searches and Wikipedia searches. Thus, the application of Shannon transfer entropy seems to be a reasonable choice.

---

<sup>39</sup>Neither stationarity tests nor providing statistical inference for parts of our empirical analysis are trivial tasks when using count data. Another reason why we consider measures of relative change.

<sup>40</sup>Note that it is not possible to calculate usual (log-) growth rates since for some trading days, we observe zero page views. Besides, given that we discretize each time series for the calculation of the Shannon transfer entropy, the scaling factor does not distort our analysis.

**Table 5.1: Descriptive statistics**

This table summarizes the data used in the empirical analysis. The data set covers 2,505 trading days from January 2008 to December 2017. For each ticker symbol, Panel A and B depict descriptive statistics for Google searches and Wikipedia searches, respectively. More precisely, we report the sample mean, standard deviation, maximum, minimum, 25%- and 75%-quantile, skewness, and kurtosis for each time series. The stock tickers are listed in descending order based on their average market capitalization over the considered time period.

Ticker Symbol	Mean	St. Dev.	Max.	Min.	25%-Quantile	75%-Quantile	Skewness	Kurtosis
<b>Panel A: Google stock ticker searches</b>								
MSFT	0.0036	8.5155	98.8809	-88.5329	-2.5520	2.2996	0.4143	33.9037
JPM	0.0057	11.0025	129.3559	-105.8366	-5.2708	4.7882	1.0868	25.5388
JNJ	0.0072	10.4029	62.3015	-56.7172	-6.2001	5.9019	0.3295	2.7980
XOM	0.0227	9.4860	48.5742	-39.3170	-5.7126	5.7267	0.0446	1.7196
WMT	0.0056	4.5596	72.0000	-49.0000	-2.1818	2.0627	1.8462	42.0606
HD	0.0266	1.7603	9.4842	-11.3710	-0.5896	0.8175	-0.7817	5.1927
CVX	0.0052	10.6177	50.7966	-50.8577	-6.4534	6.4908	-0.0567	1.4313
UNH	-0.0025	9.4140	46.7464	-39.8564	-5.6194	5.0000	0.5121	2.1340
PFE	-0.0016	17.6060	84.7236	-81.8101	-10.9142	10.5164	0.0705	1.6019
VZ	-0.3554	33.2952	245.7772	-282.6438	-7.6227	8.0000	-0.6120	14.2834
INTC	0.0062	6.6164	62.4392	-55.0000	-2.7371	2.6927	0.2625	15.1741
PG	0.0103	4.0338	47.8982	-44.4769	-2.3589	2.2375	0.7117	20.1832
BA	0.0103	3.6961	42.2330	-24.3159	-2.0276	2.0000	0.9175	12.0360
CSCO	-0.0006	13.5290	162.6790	-132.5843	-4.7613	4.7709	0.2900	21.7660
KO	0.0207	2.4997	19.4060	-16.7014	-1.2819	1.5087	-0.3954	4.6483
DIS	0.0116	6.4454	104.1616	-78.5481	-3.3270	3.1654	1.7504	50.8785
MRK	0.0123	15.1556	238.0964	-323.6623	-6.6556	6.8422	-1.9855	120.6311
IBM	-0.0481	10.2426	97.0213	-62.3708	-6.1804	5.4919	0.5967	6.8201
MMM	-0.0050	12.7328	305.3183	-200.0361	-4.6204	4.5956	5.4047	184.5162
GE	-0.0068	3.6885	34.0000	-18.0715	-2.2589	2.0041	0.6637	5.2744
MCD	0.0159	78.6018	2723.7182	-2635.8564	-3.2446	3.4070	1.6019	1081.6937
UTX	0.0072	7.1440	60.0000	-54.2461	-4.1601	4.0168	0.4228	6.4256
GS	-0.0034	5.7857	53.4519	-48.5927	-1.6198	1.2854	1.0121	21.1975
CAT	0.0067	3.4349	72.1067	-52.1623	-1.2753	1.5243	1.3325	109.6793
NKE	0.0016	7.0113	59.1396	-65.0000	-3.9494	3.8354	0.2681	11.9163
AXP	-0.0021	10.7240	101.9611	-98.5048	-5.2489	5.2134	0.4808	11.1597
TRV	-0.0184	14.8387	78.9392	-70.6881	-8.6756	8.4352	0.0317	1.4904
<b>Panel B: company-specific Wikipedia searches</b>								
MSFT	0.0331	0.4102	11.1894	-7.5809	-0.0513	0.1050	6.0860	352.0767
JPM	0.0591	0.3929	12.5611	-2.2692	-0.0589	0.1522	16.1286	453.3551
JNJ	0.0383	0.4206	14.0135	-8.6522	-0.0793	0.1196	11.3026	566.3033
XOM	0.0306	0.5075	16.3364	-11.4447	-0.0681	0.1231	8.0495	543.9656
WMT	0.0243	0.1998	2.6381	-2.5623	-0.0516	0.0736	1.3042	44.5208
HD	0.0173	0.4025	11.5462	-11.0295	-0.0728	0.0963	1.1862	530.7759
CVX	0.0344	0.6357	24.6645	-14.4966	-0.0698	0.1202	18.0665	1010.6628
UNH	0.1003	0.3033	2.3425	-1.4180	-0.0626	0.1993	1.2871	4.1853
PFE	0.0397	0.3284	8.5818	-3.2055	-0.0779	0.1297	7.9407	205.6432
VZ	0.0405	0.6327	24.2738	-11.4209	-0.0632	0.1235	19.0514	916.6305
INTC	0.0218	0.7413	25.3478	-24.8459	-0.0576	0.0930	0.8585	1046.6955
PG	0.0201	0.2711	5.2542	-5.3414	-0.0667	0.0857	0.6318	170.5701
BA	0.0118	0.3337	6.9963	-8.4476	-0.0610	0.0774	-4.8762	314.2858
CSCO	0.0582	0.2222	2.2607	-1.6251	-0.0678	0.1440	0.9922	9.4111
KO	0.0014	0.4209	7.7352	-15.0030	-0.0710	0.0764	-19.7276	777.7927
DIS	-0.0075	0.3235	10.2804	-4.3847	-0.0552	0.0262	16.4048	513.3025
MRK	0.0609	0.5521	19.7673	-8.9945	-0.0906	0.1553	16.2657	690.9885
IBM	0.0369	0.4088	13.0077	-12.7034	-0.0670	0.1180	0.7498	778.8969
MMM	0.0476	0.4555	12.5563	-12.5409	-0.0703	0.1224	-0.1262	507.3429
GE	0.0370	0.2178	3.5221	-2.8040	-0.0656	0.1069	2.1222	50.1355
MCD	-0.0034	0.3121	6.5226	-6.4800	-0.0646	0.0546	0.3421	212.9224
UTX	0.0633	0.4331	10.9561	-7.6075	-0.0761	0.1508	7.0914	238.6739
GS	0.0335	0.6428	21.1105	-10.3895	-0.0687	0.1240	12.6395	540.6940
CAT	0.0400	0.2505	4.4850	-4.1208	-0.0614	0.1195	1.9718	98.2991
NKE	0.0197	0.1918	2.5863	-2.3009	-0.0670	0.0787	0.6282	31.2509
AXP	0.0411	0.1829	1.4826	-1.2208	-0.0609	0.1181	0.8714	7.3687
TRV	0.0924	0.3241	2.2022	-2.3179	-0.0814	0.2271	0.6199	4.3961

## 5.4 Empirical results

In order to investigate whether Google searches and Wikipedia searches are equivalent proxies for online investor attention, we rely on an information-theoretical approach. Thus, for each of the considered companies' time series, we estimate Shannon transfer entropy and determine the *dominant direction* of the information transfer. We provide effective transfer entropy estimates based on 300 shuffles, and statistical inference rests on 400 bootstrap replications.<sup>41</sup> Moreover, we also consider the usual linear Granger causality test and effective transfer entropies computed using the residuals obtained from a bi-variate VAR model, which are purged of any auto and cross-correlations. The latter allow us to detect potentially nonlinear relations between the online search series. Thus, the linear Granger causality test does not constitute a benchmark for Shannon transfer entropy but merely a means to illustrate the potential existence of nonlinear dynamic relations. Denoting by  $G_t$  and  $W_t$  our measures of daily Google searches and Wikipedia searches, respectively, we estimate the following VAR for every company:

$$\begin{bmatrix} G_t \\ W_t \end{bmatrix} = \mathbf{C} + \sum_{j=1}^p \mathbf{B}^j \begin{bmatrix} G_{t-j} \\ W_{t-j} \end{bmatrix} + \begin{bmatrix} \varepsilon_{G,t} \\ \varepsilon_{W,t} \end{bmatrix}, \quad (5.6)$$

where  $\mathbf{C}$  refers to the vector of constants and the  $\mathbf{B}^j$  to the autoregressive coefficient matrices. The lag length  $p$  is determined via the BIC. We consider two estimation periods: The full sample contains all data from 2008 until 2017, whereas a restricted sample includes the data from 2010 until 2017, excluding the financial crisis.

Tables 5.2 and 5.3 depict the results for a discretization based on the 5%- and 95%-quantiles of the empirical distributions of Google stock ticker searches and company-specific Wikipedia searches. Besides, Tables 5.4 and 5.5 illustrate similar results for a discretization based on the 10%- and 90%-quantiles. We only show results for two Markov orders,  $l = h = 1$  and  $l = h = 2$ , in order to provide a reasonable summary of our findings across all companies. For the residual series, we set  $l = h = 1$ . In general, determining the Markov order is a nontrivial task, but our choices are guided by the amount of data at hand and by the fact that the Markov order of the residual series is not likely to be larger than that for the original series. Results for a range of different Markov orders are available upon request. Note that there are a few companies for which the above Markov orders do not lead to statistically significant Shannon transfer entropy estimates, while Granger causality does reveal a linear relation between the online search series. In these cases, a higher Markov order is necessary to detect a significant information flow. For example, considering Markov orders  $l = h = 6$  reveals a significant information transfer from Google to Wikipedia for “UNH”, whereas no significant information transfer for the online search series is found for the Markov orders presented in Tables 5.2–5.5.

---

<sup>41</sup>Computations are easily reproducible with the R package **RTransferEntropy** (<https://cran.r-project.org/package=RTransferEntropy>). See also Behrendt *et al.* (2019).

**Table 5.2: Information transfer between Google and Wikipedia searches, 2008–2017,  $q(5, 95)$** 

This table provides information transfer estimates for the sample of search queries from January 2008 to December 2017. For each ticker symbol, the table presents (a) effective transfer entropies, (b) F-statistics of Granger causality tests, and (c) effective transfer entropies for residual series, which are purged of any linear auto and cross-correlations. Granger causality tests and residual series are based on a bi-variate VAR, where the lag length is determined by the BIC.  $G \rightarrow W$  corresponds to the information transfer from Google to Wikipedia,  $W \rightarrow G$  indicates the information transfer from Wikipedia to Google. *Diff* calculates the difference between effective transfer entropy estimates. Positive (negative) values indicate that the *dominant direction* of information transfer points towards Wikipedia (Google). All observations are discretized based on the 5% and 95% quantiles. The Markov order is  $l = h = 1$  and  $l = h = 2$  for the original series and  $l = h = 1$  for the residual series. 300 shuffles are used. \*\*\*, \*\*, and \* denote statistical significance at the 1%, 5%, and 10% level, respectively. The stock tickers are listed in descending order based on their average market capitalization over the ten years time period from 2008 to 2017.

Ticker Symbols	(a) Effective transfer entropies						(b) Granger causalities		(c) Effective transfer entropies for residual series		
	Markov order: $l=h=1$			Markov order: $l=h=2$			$G \not\rightarrow W$	$W \not\rightarrow G$	$G \rightarrow W$	$W \rightarrow G$	<i>Diff</i>
	$G \rightarrow W$	$W \rightarrow G$	<i>Diff</i>	$G \rightarrow W$	$W \rightarrow G$	<i>Diff</i>					
MSFT	0.0000	0.0027**	-0.0027	0.0098***	0.0074***	0.0024	2.1909*	1.4243	0.0005	0.0021*	-0.0016
JPM	0.0081***	0.0041***	0.0039	0.0176***	0.0011	0.0165	6.5804	1.9442*	0.0116***	0.0000	0.0116
JNJ	0.0011	0.0017	-0.0006	0.0000	0.0000	0.0000	1.5349	2.3034**	0.0000	0.0014	-0.0014
XOM	0.0000	0.0040**	-0.0040	0.0000	0.0057*	-0.0057	1.7204	2.2523*	0.0011	0.0019*	-0.0008
WMT	0.0000	0.0000	0.0000	0.0020	0.0009	0.0011	0.7158	2.3840**	0.0000	0.0009	-0.0009
HD	0.0000	0.0020*	-0.0020	0.0011	0.0054**	-0.0044	5.7531	3.5312***	0.0004	0.0000	0.0004
CVX	0.0001	0.0000	0.0001	0.0047**	0.0008	0.0039	0.4720	1.0060	0.0000	0.0023*	-0.0023
UNH	0.0006	0.0011	-0.0005	0.0000	0.0000	0.0000	3.3981***	10.5720	0.0022*	0.0019*	0.0003
PFE	0.0044**	0.0000	0.0044	0.0071***	0.0077**	-0.0006	2.1144**	5.9872	0.0006	0.0000	0.0006
VZ	0.0043***	0.0054***	-0.0010	0.0069**	0.0000	0.0069	0.2331	0.1966	0.0009	0.0035**	-0.0026
INTC	0.0007	0.0000	0.0007	0.0106***	0.0064**	0.0042	0.4937	0.5561	0.0004	0.0000	0.0004
PG	0.0006	0.0033**	-0.0026	0.0000	0.0046	-0.0046	5.6824	6.7879	0.0010	0.0000	0.0010
BA	0.0000	0.0000	0.0000	0.0050**	0.0000	0.0050	1.3017	6.9726	0.0004	0.0000	0.0004
CSCO	0.0027**	0.0074***	-0.0047	0.0270***	0.0038**	0.0232	5.0272	5.0021	0.0001	0.0013	-0.0012
KO	0.0050***	0.0053***	-0.0002	0.0030*	0.0106***	-0.0076	5.8341	4.6413***	0.0039**	0.0046***	-0.0007
DIS	0.0000	0.0000	0.0000	0.0042**	0.0028	0.0014	10.4021	0.3308	0.0000	0.0017	-0.0017
MRK	0.0016	0.0002	0.0014	0.0037*	0.0048	-0.0011	1.7726*	1.9603**	0.0000	0.0011	-0.0011
IBM	0.0018*	0.0016	0.0001	0.0057**	0.0026	0.0032	8.8786	8.4047	0.0050***	0.0000	0.0050
MMM	0.0012	0.0024**	-0.0012	0.0008	0.0038	-0.0030	0.9220	2.2400**	0.0018*	0.0029**	-0.0011
GE	0.0024**	0.0022*	0.0002	0.0050***	0.0060**	-0.0010	1.9718**	6.5586	0.0030**	0.0000	0.0030
MCD	0.0011	0.0044***	-0.0033	0.0059**	0.0042	0.0016	0.4959	1.3882	0.0023*	0.0106***	-0.0083
UTX	0.0072***	0.0042***	0.0030	0.0138***	0.0155***	-0.0017	3.3332***	7.8645	0.0039**	0.0035**	0.0004
GS	0.0000	0.0046***	-0.0046	0.0000	0.0042	-0.0042	0.4552	0.5712	0.0011	0.0010	0.0002
CAT	0.0058***	0.0029**	0.0029	0.0039**	0.0084**	-0.0045	3.5671***	6.7214	0.0000	0.0028**	-0.0028
NKE	0.0007	0.0000	0.0007	0.0050**	0.0027	0.0023	0.9367	0.7022	0.0000	0.0011	-0.0011
AXP	0.0002	0.0000	0.0002	0.0011	0.0052*	-0.0041	0.8267	2.4458***	0.0011	0.0000	0.0011
TRV	0.0065***	0.0041**	0.0024	0.0071**	0.0026	0.0045	1.1421	1.7887*	0.0053***	0.0015	0.0037

**Table 5.3: Information transfer between Google and Wikipedia searches, 2010–2017,  $q(5, 95)$**

This table provides information transfer estimates for the sample of search queries from January 2010 to December 2017. For each ticker symbol, the table presents (a) effective transfer entropies, (b) F-statistics of Granger causality tests, and (c) effective transfer entropies for residual series, which are purged of any linear auto and cross-correlations. Granger causality tests and residual series are based on a bi-variate VAR, where the lag length is determined by the BIC.  $G \rightarrow W$  corresponds to the information transfer from Google to Wikipedia,  $W \rightarrow G$  indicates the information transfer from Wikipedia to Google. *Diff* calculates the difference between effective transfer entropy estimates. Positive (negative) values indicate that the *dominant direction* of information transfer points towards Wikipedia (Google). All observations are discretized based on the 5% and 95% quantiles. The Markov order is  $l = h = 1$  and  $l = h = 2$  for the original series and  $l = h = 1$  for the residual series. 300 shuffles are used. \*\*\*, \*\*, and \* denote statistical significance at the 1%, 5%, and 10% level, respectively. The stock tickers are listed in descending order based on their average market capitalization over ten years time period from 2008 to 2017.

Ticker Symbols	(a) Effective transfer entropies						(b) Granger causalities		(c) Effective transfer entropies for residual series		
	Markov order: $l=h=1$			Markov order: $l=h=2$			$G \not\rightarrow W$	$W \not\rightarrow G$	$G \rightarrow W$	$W \rightarrow G$	<i>Diff</i>
	$G \rightarrow W$	$W \rightarrow G$	<i>Diff</i>	$G \rightarrow W$	$W \rightarrow G$	<i>Diff</i>					
MSFT	0.0036**	0.0019	0.0016	0.0155***	0.0142***	0.0013	1.1845	1.0161	0.0017	0.0014	0.0003
JPM	0.0059***	0.0012	0.0047	0.0130***	0.0033	0.0097	18.8895	1.1839	0.0117***	0.0000	0.0117
JNJ	0.0038**	0.0007	0.0030	0.0067**	0.0028	0.0039	4.4924	3.4355***	0.0000	0.0063***	-0.0063
XOM	0.0033**	0.0019	0.0014	0.0000	0.0037	-0.0036	1.6658	2.0715*	0.0000	0.0027**	-0.0027
WMT	0.0000	0.0020	-0.0020	0.0026	0.0000	0.0026	0.6499	2.1437*	0.0000	0.0008	-0.0008
HD	0.0000	0.0026*	-0.0026	0.0012	0.0078**	-0.0066	4.6972	2.9357***	0.0007	0.0009	-0.0002
CVX	0.0007	0.0000	0.0007	0.0040*	0.0000	0.0040	0.3320	0.9575	0.0000	0.0000	0.0000
UNH	0.0000	0.0015	-0.0015	0.0000	0.0023	-0.0023	4.6651***	20.5757	0.0003	0.0000	0.0003
PFE	0.0053***	0.0000	0.0053	0.0066**	0.0069*	-0.0003	2.5209***	6.9042	0.0011	0.0004	0.0007
VZ	0.0019	0.0000	0.0019	0.0011	0.0000	0.0011	0.5087	0.3930	0.0000	0.0012	-0.0012
INTC	0.0013	0.0000	0.0013	0.0102***	0.0071**	0.0032	0.4499	0.6440	0.0000	0.0027*	-0.0027
PG	0.0003	0.0035**	-0.0032	0.0003	0.0031	-0.0029	4.8252***	5.6234	0.0001	0.0001	0.0000
BA	0.0000	0.0000	0.0000	0.0032*	0.0000	0.0032	0.6678	5.8946***	0.0000	0.0000	0.0000
CSCO	0.0024*	0.0077***	-0.0054	0.0363***	0.0056**	0.0307	10.6670	6.8313	0.0001	0.0007	-0.0006
KO	0.0048***	0.0020	0.0029	0.0008	0.0059*	-0.0051	5.1089***	3.7690***	0.0009	0.0028*	-0.0019
DIS	0.0000	0.0000	0.0000	0.0058**	0.0081**	-0.0024	10.4184	0.3130	0.0000	0.0000	0.0000
MRK	0.0020	0.0004	0.0016	0.0028	0.0065*	-0.0037	1.6370	1.6067	0.0013	0.0025*	-0.0012
IBM	0.0000	0.0022*	-0.0022	0.0046*	0.0059**	-0.0013	9.6980	8.2325	0.0015	0.0000	0.0015
MMM	0.0000	0.0024*	-0.0024	0.0000	0.0022	-0.0022	2.3358*	6.6019	0.0000	0.0038**	-0.0038
GE	0.0029**	0.0062***	-0.0033	0.0091***	0.0096**	-0.0005	1.6001	6.4794	0.0000	0.0000	0.0000
MCD	0.0000	0.0019	-0.0019	0.0026	0.0049*	-0.0023	0.4339	1.4200	0.0029*	0.0200***	-0.0171
UTX	0.0064***	0.0041**	0.0023	0.0203***	0.0183***	0.0020	3.0778***	7.6657	0.0045**	0.0031**	0.0014
GS	0.0035**	0.0006	0.0030	0.0000	0.0000	0.0000	0.6221	0.8397	0.0000	0.0000	0.0000
CAT	0.0056***	0.0004	0.0051	0.0029*	0.0053	-0.0024	3.5451***	5.8414	0.0000	0.0030*	-0.0030
NKE	0.0004	0.0002	0.0002	0.0034	0.0021	0.0013	1.0722	0.7021	0.0000	0.0031**	-0.0031
AXP	0.0023*	0.0000	0.0023	0.0041	0.0043	-0.0002	0.5804	2.5608***	0.0023*	0.0000	0.0023
TRV	0.0028*	0.0000	0.0028	0.0044*	0.0000	0.0044	0.4357	2.0712**	0.0004	0.0013	-0.0009

**Table 5.4: Information transfer between Google and Wikipedia searches, 2008–2017,  $q(10, 90)$** 

This table provides information transfer estimates for the sample of search queries from January 2008 to December 2017. For each ticker symbol, the table presents (a) effective transfer entropies, (b) F-statistics of Granger causality tests, and (c) effective transfer entropies for residual series, which are purged of any linear auto and cross-correlations. Granger causality tests and residual series are based on a bi-variate VAR, where the lag length is determined by the BIC.  $G \rightarrow W$  corresponds to the information transfer from Google to Wikipedia,  $W \rightarrow G$  indicates the information transfer from Wikipedia to Google. *Diff* calculates the difference between effective transfer entropy estimates. Positive (negative) values indicate that the *dominant direction* of information transfer points towards Wikipedia (Google). All observations are discretized based on the 10% and 90% quantiles. The Markov order is  $l = h = 1$  and  $l = h = 2$  for the original series and  $l = h = 1$  for the residual series. 300 shuffles are used. \*\*\*, \*\*, and \* denote statistical significance at the 1%, 5%, and 10% level, respectively. The stock tickers are listed in descending order based on their average market capitalization over ten years time period from 2008 to 2017.

Ticker Symbols	(a) Effective transfer entropies						(b) Granger causalities		(c) Effective transfer entropies for residual series		
	Markov order: $l=h=1$			Markov order: $l=h=2$			$G \not\rightarrow W$	$W \not\rightarrow G$	$G \rightarrow W$	$W \rightarrow G$	<i>Diff</i>
	$G \rightarrow W$	$W \rightarrow G$	<i>Diff</i>	$G \rightarrow W$	$W \rightarrow G$	<i>Diff</i>					
MSFT	0.0036***	0.0043***	-0.0007	0.0093**	0.0160***	-0.0067	2.1909*	1.4243	0.0003	0.0062***	-0.0058
JPM	0.0019	0.0019	-0.0000	0.0135***	0.0072	0.0064	6.5804	1.9442*	0.0144***	0.0029**	0.0115
JNJ	0.0060***	0.0034**	0.0026	0.0024	0.0000	0.0024	1.5349	2.3034**	0.0001	0.0024*	-0.0023
XOM	0.0037**	0.0049***	-0.0011	0.0000	0.0065	-0.0065	1.7204	2.2523*	0.0003	0.0054***	-0.0052
WMT	0.0000	0.0039**	-0.0039	0.0000	0.0009	-0.0009	0.7158	2.3840**	0.0000	0.0035**	-0.0035
HD	0.0106***	0.0061***	0.0045	0.0080**	0.0233***	-0.0153	5.7531	3.5312***	0.0059***	0.0014	0.0045
CVX	0.0000	0.0041***	-0.0041	0.0000	0.0000	0.0000	0.4720	1.0060	0.0000	0.0038**	-0.0038
UNH	0.0056***	0.0065***	-0.0010	0.0048*	0.0097**	-0.0049	3.3981***	10.5720	0.0017	0.0020	-0.0003
PFE	0.0062***	0.0008	0.0054	0.0100***	0.0072	0.0028	2.1144**	5.9872	0.0030**	0.0006	0.0024
VZ	0.0109***	0.0099***	0.0010	0.0058	0.0017	0.0040	0.2331	0.1966	0.0066***	0.0056***	0.0011
INTC	0.0008	0.0002	0.0006	0.0097**	0.0089**	0.0008	0.4937	0.5561	0.0012	0.0011	0.0001
PG	0.0017	0.0060***	-0.0043	0.0053***	0.0150***	-0.0097	5.6824	6.7879	0.0040**	0.0055***	-0.0015
BA	0.0004	0.0000	0.0004	0.0014	0.0007	0.0007	1.3017	6.9726	0.0000	0.0016	-0.0016
CSCO	0.0079***	0.0252***	-0.0174	0.0254***	0.0206***	0.0049	5.0272	5.0021	0.0028**	0.0058***	-0.0030
KO	0.0119***	0.0314***	-0.0195	0.0124***	0.0263***	-0.0139	5.8341	4.6413***	0.0058***	0.0112***	-0.0054
DIS	0.0000	0.0000	0.0000	0.0000	0.0057	-0.0057	10.4021	0.3308	0.0000	0.0000	0.0000
MRK	0.0024*	0.0028**	-0.0004	0.0063***	0.0034	0.0029	1.7726*	1.9603**	0.0001	0.0023*	-0.0022
IBM	0.0128***	0.0068***	0.0060	0.0118***	0.0070**	0.0048	8.8786	8.4047	0.0000	0.0028**	-0.0028
MMM	0.0021*	0.0114***	-0.0093	0.0000	0.0143***	-0.0143	0.9220	2.2400**	0.0013	0.0024*	-0.0011
GE	0.0068***	0.0068***	0.0000	0.0097***	0.0164***	-0.0067	1.9718**	6.5586	0.0031**	0.0006	0.0025
MCD	0.0015	0.0032**	-0.0017	0.0003	0.0128***	-0.0124	0.4959	1.3882	0.0107***	0.0103***	0.0004
UTX	0.0045***	0.0053***	-0.0008	0.0123***	0.0079*	0.0045	3.3332***	7.8645	0.0051***	0.0006	0.0046
GS	0.0003	0.0037**	-0.0034	0.0025	0.0101	-0.0075	0.4552	0.5712	0.0011	0.0000	0.0011
CAT	0.0057***	0.0102***	-0.0045	0.0079**	0.0058*	0.0020	3.5671***	6.7214	0.0000	0.0002	-0.0002
NKE	0.0011	0.0030**	-0.0020	0.0024*	0.0000	0.0024	0.9367	0.7022	0.0002	0.0000	0.0002
AXP	0.0003	0.0025*	-0.0021	0.0047**	0.0018	0.0030	0.8267	2.4458***	0.0003	0.0019	-0.0016
TRV	0.0083***	0.0038**	0.0045	0.0132***	0.0002	0.0130	1.1421	1.7887*	0.0020*	0.0019	0.0001

**Table 5.5: Information transfer between Google and Wikipedia searches, 2010–2017,  $q(10, 90)$**

This table provides information transfer estimates for the sample of search queries from January 2010 to December 2017. For each ticker symbol, the table presents (a) effective transfer entropies, (b) F-statistics of Granger causality tests, and (c) effective transfer entropies for residual series, which are purged of any linear auto and cross-correlations. Granger causality tests and residual series are based on a bi-variate VAR, where the lag length is determined by the BIC.  $G \rightarrow W$  corresponds to the information transfer from Google to Wikipedia,  $W \rightarrow G$  indicates the information transfer from Wikipedia to Google. *Diff* calculates the difference between effective transfer entropy estimates. Positive (negative) values indicate that the *dominant direction* of information transfer points towards Wikipedia (Google). All observations are discretized based on the 10% and 90% quantiles. The Markov order is  $l = h = 1$  and  $l = h = 2$  for the original series and  $l = h = 1$  for the residual series. 300 shuffles are used. \*\*\*, \*\*, and \* denote statistical significance at the 1%, 5%, and 10% level, respectively. The stock tickers are listed in descending order based on their average market capitalization over ten years time period from 2008 to 2017.

Ticker Symbols	(a) Effective transfer entropies						(b) Granger causalities		(c) Effective transfer entropies for residual series		
	Markov order: $l=h=1$			Markov order: $l=h=2$			$G \not\rightarrow W$	$W \not\rightarrow G$	$G \rightarrow W$	$W \rightarrow G$	<i>Diff</i>
	$G \rightarrow W$	$W \rightarrow G$	<i>Diff</i>	$G \rightarrow W$	$W \rightarrow G$	<i>Diff</i>					
MSFT	0.0044**	0.0025	0.0019	0.0078*	0.0141***	-0.0062	1.1845	1.0161	0.0000	0.0047***	-0.0047
JPM	0.0009	0.0000	0.0009	0.0182***	0.0079*	0.0103	18.8895	1.1839	0.0214***	0.0007	0.0207
JNJ	0.0002	0.0056**	-0.0055	0.0000	0.0010	-0.0010	4.4924	3.4355***	0.0000	0.0063***	-0.0063
XOM	0.0030*	0.0049**	-0.0019	0.0000	0.0122	-0.0122	1.6658	2.0715*	0.0003	0.0068***	-0.0066
WMT	0.0000	0.0068***	-0.0068	0.0000	0.0026	-0.0026	0.6499	2.1437*	0.0001	0.0062**	-0.0061
HD	0.0074***	0.0069***	0.0005	0.0071**	0.0304***	-0.0233	4.6972	2.9357***	0.0027*	0.0041**	-0.0014
CVX	0.0000	0.0022*	-0.0022	0.0014	0.0000	0.0014	0.3320	0.9575	0.0000	0.0023*	-0.0023
UNH	0.0035*	0.0061***	-0.0026	0.0038	0.0091**	-0.0053	4.6651***	20.5757	0.0000	0.0019	-0.0019
PFE	0.0062***	0.0008	0.0053	0.0024	0.0039	-0.0015	2.5209***	6.9042	0.0006	0.0000	0.0006
VZ	0.0016	0.0011	0.0005	0.0038	0.0000	0.0038	0.5087	0.3930	0.0000	0.0007	-0.0007
INTC	0.0002	0.0037**	-0.0035	0.0108**	0.0127***	-0.0018	0.4499	0.6440	0.0005	0.0000	0.0005
PG	0.0018	0.0043**	-0.0025	0.0045**	0.0099**	-0.0054	4.8252***	5.6234	0.0027*	0.0014	0.0013
BA	0.0000	0.0000	0.0000	0.0000	0.0042	-0.0042	0.6678	5.8946***	0.0000	0.0010	-0.0010
CSCO	0.0059***	0.0196***	-0.0138	0.0195***	0.0052**	0.0144	10.6670	6.8313	0.0014	0.0052**	-0.0039
KO	0.0112***	0.0206***	-0.0094	0.0119***	0.0203***	-0.0084	5.1089***	3.7690***	0.0087***	0.0065***	0.0022
DIS	0.0000	0.0000	0.0000	0.0000	0.0055	-0.0055	10.4184	0.3130	0.0000	0.0000	0.0000
MRK	0.0011	0.0058***	-0.0047	0.0053	0.0022	0.0031	1.6370	1.6067	0.0023	0.0002	0.0021
IBM	0.0161***	0.0103***	0.0058	0.0155***	0.0054*	0.0101	9.6980	8.2325	0.0028*	0.0000	0.0028
MMM	0.0044**	0.0153***	-0.0109	0.0031	0.0186***	-0.0155	2.3358*	6.6019	0.0003	0.0048**	-0.0045
GE	0.0044**	0.0138***	-0.0094	0.0082**	0.0203***	-0.0122	1.6001	6.4794	0.0006	0.0022	-0.0016
MCD	0.0012	0.0030*	-0.0018	0.0027	0.0101*	-0.0073	0.4339	1.4200	0.0072***	0.0183***	-0.0110
UTX	0.0040**	0.0040**	0.0000	0.0173***	0.0063	0.0110	3.0778***	7.6657	0.0038**	0.0036**	0.0002
GS	0.0002	0.0015	-0.0013	0.0000	0.0009	-0.0009	0.6221	0.8397	0.0000	0.0007	-0.0007
CAT	0.0093***	0.0130***	-0.0038	0.0020	0.0055	-0.0035	3.5451***	5.8414	0.0000	0.0001	-0.0001
NKE	0.0009	0.0044**	-0.0034	0.0018	0.0000	0.0018	1.0722	0.7021	0.0000	0.0000	0.0000
AXP	0.0000	0.0007	-0.0007	0.0023	0.0037	-0.0014	0.5804	2.5608***	0.0000	0.0015	-0.0015
TRV	0.0018	0.0000	0.0018	0.0000	0.0000	0.0000	0.4357	2.0712**	0.0008	0.0000	0.0008



Nonetheless, several interesting findings can be obtained from these tables: Firstly, no clear pattern is visible regarding the *dominant direction* of the information transfer as indicated by the *Diff* columns in the tables, where positive (negative) values indicate that the dominant direction points towards Wikipedia (Google). For some companies, the dominant direction points from Google to Wikipedia, for other companies, it points in the opposite direction. Note, that this value only holds meaning if at least one of the transfer entropy estimates is statistically significant. As a result, these online search series do not measure the same online investor attention across the companies in our sample. A similar result is obtained by the Granger causality tests, which do not unambiguously point into one direction (here, an unambiguous statement about direction is only possible if the detected information transfer is only statistically significant in one direction). However, secondly, there is some nonlinear information transfer, indicated by the significant effective transfer entropy estimates for the residual series that are purged of any auto and cross-correlations. In these cases, linear Granger causality tests do not provide a reliable measure, while Shannon transfer entropy detects the dependencies. Thirdly, the number of companies for which such nonlinear information transfer between the online search series is detected decreases for the post-crisis sample. Thus, such nonlinear dependencies between these measures of online investor attention become more relevant in crisis periods, which is in line with an increased demand for information in such times. Lastly, results are not completely robust to changes in the quantiles that are used for discretization. For some stocks, results are driven by some extremely low or high Google searches and Wikipedia searches. However, Shannon transfer entropy still detects the relevant dependencies, only the direction of the dominant information transfer may change. Overall, we cannot confirm that Google stock ticker searches and company-specific Wikipedia searches constitute equivalent proxies for online investor attention, and we find that model-free measures such as Shannon transfer entropy provide valuable tools for such investigations. Our results are independent of the average market capitalization of the considered companies' stocks or the primary business fields they are engaged in.

## 5.5 Conclusion

Both researchers and practitioners are interested in proxies for latent investor attention, which are used in a variety of financial applications. In particular, measures obtained from online sources have increasingly been employed in applied research. Google stock ticker searches and company-specific Wikipedia searches provide indirect measures of investor attention that can easily be computed for individual-level stocks. However, these online search series do not provide equivalent proxies when considering information-theoretical arguments. Moreover, linear correlations do not suffice to investigate the information transfer between such different measures of online investor attention. Although our analysis does not determine the specific usefulness of the considered online investor attention measures in financial applications, one should keep in mind that they do not necessarily capture the same latent investor attention.

# Chapter 6

## News impact dynamics in the correlations of global equity returns for systemic risk measurement

### 6.1 Introduction

This article introduces a parsimonious model to investigate the dynamic correlations between a global cross-section of equity market indices and to reveal the impact of news on their dependence over time. The model is based on [Engle \(2002\)](#)'s well-established DCC model and complements the asymmetric extension suggested in [Cappiello \*et al.\* \(2006\)](#). In compliance both with price variation theory outlined in [Mandelbrot \(1963\)](#) as well as investigations on the impact of shocks on asset volatility in spirit of [Engle and Ng \(1993\)](#) and [Jondeau and Rockinger \(2009\)](#), we argue that the impact of news on second central moments is highly dynamic. In the multivariate case, it is therefore not reasonable to assume that the impact of news on the co-movement between assets remains constant over time. For this reason, we introduce a new model which permits the dynamic dependence between news and correlations to be anchored in a single time-varying parameter. The recursion to update the parameter is based on the scaled shape of the conditional observation density. In turn, this dynamic parameter may capture the “severity” of news for every single point in time over the entire observation interval.

Our contribution to the literature is twofold. Firstly, we add to the extensive strand of literature on MGARCH models. Throughout the last decades, MGARCH models have gained wide popularity in modelling and forecasting conditional (co)variances of financial time series. For instance, [Engle and Kroner \(1995\)](#) suggest the Baba-Engle-Kraft-Kroner (BEKK) model which provides a natural extension of [Engle \(1982\)](#)'s ARCH and [Bollerslev \(1986\)](#)'s GARCH model to the multivariate setting. Whilst the BEKK model reliably ensures positive definiteness of the conditional covariance matrix, practical applications are largely limited due to the curse of dimensionality. For this reason,

Tse and Tsui (2002) propose the varying conditional correlation (VCC) model and Engle (2002) introduces the well-known DCC model. In contrast to the BEKK specification, both models allow for a parsimonious modelling of correlation dynamics over time. Acknowledging the presence of leverage effects provoked in Black (1976) and Christie (1982), namely that variances (and covariances in the multivariate setting) exhibit different responses depending on the sign of past news, Cappiello *et al.* (2006) forward the DCC model to account for potentially asymmetric effects in the evolution of conditional correlations.

The above models restrict the impact of news on correlation dynamics to be constant over time. In many empirical applications, however, the influence of news on market linkages shows large changes over the observation interval. The assumption of a single static parameter to capture this impact can therefore be unreasonable, especially when market dynamics are exposed to incisive events such as financial crises or events provoking changes of similar scope. Thus, we propose to advance MGARCH models along this dimension. More precisely, our extension complements DCC-type models in considering an adaptive weighting of squared standardized innovations to model and forecast conditional correlations over time. We employ the GAS framework introduced in Creal *et al.* (2011), Creal *et al.* (2013), and Harvey (2013) to account for potential time-variation in the news impact parameter. The updating function of the time-varying parameter is similar to the recursion of parent GARCH volatility models and offers a flexible linkage between past innovations and current estimates of the conditional correlation. Consequently, the response from correlation estimates to news varies over time and allows for a much quicker, score-driven adaption of the conditional correlation to the observed data. We interpret the magnitude of the time-varying parameter as an indicator for the “severity” of news. We additionally conduct a simulation study to highlight the model’s ability to pattern a wide range of time-varying correlation processes.

Secondly, we contribute to the literature studying financial systemic risk within large economic networks. For instance, Rua and Nunes (2009) investigate international equity return co-movement using wavelet analyses. Along this line, Rodriguez (2007) and Kenourgios *et al.* (2011) employ regime-switching copulas to model financial market linkages over multiple crisis periods. Moreover, Chiang *et al.* (2007) find correlation linkages across crisis-hit markets during the late 1990 Asian financial crises to be significantly impacted by news on changes in foreign-currency sovereign credit ratings.

Our approach distinguishes from the studies above since we study changes to cross-market linkages not only by using a framework revealing bi-variate estimates, but also by offering a single time-varying parameter which can capture the (potentially) changing relevance of news for the correlation dynamics of the entire cross-section. Besides, our model provides the means to detect precise event windows over which we observe significant increases in the impact of shocks on market linkages. Such changes to correlation dynamics are directly related to Forbes and Rigobon (2002)’s definition of contagion as a significant increase in cross-market linkages in response to shocks. For further prominent literature on the subject and measuring of financial contagion, we refer to Bae

*et al.* (2003), *Bekaert et al.* (2009), and *Bekaert et al.* (2014). Consequently, the proposed dynamic news impact parameter provides an indicator for the evolution of financial systemic risk and the market exposure to the risk of contagion over time.

The remainder of this paper is structured as follows. Section 6.2 introduces score-driven dynamics to the news parameter in dynamic conditional correlation models, Section 6.3 provides a Monte Carlo study to demonstrate the fit of the model in different situations, and Section 6.4 describes the data and offers an empirical application. Lastly, Section 6.5 concludes.

## 6.2 Time-varying correlation models with score-driven dynamics

Consider an  $n$ -dimensional vector stochastic process  $r_t$  with mean zero and covariance matrix  $\Sigma_t$ . The conditional correlation between any two  $r_{i,t}$  and  $r_{j,t}$  with  $i = 1, \dots, n$  and  $j = 1, \dots, n$  is defined:

$$\rho_{ij,t} = \frac{E_{t-1}(r_{i,t}r_{j,t})}{\sqrt{E_{t-1}(r_{i,t}^2)}\sqrt{E_{t-1}(r_{j,t}^2)}}, \quad (6.1)$$

such that the correlation in any period depends on all information available prior to that period and cannot exceed unity in absolute terms. The linkage between conditional covariance and conditional correlation can be demonstrated as follows. Denote  $r_{k,t}$  as the conditional standard deviation multiplied by a mean zero, unit variance disturbance term  $\varepsilon_{k,t}$ :

$$\sigma_{k,t}^2 = E_{t-1}(r_{k,t}^2), \quad r_{k,t} = \sigma_{k,t}\varepsilon_{k,t}, \quad k = 1, \dots, n, \quad (6.2)$$

Substitution into Equation 6.1 provides a means to depict the conditional correlation between  $r_{i,t}$  and  $r_{j,t}$  as the conditional covariance between standardized disturbances:

$$\begin{aligned} \rho_{ij,t} &= \frac{E_{t-1}(\varepsilon_{i,t}\varepsilon_{j,t})}{\sqrt{E_{t-1}(\varepsilon_{i,t}^2)}\sqrt{E_{t-1}(\varepsilon_{j,t}^2)}} \\ &= E_{t-1}(\varepsilon_{i,t}\varepsilon_{j,t}). \end{aligned} \quad (6.3)$$

### 6.2.1 Dynamic conditional correlation with static news impact

Investigations on correlation dynamics have sparked large strands of theoretic and applied econometric literature. Amongst others, well-known models to estimate conditional correlations are *Engle* (2002)'s DCC model and *Cappiello et al.* (2006)'s more adaptive ADCC model to capture potentially asymmetric effects on correlations in response to the sign of past innovations. By decomposing the conditional covariance matrix  $\Sigma_t$  in its variance- and correlation constituents,

$D_t$  and  $R_t$ , respectively, the ADCC model can be formulated:

$$\begin{aligned}
 r_t | \mathfrak{F}_{t-1} &\sim \mathcal{N}(0, D_t R_t D_t), \\
 D_t^2 &= \text{diag}(\omega_i) + \text{diag}(\alpha_i) \circ r_{t-1} r'_{t-1} + \text{diag}(\beta_i) \circ D_{t-1}^2, \\
 \varepsilon_t &= D_t^{-1} r_t, \\
 Q_t &= \bar{Q} (\iota' - \psi_1 - \psi_2) - \psi_3 \bar{N} + \psi_1 \varepsilon_{t-1} \varepsilon'_{t-1} \\
 &\quad + \psi_3 n_{t-1} n'_{t-1} + \psi_2 Q_{t-1}, \\
 R_t &= \text{diag}(Q_t)^{-1/2} Q_t \text{diag}(Q_t)^{-1/2},
 \end{aligned} \tag{6.4}$$

where  $\mathfrak{F}_t$  is the information set at time  $t$ ,  $\circ$  is the Hadamard product, and  $D_t$  is a diagonal matrix comprising univariate volatility estimates of (standard) GARCH models based on the unknown parameter vectors  $\omega$ ,  $\alpha$ , and  $\beta$ .<sup>42</sup> The correlation equation consists of the auxiliary matrix  $Q_t$  where  $\iota$  denotes a  $(n \times 1)$  vector of ones,  $n_t = \mathbb{1}\{\varepsilon_t < 0\} \circ \varepsilon_t$  with  $\mathbb{1}\{\cdot\}$  as the indicator function,  $\bar{Q}$  and  $\bar{N}$  are the unconditional covariance matrix of  $\varepsilon_t \varepsilon'_t$  and  $n_t n'_t$ , respectively, and  $\psi_1$ ,  $\psi_2$ , and  $\psi_3$  are three unknown scalar parameters to describe the evolution of correlations over time. Finally, elements of  $R_t$  contain estimates of the conditional correlation of form  $\rho_{ij,t} = q_{ij,t} / \sqrt{q_{ii,t} q_{jj,t}}$ , whereby  $q_{ij,t}$  is the  $ij$ -th entry of  $Q_t$ . Note, that the ADCC model nests the DCC model as a special case for  $\psi_3 = 0$ . For positive definiteness of  $Q_t$ , a necessary and sufficient condition is  $\psi_1 + \psi_2 + \delta \psi_3 < 1$  where  $\delta$  is the largest eigenvalue of  $[\bar{Q}^{-1/2} \bar{N} \bar{Q}^{-1/2}]$  (see, e.g., [Ding and Engle, 2001](#); [Cappiello et al., 2006](#)).

Coefficients of DCC-type models are commonly obtained via two-stage maximum likelihood estimation. In the first stage, GARCH-type models are employed to estimate the parameters of the mean and variance equations comprised in  $\theta_1$ . In the second stage, the univariate volatility series from the first stage are used to standardize the vector stochastic process and, in turn, estimate the unknown parameter vector  $\theta_2 = (\psi_1, \psi_2, \psi_3)'$  to compute the conditional correlation matrices.

### 6.2.2 Dynamic conditional correlation with score-driven news impact

In the ADCC model, correlation dynamics are subject to three parameters, exclusively. More broadly,  $\psi_1$  covers the influence of past innovations on correlations,  $\psi_2$  refers to the autoregressive parameter of the recursion, and  $\psi_3$  captures potentially asymmetric responses to the sign of past innovations.<sup>43</sup> In many empirical applications which require the estimation of time-varying correlations, it is not reasonable to assume that the influence of past news on correlations remains constant over the entire observation period.

For this reason, we introduce a time-varying parameter to capture the dynamic influence of past

---

<sup>42</sup>In our empirical study, we consider four distinct GARCH models to describe the evolution of univariate volatilities over time.

<sup>43</sup>Similar to [Engle and Ng \(1993\)](#),  $\varepsilon_t$  is treated as a collective measure of standardized news at time  $t$  in this paper. Consequently, we interpret positive (negative)  $\varepsilon_t$  as the arrival of “good” (“bad”) news.

news on correlations. We propose to model the evolution of correlation dynamics by using flexible estimates for  $\psi_1$ :

$$Q_t = \bar{Q} (\omega' - \psi_{1,t} - \psi_2) + \psi_{1,t} \varepsilon_{t-1} \varepsilon'_{t-1} + \psi_2 Q_{t-1}, \quad (6.5)$$

where  $\psi_{1,t} = h(f_t)$  is a strictly monotonic transformation of the parameter  $f_t \in \mathbb{R}$  with  $t = 1, \dots, T$ . More particularly, we suggest  $h(f_t) = \exp(f_t)/(1 + \exp(f_t))$  as the link function to be used in the remainder of this paper. The choice for  $\psi_3 = 0$  is intuitive as potential asymmetry effects can be captured in a flexible adaption of  $\psi_{1,t}$  to these effects at any point in time. We use the GAS framework to model the evolution of  $f_t$  over time (Creal *et al.*, 2011, 2013; Harvey, 2013). Recently, GAS-type models have been employed in a variety of different econometric settings to permit time-varying dynamics based on information received from the score of the conditional observation density. For instance, Creal *et al.* (2011) suggest a novel multivariate Student-t GAS model to estimate volatilities and correlations, and Blasques *et al.* (2019) use score-driven dynamics to introduce time-variation to magnitude parameters of univariate GARCH-type models. Along this line, Blasques *et al.* (2016b) propose a score-driven spatial dependence model, and Oh and Patton (2018) use the GAS framework to enhance their model for dynamic systematic risk. In conformity with the parsimonious structure of DCC-type models, we assume the updating function of  $f_t$  to follow a GAS(1-1)-type process:

$$f_{t+1} = \omega^s + AS(f_t) \nabla_t + B f_t, \quad (6.6)$$

where  $\omega^s$ ,  $A$  and  $B$  are unknown parameters and  $S(f_t)$  provides a means for local scaling of the score function  $\nabla_t$ . In our case, the scaling function equals unity for all arguments  $f_t$  which is in line with the approach of Blasques *et al.* (2016b).<sup>44</sup> Thus, for each iteration, the (scaled) score of the conditional density relates the direction of the steepest ascent of the observation density to the recursion of  $f_t$ . Denote the score as:

$$\nabla_t = \frac{\partial \log p(r_t | f_t, \mathfrak{F}_t; \theta_2)}{\partial f_t}, \quad (6.7)$$

where  $\theta_2 = (\psi_2, \omega^s, A, B)'$  comprises all static parameters used in the second stage of the estimation procedure. In line with Engle (2002), the log-likelihood is given by the sum of a volatility ( $\ell_{v,t}$ ) and a correlation ( $\ell_{c,t}$ ) part:

$$\mathcal{L} = \sum_{t=1}^T \ell_{v,t} + \ell_{c,t}, \quad (6.8)$$

---

<sup>44</sup>Please see, e.g., Creal *et al.* (2013) for an extensive discussion on alternative specifications for the scaling function  $S(f_t)$ .

where the time  $t$  contribution to the volatility part of the log-likelihood function is given by:

$$\ell_{v,t} = -\frac{1}{2} \left( n \log(2\pi) + \log|D_t|^2 + r_t' D_t^{-2} r_t \right), \quad (6.9)$$

whilst the time  $t$  contribution to the correlation part of the log-likelihood function can be written as:

$$\ell_{c,t} = -\frac{1}{2} \left( \log|R(f_t)| + \varepsilon_t' R(f_t)^{-1} \varepsilon_t - \varepsilon_t' \varepsilon_t \right). \quad (6.10)$$

Note, that the derivative of the log-likelihood function in Equation 6.8 with respect to  $f_t$  is equal to the derivative of the correlation part of the log-likelihood function given in Equation 6.10 with respect to  $f_t$ . Thus, the score can be denoted:

$$\begin{aligned} \nabla_t &= \frac{\partial \ell_{c,t}}{\partial f_t} \\ &= -\frac{1}{2} \left[ \text{Tr} \left( R(f_t)^{-1} C_t \right) + \varepsilon_t' \left( -R(f_t)^{-1} C_t R(f_t)^{-1} \right) \varepsilon_t \right] \\ &= \frac{1}{2} \text{vec} \left( R(f_t)^{-1} C_t \right)' \text{vec} \left( R(f_t)^{-1} \varepsilon_t \varepsilon_t' - I \right), \end{aligned} \quad (6.11)$$

where  $\text{Tr}(\cdot)$  and  $\text{vec}(\cdot)$  are the trace and vectorization operators, respectively, whilst  $C_t$  is an auxiliary ( $n \times n$ ) matrix defined by:

$$\begin{aligned} C_t &= -\frac{1}{2} \text{diag} \left( \frac{\partial Q}{\partial f_t} \right) \text{diag}(Q_t)^{-1} R(f_t) + \text{diag}(Q_t)^{-1/2} \frac{\partial Q}{\partial f_t} \text{diag}(Q_t)^{-1/2} \\ &\quad - \frac{1}{2} R(f_t) \text{diag} \left( \frac{\partial Q}{\partial f_t} \right) \text{diag}(Q_t)^{-1}, \end{aligned} \quad (6.12)$$

with:

$$\frac{\partial Q}{\partial f_t} = \dot{h}(f_t) \cdot \left( \varepsilon_{t-1} \varepsilon_{t-1}' - \bar{Q} \right), \quad (6.13)$$

where  $\dot{h}(f_t)$  is the first derivative of the link function with respect to  $f_t$ . In our case,  $\dot{h}(f_t) = \exp(f_t)/(1 + \exp(f_t))^2$ . The introduction of score-driven dynamics to the DCC framework is a statistically attractive tool to broaden the range of the innovation parameter based on the probability density. More particularly, the proposed score-driven model allows the impact of news on conditional correlation estimates to vary over time. Furthermore, the model adopts the appealing considerations of DCC-type models for applications with large cross-sections. For simplicity, we henceforth refer to the model as probability-range DCC, or p-range DCC.

### 6.3 Monte Carlo study

To evaluate the performance of the p-range DCC model in finding different correlation structures, we conduct a simulation study. The performance evaluation relies on 200 replications of five simulated data sets which follow the patterns in Engle (2002). We set the number of observations to 1000 which is similar to the empirical application in the subsequent section. The data generating process consists of two Gaussian standard GARCH models and is given by:

$$\begin{aligned} \begin{pmatrix} \varepsilon_{1,t} \\ \varepsilon_{2,t} \end{pmatrix} &\sim \mathcal{N} \left[ \begin{pmatrix} 0 \\ 0 \end{pmatrix}, \begin{pmatrix} 1 & \rho_t \\ \rho_t & 1 \end{pmatrix} \right], \quad r_t = D_t \varepsilon_t, \\ D_t^2 &= \begin{pmatrix} 0.01 & 0 \\ 0 & 0.5 \end{pmatrix} + \begin{pmatrix} 0.05 & 0 \\ 0 & 0.2 \end{pmatrix} \circ r_{t-1} r'_{t-1} + \begin{pmatrix} 0.94 & 0 \\ 0 & 0.5 \end{pmatrix} \circ D_{t-1}^2, \end{aligned} \quad (6.14)$$

where the simulated correlations processes are:

- Constant:  $\rho_t = 0.9$
- Sine:  $\rho_t = 0.5 + 0.4 \cos 2\pi t/200$
- Fast sine:  $\rho_t = 0.5 + 0.4 \cos 2\pi t/20$
- Step:  $\rho_t = 0.9 - 0.5 \cdot \mathbf{1}(t > 500)$
- Ramp:  $\rho_t = \text{mod } t/200$

Figure 6.1 depicts each of the simulated correlation processes (black lines), mean estimates (yellow lines), and the corresponding 5% and 95% quantiles (red lines). The figure demonstrates that the model parameters are capable of replicating the simulated correlation processes quite well.

We consider three measures to document the performance of different correlation models in finding the simulated correlation structures. Firstly, we compute mean absolute errors between estimates and true values defined by  $T^{-1} \sum_{t=1}^T |\hat{\rho}_t - \rho_t|$ . Naturally, the model performance is better for lower values of this measure. Secondly, we provide root mean squared errors given by  $(T^{-1} \sum_{t=1}^T (\hat{\rho}_t - \rho_t)^2)^{1/2}$  to increase the penalizing related to large deviations from the true values. Finally, a value at risk (VaR) based dynamic quantile test is conducted (Engle and Manganelli, 2004). VaR is calculated as  $VaR_t = 1.65(w_1^2 \Sigma_{11,t} + w_2^2 \Sigma_{22,t} + 2w_1 w_2 \hat{\rho}_t \sqrt{\Sigma_{11,t} \Sigma_{22,t}})^{1/2}$  where  $w_1$  and  $w_2$  denote the portfolio weights of the two assets. In addition, a  $hit_t$  variable is defined by  $hit_t = \mathbf{1}(w_1 r_{1,t} + w_2 r_{2,t} < VaR_t) - 0.05$  which assumes 0.95 each time the portfolio return falls below VaR and  $-0.05$  otherwise. The conditional expectation of  $hit_t$  must be zero given all available information before  $t$ . The dynamic quantile test proposed in Engle and Manganelli (2004) is conducted as an F-test under the null hypothesis that all independent variables are zero in a regression of  $hit_t$  on current VaR and the history of  $hit_t$ . Following Engle (2002), we report the rejection rates using an intercept, current VaR and 5 lags of  $hit_t$  in the regression, a 5% critical



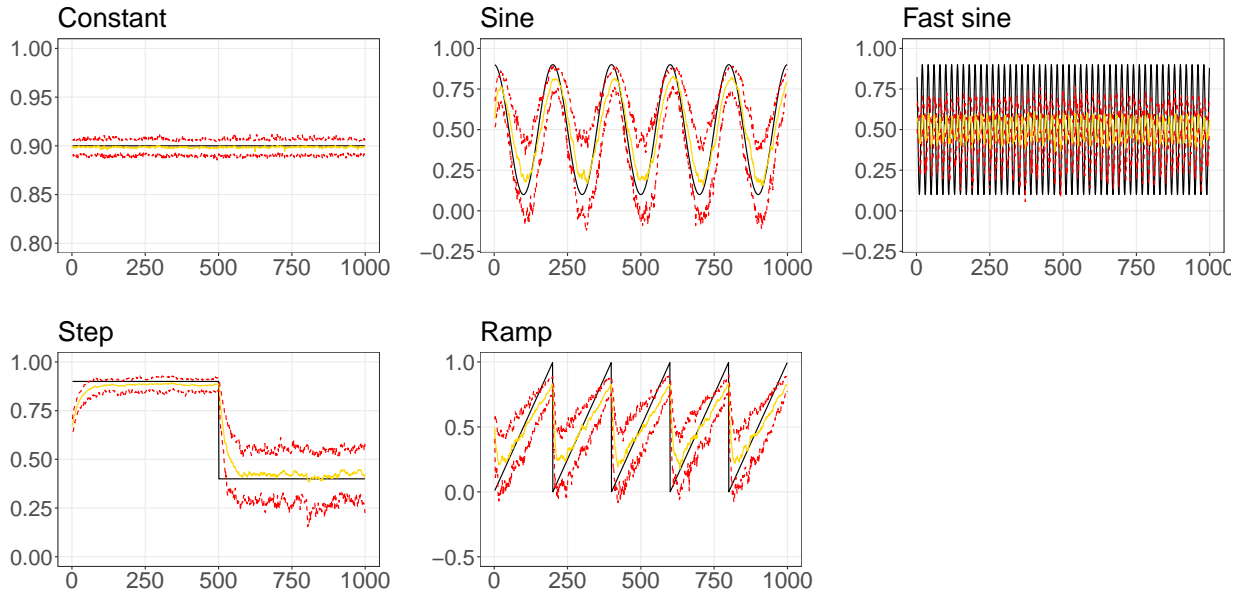


**Figure 6.1: Simulated true correlation processes**

This figure depicts five simulated true correlation processes (black lines), mean estimates (yellow lines), and 5% and 95% quantiles of the estimates (red lines). The figures are based on 200 simulations and 1000 observations.

value for the F-test, and an equally weighted portfolio with weights  $w_1 = w_2 = 0.5$  as well as a hedged portfolio with weights  $w_1 = 1, w_2 = -1$ .

Table 6.1 documents the performance of different correlation models in finding the simulated correlation structures. First, the p-range DCC model has the smallest mean absolute error in four out of five cases. The sum over all cases is also the smallest for the p-range DCC specification, ranking this model the best. Second and third place are the DCC and ADCC model, respectively. Note, that the rather weak performance of the asymmetric model is not surprising since there is no asymmetry in the generated data. Along this line, it is also very reasonable for the DCC model to perform best when the correlation process remains constant over the entire observation period.

Second, root mean squared errors are considered to evaluate the model performances with an increased penalty towards large departures from the true correlation. The p-range DCC model ranks best in four out of five instances and when summed over all cases. Using this evaluation measure, we again find the standard DCC model on second place, closely followed by the asymmetric specification.

Third, the table reports model performances with respect to the VaR based dynamic quantile test for an equal-weighted and a long-short portfolio, i.e., weights 0.5 for each asset and weights +1 and -1, respectively. The sum of the share of 5% rejections over all cases is lowest for the p-range DCC model in both portfolio weighting schemes.

Overall, the different measures point towards a strong performance of the p-range DCC specification in finding the true correlation structure. Whilst there is no asymmetry in the generated

**Table 6.1: Performance of different correlation models**

This table provides three measures to evaluate the performance of different correlation models in finding five distinct correlation structures. We consider mean absolute errors, root mean squared errors, and VaR based dynamic quantile tests for equal-weighted and long-short portfolios.

	Constant	Sine	Fast sine	Step	Ramp
<b>Mean absolute error</b>					
DCC	0.0056	0.1375	0.2261	0.0701	0.1565
ADCC	0.0061	0.1374	0.2262	0.0702	0.1568
p-range DCC	0.0057	0.1369	0.2259	0.0699	0.1561
<b>Root mean squared error</b>					
DCC	0.0064	0.1729	0.2601	0.1039	0.2104
ADCC	0.0082	0.1733	0.2604	0.1047	0.2109
p-range DCC	0.0065	0.1723	0.2600	0.1035	0.2083
<b>VaR based dynamic quantile test (equal-weighted)</b>					
DCC	0.0750	0.0350	0.0400	0.0450	0.0400
ADCC	0.0750	0.0350	0.0500	0.0450	0.0400
p-range DCC	0.0750	0.0300	0.0450	0.0400	0.0400
<b>VaR based dynamic quantile test (long-short)</b>					
DCC	0.0750	0.0350	0.0400	0.0450	0.0400
ADCC	0.0750	0.0350	0.0500	0.0450	0.0400
p-range DCC	0.0750	0.0300	0.0450	0.0400	0.0400

data which could be captured by the asymmetric specification, four out of the five true correlation processes contain at least one significant change in level over the observation period. In contrast to the standard DCC model, the more flexible p-range DCC specification detects the innovations at these change points to have a stronger impact on the correlation structure (instead of one common value), allowing for a quick adaption towards the true level of the simulated correlation process.

## 6.4 Empirical study

### 6.4.1 Data

The data employed comprises 30 equity indices over the observation period from January 2017 to March 2021 in daily frequency. More particularly, the global cross-section in our empirical analysis consists of data from 5 American stock markets (Argentina, Canada, Chile, Mexico, and the US), 19 European stock markets (Austria, Belgium, Czech Republic, Denmark, France, Germany, Hungary, Ireland, Italy, Netherlands, Norway, Poland, Portugal, Russia, Spain, Sweden, Switzerland, Turkey, and the UK), and 6 Asian-Pacific stock markets (Australia, China, Hong Kong, Japan, New Zealand, and Singapore). Given the extensive sample considered in this study, we employ the p-range DCC model to investigate global market dynamics by quantifying the dynamic impact of news on equity return correlations over time. Stock market price data are sourced from Refinitiv Eikon in daily

frequency, leaving us with 1,100 observations per time series. Continuously compounded returns are calculated as the log-price change between two consecutive trading days.

Table 6.2 comprises descriptive statistics for all data used in the empirical analysis. Clearly, the (log-)return series are negatively skewed which indicates tails on the left side of the empirical distributions. Further, and corresponding to the expectations of financial return characteristics, most time series exhibit excess kurtosis. Accordingly, we find the Jarque-Bera test statistics to report significant departure from normality for each of the sample constituents. We therefore base the first stage of the estimation in our analysis on a multivariate Student-t distribution for the disturbances.

Table 6.3 provides the unconditional correlation between each pair of market returns. The average unconditional correlation over the entire cross-section of market indices is 0.5289. Our data further points towards a positive relation between the geographic closeness of countries and their unconditional market correlation. For instance, whilst the mean value of the correlation is 0.6872 when considering only European stock indices, it is given by 0.4716 in the case of Asian-Pacific markets. For America, the average regional correlation is 0.4810 which is close to the mean value of the correlation witnessed in the global cross-section.

To receive additional insights on our data, we investigate the role of economic closeness on stock market integration. In line both with trade linkage theories based on [Winters and Italianer \(1987\)](#) and [Imbs \(2004\)](#) as well as the synchronization of business cycles in the vein of [Frankel and Rose \(1998\)](#), international trade is widely considered to foster market co-movement. We employ a measure of GDP normalized trade in spirit of [Asgharian et al. \(2013\)](#) to measure the economic relation between countries. Bi-variate yearly nominal export values and country-specific GDP with a lag of one year are obtained from the OECD and Worldbank database, respectively. All data are denoted in US-dollars. The measure of average economic distance between two countries over the entire observation period is thus given by  $\bar{E}_{ij} = (1/T) \sum_{t=1}^T 2 - (ex_{ij,t}/GDP_{j,t} + ex_{ji,t}/GDP_{i,t})$ , where  $ex_{ij,t}$  is the export value from country  $i$  to  $j$  and  $GDP_{i,t}$  is the GDP of country  $i$ . Similarly,  $ex_{ji,t}$  is the export value from country  $j$  to  $i$  and  $GDP_{j,t}$  is the GDP of country  $j$ .

Figure 6.2 condenses the information on the relation between economic distance and equity market correlation. Partner countries which are affiliated with lower quantiles of the empirical distribution of the measure of economic distance in the upper panel (high trade intensity, red color scheme) are largely accompanied by a high degree of market co-movement in the lower panel (high unconditional correlation, red color scheme). For instance, most European countries show low economic distances to European partner countries and a high degree of market integration. On the opposite side of the spectrum, and with the exception of the US and China, our data for American and Asian-Pacific countries suggest both higher economic distances to other regions as well as less integrated equity markets.

**Table 6.2: Descriptive statistics**

This table provides descriptive statistics for the log-price changes between two consecutive trading days for each of the 30 market indices used in the empirical analysis. The sample period spans from January 2017 to March 2021, containing 1,100 observations per market. In more detail, we report the sample mean, standard deviation, minimum, maximum, skewness, kurtosis, Jarque-Bera (JB) and ADF test statistics, and lag-1 autocorrelation for each time series. \*\*\*, \*\*, and \* denote statistical significance at the 1%, 5%, and 10% level, respectively.

	Mean	Median	St. Dev.	Min.	Max.	Skewness	Kurtosis	Autocorr.	JB test	ADF test
Argentina	-0.0006	0.0007	0.0340	-0.6765	0.1025	-7.3474	142.1096	-0.0861	938979***	-9.0454***
Canada	0.0003	0.0007	0.0125	-0.1407	0.1170	-2.2687	38.6202	-0.1069	69576***	-8.8698***
Chile	0.0001	0.0003	0.0155	-0.1576	0.1105	-1.2464	20.4932	0.0397	19615***	-9.6002***
Mexico	0.0000	0.0001	0.0157	-0.1071	0.0584	-0.8993	6.0824	0.0700	1854***	-8.2911***
United States	0.0005	0.0006	0.0126	-0.1277	0.0897	-1.1501	21.5941	-0.2422	21704***	-9.0651***
Austria	0.0003	0.0003	0.0145	-0.1643	0.1009	-1.5718	23.1177	0.0970	25050***	-9.6688***
Belgium	0.0002	0.0004	0.0132	-0.1708	0.0771	-2.1673	29.6330	0.0442	41272***	-9.8731***
Czech Republic	0.0003	0.0006	0.0118	-0.1176	0.0814	-2.0617	23.9983	0.1104	27286***	-9.2800***
Denmark	0.0006	0.0007	0.0109	-0.0958	0.0525	-0.6961	6.7184	0.0132	2169***	-10.7736***
France	0.0003	0.0008	0.0129	-0.1485	0.0840	-1.5438	22.0065	0.0300	22727***	-10.4871***
Germany	0.0003	0.0008	0.0132	-0.1481	0.1076	-1.2262	21.3134	0.0091	21183***	-10.3031***
Hungary	0.0002	0.0009	0.0146	-0.1525	0.0649	-1.4268	14.6812	0.0708	10296***	-10.8512***
Ireland	0.0003	0.0007	0.0130	-0.1222	0.0706	-1.0568	12.9206	0.0605	7891***	-9.9888***
Italy	0.0003	0.0008	0.0147	-0.2029	0.0890	-2.7185	37.8030	-0.0543	67115***	-9.7519***
Netherlands	0.0004	0.0010	0.0114	-0.1313	0.0894	-1.5380	21.5745	0.0153	21857***	-10.1952***
Norway	0.0002	0.0005	0.0150	-0.1469	0.0702	-1.3648	12.8318	-0.0360	7923***	-9.5029***
Poland	0.0001	0.0000	0.0158	-0.1743	0.0698	-1.3352	15.3002	0.0278	11104***	-10.0622***
Portugal	0.0001	0.0001	0.0117	-0.1202	0.0788	-1.1233	14.7594	0.0526	10260***	-9.9722***
Russia	0.0002	0.0005	0.0158	-0.1243	0.0863	-1.3462	11.7247	0.0126	6663***	-9.4301***
Spain	0.0000	0.0002	0.0135	-0.1690	0.0788	-1.7750	26.2801	-0.0129	32362***	-10.0976***
Sweden	0.0004	0.0007	0.0134	-0.1465	0.0836	-1.2992	16.1332	-0.0254	12291***	-10.4588***
Switzerland	0.0003	0.0005	0.0097	-0.1176	0.0692	-1.6815	24.3041	-0.0017	27704***	-10.6602***
Turkey	0.0000	0.0008	0.0203	-0.1722	0.0799	-0.9349	7.5063	0.0252	2756***	-10.4977***
United Kingdom	0.0000	0.0007	0.0124	-0.1421	0.1117	-1.2339	24.7671	-0.0067	28509***	-9.5636***
Australia	0.0002	0.0005	0.0130	-0.1122	0.0740	-1.4715	15.6365	-0.0852	11653***	-8.1531***
China	0.0001	0.0000	0.0118	-0.0938	0.0603	-0.6930	6.7851	-0.0193	2209***	-9.5452***
Hong Kong	0.0002	0.0005	0.0114	-0.0573	0.0499	-0.4343	2.7054	-0.0372	373***	-10.0651***
Japan	0.0005	0.0005	0.0112	-0.0767	0.0777	-0.0964	7.2110	-0.0170	2397***	-9.9858***
New Zealand	0.0004	0.0005	0.0107	-0.0916	0.0913	-0.5321	15.9829	0.1061	11811***	-9.9205***
Singapore	0.0001	0.0001	0.0101	-0.0816	0.0650	-0.6281	10.5700	0.0143	5217***	-9.6042***

**Table 6.3: Unconditional correlations between market returns**

This table provides the unconditional correlation between each pair of market returns for the sample period from January 2017 to March 2021. To improve readability, country names in each column are abbreviated by the corresponding Alpha-3 code of the ISO 3166-1 country encoding list.

	CAN	CHL	MEX	USA	AUT	BEL	CZE	DNK	FRA	DEU	HUN	IRL	ITA	NLD	NOR	POL	PRT	RUS	ESP	SWE	CHE	TUR	GBR	AUS	CHN	HKG	JPN	NZL	SGP
Argentina	0.32	0.35	0.29	0.30	0.27	0.25	0.22	0.18	0.27	0.25	0.22	0.24	0.23	0.24	0.27	0.21	0.27	0.23	0.25	0.25	0.20	0.18	0.25	0.20	0.11	0.16	0.09	0.15	0.20
Canada		0.59	0.62	0.80	0.67	0.67	0.65	0.47	0.73	0.71	0.59	0.66	0.68	0.72	0.68	0.58	0.64	0.60	0.68	0.70	0.66	0.35	0.75	0.63	0.26	0.38	0.28	0.42	0.49
Chile			0.54	0.49	0.54	0.50	0.54	0.34	0.55	0.53	0.49	0.51	0.46	0.54	0.52	0.48	0.49	0.51	0.53	0.52	0.45	0.37	0.54	0.47	0.26	0.41	0.21	0.30	0.43
Mexico				0.52	0.55	0.58	0.53	0.36	0.61	0.57	0.53	0.56	0.54	0.57	0.57	0.53	0.52	0.55	0.59	0.57	0.50	0.37	0.61	0.45	0.22	0.32	0.24	0.36	0.45
United States					0.53	0.54	0.48	0.38	0.60	0.59	0.44	0.53	0.57	0.58	0.53	0.46	0.52	0.42	0.57	0.58	0.53	0.30	0.59	0.46	0.20	0.28	0.17	0.25	0.34
Austria						0.84	0.80	0.49	0.84	0.82	0.67	0.77	0.80	0.80	0.73	0.67	0.76	0.62	0.81	0.75	0.64	0.40	0.78	0.54	0.28	0.43	0.31	0.40	0.51
Belgium							0.73	0.58	0.90	0.88	0.66	0.80	0.86	0.87	0.74	0.69	0.77	0.58	0.88	0.84	0.75	0.41	0.85	0.53	0.28	0.44	0.31	0.45	0.54
Czech Republic								0.50	0.74	0.72	0.71	0.69	0.69	0.72	0.68	0.64	0.68	0.59	0.72	0.68	0.58	0.40	0.71	0.58	0.28	0.45	0.36	0.44	0.56
Denmark									0.62	0.63	0.49	0.58	0.57	0.67	0.57	0.57	0.59	0.43	0.53	0.64	0.69	0.30	0.59	0.45	0.21	0.33	0.26	0.38	0.37
France										0.94	0.68	0.83	0.88	0.93	0.77	0.70	0.81	0.64	0.90	0.88	0.80	0.42	0.89	0.57	0.28	0.46	0.32	0.44	0.55
Germany											0.67	0.82	0.87	0.92	0.75	0.70	0.79	0.62	0.87	0.88	0.79	0.42	0.86	0.56	0.28	0.44	0.32	0.44	0.53
Hungary												0.64	0.64	0.65	0.60	0.67	0.66	0.54	0.65	0.63	0.56	0.41	0.65	0.50	0.25	0.40	0.29	0.37	0.50
Ireland													0.75	0.80	0.68	0.62	0.73	0.56	0.78	0.78	0.67	0.38	0.81	0.54	0.23	0.41	0.28	0.41	0.50
Italy														0.85	0.73	0.67	0.77	0.58	0.88	0.82	0.74	0.38	0.80	0.48	0.22	0.38	0.23	0.36	0.46
Netherlands															0.78	0.69	0.80	0.65	0.84	0.88	0.84	0.43	0.89	0.58	0.31	0.47	0.35	0.45	0.53
Norway																0.67	0.72	0.64	0.74	0.79	0.68	0.39	0.78	0.59	0.28	0.42	0.30	0.44	0.51
Poland																	0.67	0.59	0.69	0.70	0.64	0.40	0.67	0.50	0.28	0.41	0.27	0.40	0.48
Portugal																		0.56	0.81	0.76	0.68	0.40	0.76	0.54	0.27	0.41	0.30	0.44	0.50
Russia																			0.58	0.61	0.55	0.40	0.65	0.47	0.24	0.36	0.24	0.35	0.40
Spain																				0.82	0.72	0.41	0.83	0.54	0.24	0.40	0.28	0.41	0.49
Sweden																					0.81	0.40	0.85	0.55	0.31	0.46	0.32	0.43	0.54
Switzerland																						0.34	0.79	0.52	0.26	0.39	0.30	0.45	0.46
Turkey																							0.40	0.29	0.15	0.25	0.18	0.24	0.30
United Kingdom																								0.64	0.31	0.49	0.35	0.51	0.58
Australia																									0.33	0.49	0.49	0.59	0.59
China																										0.62	0.34	0.27	0.47
Hong Kong																											0.46	0.36	0.68
Japan																												0.39	0.51
New Zealand																													0.49

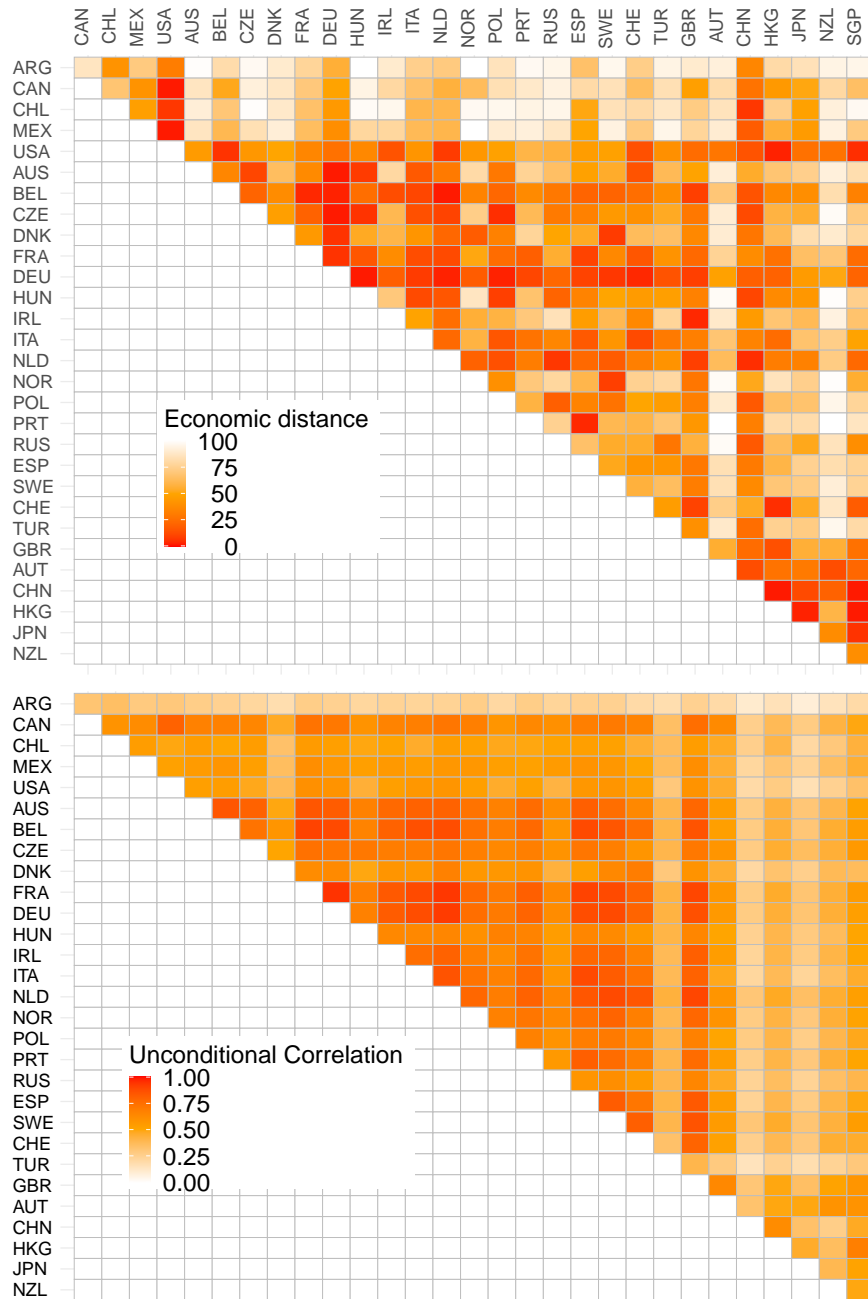


**Figure 6.2: Economic distance and stock market integration**

This figure depicts the relation between economic distance and market integration for all partner countries over the sample period from January 2017 to March 2021. Economic distance is reported as a GDP normalized measure of bi-variate trade between countries. The color indicates the affiliation of each pair with the respective quantile of the empirical distribution of this measure. Moreover, the figure contains a graphical representation of the unconditional correlations between corresponding market returns. Since each pair of the unconditional correlation is positive over the sample period, color scales are limited to positive values, exclusively. To improve readability, country names are abbreviated by the corresponding Alpha-3 code of the ISO 3166-1 country encoding list.

## 6.4.2 Empirical results

### Volatility dynamics

The model estimation procedure consists of two stages. In the first stage, univariate GARCH specifications are fit to each of the 30 return series. Appendix 6.6.1 comprises an overview of all volatility models considered in this study. The selection of the appropriate volatility model for each time series of asset returns is based on the BIC.

Table 6.4 provides information on the chosen GARCH specification as well as corresponding parameter estimates for the global sample of equity markets. Firstly, the table reports positive magnitude parameters, i.e.,  $\alpha$ -estimates in case of standard GARCH, GJR-GARCH, and asymmetric power ARCH specifications, and  $\gamma$ -estimates in case of exponential GARCH specifications, for each of the equity return series. The sign of the parameters is in line with prior literature and hints towards the clustering of volatility that is usually observed in financial markets. However, we only find 16 out of the 30 magnitude parameters to be significant at the 5% level. The results further suggest large differences between the impact of the size of news within (and across) the selected models. Secondly, the table reports negative  $\alpha$ -estimates and positive  $\gamma$ -estimates in case of the exponential GARCH, and both the GJR-GARCH and the asymmetric power ARCH model, respectively. In more detail, we find 21 of the 27 asymmetry terms to be significant at the 5% level which is consistent with the prominent literature on asymmetry in second central moments of equity returns.

Figure 6.3 illustrates volatility news impact curves for three assets which share the same GJR-GARCH structure in their conditional variance equation. The selected assets are chosen as they represent the estimated GJR-GARCH models with the highest, “closest to average”, and lowest magnitude parameters within our sample. In turn, the figure demonstrates the effects that magnitude parameters of different size exert on the conditional volatility estimates. For instance, Argentinian equity return volatility shows the strongest response to shocks of either sign compared to the Belgian and Swedish equity returns. In contrast, Belgian equity return volatility shows a much weaker reaction to both negative and positive market shocks. Finally, Swedish equity returns comprise the news impact curve with the lowest response to shocks overall. The depicted volatility news impact curves further suggest negative shocks to have stronger impacts on the conditional volatility than positive shocks.

**Table 6.4: GARCH model selection**

This table offers both the selected GARCH specification based on the BIC and the corresponding parameter estimates for each of the financial equity return series over the sample period from January 2017 to March 2021.

Market	Model	$\omega$	$\alpha$	$\beta$	$\gamma$	$\delta$
Argentina	GJR-GARCH	0.0000	0.0492	0.7931	0.2576	
Canada	GJR-GARCH	0.0000	0.0293	0.8697	0.1650	
Chile	eGARCH	-0.1715	-0.0721	0.9805	0.1461	
Mexico	GJR-GARCH	0.0000	0.0308	0.9015	0.0908	
United States	apARCH	0.0008	0.1563	0.8703	0.9369	0.8316
Austria	GJR-GARCH	0.0000	0.0141	0.9212	0.0960	
Belgium	GJR-GARCH	0.0000	0.0152	0.9278	0.0939	
Czech Republic	GJR-GARCH	0.0000	0.0274	0.9160	0.0691	
Denmark	eGARCH	-0.2853	-0.0848	0.9684	0.1286	
France	GJR-GARCH	0.0000	0.0034	0.9114	0.1482	
Germany	GJR-GARCH	0.0000	0.0000	0.9340	0.1034	
Hungary	sGARCH	0.0000	0.0793	0.8874		
Ireland	GJR-GARCH	0.0000	0.0056	0.9415	0.0822	
Italy	eGARCH	-0.1718	-0.0978	0.9804	0.0965	
Netherlands	GJR-GARCH	0.0000	0.0056	0.9184	0.1205	
Norway	GJR-GARCH	0.0000	0.0000	0.9399	0.0890	
Poland	eGARCH	-0.1026	-0.0681	0.9880	0.0782	
Portugal	eGARCH	-0.3683	-0.0794	0.9600	0.2170	
Russia	eGARCH	-0.1797	-0.0636	0.9791	0.1106	
Spain	GJR-GARCH	0.0000	0.0202	0.9042	0.1087	
Sweden	GJR-GARCH	0.0000	0.0000	0.9384	0.0984	
Switzerland	GJR-GARCH	0.0000	0.0004	0.8627	0.1834	
Turkey	eGARCH	-0.3015	-0.1146	0.9621	0.1141	
United Kingdom	GJR-GARCH	0.0000	0.0081	0.9320	0.0936	
Australia	GJR-GARCH	0.0000	0.0252	0.9201	0.0747	
China	sGARCH	0.0000	0.0671	0.9265		
Hong Kong	GJR-GARCH	0.0000	0.0022	0.9275	0.0982	
Japan	GJR-GARCH	0.0000	0.0332	0.7949	0.2306	
New Zealand	GJR-GARCH	0.0000	0.0337	0.9206	0.0538	
Singapore	GJR-GARCH	0.0000	0.0320	0.8961	0.0992	



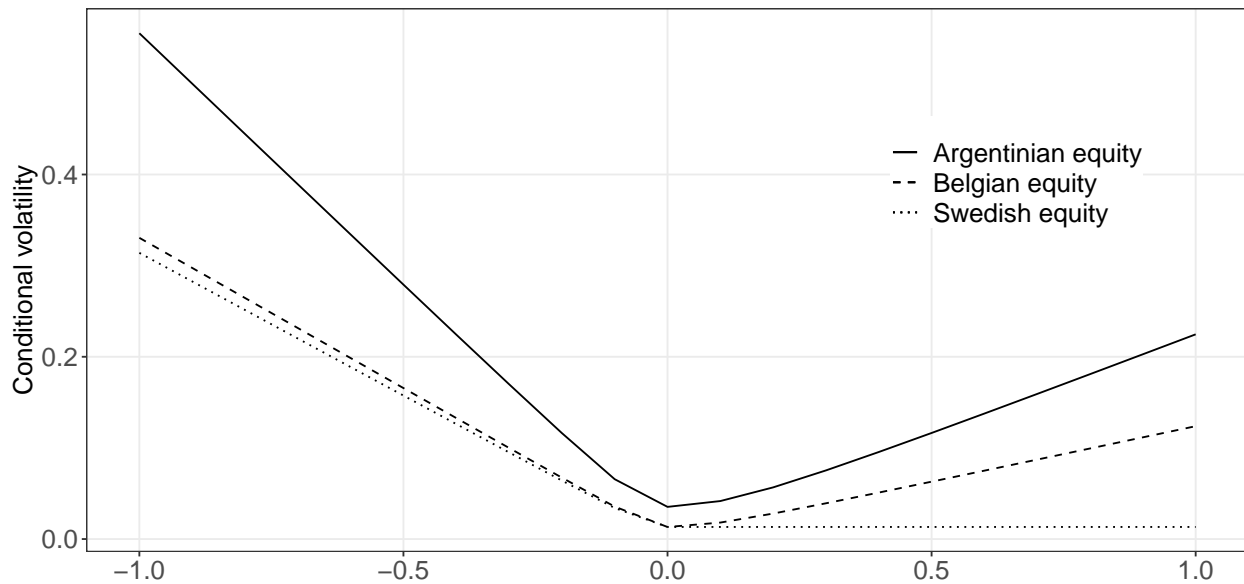


**Figure 6.3: Volatility news impact curves for three assets**

This figure shows volatility news impact curves based on GJR-GARCH models for Argentinian (solid line), Belgian (dashed line), and Swedish (dotted line) equity returns. The volatility dynamics highlight the different reactions in terms of asymmetry and magnitude in response to market shocks.

### Correlation dynamics

In the second stage, four different DCC-type specifications are used to estimate time-varying correlation dynamics between markets. The most simplistic specification is the standard DCC model where neither asymmetry nor time-varying news impact is considered (Equation 6.4 with  $\psi_3 = 0$ ). The second specification, the asymmetric DCC model, provides a means to include the potentially asymmetric response of correlations to negative past innovations (Equation 6.4). Next, the p-range DCC specification is estimated to introduce time-variation towards the news impact factor (Equation 6.5).

Table 6.5 provides estimates based on these specifications for the time period from January 2017 to March 2021. The estimated parameters are significantly different from zero and indicate high persistence of the conditional correlation across models. Further, the log-likelihood values and information criteria reported in the table suggest that the p-range DCC model outperforms both the standard DCC model and its asymmetric extension in our empirical application. In line with our results suggested in the simulation study, the increased flexibility of the news impact parameter seems to be a reasonable addition to DCC-type models when markets are exposed to periods of turmoil and uncertainty. In the following, we examine how the incorporation of additional information to the standard DCC specification impacts the conditional correlation estimates. To this end, we focus on the case of the US-German equity return correlation. However, results for all pairs of equity returns are available from the authors upon request.

**Table 6.5: Parameter estimates of DCC-type models**

This table provides mean estimates of DCC-type model parameters with static and score-driven impact of news. The estimated parameters are based on the sample period from January 2017 to March 2021. In addition, we provide the log-likelihood ( $\mathcal{L}$ ), the Akaike information criterion (AIC), and the Bayesian information criterion (BIC). \*\*\*, \*\*, and \* denote statistical significance at the 1%, 5%, and 10% level, respectively.

	DCC	ADCC	p-range DCC
$\psi_1$	0.0061***	0.0026***	
$\psi_2$	0.9366***	0.9468***	0.9316***
$\psi_3$		0.0095***	
$\omega$			-0.0819***
$A$			-0.3372***
$B$			0.9833***
$\mathcal{L}$	117381	117412	117420
AIC	-234426	-234485	-234499
BIC	-233585	-233640	-233649

The upper panel of Figure 6.4 depicts daily estimates of the conditional correlation between US and German equity returns for the period from January 2017 to March 2021 based on the three DCC-type models considered in this study. Correlation estimates are generally close to 0.5, whilst large increases can be witnessed towards the end of February 2020 when equity markets plunge in response to the outbreak of COVID-19. Clearly, both the ADCC and the p-range DCC model provide a means for the fit correlation to show a stronger reaction to this event in comparison to the standard DCC model. However, whilst estimates of the ADCC model quickly readjust to standard DCC estimates when both markets recover simultaneously from March 2020 on-wards, the p-range DCC specification permits correlation estimates to remain above their initial level during this period of joint recovering. We additionally shed light on the time-varying dynamics of the impact of news on market linkages over time.

More particularly, the lower panel of Figure 6.4 plots the global dynamic news impact parameter over the full sample period. By construction, the time-varying parameter allows estimates of the p-range DCC model to depart from standard DCC estimates when its magnitude differs from the otherwise static news impact factor. Upon closer inspection of both the figure and our fit correlations, we find such deviation to be prevalent in multiple instances over the sample period. Most notable are the increases of the parameter in early 2018 as well as February 2020 and January 2021, suggesting that the “severity” of news for cross-market linkages is on a high level during these periods.

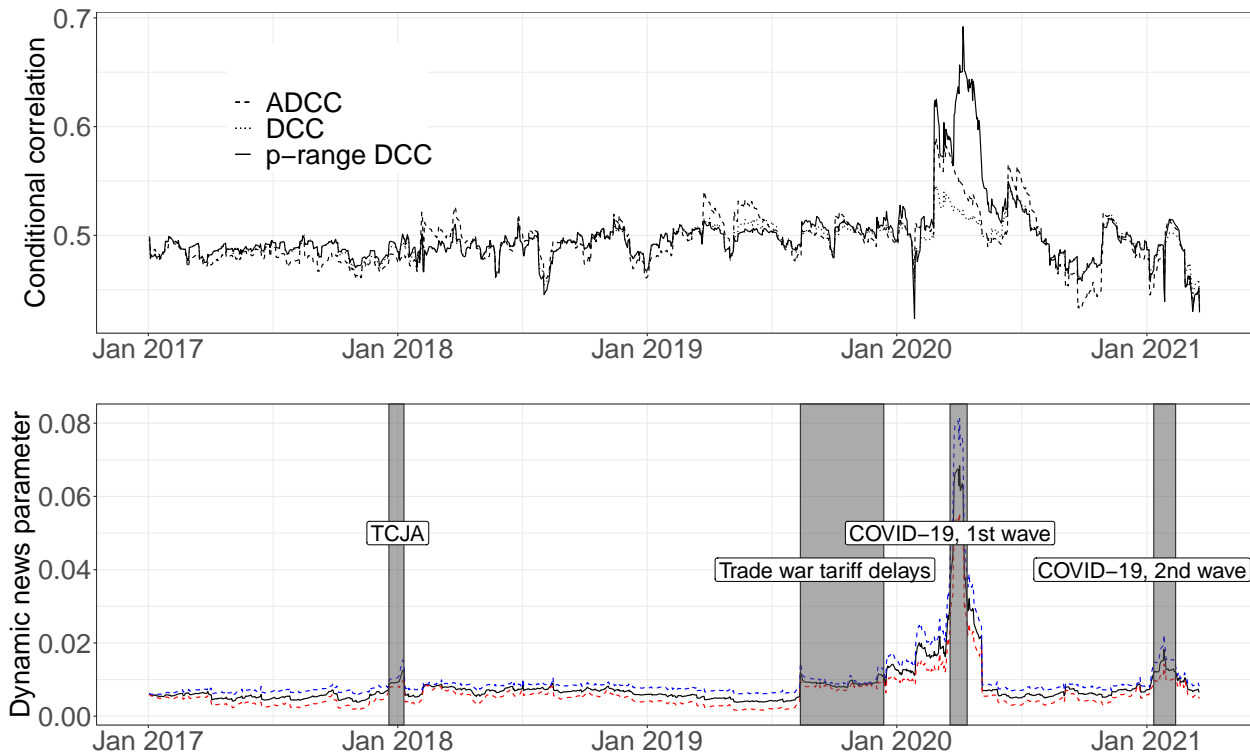


**Figure 6.4: US-German equity return correlation and global news impact**

This figure depicts the conditional correlation between US and German equity returns. The upper panel shows correlation estimates based on the DCC (dotted lines), ADCC (dashed lines) and p-range DCC (solid lines) model. The lower panel highlights the dynamic news impact factor over time. Red and blue lines depict the 2.5% and 97.5% quantiles of the distribution, respectively. The time-varying news impact is used to define event-periods between January 2017 and March 2021.

### 6.4.3 The impact of news on global cross-market linkages

An additional benefit of the p-range DCC model is that it provides a straightforward interpretation of the impact of news on market linkages on a scale which comprises the entire cross-section used in empirical applications. In this section, we assess whether there is empirical evidence of significant increases in the exposure of global market linkages to shocks between January 2017 and March 2021. Using the time-varying news impact parameter, tests for increased exposure to the risk of financial contagion are not based on arbitrarily set event windows and subsequent comparison of (multiple) bi-variate correlation estimates, but can be identified and conducted based on a single parameter resulting from the score-driven detection of such events.

Accordingly, we estimate confidence bounds for the dynamic news impact parameter based on the in-sample cumulative Delta-method bands for observation driven models suggested in Blasques *et al.* (2016a). We define significant increases in the “severity” of news as a non-overlapping of at least seven continuous days of the event/post-event lower ( $c_{tc}^{LOW}$ ) confidence bounds and the moving

arithmetic average of the pre-event upper ( $c_{t_p}^{UP}$ ) confidence bounds:

$$\frac{1}{N} \sum_{p=s}^{s+N} c_{t_p}^{UP} < c_{t_c}^{LOW} \quad t_c \in \{t_m, t_{m+1}, \dots, t_{m+M}\}$$

$$\text{with } t_{s+N} < t_m, \tag{6.15}$$

where the pre-event period is defined as 30 days preceding the start of the event. We consider the 2.5% and 97.5% quantiles for lower- and upper bounds, respectively.

Referring to the terminology provided in [Forbes and Rigobon \(2002\)](#), contagion concerns rise with the outbreak of COVID-19 in early 2020 and the subsequent, joint economic recoveries in response to non-standard national and supranational regulating policies. Alleviation of distress is only visible long after these policy events when market linkages, approximated by the conditional correlations, begin to reach and fall from their preceding level. The behavior of the dynamic news impact parameter can be related to various key political actions, particularly during the time of the COVID-19 pandemic. Using the time-variation in the “severity” of news, we find some of these actions to have a clear, visible impact on the way that shocks are transmitted across financial markets. The lower panel of [Figure 6.4](#) depicts our results. The time-varying parameter detects four events which induce significant increases in the impact of news on global cross-market linkages.

Firstly, the impact of news on correlation dynamics rises significantly in the period between 2017-12-19 and 2018-01-10 when global equity markets collectively responded to heightened expectations of the US Tax Cuts and Jobs Act of 2017 (TCJA). The day prior, for instance, American equity markets closed on 2.5% returns on average, whilst European and Asian-Pacific markets experienced mean returns of 1.55% and 0.53%, respectively. Overall, only Russian, New Zealand, and Chinese equity markets showed negative returns that day whilst the remaining 27 sample constituents responded positively to the major US tax rate reductions for businesses and individuals, leading to increased cross-market linkages in response.

Secondly, we detect a significant increase over the period from 2019-08-13 to 2019-12-13. A potential explanation for the high “severity” of news during that time is the US delay to the drastic imposition of tariffs on 152 billion US-Dollars of Chinese imports until mid December. By and large, global equity markets reacted positively to the delay of the US-China trade war. In turn, the significant increase in the parameter during this time frame allows the fit market linkages to adapt accordingly to the homogeneous reaction of equity markets.

Thirdly, and perhaps most importantly, we detect the period around COVID-19 to induce gradual increases to the dynamic news impact parameter. The parameter rises in early January 2020 and jumps again in late February amid market uncertainties related to the global outbreak of COVID-19. Throughout March, equity markets jointly recover from their early response when economies began to reopen. We find this joint market recovering to accompany the significant increase observable from 2020-03-19 towards 2020-04-13.

Finally, the S&P 500 climbed to all-time highs on 2021-01-08 when the US president elect Joe

Biden calls for trillions of dollars in market stimulus. Asian-Pacific equity markets also gained 1.36% in average returns that day. The day after, we detect a significant increase in the global news impact parameter with an event window ranging from 2021-01-09 to 2021-02-12. During this time frame, the impact of news on correlation dynamics peaks on 2021-01-26 when European equity markets collectively tumbled against the backdrop of European restrictions related to the COVID-19 pandemic.

#### 6.4.4 Correlation news impact surfaces

In this section, we demonstrate the distinct responses of correlation dynamics to “good” and “bad” news of different magnitudes for each correlation model by employing correlation news impact surfaces as introduced in [Kroner and Ng \(1998\)](#). The correlation news impact surfaces for multivariate GARCH models resemble the volatility news impact curves for univariate time series. With respect to the model presented in this article, the impact surface is illustrated only for the minimum and maximum value of the time-varying news impact parameter. Note, however, that the impact of standardized residuals on correlation dynamics fluctuates between these outer surfaces over time. The news impact surface for correlations is:

$$\begin{aligned}
 f(\varepsilon_i, \varepsilon_j) &= \frac{c_{ij} + (\psi_1 + \psi_3)\varepsilon_i\varepsilon_j + \psi_2\bar{q}_{ij}}{\sqrt{[c_{ii} + (\psi_1 + \psi_3)\varepsilon_i^2 + \psi_2] \cdot [c_{jj} + (\psi_1 + \psi_3)\varepsilon_j^2 + \psi_2]}}, & \text{if } \varepsilon_i < 0 \text{ and } \varepsilon_j < 0, \\
 f(\varepsilon_i, \varepsilon_j) &= \frac{c_{ij} + \psi_1\varepsilon_i\varepsilon_j + \psi_2\bar{q}_{ij}}{\sqrt{[c_{ii} + \psi_1\varepsilon_i^2 + \psi_2] \cdot [c_{jj} + (\psi_1 + \psi_3)\varepsilon_j^2 + \psi_2]}}, & \text{if } \varepsilon_i \geq 0 \text{ and } \varepsilon_j < 0, \\
 f(\varepsilon_i, \varepsilon_j) &= \frac{c_{ij} + \psi_1\varepsilon_i\varepsilon_j + \psi_2\bar{q}_{ij}}{\sqrt{[c_{ii} + (\psi_1 + \psi_3)\varepsilon_i^2 + \psi_2] \cdot [c_{jj} + \psi_1\varepsilon_j^2 + \psi_2]}}, & \text{if } \varepsilon_i < 0 \text{ and } \varepsilon_j \geq 0, \\
 f(\varepsilon_i, \varepsilon_j) &= \frac{c_{ij} + \psi_1\varepsilon_i\varepsilon_j + \psi_2\bar{q}_{ij}}{\sqrt{[c_{ii} + \psi_1\varepsilon_i^2 + \psi_2] \cdot [c_{jj} + \psi_1\varepsilon_j^2 + \psi_2]}}, & \text{if } \varepsilon_i \geq 0 \text{ and } \varepsilon_j \geq 0, \quad (6.16)
 \end{aligned}$$

where  $c_{ij}$  denotes the  $ij$ -th element of the intercept matrix in the correlation equation,  $\bar{q}_{ij}$  is the corresponding element of the unconditional correlation matrix  $\bar{Q}$ , and  $\psi_3 = 0$  when considering the standard DCC- and p-range DCC model.

Figure 6.5 depicts news impact surfaces for the US and German equity return correlations. For each model and equity market, standardized shocks range from -5 to +5. The important difference between the distinct DCC-type models is the way in which past innovations of equity returns may impact market linkages. In the standard DCC model, function values over the given set of arguments are bound between 0.29 and 0.55, referring to the most extreme responses of return correlations to shocks of unequal and equal sign, respectively. In comparison to its alternative specifications, the standard DCC model imposes several restrictions on the dynamic behavior of correlations. For instance, when considering the ADCC model instead, the correlation news impact surface shows to

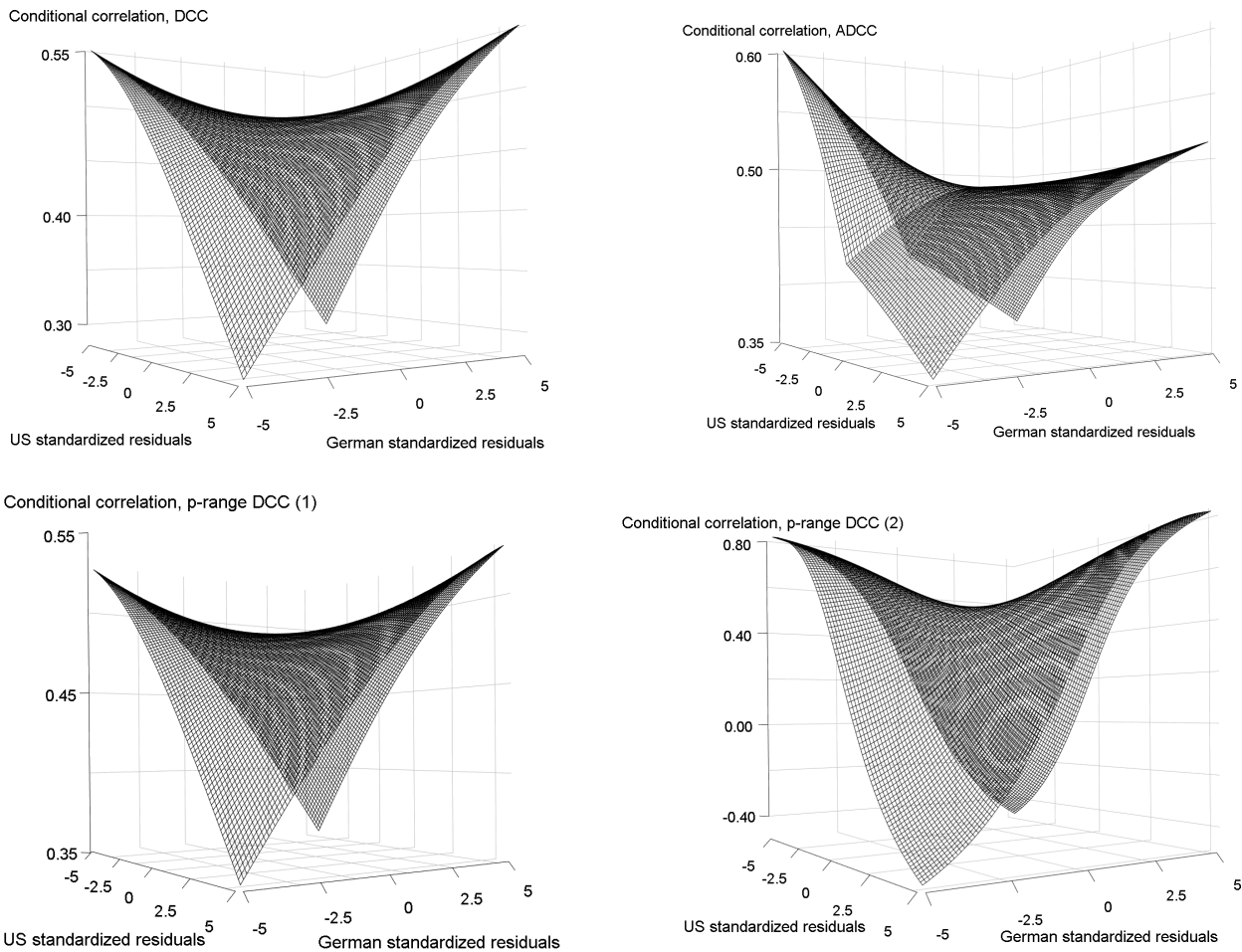


**Figure 6.5: Correlation news impact surfaces**

This figure depicts news impact surfaces for US and German equity returns based on the DCC-, ADCC-, and p-range DCC model. The ADCC news impact surface shows clear asymmetry between the  $-/-$  and  $+/+$  quadrant. The p-range DCC model contains no asymmetry but instead attributes dynamic news impacts between (1), the minimum value of the parameter, and (2), the maximum value of the parameter, to each observation.

be highly asymmetric and ranges from 0.35 to 0.60. More particularly, the asymmetric behavior becomes apparent when comparing the impact between the  $-/-$  and the  $+/+$  quadrant, showing joint “bad” news to induce a stronger impact on correlation dynamics than joint “good” news.

Likewise, the figure depicts two news impact surfaces for correlations based on the p-range DCC model which refer to the minimum and maximum value of the dynamic news impact parameter.<sup>45</sup> In contrast to the asymmetric specification, our model does not distinguish between the average impact of joint “bad” or joint “good” news. Instead, the p-range DCC model takes a more general approach to distinguish between the impact of each single observation of news over time. Using this approach, the figure suggests large differences in the impact that past shocks of any combination of signs can have on correlation dynamics. By construction, small values of the dynamic parameter highly limit the impact of shocks, whereas large values endow shocks with a strong impact on correlations. Figure 6.6 provides four views on the difference between the two news impact surfaces to shed further light on the importance of considering the dynamic behavior of the parameter. The difference notably distinguishes from a flat plane.

---

<sup>45</sup>Additional news impact surfaces for correlations are plotted for a wide range of values that the news impact parameter takes in the empirical application. All plots are available upon request.

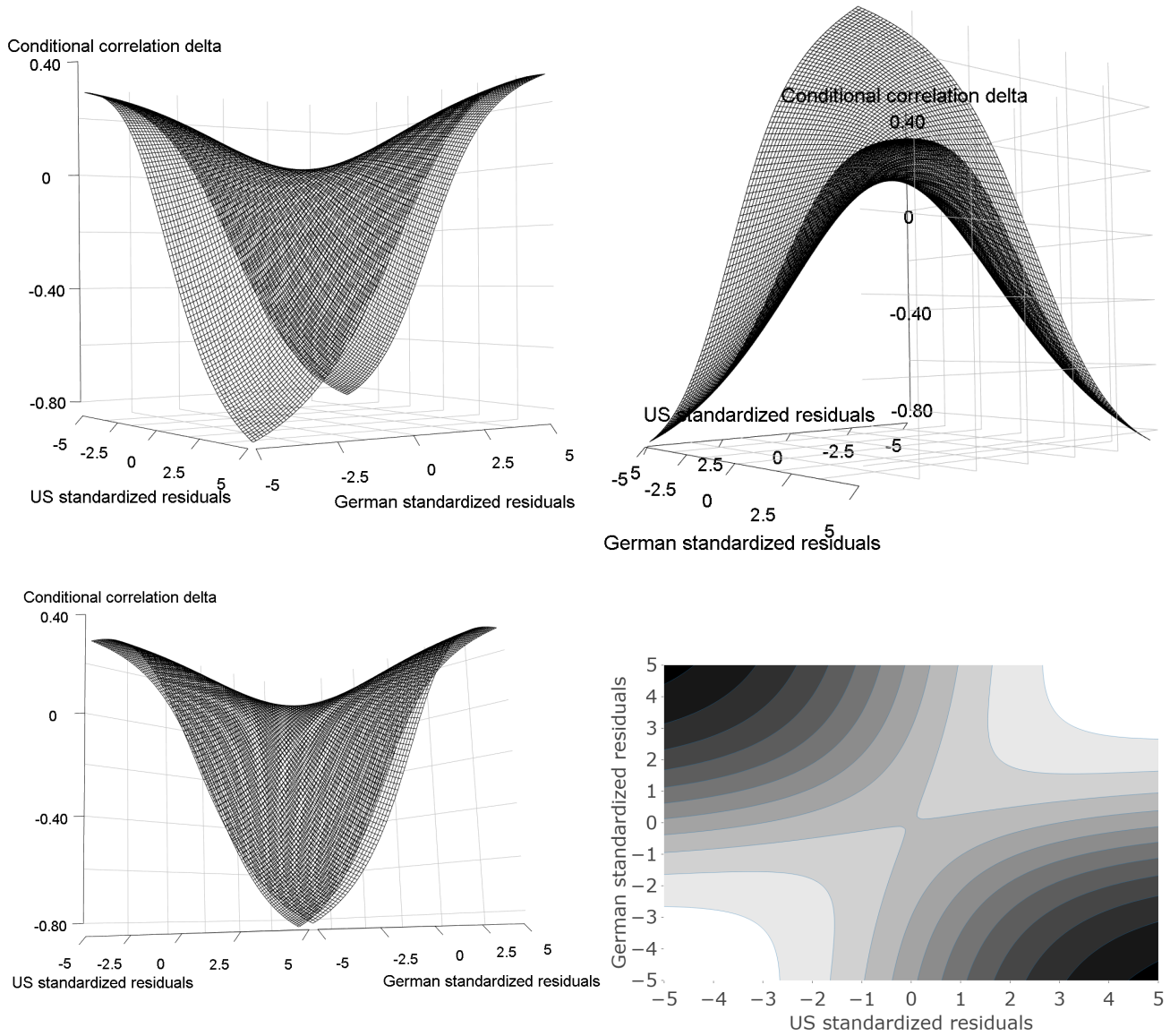


**Figure 6.6: Difference between correlation news impact surfaces**

This figure depicts four views on the difference in the news impact surface between maximum and minimum value for US and German equity returns. The difference between the two correlation news impact surfaces (Conditional correlation delta) ranges from -0.83 to 0.29.



### 6.4.5 Model alternatives and extensions

In this section, we extend the p-range DCC model towards two dimensions. First, we consider time-variation in the asymmetry dynamics. We refer to this model as the p-range ADCC model. Second, we allow for series-specific, time-varying news impact. The resulting p-range GDCC model extends the initial specification by adding a time-varying  $(n \times n)$  diagonal matrix to account for the impact of individual news on correlation estimates.

#### Time-varying asymmetry dynamics

The first extension allows to unravel potentially changing asymmetry effects when comparing times of financial tranquility against times of financial turmoil. More particularly, we introduce the time-varying asymmetry parameter to DCC-type models as follows:

$$Q_t = \bar{Q} (\omega' - \psi_1 - \psi_2) - \psi_{3,t} \bar{N} + \psi_1 \varepsilon_{t-1} \varepsilon'_{t-1} + \psi_{3,t} \eta_{t-1} \eta'_{t-1} + \psi_2 Q_{t-1}, \quad (6.17)$$

where  $\psi_{3,t} = h(f_t)$  is again a strictly monotonic transformation of the time-varying parameter  $f_t$ . The introduction of score updating functions is identical to both Equations 6.6 and 6.7, while  $\partial Q / \partial f_t = \dot{h}(f_t) \cdot (\eta_{t-1} \eta'_{t-1} - \bar{N})$ .

Figure 6.7 shows the evolution of the asymmetry impact on global correlation dynamics over time. The asymmetry impact generally fluctuates around the estimate of  $\psi_3$  suggested in the standard ADCC model. Given that the estimate of the static asymmetry impact is much smaller than the estimate of the static news impact, it is hardly surprising that the observed deviations over time are of smaller size. Finally, global asymmetry considerations seem to be particularly important in the early 2018 period and in response to the outbreak of COVID-19.

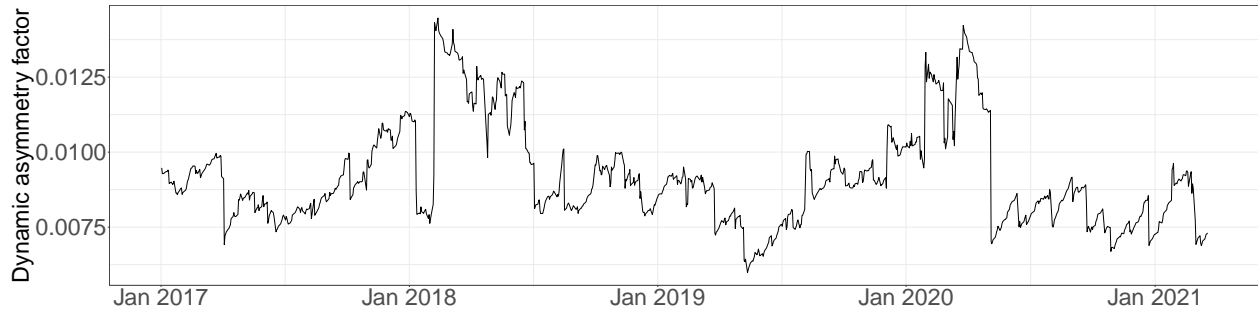


**Figure 6.7: Time-varying global asymmetry impact**

This figure depicts the time-varying asymmetry impact factor based on the p-range ADCC model. The time period ranges from January 2017 to March 2021.

### Series-specific news impact dynamics

The second extension further broadens the flexibility of the proposed p-range DCC specification by considering potential differences in heterogeneous data. Note, that the p-range DCC specification allows to relax unrealistic assumptions of a time-invariant news impact over long sample periods. In large cross-sections, and in line with [Cappiello \*et al.\* \(2006\)](#), it is neither reasonable to assume the resulting, time-varying news impact dynamics to be common for the entire cross-section used in empirical applications. We therefore extend the scalar p-range DCC model to the general case, where the correlation evolution equation is given by:

$$Q_t = \bar{Q} \circ \left( u' - \psi_{1,t} \psi'_{1,t} - \psi_2 \psi'_2 \right) + \psi_{1,t} \psi'_{1,t} \circ \varepsilon_{t-1} \varepsilon'_{t-1} + \psi_2 \psi'_2 \circ Q_{t-1}, \quad (6.18)$$

with  $\psi_{1,t} := \psi_1(\mathbf{f}_t) = (h(f_{1,t}), h(f_{2,t}), \dots, h(f_{n,t}))'$ . The sufficient condition for  $Q_t$  to be positive definite for all  $t$  is that the intercept of Equation 6.18 is positive semi-definite and that  $Q_0$  is positive definite (compare, e.g., [Cappiello \*et al.\*, 2006](#)). Similar to the initial specification, the parameter vector  $\mathbf{f}_t$  is endowed with time-varying features. To ensure parsimony in spirit of DCC-type models we permit series-specific intercepts and sensitivity parameters in the updating function of  $\mathbf{f}_t$ , yet restrict the updating equation to a common smoothing factor. Consequently,  $f_{i,t+1} = \omega_i^s + A_i \nabla_{i,t} + B f_{i,t}$ .<sup>46</sup> The generalized specification comes at the cost of additional parameters that need to be estimated in the second step of the estimation procedure and a less intuitive interpretation. The total amount of parameters required for the estimation of correlation dynamics in the p-range GDCC model equals  $3n + 1$  and grows linearly in the number of time series.

### Goodness of fit comparison and discussion

Table 6.6 compares the goodness of fit between all models considered in this study. The table highlights that each extension improves the performance of the standard DCC model. The p-range

<sup>46</sup>Please refer to Appendix 6.6.2 for further details.

**Table 6.6: Goodness of fit comparison between models**

This table provides a goodness of fit comparison between all models considered in this study. The estimation period is January 2017 to March 2021. The largest log-likelihood value and the smallest value of the AIC and BIC are depicted in boldface.

	DCC	ADCC	p-range DCC	p-range ADCC	p-range GDCC
$\mathcal{L}$	117381	117412	117420	117413	<b>117485</b>
AIC	-234426	-234485	<b>-234499</b>	-234484	-234456
BIC	-233585	-233640	<b>-233649</b>	-233628	-233170

GDCC specification, accounting for series-specific news impact dynamics, performs best as indicated by the highest value of the maximized log-likelihood function. This comes to no surprise, as this particular specification nests the others. When considering the information criteria, the table further suggests that the better fit of the p-range GDCC model is not enough to justify the additional parameters introduced for the measuring of asset-specific news. Accordingly, we conclude that the p-range DCC specification is well-suited for measuring international market co-movement during times of turmoil and uncertainty.

Table 6.7 comprises the corresponding parameter estimates of the p-range ADCC and p-range GDCC model specification. First, we find the influence of scores to be larger in case of the dynamic asymmetry impact factor compared against the dynamic news impact factor. In contrast, the asymmetry parameter seems to be less persistent. Second, intercept and sensitivity estimates differ between markets in case of the series-specific dynamic news impact factor, whilst the behavior over time captured in  $B$  is less persistent than in the scalar p-range DCC specification.

**Table 6.7: Parameter estimates of extended p-range DCC models**

This table offers dynamic conditional correlation parameter estimates for the p-range ADCC and the p-range GDCC specification over the sample period from January 2017 to March 2021. \*\*\*, \*, and \* denote statistical significance at the 1%, 5%, and 10% level, respectively.

Market	$\psi_1$	$\psi_2$	$\omega^s$	$A$	$B$
<b>Panel A: P-range ADCC</b>					
	0.0024***	0.9495***	-0.1126*	-0.3503	0.9755***
<b>Panel B: P-range GDCC</b>					
Argentina		0.7587***	-0.6911***	-0.3653	
Canada		0.8551***	-0.3669	-0.2160	
Chile		0.9418***	-0.7693***	-0.3488	
Mexico		0.9856***	-0.7887	0.2426	
United States		0.8476***	-0.3359	0.3168	
Austria		0.9905***	-0.6910***	0.4663	
Belgium		0.9874***	-0.6743***	0.2364	
Czech Republic		0.9897***	-0.7922	-0.0092	
Denmark		0.9162***	-0.6061	-0.2867	
France		0.9946***	-0.7656***	-0.6598	
Germany		0.9803***	-0.7029**	0.3448	
Hungary		0.9596***	-0.7018	-0.4983	
Ireland		0.9859***	-0.7390	-0.4964	
Italy		0.9845***	-0.6248***	-0.7551***	
Netherlands		0.9834***	-0.7336	0.0648	
Norway		0.9831***	-0.7640***	-0.2058	
Poland		0.9856***	-0.8869***	0.2913	
Portugal		0.9795***	-0.7802***	-0.1124	
Russia		0.9934***	-0.9447	-0.2735	
Spain		0.9947***	-0.6940***	-0.0037	
Sweden		0.9817***	-0.7187**	-0.2638	
Switzerland		0.9677***	-0.6762*	-0.2352	
Turkey		0.9923***	-0.9306	-0.5353	
United Kingdom		0.9892***	-0.7236***	0.1004	
Australia		0.9158***	-0.9010***	0.2625	
China		0.7698	-0.8009	-0.7999	
Hong Kong		0.9137***	-0.5780***	-0.1052	
Japan		0.8631***	-0.7570***	-0.4234	
New Zealand		0.7575	-0.8290	-0.5123	
Singapore		0.9135**	-0.6394	0.1450	
					0.7141***

## 6.5 Concluding remarks

In this article, we propose a new model for the estimation of time-varying conditional correlations. The model extends the widely employed DCC model introduced in [Engle \(2002\)](#) in allowing for a time-varying impact of news on correlation dynamics. Allowing for time-variation is especially useful if DCC-type models are employed over longer time periods, when it is not reasonable to assume that the impact of news on correlation dynamics remains constant. In such instances, we suggest an adaptive, score-driven weighting of past innovations based on the generalized autoregressive score framework to model the evolution of conditional correlations. The proposed probability-range DCC model, or simply p-range DCC model, is both flexible and empirically feasible for applications with large cross-sections. Using this model, potential differences in the importance of news over time can appropriately be reflected by their respective impact on correlation dynamics.

We show that the model performs well in approximating time-varying correlation processes in a variety of different situations and often outperforms alternative DCC-type models. This finding holds whether performance measures are based on mean absolute errors, root mean squared errors, or VaR-based computations.

In our empirical study, we employ the p-range DCC specification to investigate the time-varying impact of news on cross-market linkages for a global sample of national equity indices. We demonstrate that global market linkages exhibit a strong, time-varying degree to which they depend on past market shocks from either sign. Using the evolution of the news impact parameter over time, we find empirical evidence for significant changes in the “severity” of news for correlation dynamics. The most notable increase of our measure is detected in early 2020, i.e., during the outbreak of COVID-19, and when equity markets began to recover from global uncertainties whilst economies started to reopen under the aiding guidance of national and supranational monetary and fiscal policies. This finding points towards increased risks of contagion in the sense of [Forbes and Rigobon \(2002\)](#) during times when the degree of shock transmission in financial markets is on a high level. On the bright side, however, our finding also hints towards the effectiveness of regulating policies to prevent worse when global markets collapsed in response to the COVID-19 pandemic.

The evolution of the correlation dynamics reported in this article motivate interesting avenues both for researchers and financial practitioners. Amongst other, what causes fluctuations in the dynamic news impact parameter? Can the risk of increased cross-market linkages during times of “severe” news be hedged by other financial assets? Has the COVID-19 pandemic lead to persistent long-term changes in financial markets, and how will this influence risk management decision making and asset allocation strategies?

## 6.6 Appendices

### 6.6.1 Univariate GARCH models

In our empirical application, we use the BIC to choose the univariate GARCH specification from a selection of four models. The set of GARCH models comprises:

- Standard GARCH (Bollerslev, 1986)

$$\sigma_t^2 = \omega + \alpha r_{t-1}^2 + \beta \sigma_{t-1}^2 \quad (6.19)$$

- Exponential GARCH (Nelson, 1991)

$$\log \sigma_t^2 = \omega + \alpha \frac{r_{t-1}}{\sigma_{t-1}} + \gamma \left( \frac{|r_{t-1}|}{\sigma_{t-1}} - E \left[ \frac{|r_{t-1}|}{\sigma_{t-1}} \right] \right) + \beta \log \sigma_{t-1}^2 \quad (6.20)$$

- GJR-GARCH (Glosten *et al.*, 1993)

$$\sigma_t^2 = \omega + \alpha r_{t-1}^2 + \gamma \mathbb{1}\{r_{t-1}^2\} + \beta \sigma_{t-1}^2 \quad (6.21)$$

- Asymmetric power ARCH (Ding and Engle, 2001)

$$\sigma_t^\delta = \omega + \alpha (|r_{t-1}| - \gamma r_{t-1})^\delta + \beta \sigma_{t-1}^\delta \quad (6.22)$$

The employed GARCH models are capable to account for the characteristic properties observable in univariate financial time series to different extents. The asymmetric power ARCH (apARCH) model, for instance, can capture volatility persistence in addition to potential leverage and asymmetry effects. Besides, it nests a variety of alternative GARCH models such as the absolute value GARCH, nonlinear ARCH, and threshold GARCH (Schwert, 1990; Higgins and Bera, 1992; Zakoian, 1994).

### 6.6.2 Series-specific news impact dynamics

We assume that the vector of series specific news impact is a strictly monotonic vector transformation of  $\mathbf{f}_t$  which follows the  $n$ -dimensional updating function:

$$\mathbf{f}_{t+1} = \boldsymbol{\omega}^s + \text{diag}\{A_i\}\boldsymbol{\nabla}_t + B\mathbf{f}_t, \quad (6.23)$$

where  $\boldsymbol{\omega}^s$  is an unknown, series-specific ( $n \times 1$ ) parameter vector,  $\text{diag}\{A_i\}$  is a ( $n \times n$ ) diagonal parameter matrix, and  $B \in \mathbb{R}$ . Thus, we allow for series-specific intercept and sensitivity parameters in the score-updating of news impacts, yet ensure parsimony by employing joint  $B$  for all equity return series. The  $i$ -th element of the score vector at time  $t$  is then given by the first derivative of the likelihood function with respect to  $f_{i,t}$ :

$$\nabla_{i,t} = -\frac{1}{2} \left[ \text{Tr} \left( R(\mathbf{f}_t)^{-1} C_{i,t} \right) + \varepsilon_t' \left( -R(\mathbf{f}_t)^{-1} C_{i,t} R(\mathbf{f}_t)^{-1} \right) \varepsilon_t \right], \quad (6.24)$$

where  $C_{i,t}$  is an auxiliary ( $n \times n$ ) matrix defined by:

$$\begin{aligned} C_{i,t} = & -\frac{1}{2} \text{diag} \left( \frac{\partial Q}{\partial f_{i,t}} \right) \text{diag}(Q_t)^{-1} R(\mathbf{f}_t) + \text{diag}(Q_t)^{-1/2} \frac{\partial Q}{\partial f_{i,t}} \text{diag}(Q_t)^{-1/2} \\ & - \frac{1}{2} R(\mathbf{f}_t) \text{diag} \left( \frac{\partial Q}{\partial f_{i,t}} \right) \text{diag}(Q_t)^{-1}, \end{aligned} \quad (6.25)$$

with:

$$\begin{aligned} \frac{\partial Q}{\partial f_{1,t}} &= \left( \left[ \dot{h}(f_{1,t}), 0, \dots, 0 \right] h(\mathbf{f}_t)' + h(\mathbf{f}_t) \left[ \dot{h}(f_{1,t}), 0, \dots, 0 \right]' \right) \circ \left( \varepsilon_{t-1} \varepsilon_{t-1}' - \bar{Q} \right) \\ &\quad \vdots \\ \frac{\partial Q}{\partial f_{n,t}} &= \left( \left[ 0, \dots, 0, \dot{h}(f_{n,t}) \right] h(\mathbf{f}_t)' + h(\mathbf{f}_t) \left[ 0, \dots, 0, \dot{h}(f_{n,t}) \right]' \right) \circ \left( \varepsilon_{t-1} \varepsilon_{t-1}' - \bar{Q} \right), \end{aligned} \quad (6.26)$$

where, in our case,  $\dot{h}(f_{i,t}) = \exp(f_{i,t}) / (1 + \exp(f_{i,t}))^2$  for  $i = 1, \dots, n$  and  $t = 1, \dots, T$ .

# Chapter 7

## Critical assessment and conclusion

As introduced in Chapter 1, this dissertation is concerned with an investigation on financial market linkages and the behavior of financial investors in times of market turmoil and uncertainty. Whilst the overarching theme is relevant to each of the research papers presented in Chapters 2–6, the latter investigate and contribute to distinct yet highly interrelated fields within this area of financial econometrics. To conclude this dissertation, this final chapter complements the preceding research papers in summarizing their main findings, critically assessing their limitations and shortcomings, and stimulating avenues for further research.

Given the large interest in and the practical relevance of the many different periods of market turmoil that have occurred over the last two decades, Chapter 2 provides a thorough investigation on both the time-varying co-movement and the presence of financial contagion within a large sample of 38 equity markets over the period from January 1995 to July 2020. Since the chapter is particularly interested in studying (shifts in) these linkages on a broad scale beyond pair-wise investigations, the empirical methodology considers a dynamic spatial model which is also capable to account for increases in volatilities arising during the respective periods of market turmoil. The results of this research paper are twofold: First, the paper provides a generalized view on the co-movement between equity markets, demonstrating an increase in global stock market integration over time. Turning towards the continent-specific analysis, European markets are shown to exhibit a stronger co-movement than their American or Asian-Pacific counterparts. Second, when accounting for the increased parameter uncertainty during periods of market turmoil, the chapter suggests the shifts in global equity market linkages to be significant only in response to the outbreak of the COVID-19 pandemic in early 2020. Thus, in line with [Forbes and Rigobon \(2002\)](#), most of the investigated increases in global equity market co-movement in response to shocks should be considered interdependence rather than contagion.

Importantly, the thorough empirical investigation on and comparison of different periods of market turmoil, using a dynamic spatial model with time-varying volatilities, is a novel addition to the existing literature. Note, however, that the Delta-method in-sample confidence bands, as proposed in [Blasques \*et al.\* \(2016a\)](#) and employed in Chapter 2 to investigate shifts in market



---

linkages, impose several assumptions on the sources of uncertainty for the dynamic spatial dependence parameter. In general, three potential sources of uncertainty, i.e., parameter uncertainty (the true value of the parameter vector is unknown and replaced by its maximum likelihood estimate), filtering uncertainty (the true underlying time-varying parameter process is unknown), and model uncertainty (the true data generating process is unknown) can be identified for the dynamic spatial dependence parameter (Blasques *et al.*, 2016a). The approach used in the chapter accounts for the first of these sources. In that regard, the methodology additionally considers the accumulation of parameter uncertainty in the updating process which is reasonable given that the autoregressive component, i.e., the estimate of  $B$  in Equation 2.3 of Chapter 2, is non-zero. Besides, the fact that Delta-method in-sample confidence bands are of fully analytical nature renders their application appropriate for the extensive data set that is used in the chapter. We acknowledge, however, that computationally intense, simulation-based or bootstrap methods would be able to account for other potential sources of uncertainty for the dynamic spatial dependence parameter (see, e.g., Blasques *et al.*, 2016a; Zamojski, 2017; Beutner *et al.*, 2020). As the corresponding, formal results are not yet developed for the dynamic SAR model with time-varying volatilities, this consideration reflects a promising avenue for further research.

Whilst Chapter 2 is exclusively devoted to the linkages between equity markets, the focus of Chapters 3 and 4 is set on the dependencies between equity markets and a selection of associated safe haven assets and/ or hedges in times of turmoil and uncertainty. Specifically, Chapter 3 contributes to the existing research on flights to quality and gold and offers preliminary findings on the role of liquidity and tangibility during times of market turmoil. In the empirical analysis, the chapter employs an extensive sample of gold mining companies traded on four different markets as well as data on corresponding equity market indices and gold bullion to identify different types of flight to quality. The results of this chapter are manifold: First, the chapter offers novel insights on the relation between the severity of shocks to the equity market and the type of flight to quality. In more detail, the paper reveals that after extreme shocks (e.g., the collapse of Lehman Brothers in September 2008), investors flee from stocks including gold mining company shares to gold bullion. This temporary decoupling implies long-term profit opportunities given the expected recoupling of gold mining company shares with the price of gold bullion. After less severe shocks (e.g., the September 11, 2001, terrorist attacks), flights to gold bullion are less pronounced and no clear flights from gold mining company shares can be witnessed. On the opposite side of the spectrum, when shocks to the market are comparatively small (e.g., the Brexit vote in June 2016), investors partially reallocate their equity market investments towards both gold bullion and gold mining company shares, speculating on the safe haven effect to increase the price of gold bullion and gold mining company shares alike. Second, the findings suggest a negative relation between the broadness of the flight to quality and the safe haven effect of gold bullion. Beyond, differences in the size of companies as well as the importance of liquidity and tangibility of financial assets in times of market turmoil are also analyzed.

Chapter 3 contributes towards filling several gaps in the existing literature, particularly by demonstrating the dependence between the severity of crises and differences in flights to quality. Nevertheless, some shortcomings and limitations of the study need to be reflected. For instance, the sourcing, cleaning, and managing of data is generally challenging when considering large sets of data. Based on the extensive sample of gold mining companies considered in the chapter, it should be noted that reproducing this study or conducting subsequent research is associated with high efforts along this dimension. Nevertheless, this consideration is a common issue when empirical analyses are built on large data sets which are compiled manually. Another potential limitation of the chapter is the analysis devoted to the role of liquidity and tangibility during times of market turmoil. Turning towards this concern, the empirical findings in the chapter partially depart from the theory outlined in, e.g., [Vayanos \(2004\)](#), who suggests that liquidity considerations change over time and become increasingly relevant during periods of high market volatility. In contrast, the results of Chapter 3 report that financial investors flee from (and not to) the relatively liquid gold mining company shares with large market capitalization when shocks are severe. The chapter provides an explanation for this observation by suggesting a preference of financial investors for the physicality of underlying assets in times of market turmoil. Whilst an in-depth investigation on that matter is beyond the scope of the chapter, further research would be required to test this hypothesis.

Similar to Chapter 3, Chapter 4 is concerned with the dependencies between the equity market and gold, as well as other derivatives such as silver and energy future contracts. More explicitly, the chapter augments the standard DCC model of [Engle \(2002\)](#) to include information received from Google search queries for financial terms in the estimation of the time-varying correlation between the daily returns of the DJIA and gold, silver, crude oil, and natural gas future contracts. Before conducting any econometric analysis, the corresponding relative Google search volume data must be sourced from Google Trends in daily frequency. Receiving such data over the close to six years period of interest from January 2015 to September 2020 is challenging, however, as daily data can only be accessed for requests up to 270 continuous days. To address this concern, Chapter 4 makes use of the algorithm proposed in [Bleher and Dimpfl \(2019\)](#) which provides a means to construct consistent, multi-annual time series of daily relative observations from Google Trends' initial data. It should be acknowledged, however, that although the use of publicly available Google Trends data benefits the replicability of the presented findings in the chapter, the exact methodologies used for the computation of the relative measure for online investor attention remain unclear as the underlying algorithms are not disclosed by the provider. This concern is not further addressed in the chapter and is commonly not addressed in the related behavioral finance literature either, irrespective of the considered source of online search queries. Making the assumption that Google Trends' search volume data is a reasonable measure for latent online investor attention, the chapter provides a novel empirical application to this data in demonstrating its usefulness towards the modelling of the dynamic linkages between financial markets. On an additional note, the empirical results are used in a financial exercise to highlight the subsequent implications for the performance

---

and hedging effectiveness of combined portfolios. Along this line, it is shown in the chapter that the measure is less useful in the designing of optimal portfolios and their corresponding risk reduction, as portfolios' hedging effectiveness does not improve by more than 1% when incorporating the additional information.

Notably, since the majority of related studies only applies measures for investor attention to measure and predict first and second moments of individual financial time series, their innovative use in Chapter 4, building on the theoretical foundation of Peng and Xiong (2006), Veldkamp (2006), and Veldkamp and Wolfers (2007), provides novel empirical evidence on their usefulness in the modelling of the linkages between such time series. However, as the analysis in the likes of Vargas (2008) is based on a small selection of assets, exclusively, the empirical results provided in the chapter can hardly be generalized. Instead, further research should make similar endeavors using a broader selection of assets with a high proportion of shares or contracts held by retail investors. To reduce the number of required parameters in such exercise, one could consider the use of aggregate measures of investor attention that are relevant to all time series employed in the estimation. In that concern, promising aggregate measures to capture online investor attention based on Google search queries are provided in, e.g., the Financial and Economic Attitudes Revealed by Search (FEARS) index or the Global Risk Awareness (GRA) index of Da *et al.* (2015) and Costola *et al.* (2022), respectively. In contrast to measuring investor attention towards individual assets, these aggregate measures constitute search-based sentiment measures in depicting the overall perceived market risks by financial investors. According to the theory outlined in Barberis *et al.* (2005) and Kumar and Lee (2006), such measures of online investors' perceived risks may contain valuable information to the estimation and prediction of the co-movement between assets, raising the attention of institutional investors which are willing to incorporate this information into their wealth allocation strategies.

Chapter 5 adds to the research of Chapter 4 and investigates the question whether different online search queries in the form of Google searches for stock tickers and company-specific Wikipedia page views constitute equivalent measures for latent investor attention. Whilst a variety of different measures to quantify the latent variable have been employed in the empirical literature, the existing research has so far disregarded such comparison. However, given the increasing interest in and the many empirical applications of measures for online investor attention, a thorough investigation on their informational equivalence is highly relevant to researchers and practitioners alike since differences between them may impact empirical findings. Beyond, such investigation is closely associated with the ongoing search for a preferred measure of investor attention in general, including more traditional measures estimated from, e.g., market variables or newspaper appearances. Setting the focus on publicly available Google and Wikipedia search queries, Chapter 5 tests and quantifies the bi-directional information transfer between the respective search series for the constituents of the DJIA over the period from January 2008 to December 2017. The empirical methodology employs Shannon transfer entropy, a model-free measure to test for and quantify any kind of statistical dependencies between time series. In turn, the methodology allows to unravel

potentially nonlinear dependencies which would otherwise not be revealed by more traditional VAR approaches. Further, Shannon transfer entropy allows to infer the dominant direction of the information transfer, which cannot be identified with Granger (1969)'s causality test and its nonlinear extensions (e.g., Nishiyama *et al.*, 2011). In the empirical analysis, the chapter finds significant bi-directional information transfer between the different online search series for the stock tickers of the DJIA constituents. In turn, different online search series cannot be considered equivalent measures for online investor attention. Further, a considerable part of the identified information transfer is nonlinear, indicating that linear correlations and Granger causality tests are less useful when comparing different measures for online investor attention. Instead, Shannon transfer entropy constitutes a sound method for such investigation. Moreover, the chapter finds that taking nonlinear dependencies between search series into account becomes increasingly important during periods of market turmoil.

Turning towards the limitations of Chapter 5, a potential methodological shortcoming is the partitioning of the time series into three bins to compute Shannon transfer entropy based on discretized time series. In the chapter, this particular choice of partitioning is justified based on the limited amount of data that is considered in the study. Whilst the use of more bins to discretize the time series would be possible in theory, any reasonable partitioning into higher numbers of bins would require more data to be used in the empirical application. Besides, given the specific interest in the tail events of the empirical distribution, i.e., extremely low or high Google or Wikipedia searches, a partitioning into three bins seems to be a reasonable choice. In this case, using the 5% and 95% quantiles (or the 10% and 90% quantiles) of the empirical distribution results in the first and third bin capturing extremely negative and positive returns, respectively. A second potential shortcoming is related to the limited explanations behind the findings reported in the study. In particular, the investigation on the dominant direction of information transfer suggests the latter to be independent of the average market capitalization of the considered companies' stocks or the primary business fields they are engaged in. In turn, it would be interesting for future research to identify the common characteristics of companies for which the dominant direction of information flow unambiguously points into one direction. Such finding would significantly contribute towards the search for a preferred measure for online investor attention and, in consequence, be interesting for professional investors who consider these measures in the construction of their investment portfolios.

Finally, the research paper presented in Chapter 6 proposes an extension to the DCC model of Engle (2002) which improves the estimation of time-varying correlations between (financial) time series. The extended version considers and allows for changes in the impact of past news on correlation dynamics. Since financial applications of correlation models often revolve around times characterized by turmoil and uncertainty, the adaptable response of the model to news seems highly reasonable and relevant to researchers and practitioners alike (compare, e.g., Cappiello *et al.*, 2006). The updating is based on the observations of past periods, linking information from the shape of the conditional observation density directly to the dynamics of the time-varying news impact parameter

---

(Creal *et al.*, 2011, 2013; Harvey, 2013). In turn, the proposed model increases both flexibility and interpretability of DCC-type models beyond pair-wise correlations, whilst maintaining their appealing nature for applications with large cross-sections. It is demonstrated in a simulation study that the proposed p-range DCC model performs well in a variety of different situations. Besides, relying on an extensive data set of 30 equity indices over the period from January 2017 to March 2021, the model finds empirical evidence for significant increases in the impact of news for global correlation dynamics in response to several events. The most notable increases of the measure are detected in the aftermath of two instances in early 2020, namely (i) following the outbreak of COVID-19 and (ii) when equity markets began to recover from global uncertainties whilst economies started to reopen under the aiding guidance of national and supranational monetary and fiscal policies. The findings further suggest increases (decreases) in the impact of news to have direct implications for correlation news impact surfaces, pointing towards increased (decreased) risks of financial contagion. On a final note, the research paper further considers changes in the relevance of asymmetries for correlation dynamics, which become more pronounced during crisis events, and provides a generalized version of the extended model.

Whereas Chapters 2–5 are primarily concerned with empirical applications to investigate market linkages and investor behavior in times of turmoil and uncertainty, the nature and perspective of Chapter 6 on the topic is slightly more theoretical. Consequently, most of the chapter’s shortcomings are ingrained in its methodological setting which can and should be substantially extended along several dimensions. For instance, the p-range DCC model is estimated based on the assumption of conditional multivariate normality. This assumption is attractive from a modelling point of view in the chapter and, equally so, stated in the related literature (e.g., Engle and Kroner, 1995; Engle, 2002; Tse and Tsui, 2002; Cappiello *et al.*, 2006). However, the multivariate normal distribution places little mass on the joint tails between variables compared with other multivariate distributions such as, e.g., the multivariate Student-t distribution. In contrast, empirical findings on the multivariate behavior of financial assets and markets suggest the presence of extreme joint movements, rendering the multivariate Gaussian assumption less adequate for such applications (e.g., Richardson and Smith, 1993; Karolyi and Stulz, 1996; Longin and Solnik, 2001). Given the p-range DCC model’s financial application proposed in Chapter 6, it would therefore be interesting to explore how the model generalizes to the non-Gaussian setting. Similarly, efforts should be made by future research to compare the performance of the model against further competitors such as the copula-based MGARCH model of Lee and Long (2009), Creal *et al.* (2011)’s dynamic multivariate heavy-tailed model for time-varying correlations, or dynamic equicorrelation models based on Engle and Kelly (2012). In its current form, rather than competing with these models, the research paper solely focuses on providing an extension to the standard and asymmetric DCC models whilst offering the intuitively interpretable news impact parameter. A further limitation and promising avenue for future research is the investigation on the effects that alternative scaling functions have in the updating of the time-varying parameter on estimated correlation matrices. The current choice of

unity in the paper is in line with the selections in other settings considered in prior literature (compare, e.g., Blasques *et al.*, 2016b). Nevertheless, as stated in the paper, alternative choices in spirit of Creal *et al.* (2013) should be considered. Finally, we acknowledge that the investigation on the relation between economic distance and stock market integration could potentially be regarded as another shortcoming of the paper. Importantly, the paper touches upon this topic to provide a more detailed illustration of the data considered in the empirical application. However, a detailed analysis of differences in the dynamic news impact parameter across several regional samples is beyond the scope of the paper.

In conclusion, the original research conducted in this dissertation contributes to several strands of the financial literature concerned with market linkages and investor behavior in times of turmoil and uncertainty. Most remarkably, even though some methodological shortcomings or empirical limitations may still remain in the preceding chapters, each of the five presented research papers encourages promising avenues for future research on its respective matter. Further investigations on the overarching topic of this dissertation – particularly considering current and future crisis events – are inevitable, and of the uttermost importance. We hope that this dissertation may serve as a starting point and guiding light for future research. To those concerned with pursuing the suggested research ideas, we wish you all the best on your respective journeys.

*It is good to have an end to journey toward;  
But it is the journey that matters, in the end.*  
– Ursula K. Le Guin

# Bibliography

- Abuzayed, B., Bouri, E., Al-Fayoumi, N. and Jalkh, N. (2021) Systemic risk spillover across global and country stock markets during the COVID-19 pandemic, *Economic Analysis and Policy*, **71**, 180–197.
- Acemoglu, D., Ozdaglar, A. and Tahbaz-Salehi, A. (2015) Systemic risk and stability in financial networks, *American Economic Review*, **105**, 564–608.
- Adam, T. R., Fernando, C. S. and Salas, J. M. (2017) Why do firms engage in selective hedging? Evidence from the gold mining industry, *Journal of Banking & Finance*, **77**, 269–282.
- Afkhami, M., Cormack, L. and Ghoddsi, H. (2017) Google search keywords that best predict energy price volatility, *Energy Economics*, **67**, 17–22.
- Ahmad, W., Bhanumurthy, N. R. and Sehgal, S. (2013) Eurozone crisis and BRIICKS stock markets: Contagion or market interdependence?, *Economic Modelling*, **33**, 209–225.
- Ahmad, W., Bhanumurthy, N. R. and Sehgal, S. (2014) The Eurozone crisis and its contagion effects on the European stock markets, *Studies in Economics and Finance*, **31**, 325–352.
- Aielli, G. P. (2013) Dynamic conditional correlation: On properties and estimation, *Journal of Business & Economic Statistics*, **31**, 282–299.
- Ali, M., Alam, N. and Rizvi, S. A. R. (2020) Coronavirus (COVID-19) – An epidemic or pandemic for financial markets, *Journal of Behavioral and Experimental Finance*, **27**, 100341.
- Allen, F. and Douglas, G. (2000) Financial contagion, *Journal of Political Economy*, **108**, 1–33.
- Amihud, Y. (2002) Illiquidity and stock returns: Cross-section and time-series effects, *Journal of Financial Markets*, **5**, 31–56.
- Anand, A., Puckett, A., Irvine, P. J. and Venkataraman, K. (2013) Institutional trading and stock resiliency: Evidence from the 2007–2009 financial crisis, *Journal of Financial Economics*, **108**, 773–797.

## BIBLIOGRAPHY

---

- Ang, A. and Bekaert, G. (2002) International asset allocation with regime shifts, *The Journal of Finance*, **15**, 1137–1187.
- Anselin, L. (1982) A note on small sample properties of estimators in a first-order spatial autoregressive model, *Environment and Planning A*, **14**, 1023–1030.
- Areal, N., Benilde, O. and Sampaio, R. (2013) When times get tough, gold is golden, *The European Journal of Finance*, **22**, 507–526.
- Arnold, M., Stahlberg, S. and Wied, D. (2013) Modeling different kinds of spatial dependence in stock returns, *Empirical Economics*, **44**, 761–774.
- Aromi, D. and Clements, A. (2019) Spillovers between the oil sector and the S&P500: The impact of information flow about crude oil, *Energy Economics*, **81**, 187–196.
- Arouri, M. E. H., Jouini, J. and Duc, K. N. (2011) Volatility spillovers between oil prices and stock sector returns: Implications for portfolio management, *Journal of International Money and Finance*, **30**, 1387–1405.
- Arouri, M. E. H., Lahiani, A. and Duc, K. N. (2015) World gold prices and stock returns in China: Insights for hedging and diversification strategies, *Economic Modelling*, **44**, 273–283.
- Asai, M. and McAleer, M. (2009) Multivariate stochastic volatility, leverage and news impact surfaces, *The Econometrics Journal*, **12**, 145–175.
- Asgharian, H., Hess, W. and Lu, L. (2013) A spatial analysis of international stock market linkages, *Journal of Banking & Finance*, **37**, 4738–4754.
- Ashraf, B. N. (2020) Stock markets' reaction to COVID-19: Cases or fatalities?, *Research in International Business and Finance*, **54**, 101249.
- Audrino, F., Ballinari, D. and Sigris, F. (2020) The impact of sentiment and attention measures on stock market volatility, *International Journal of Forecasting*, **36**, 334–357.
- Aviat, A. and Coeurdacier, N. (2007) The geography of trade in goods and asset holdings, *Journal of International Economics*, **71**, 22–51.
- Bae, K.-H., Karolyi, G. A. and Stulz, R. M. (2003) A new approach to measuring financial contagion, *The Review of Financial Studies*, **16**, 717–763.
- Baele, L., Bekaert, G., Inghelbrecht, K. and Wei, M. (2018) Flights to safety, *National Bank of Belgium Working Paper No. 230*.
- Baele, L. and Soriano, P. (2010) The determinants of increasing equity market comovement: Economic or financial integration?, *Review of World Economics*, **146**, 573–589.



- Baig, T. and Goldfajn, I. (1999) Financial market contagion in the Asian crisis, *IMF Economic Review*, **46**, 167–195.
- Baig, T. and Goldfajn, I. (2000) The Russian default and the contagion to Brazil, IMF Working Paper 00/160, International Monetary Fund.
- Baker, S. R., Bloom, N., Davis, S. J., Kost, K., Sammon, M. and Viratyosin, T. (2020) The unprecedented stock market reaction to COVID-19, *The Review of Asset Pricing Studies*, **10**, 742–758.
- Barber, B. M. and Odean, T. (2008) All that glitters: The effect of attention and news on the buying behavior of individual and institutional investors, *The Review of Financial Studies*, **21**, 785–818.
- Barberis, N., Shleifer, A. and Wurgler, J. (2005) Comovement, *Journal of Financial Economics*, **75**, 283–317.
- Batten, J. A., Ciner, C., Kosedag, A. and Lucey, B. M. (2017) Is the price of gold to gold mining stocks asymmetric?, *Economic Modelling*, **60**, 402–407.
- Baur, D. (2006) A flexible dynamic correlation model, *Advances in Econometrics*, **20**, 3–31.
- Baur, D. G. (2014) Gold mining companies and the price of gold, *Review of Financial Economics*, **23**, 174–181.
- Baur, D. G. and Lucey, B. M. (2009) Flights and contagion. An empirical analysis of stock-bond correlations, *Journal of Financial Stability*, **5**, 339–352.
- Baur, D. G. and Lucey, B. M. (2010) Is gold a hedge or a safe haven? An analysis of stocks, bonds and gold, *The Financial Review*, **45**, 217–229.
- Baur, D. G. and McDermott, T. K. (2010) Is gold a safe haven? International evidence, *Journal of Banking & Finance*, **34**, 1886–1898.
- Bauwens, L., Laurent, S. and Rombouts, J. V. K. (2006) Multivariate GARCH models: A survey, *Journal of Applied Econometrics*, **21**, 79–109.
- Beber, A., Brandt, M. W. and Kenneth, A. (2009) Flight-to-quality or flight-to-liquidity? Evidence from the Euro-area bond market, *The Review of Financial Studies*, **22**, 925–957.
- Beckmann, J., Berger, T. and Czudaj, R. (2013) Does gold act as a hedge or a safe haven for stocks? A smooth transition approach, *Economic Modelling*, **48**, 16–24.
- Behrendt, S., Dimpfl, T., Peter, F. J. and Zimmermann, D. J. (2019) RTransferEntropy: Quantifying information flow between different time series using effective transfer entropy, *SoftwareX*, **10**, 100265.

## BIBLIOGRAPHY

---

- Behrendt, S., Peter, F. J. and Zimmermann, D. J. (2020) An encyclopedia for stock markets? Wikipedia searches and stock returns, *International Review of Financial Analysis*, **79**, 101563.
- Behrendt, S. and Schmidt, A. (2021) Nonlinearity matters: The stock price – trading volume relation revisited, *Economic Modelling*, **98**, 371–385.
- Beirne, J. and Fratzscher, M. (2013) The pricing of sovereign risk and contagion during the European sovereign debt crisis, *Journal of International Money and Finance*, **34**, 60–82.
- Bekaert, G., Ehrmann, M., Fratscher, M. and Mehl, A. (2014) The global crisis and equity market contagion, *The Journal of Finance*, **69**, 2597–2649.
- Bekaert, G., Harvey, C. and Lundblad, C. (2007) Liquidity and expected returns: Lessons from emerging markets, *The Review of Financial Studies*, **20**, 1783–1831.
- Bekaert, G., Hodrick, R. J. and Zhang, X. (2009) International stock return comovements, *The Journal of Finance*, **64**, 2591–2626.
- Benjamin, M. A., Rigby, R. A. and Stasinopoulos, M. (2003) Generalized autoregressive moving average models, *Journal of the American Statistical Association*, **98**, 214–223.
- Benoit, S., Colliard, J.-E., Hurlin, C. and Pérignon, C. (2017) Where the risks lie: A survey on systemic risk, *Review of Finance*, **21**, 109–152.
- Berben, R.-P. and Jansen, W. J. (2005) Comovement in international equity markets: A sectoral view, *Journal of International Money and Finance*, **24**, 832–857.
- Beutner, E., Heinemann, A. and Smeekes, S. (2020) A residual bootstrap for conditional Value-at-Risk, Working paper.
- Black, F. (1976) Studies of stock price volatility changes, in *Proceedings of the 1976 meetings of the Business and Economics Statistics section, American Statistical Association*, pp. 177–181.
- Black, F. (1986) Noise, *The Journal of Finance*, **41**, 528–543.
- Blasques, F., Gorgi, P. and Koopman, S. J. (2019) Accelerating score-driven time series models, *Journal of Econometrics*, **212**, 359–376.
- Blasques, F., Koopman, S. J., Lasak, K. and Lucas, A. (2016a) In-sample confidence bands and out-of-sample forecast bands for time-varying parameters in observation-driven models, *International Journal of Forecasting*, **32**, 875–887.
- Blasques, F., Koopman, S. J., Lucas, A. and Schaumburg, J. (2016b) Spillover dynamics for systemic risk measurement using spatial financial time series models, *Journal of Econometrics*, **195**, 255–271.

- Blasques, F., Van Brummelen, J., Koopman, S. J. and Lucas, A. (2022) Maximum likelihood estimation for score-driven models, *Journal of Econometrics*, **227**, 325–346.
- Bleher, J. and Dimpfl, T. (2019) Today I got a million, tomorrow, I don't know: On the predictability of cryptocurrencies by means of Google search volume, *International Review of Financial Analysis*, **63**, 147–159.
- Bloomberg (2021) Barrick Gold Corp, <https://www.bloomberg.com/quote/GOLD:US>, [Online; accessed 2022-04-08].
- Bollerslev, T. (1986) Generalized autoregressive conditional heteroskedasticity, *Journal of Econometrics*, **31**, 307–327.
- Bollerslev, T., Engle, R. F. and Wooldridge, J. M. (1988) A capital asset pricing model with time-varying covariances, *Journal of Political Economy*, **96**, 116–131.
- Borenstein, S. and Farrell, J. (2008) Do investors forecast fat firms? Evidence from the gold-mining industry, *RAND Journal of Economics*, **38**, 56–63.
- Boubaker, S., Jouini, J. and Lahiani, A. (2016) Financial contagion between the US and selected developed and emerging countries: The case of the subprime crisis, *The Quarterly Review of Economics and Finance*, **61**, 14–28.
- Boyer, B. H., Gibson, M. S. and Loretan, M. (1997) Pitfalls in tests for changes in correlations, International Finance Discussion Papers 597, Board of Governors of the Federal Reserve System (US).
- Bräuning, F. and Koopman, J. S. (2014) Forecasting macroeconomic variables using collapsed dynamic factor analysis, *International Journal of Forecasting*, **30**, 572–584.
- Bredin, D., Conlon, T. and Potì, V. (2015) Does gold glitter in the long-run? Gold as a hedge and safe haven across time and investment horizon, *International Review of Financial Analysis*, **48**, 320–328.
- Broto, C. and Perez-Quiros, G. (2015) Disentangling contagion among sovereign CDS spreads during the European debt crisis, *Journal of Empirical Finance*, **32**, 165–179.
- Brunnermeier, M. K. (2009) Deciphering the liquidity and credit crunch 2007–2008, *Journal of Economic Perspectives*, **23**, 77–100.
- Buiter, W., Corsetti, G. and Pesenti, P. (1998) *Financial markets and European monetary cooperation. The lessons of the 1992–1993 exchange rate mechanism crisis*, Cambridge University Press, Cambridge.

## BIBLIOGRAPHY

---

- Calvo, G. A. (2004) Contagion in emerging markets: When Wall Street is a carrier, in *Latin American economic crises* (Eds.) E. Bour, D. Heymann and F. Navajas, Palgrave Macmillan, pp. 81–91.
- Calvo, G. A. and Reinhart, C. M. (1996) Capital flows to Latin America: Is there evidence of contagion effects?, in *Private capital flows to emerging markets after the Mexican crisis* (Eds.) G. A. Calvo, M. Goldstein and E. Hochreiter, Institute for International Economics, pp. 151–171.
- Capie, F., Mills, T. C. and Wood, G. (2005) Gold as a hedge against the Dollar, *Journal of International Financial Markets, Institutions & Money*, **15**, 343–352.
- Caporale, G. M., Cipollini, A. and Spagnolo, N. (2005) Testing for contagion: A conditional correlation analysis, *Journal of Empirical Finance*, **12**, 476–489.
- Caporin, M., Pelizzon, L., Ravazzolo, F. and Rigobon, R. (2018) Measuring sovereign contagion in Europe, *Journal of Financial Stability*, **34**, 150–181.
- Cappiello, L., Engle, R. F. and Sheppard, K. (2006) Asymmetric dynamics in the correlations of global equity and bond returns, *Journal of Financial Econometrics*, **4**, 537–572.
- Chakrabarti, P., Jawed, M. S. and Sarkhel, M. (2021) COVID-19 pandemic and global financial market interlinkages: A dynamic temporal network analysis, *Applied Economics*, **53**, 2930–2945.
- Chan, K. F., Treepongkaruna, S., Brooks, R. and Gray, S. (2011) Asset market linkages: Evidence from financial, commodity and real estate assets, *Journal of Banking & Finance*, **35**, 1415–1426.
- Chang, Y., Faff, R. and Hwang, C.-Y. (2010) Liquidity and stock returns in Japan: New evidence, *Pacific-Basin Finance Journal*, **18**, 90–115.
- Chiang, T. C., Jeon, B. N. and Li, H. (2007) Dynamic correlation analysis of financial contagion: Evidence from Asian markets, *Journal of International Money and Finance*, **26**, 1206–1228.
- Chkili, W. (2016) Dynamic correlations and hedging effectiveness between gold and stock markets: Evidence for BRICS countries, *Research in International Business and Finance*, **38**, 22–34.
- Chordia, T., Roll, R. and Subrahmanyam, A. (2000) Commonality in liquidity, *Journal of Financial Economics*, **56**, 3–28.
- Chordia, T., Roll, R. and Subrahmanyam, A. (2001) Market liquidity and trading activity, *The Journal of Finance*, **56**, 501–530.
- Chordia, T., Roll, R. and Subrahmanyam, A. (2004) Order imbalance, liquidity, and market returns, *Journal of Financial Economics*, **72**, 485–518.

- Chordia, T., Sarkar, A. and Subrahmanyam, A. (2005) An empirical analysis of stock and bond market liquidity, *The Review of Financial Studies*, **18**, 85–129.
- Christie, A. A. (1982) The stochastic behavior of common stock variances: Value, leverage and interest rate effects, *Journal of Financial Economics*, **10**, 407–432.
- Christoffersen, P., Errunza, V., Jacobs, K. and Jin, X. (2014) Correlation dynamics and international diversification benefits, *International Journal of Forecasting*, **30**, 807–824.
- Chronopoulos, D. K., Papadimitriou, F. I. and Vlastakis, N. (2018) Information demand and stock return predictability, *Journal of International Money and Finance*, **80**, 59–74.
- Ciner, C., Gurdgiev, C. and Lucey, B. M. (2013) Hedges and safe havens: An examination of stocks, bonds, gold, oil and exchange rates, *International Review of Financial Analysis*, **29**, 202–211.
- Claessens, S., Dornbusch, R. and Park, Y. C. (2001) Contagion: Why crises spread and how this can be stopped, in *International financial contagion* (Eds.) S. Claessens and K. J. Forbes, Kluwer Academic Publishers, pp. 19–41.
- Cliff, A. D. and Ord, J. K. (1973) Spatial autocorrelation, Tech. rep., London, Pion.
- Cliff, A. D. and Ord, J. K. (1981) Spatial processes, models and applications, Tech. rep., London, Pion.
- Connolly, R., Stivers, C. and Sun, L. (2005) Stock market uncertainty and the stock-bond return relation, *Journal of Financial and Quantitative Analysis*, **40**, 161–194.
- Corbet, S., Goodell, J. W. and Günay, S. (2020) Co-movements and spillovers of oil and renewable firms under extreme conditions: New evidence from negative WTI prices during COVID-19, *Energy Economics*, **92**, 104978.
- Corsetti, G., Pesenti, P. and Roubini, N. (1999) What caused the Asian currency and financial crisis?, *Japan and the World Economy*, **11**, 305–373.
- Corsetti, G., Pesenti, P., Roubini, N. and Tille, C. (2000) Competitive devaluations: Toward a welfare-based approach, *European Journal of Political Economy*, **51**, 217–241.
- Costola, M., Donadelli, M., Gerotto, L. and Gufler, I. (2022) Global risks, the macroeconomy, and asset prices, *Empirical Economics*, pp. 1–32.
- Cox, D. R. (1981) Statistical analysis of time series: Some recent developments, *Scandinavian Journal of Statistics*, **8**, 93–115.

## BIBLIOGRAPHY

---

- Creal, D., Koopman, S. J. and Lucas, A. (2011) A dynamic multivariate heavy-tailed model for time-varying volatilities and correlations, *Journal of Business & Economic Statistics*, **29**, 552–563.
- Creal, D., Koopman, S. J. and Lucas, A. (2013) Generalized autoregressive score models with applications, *Journal of Applied Econometrics*, **28**, 777–795.
- Creti, A., Joëts, M. and Mignon, V. (2013) On the links between stock and commodity markets' volatility, *Energy Economics*, **37**, 16–28.
- Da, Z., Engelberg, J. and Gao, P. (2011) In search of attention, *The Journal of Finance*, **66**, 1461–1499.
- Da, Z., Engelberg, J. and Gao, P. (2015) The sum of all FEARS investor sentiment and asset prices, *The Review of Financial Studies*, **28**, 1–32.
- Dar, A., Bhanja, N. and Paul, M. (2019) Do gold mining stocks behave like gold or equities? Evidence from the UK and the US, *International Review of Economics & Finance*, **59**, 369–384.
- Daskalaki, C. and Skiadopoulos, G. (2011) Should investors include commodities in their portfolios after all? New evidence, *Journal of Banking & Finance*, **35**, 2606–2626.
- De Gregorio, J. and Valdé, R. O. (2001) Crisis transmission: Evidence from the debt, tequila, and Asian flu crises, *The World Bank Economic Review*, **15**, 289–314.
- De Long, J. B., Shleifer, A., Summers, L. H. and Waldmann, R. J. (1990) Noise trader risk in financial markets, *Journal of Political Economy*, **98**, 703–738.
- Dellas, H. (1986) A real model of the world business cycle, *Journal of International Money and Finance*, **5**, 381–394.
- Diebold, F. X. and Yilmaz, K. (2012) Better to give than to receive: Predictive directional measurement of volatility spillovers, *International Journal of Forecasting*, **28**, 57 – 66.
- Dimitriou, D., Kenourgios, D. and Simos, T. (2011) Global financial crisis and emerging stock market contagion: A multivariate FIAPARCH-DCC approach, *International Review of Financial Analysis*, **20**, 717 – 732.
- Dimpfl, T. and Jank, S. (2016) Can internet search queries help to predict stock market volatility?, *European Financial Management*, **22**, 171–192.
- Dimpfl, T. and Peter, F. J. (2013) Using transfer entropy to measure information flows between financial markets, *Studies in Nonlinear Dynamics & Econometrics*, **17**, 85–102.

- Dimpfl, T. and Peter, F. J. (2018) Analyzing volatility transmission using group transfer entropy, *Energy Economics*, **75**, 368–376.
- Ding, Z. and Engle, R. F. (2001) Large scale conditional covariance matrix modeling, estimation and testing, *Academia Economic Papers*.
- Drazen, A. (2000) Political contagion in currency crises, in *Currency crises* (Ed.) P. Krugman, University of Chicago Press, pp. 47–70.
- Driessen, J. and Laeven, L. (2007) International portfolio diversification benefits: Cross-country evidence from a local perspective, *Journal of Banking & Finance*, **31**, 1693–1712.
- Dungey, M., Fry, R., Gonzáles-Hermosillo, B. and Martin, V. L. (2005) Empirical modelling of contagion: A review of methodologies, *The Journal of Finance*, **5**, 9–24.
- Durbin, J. and Koopman, S. J. (1997) Monte Carlo maximum likelihood estimation for non-Gaussian state space models, *Biometrika*, **84**, 669–684.
- Dzielinski, M. (2012) Measuring economic uncertainty and its impact on the stock market, *Finance Research Letters*, **9**, 167–175.
- Eichengreen, B., Rose, A. K. and Wyplosz, C. (1996) Contagious currency crises, NBER Working Paper 5681, National Bureau of Economic Research.
- Engle, R. F. (1982) Autoregressive conditional heteroscedasticity with estimates of the variance of United Kingdom inflation, *Econometrica*, **50**, 987–1007.
- Engle, R. F. (2002) Dynamic conditional correlation: A simple class of multivariate generalized autoregressive conditional heteroskedasticity models, *Journal of Business & Economic Statistics*, **20**, 339–350.
- Engle, R. F. (2009) *Anticipating correlations: A new paradigm for risk management*, Oxford University Press, Princeton, NJ.
- Engle, R. F., Ito, T. and Lin, W.-L. (1990) Meteor showers or heat waves? Heteroskedastic intraday volatility in the foreign exchange market, *Econometrica*, **58**, 525–542.
- Engle, R. F. and Kelly, B. (2012) Dynamic equicorrelation, *Journal of Business & Economic Statistics*, **30**, 212–228.
- Engle, R. F. and Kroner, K. F. (1995) Multivariate simultaneous generalized ARCH, *Econometric Theory*, **11**, 122–150.
- Engle, R. F. and Manganelli, S. (2004) CAViaR: Conditional autoregressive Value at Risk by regression quantiles, *Journal of Business & Economic Statistics*, **22**, 367–381.

## BIBLIOGRAPHY

---

- Engle, R. F. and Ng, V. K. (1993) Measuring and testing the impact of news on volatility, *The Journal of Finance*, **48**, 1749–1778.
- Engle, R. F. and Russel, J. R. (2005) A discrete-state continuous-time model of financial transactions prices and times: The autoregressive conditional multinomial-autoregressive conditional duration model, *Journal of Business & Economic Statistics*, **23**, 166–180.
- Engle, R. F. and Russell, J. R. (1998) Autoregressive conditional duration: A new model for irregularly spaced transaction data, *Econometrica*, **66**, 1127–1162.
- Engle, R. F. and Sheppard, K. (2001) Theoretical and empirical properties of dynamic conditional correlation multivariate GARCH, NBER Working Paper 8554, National Bureau of Economic Research.
- English, W. B. and Loretan, M. (1997) Evaluating “correlation breakdowns” during periods of market volatility, International Finance Discussion Papers 658, Board of Governors of the Federal Reserve System (US).
- Fama, E. F. (1965) The behavior of stock-market prices, *The Journal of Business*, **38**, 34–105.
- Faugère, C. and Van Erlich, J. (2005) The price of gold: A global required yield theory, *The Journal of Investing*, **14**, 99–111.
- Fernandez, V. (2011) Spatial linkages in international financial markets, *Quantitative Finance*, **11**, 237–245.
- Florackis, C., Kontonikas, A. and Kostakis, A. (2014) Stock market liquidity and macro-liquidity shocks: Evidence from the 2007–2009 financial crisis, *Journal of International Money and Finance*, **44**, 97–117.
- Forbes, K. (2012) The “Big C”: Identifying contagion, NBER Working Paper 18465, National Bureau of Economic Research.
- Forbes, K. and Rigobon, R. (2001) Measuring contagion: Conceptual and empirical issues, in *International financial contagion* (Eds.) S. Claessens and K. J. Forbes, Kluwer Academic Publishers, pp. 43–66.
- Forbes, K. J. and Chinn, M. D. (2004) A decomposition of global linkages in financial markets over time, *Review of Economics and Statistics*, **86**, 705–722.
- Forbes, K. J. and Rigobon, R. (2002) No contagion, only interdependence: Measuring stock market comovements, *The Journal of Finance*, **57**, 2223–2261.
- Frankel, J. and Rose, A. (1998) The endogeneity of the optimum currency area criteria, *The Economic Journal*, **108**, 1009–1025.



- Gai, P., Haldane, A. and Kapadia, S. (2011) Complexity, concentration and contagion, *Journal of Monetary Economics*, **58**, 453–470.
- Gasperoni, F., Luati, A., Paci, L. and D’Innocenzo, E. (2022) Score-driven modeling of spatio-temporal data, *Journal of the American Statistical Association*, **In press**.
- Gerlach, S. and Smets, F. (1995) Contagious speculative attacks, *European Journal of Political Economy*, **11**, 45–63.
- Gervais, S., Kaniel, R. and Mingelgrin, D. H. (2001) The high-volume return premium, *The Review of Financial Studies*, **56**, 877–919.
- Glick, R. and Rose, A. K. (1999) Contagion and trade: Why are currency crises regional?, *Journal of International Money and Finance*, **18**, 603–617.
- Glosten, L. R., Jagannathan, R. and Runkle, D. E. (1993) On the relation between the expected value and the volatility of the nominal excess return on stocks, *The Journal of Finance*, **48**, 1779–1801.
- Goldstein, M., Kaminsky, G. L. and Reinhart, C. M. (2000) *Assessing financial vulnerability: An early warning system for emerging markets*, Institute for International Economics, Washington.
- Goyenko, R. Y. and Ukhov, A. D. (2009) Stock and bond market liquidity: A long-run empirical analysis, *Journal of Financial and Quantitative Analysis*, **44**, 189–212.
- Granger, C. W. J. (1969) Investigating causal relations by econometric models and cross-spectral methods, *Econometrica*, **37**, 424–438.
- Griffin, H. J. H., John M., Shu, T. and Topaloglu, S. (2011) Who drove and burst the tech bubble?, *The Journal of Finance*, **66**, 1251–1290.
- Grullon, G., Kanatas, G. and Weston, J. P. (2004) Advertising, breadth of ownership, and liquidity, *The Review of Financial Studies*, **17**, 439–461.
- Gulko, L. (2002) Decoupling, *The Journal of Portfolio Management*, **28**, 59–66.
- Habib, M. M. and Stracca, L. (2012) Getting beyond carry trade: What makes a safe haven currency?, *Journal of International Economics*, **87**, 50–64.
- Hafner, C. M. and Manner, H. (2012) Dynamic stochastic copula models: Estimation, inference and applications, *Journal of Applied Econometrics*, **27**, 485–505.
- Han, L., Lv, Q. and Yin, L. (2017) Can investor attention predict oil prices?, *Energy Economics*, **66**, 547–558.

## BIBLIOGRAPHY

---

- Harvey, A. C. (2013) *Dynamic models for volatility and heavy tails: With applications to financial and economic time series*, Cambridge University Press, Cambridge.
- Harvey, A. C. and Luati, A. (2014) Filtering with heavy tails, *Journal of the American Statistical Association*, **109**, 1112–1122.
- Hervé, F., Zouaoui, M. and Belvaux, B. (2019) Noise traders and smart money: Evidence from online searches, *Economic Modelling*, **83**, 141–149.
- Higgins, M. L. and Bera, A. K. (1992) Threshold heteroskedastic models, *International Economic Review*, **33**, 137–158.
- Hillier, D., Draper, P. and Faff, R. (2006) Do precious metals shine? An investment perspective, *Financial Analysts Journal*, **62**, 98–106.
- Hirshleifer, D. and Teoh, S. H. (2003) Limited attention, information disclosure, and financial reporting, *Journal of Accounting and Economics*, **36**, 337–386.
- Horowitz, J. L. (2003) Bootstrap methods for Markov processes, *Econometrica*, **71**, 1049–1082.
- Hu, Y., Li, X., Goodell, J. and Shen, D. (2021) Investor attention shocks and stock co-movement: Substitution or reinforcement?, *International Review of Financial Analysis*, **73**, 101617.
- Imbs, J. (2004) Trade, finance, specialization, and synchronization, *Review of Economics and Statistics*, **86**, 723–734.
- Jaffe, J. F. (1989) Gold and gold stocks as investments for institutional portfolios, *Financial Analysts Journal*, **45**, 53–59.
- Jain, A. and Biswal, P. C. (2019) Does internet search interest for gold move the gold spot, stock and exchange rate markets? A study from India, *Resources Policy*, **61**, 501–507.
- Jeanne, O. (1997) Are currency crises self-fulfilling? A test, *Journal of International Economics*, **43**, 263–286.
- Ji, Q. and Gu, J.-F. (2015) Market interdependence among commodity prices based on information transmission on the internet, *Physica A: Statistical Mechanics and its Applications*, **426**, 35–44.
- Jiang, Z. and Yoon, S.-M. (2020) Dynamic co-movement between oil and stock markets in oil-importing and oil-exporting countries: Two types of wavelet analysis, *Energy Economics*, **90**, 104835.
- Jondeau, E. and Rockinger, M. (2009) The impact of shocks on higher moments, *Journal of Financial Econometrics*, **7**, 77–105.

- Joseph, K., M. Babajide, W. and Zhang, Z. (2011) Forecasting abnormal stock returns and trading volume using investor sentiment: Evidence from online search, *International Journal of Forecasting*, **27**, 1116–1127.
- Jungbacker, B. and Koopman, S. J. (2007) Monte Carlo estimation for nonlinear non-Gaussian state space models, *Biometrika*, **94**, 827–839.
- Jungbacker, B. and Koopman, S. J. (2014) Likelihood-based dynamic factor analysis for measurement and forecasting, *The Econometrics Journal*, **18**, C1–C21.
- Kahnemann, D. (1973) *Attention and effort*, Prentice-Hall, Englewood Cliffs, NJ.
- Kaminsky, G. L. and Reinhart, C. M. (2000) On crises, contagion, and confusion, *Journal of International Economics*, **51**, 145–168.
- Kaminsky, G. L. and Reinhart, C. M. (2003) The center and the periphery: The globalization of financial turmoil, in *Capital flows, crisis, and stabilization: Essays in honor of Guillermo A. Calvo* (Eds.) C. M. Reinhart, C. Vegh and A. Velasco, MIT Press, pp. 171–216.
- Karolyi, G. A. (1995) A multivariate GARCH model of international transmissions of stock returns and volatility: The case of the United States and Canada, *Journal of Business & Economic Statistics*, **13**, 11–25.
- Karolyi, G. A. and Stulz, R. M. (1996) Why do markets move together? An investigation of US-Japan stock return comovements, *The Journal of Finance*, **51**, 951–986.
- Kaul, A. and Sapp, S. (2006) Y2k fears and safe haven trading of the US Dollar, *Journal of International Money and Finance*, **5**, 760–779.
- Kelejian, H. H. and Prucha, I. R. (2010) Specification and estimation of spatial autoregressive models with autoregressive and heteroskedastic disturbances, *Journal of Econometrics*, **157**, 53–67.
- Kenourgios, D., Samitas, A. and Paltalidis, N. (2011) Financial crises and stock market contagion in a multivariate time-varying asymmetric framework, *Journal of International Financial Markets, Institutions & Money*, **21**, 92–106.
- Kilian, L. and Park, C. (2009) The impact of oil price shocks on the US stock market, *International Economic Review*, **50**, 1267–1287.
- King, M. A., Sentana, E. and Wadhvani, S. (1994) Volatility and links between national stock markets, *Econometrica*, **62**, 901–933.
- King, M. A. and Wadhvani, S. (1990) Transmission of volatility between stock markets, *The Review of Financial Studies*, **3**, 5–33.

## BIBLIOGRAPHY

---

- Kling, J. L. (1985) Oil price shocks and stock market behavior, *Journal of Portfolio Management*, **1**, 34–39.
- Koopman, S. J., Lucas, A. and Scharth, M. (2015) Numerically accelerated importance sampling for nonlinear non-Gaussian state-space models, *Journal of Business & Economic Statistics*, **33**, 114–127.
- Koopman, S. J., Lucas, A. and Scharth, M. (2016) Predicting time-varying parameters with parameter-driven and observation-driven models, *Review of Economics and Statistics*, **98**, 97–110.
- Kroner, K. F. and Ng, V. K. (1998) Modeling asymmetric comovement of asset returns, *The Review of Financial Studies*, **11**, 844–871.
- Kroner, K. F. and Sultan, J. (1993) Time-varying distributions and dynamic hedging with foreign currency futures, *Journal of Financial and Quantitative Analysis*, **28**, 535–551.
- Krugman, P. (1991) *Geography and trade*, MIT Press, Cambridge.
- Krugman, P. (1992) A dynamic spatial model, NBER Working Paper 4219, National Bureau of Economic Research.
- Ku, Y.-H. H., Chen, H.-C. and Chen, K.-H. (2007) On the application of the dynamic conditional correlation model in estimating optimal time-varying hedge ratios, *Applied Economics Letters*, **14**, 503–509.
- Kullback, S. and Leibler, R. A. (1951) On information and sufficiency, *Annals of Mathematical Statistics*, **1**, 79–86.
- Kumar, A. and Lee, C. M. C. (2006) Retail investor sentiment and return comovements, *The Journal of Finance*, **61**, 2451–2486.
- Kyle, A. S. (1985) Continuous auctions and insider trading, *Econometrica*, **53**, 1315–1335.
- Kyle, A. S. and Xiong, W. (2001) Contagion as a wealth effect, *The Journal of Finance*, **56**, 1401–1440.
- Lahrech, A. and Sylwester, K. (2011) US and Latin American stock market linkages, *Energy Economics*, **30**, 1341–1357.
- Lee, L. (2004) Asymptotic distributions for quasi-maximum likelihood estimators for spatial autoregressive models, *Econometrica*, **72**, 1899–1925.
- Lee, T.-H. and Long, X. (2009) Copula-based multivariate GARCH model with uncorrelated dependent errors, *Journal of Econometrics*, **150**, 207–218.

- Lesage, J. P. and Pace, R. K. (2009) *Introduction to spatial econometrics*, CRC Press, Boca Raton, Florida.
- Lesmond, D. A. (2005) Liquidity of emerging markets, *Journal of Financial Economics*, **77**, 411–452.
- Lesmond, D. A., Ogden, J. P. and Trzcinka, C. A. (1999) A new estimate of transaction costs, *The Review of Financial Studies*, **12**, 1113–1141.
- Lin, B., Wesseh Jr., P. K. and Appiah, M. O. (2014) Oil price fluctuation, volatility spillover and the Ghanaian equity market: Implication for portfolio management and hedging effectiveness, *Energy Economics*, **42**, 172–182.
- Ljungqvist, A. and Wilhelm Jr., W. J. (2003) IPO pricing in the dot-com bubble, *The Journal of Finance*, **58**.
- Loisel, O. and Martin, P. (2001) Coordination, cooperation, contagion and currency crises, *Journal of International Economics*, **53**, 399–419.
- Londono, J. M. (2019) Bad bad contagion, *Journal of Banking & Finance*, **108**.
- Longin, F. and Solnik, B. (2001) Extreme correlation of international equity markets, *The Journal of Finance*, **56**, 649–676.
- Longstaff, F. A. (2004) The flight-to-liquidity premium in US treasury bond prices, *The Journal of Business*, **77**, 511–526.
- Lou, D. (2014) Attracting investor attention through advertising, *The Review of Financial Studies*, **27**, 1797–1829.
- Lucey, B. M. and O’Connor, F. (2017) Are gold bugs coherent?, *Applied Economics Letters*, **24**, 90–94.
- Lucey, B. M., Poti, V. and Tully, E. (2006) International portfolio formation, skewness & the role of gold, *Frontiers in Finance and Economics*, **3**, 49–68.
- MacKinlay, A. C. (1997) Event studies in economics and finance, *Journal of Economic Literature*, **35**, 13–39.
- Malik, F. and Ewing, B. T. (2009) Volatility transmission between oil prices and equity sector returns, *International Review of Financial Analysis*, **18**, 95–100.
- Manas, P., Niyati, B. and Arif Billah, D. (2019) Gold, gold mining stocks and equities – Partial wavelet coherence evidence from developed countries, *Resources Policy*, **62**, 378–384.

## BIBLIOGRAPHY

---

- Mandelbrot, B. (1963) The variation of certain speculative prices, *The Journal of Business*, **36**, 394–419.
- Manrique, N., A. Shephard (1998) Simulation-based likelihood inference for limited dependent processes, *The Econometrics Journal*, **1**, C174–C202.
- Marschinski, R. and Kantz, H. (2002) Analysing the information flow between financial time series: An improved estimator for transfer entropy, *European Physical Journal B: Condensed Matter and Complex Systems*, **30**, 275–281.
- Masson, P. R. (1998) Contagion: Monsoonal effects, spillovers, and jumps between multiple equilibria, IMF Working Paper 142, International Monetary Fund.
- Mensi, W., Beljid, M., Boubaker, A. and Managi, S. (2013) Correlations and volatility spillovers across commodity and stock markets: Linking energies, food, and gold, *Economic Modelling*, **32**, 15–22.
- Mensi, W., Hammoudeh, S. and Kang, S. H. (2015a) Precious metals, cereal, oil and stock market linkages and portfolio risk management: Evidence from Saudi Arabia, *Economic Modelling*, **51**, 340–358.
- Mensi, W., Hammoudeh, S. and Yoon, S.-M. (2015b) Structural breaks, dynamic correlations, asymmetric volatility transmission, and hedging strategies for petroleum prices and USD exchange rate, *Energy Economics*, **48**, 46–60.
- Merton, R. C. (1987) A simple model of capital market equilibrium with incomplete information, *The Journal of Finance*, **42**, 483–510.
- Meyer, R. and Yu, J. (2006) Multivariate stochastic volatility models: Bayesian estimation and model comparison, *Econometric Reviews*, **25**, 361–384.
- Miller, E. M. (1977) Risk, uncertainty, and divergence of opinion, *The Journal of Finance*, **32**, 1151–1168.
- Moat, H. S., Curme, C., Avakian, A., Kenett, D. Y., Stanley, H. E. and Preis, T. (2013) Quantifying Wikipedia usage patterns before stock market moves, *Scientific Reports*, **3**, 1801.
- Moel, A. and Tufano, P. (2002) When are real options exercised? An empirical study of mine closings, *The Review of Financial Studies*, **15**, 35–64.
- Mollah, S., Quoreshi, S. and Zafirov, G. (2016) Equity market contagion during global financial and Eurozone crises: Evidence from a dynamic correlation analysis, *Journal of International Financial Markets, Institutions & Money*, **41**, 151–167.

- Narayan, S., Sriananthakumar, S. and Islam, S. Z. (2014) Stock market integration of emerging Asian economies: Patterns and causes, *Economic Modelling*, **39**, 19–31.
- Nelson, D. B. (1991) Conditional heteroskedasticity in asset returns: A new approach, *Econometrica*, **59**, 347–370.
- Nishiyama, Y., Hitomi, K., Kawasaki, Y. and Jeong, K. (2011) A consistent nonparametric test for nonlinear causality – Specification in time series regression, *Journal of Econometrics*, **165**, 112–127.
- Obstfeld, M. (1986) Rational and self-fulfilling balance-of-payments crises, *American Economic Review*, **76**, 72–81.
- Oh, D. H. and Patton, A. J. (2018) Time-varying systemic risk: Evidence from a dynamic copula model of CDS spreads, *Journal of Business & Economic Statistics*, **36**, 181–195.
- Opschoor, A., Janus, P., Lucas, A. and Van Dijk, D. (2018) New heavy models for fat-tailed realized covariances and returns, *Journal of Business & Economic Statistics*, **36**, 643–657.
- Ord, J. K. (1975) Estimation methods for models of spatial interaction, *Journal of the American Statistical Association*, **70**, 120–126.
- Park, J. and Ratti, R. (2008) Oil price shocks and stock markets in the US and 13 European countries, *Energy Economics*, **30**, 2587–2608.
- Pashler, H. and Johnston, J. C. (1998) Attentional limitations in dual-task performance, in *Attention* (Ed.) H. Pashler, Psychology Press/Erlbaum (UK) Taylor & Francis, pp. 155–189.
- Patton, A. J. (2006) Modelling asymmetric exchange rate dependence, *International Economic Review*, **47**, 527–556.
- Peng, L. and Xiong, W. (2006) Investor attention, overconfidence and category learning, *Journal of Financial Economics*, **80**, 563–602.
- Portes, R. and Rey, H. (2005) The determinants of cross-border equity flows, *Journal of International Economics*, **65**, 269–296.
- Pragidis, I., Aielli, G., Chionis, D. and Schizas, P. (2015) Contagion effects during financial crisis: Evidence from the Greek sovereign bonds market, *Journal of Financial Stability*, **18**, 127–138.
- Preis, T., Moat, H. S. and Stanley, H. E. (2013) Quantifying trading behavior in financial markets using Google Trends, *Scientific Reports*, **3**, 1684.
- Qu, X. and Lee, L.-f. (2015) Estimating a spatial autoregressive model with an endogenous spatial weight matrix, *Journal of Econometrics*, **184**, 209–232.

## BIBLIOGRAPHY

---

- Raddant, M. and Kenett, D. Y. (2021) Interconnectedness in the global financial market, *Journal of International Money and Finance*, **110**, 102280.
- Ranaldo, A. and Söderlind, P. (2010) Safe haven currencies, *Review of Finance*, **14**, 385–407.
- Reboredo, J. C. (2013) Is gold a safe haven or a hedge for the US Dollar? Implications for risk management, *Journal of Banking & Finance*, **37**, 2665–2676.
- Reboredo, J. C. and Ugolini, A. (2017) Quantile causality between gold commodity and gold stock prices, *Resources Policy*, **53**, 56–63.
- Richard, J.-F. and Zhang, W. (2007) Efficient high-dimensional importance sampling, *Journal of Econometrics*, **141**, 1385–1411.
- Richardson, M. and Smith, T. (1993) A test for multivariate normality in stock returns, *Journal of Business*, **66**, 295–321.
- Rigobon, R. (1998) Informational speculative attacks: Good news is no news, Federal Reserve Board IF Seminar Paper, Federal Reserve.
- Rigobon, R. (2003a) Identification through heteroskedasticity, *Review of Economics and Statistics*, **85**, 777–792.
- Rigobon, R. (2003b) On the measurement of the international propagation of shocks: Is the transmission stable?, *Journal of International Economics*, **61**, 261–283.
- Rigobon, R. (2019) Contagion, spillover, and interdependence, *Economía*, **19**, 69–100.
- Rockerbie, D. W. (1999) Gold prices and gold production: Evidence for South Africa, *Resources Policy*, **25**, 69–76.
- Rodriguez, J. C. (2007) Measuring financial contagion: A copula approach, *Journal of Empirical Finance*, **14**, 401–423.
- Roll, R. (1984) A simple implicit measure of the effective bid-ask spread in an efficient market, *The Journal of Finance*, **39**, 1127–1139.
- Ross, S. A. (1976) The arbitrage theory of capital asset pricing, *Journal of Economic Theory*, **13**, 341–360.
- Rouwenhorst, G. (1999) Local factors and turnover in emerging markets, *The Journal of Finance*, **54**, 1439–1464.
- Rua, A. and Nunes, L. C. (2009) International comovement of stock market returns: A wavelet analysis, *Journal of Empirical Finance*, **16**, 632–639.



- Sachs, J., Tornell, A. and Velasco, A. (1996) The Mexican peso crisis: Sudden death or death foretold?, *Journal of International Economics*, **41**, 265–283.
- Sadorsky, P. (1999) Oil price shocks and stock market activity, *Energy Economics*, **21**, 449–469.
- Sadorsky, P. (2014) Modeling volatility and correlations between emerging market stock prices and the prices of copper, oil and wheat, *Energy Economics*, **43**, 72–81.
- Schreiber, T. (2000) Measuring information transfer, *Physical Review Letters*, **85**, 461–464.
- Schwert, W. G. (1990) Stock volatility and the crash of '87, *The Review of Financial Studies*, **4**, 77–102.
- Seasholes, M. S. and Wu, G. (2007) Predictable behavior, profits, and attention, *Journal of Empirical Finance*, **14**, 590–610.
- Selvanathan, S. and Selvanathan, E. A. (1999) The effect of the price of gold on its production: A time-series analysis, *Resources Policy*, **25**, 265–275.
- Shannon, C. E. (1948) A mathematical theory of communication, *Bell System Technical Journal*, **27**, 379–423.
- Sharif, A., C., A. and Yarovaya, L. (2020) COVID-19 pandemic, oil prices, stock market, geopolitical risk and policy uncertainty nexus in the US economy: Fresh evidence from the wavelet-based approach, *International Review of Financial Analysis*, **70**, 101496.
- Sharpe, W. F. (1964) Capital asset prices: A theory of market equilibrium under conditions of risk, *The Journal of Finance*, **19**, 425–442.
- Shepard, N. and Pitt, M. K. (1997) Likelihood analysis of non-Gaussian measurement time series, *Biometrika*, **84**, 653–667.
- Shephard, N. (2005) *Stochastic volatility: Selected readings*, Oxford University Press, Princeton, NJ.
- Sherman, E. J. (1982) Gold: A conservative, prudent diversifier, *The Journal of Portfolio Management*, **8**, 21–27.
- Shiyang, H., Yulin, H. and Tse-Chun, L. (2019) Attention allocation and return co-movement: Evidence from repeated natural experiments, *Journal of Financial Economics*, **132**, 369–383.
- Shleifer, A. and Vishny, R. W. (1997) The limits of arbitrage, *The Journal of Finance*, **52**, 35–55.
- Silvennoinen, A. and Teräsvirta, T. (2009) Multivariate GARCH models, in *Handbook of financial time series* (Eds.) T. G. Andersen, R. A. Davis, J. P. Kreiss and T. Mikosch, Springer, pp. 201–229.

## BIBLIOGRAPHY

---

- Silvestrini, A. and Veredas, D. (2008) Temporal aggregation of univariate and multivariate time series models: A survey, *Journal of Economic Surveys*, **22**, 458–497.
- Statista (2021) Worldwide desktop market share of leading search engines from January 2010 to September 2021, <https://www.statista.com/statistics/216573/worldwide-market-share-of-search-engines/>, [Online; accessed 2022-04-08].
- Stoll, H. (2000) Presidential address: Friction, *The Journal of Finance*, **55**, 1479–1514.
- Syllignakis, M. N. and Kouretas, G. P. (2011) Dynamic correlation analysis of financial contagion: Evidence from the Central and Eastern European markets, *International Review of Economics & Finance*, **20**, 717–732.
- Tange, O. (2011) GNU parallel – The command-line power tool, *login: The USENIX Magazine*, **36**, 42–47.
- Tauchen, G. E. and Pitts, M. (1983) The price variability-volume relationship on speculative markets, *Econometrica*, **51**, 485–505.
- Tse, Y. K. and Tsui, A. K. (2002) A multivariate generalized autoregressive conditional heteroscedasticity model with time-varying correlations, *Journal of Business & Economic Statistics*, **20**, 351–362.
- Tufano, P. (1996) Who manages risk? An empirical examination of risk management practices in the gold mining industry, *The Journal of Finance*, **51**, 1097–1137.
- Ulrich, S., Trench, A. and Hagemann, S. (2019) Grade-cost relationships within Australian underground gold mines – A 2014–2017 empirical study and potential value implications, *Resources Policy*, **61**, 29–48.
- Valdés, R. (1996) Emerging market contagion: Evidence and theory, *Working Paper*.
- Vargas, G. A. (2008) What drives the dynamic conditional correlation of foreign exchange and equity returns?, MPRA Working Paper 7174, Munich Personal RePEc Archive.
- Varin, C. and Vidoni, P. (2008) Pairwise likelihood inference for general state space models, *Econometrics Review*, **28**, 170–185.
- Vayanos, D. (2004) Flight to quality, flight to liquidity, and the pricing of risk, NBER Working Paper 10327, National Bureau of Economic Research.
- Veldkamp, L. L. (2006) Information markets and the co-movement of asset prices, *The Review of Economic Studies*, **73**, 823–845.

- Veldkamp, L. L. and Wolfers, J. (2007) Aggregate shocks or aggregate information? Costly information and business cycle co-movement, *Journal of Monetary Economics*, **54**, 37–55.
- Virk, N. and Javed, F. (2017) European equity market integration and joint relationship of conditional volatility and correlations, *Journal of International Money and Finance*, **71**, 53–77.
- Wälti, S. (2011) Stock market synchronization and monetary integration, *Journal of International Money and Finance*, **30**, 96–110.
- Weng, B., Ahmed, M. A. and M., M. F. (2017) Stock market one-day ahead movement prediction using disparate data sources, *Economic Modelling*, **79**, 153–163.
- WHO (2020a) COVID-19 public health emergency of international concern (PHEIC) global research and innovation forum, [https://www.who.int/publications/m/item/covid-19-public-health-emergency-of-international-concern-\(pheic\)-global-research-and-innovation-forum](https://www.who.int/publications/m/item/covid-19-public-health-emergency-of-international-concern-(pheic)-global-research-and-innovation-forum), [Online; accessed 2022-04-08].
- WHO (2020b) WHO director-general’s opening remarks at the media briefing on COVID-19, <https://www.who.int/director-general/speeches/detail/who-director-general-s-opening-remarks-at-the-media-briefing-on-covid-19---11-march-2020>, [Online; accessed 2022-04-08].
- WHO (2020c) Weekly epidemiological update on COVID-19, <https://www.who.int/publications/m/item/weekly-epidemiological-update-on-covid-19---16-november-2021>, [Online; accessed 2022-04-08].
- Wied, D. (2013) CUSUM-type testing for changing parameters in a spatial autoregressive model for stock returns, *Journal of Time Series Analysis*, **34**, 221–229.
- Winters, L. A. and Italianer, A. (1987) Theory and practice of international trade linkage models, *The Economic Journal*, **97**, 780.
- World Gold Council (2021) Gold trading volume, <https://www.gold.org/goldhub/data/trading-volumes>, [Online; accessed 2022-04-08].
- Yuan, K. (2005) Asymmetric price movements and borrowing constraints: A REE model of crisis, contagion, and confusion, *The Journal of Finance*, **60**, 379–411.
- Yuan, Y. (2015) Market-wide attention, trading, and stock returns, *Journal of Financial Economics*, **116**, 548–564.
- Zakoian, J.-M. (1994) Threshold heteroskedastic models, *Journal of Economic Dynamics and Control*, **18**, 931–955.

## BIBLIOGRAPHY

---

- Zamojski, M. (2017) Filtering with confidence: In-sample confidence bands for GARCH filters, Working paper.
- Zangari, P. (1996) Riskmetrics – technical document, Tech. rep., MSCI Inc.
- Zhang, D., Hu, M. and Ji, Q. (2020) Financial markets under the global pandemic of COVID-19, *Finance Research Letters*, **36**, 101528.
- Zolfaghari, M., Ghoddusi, H. and Faghihian, F. (2020) Volatility spillovers for energy prices: A diagonal BEKK approach, *Econometrica*, **92**, 104965.